

University of Windsor

Scholarship at UWindor

Electronic Theses and Dissertations

Theses, Dissertations, and Major Papers

2005

Design of a research engine for homogeneous charge compression ignition (HCCI) combustion.

Philip S. Zoldak
University of Windsor

Follow this and additional works at: <https://scholar.uwindsor.ca/etd>

Recommended Citation

Zoldak, Philip S., "Design of a research engine for homogeneous charge compression ignition (HCCI) combustion." (2005). *Electronic Theses and Dissertations*. 1659.
<https://scholar.uwindsor.ca/etd/1659>

This online database contains the full-text of PhD dissertations and Masters' theses of University of Windsor students from 1954 forward. These documents are made available for personal study and research purposes only, in accordance with the Canadian Copyright Act and the Creative Commons license—CC BY-NC-ND (Attribution, Non-Commercial, No Derivative Works). Under this license, works must always be attributed to the copyright holder (original author), cannot be used for any commercial purposes, and may not be altered. Any other use would require the permission of the copyright holder. Students may inquire about withdrawing their dissertation and/or thesis from this database. For additional inquiries, please contact the repository administrator via email (scholarship@uwindsor.ca) or by telephone at 519-253-3000ext. 3208.

Design of a Research Engine for Homogeneous Charge Compression Ignition (HCCI) Combustion.

by

Philip S. Zoldak

A Thesis
Submitted to the Faculty of Graduate Studies and Research
Through the Department of Mechanical, Automotive and Materials Engineering
in Partial Fulfillment of the Requirements for
the Degree of Master of Applied Science at the
University of Windsor

Windsor, Ontario, Canada

© 2005 Philip S. Zoldak



Library and
Archives Canada

Bibliothèque et
Archives Canada

Published Heritage
Branch

Direction du
Patrimoine de l'édition

395 Wellington Street
Ottawa ON K1A 0N4
Canada

395, rue Wellington
Ottawa ON K1A 0N4
Canada

Your file *Votre référence*

ISBN: 0-494-09833-3

Our file *Notre référence*

ISBN: 0-494-09833-3

NOTICE:

The author has granted a non-exclusive license allowing Library and Archives Canada to reproduce, publish, archive, preserve, conserve, communicate to the public by telecommunication or on the Internet, loan, distribute and sell theses worldwide, for commercial or non-commercial purposes, in microform, paper, electronic and/or any other formats.

The author retains copyright ownership and moral rights in this thesis. Neither the thesis nor substantial extracts from it may be printed or otherwise reproduced without the author's permission.

AVIS:

L'auteur a accordé une licence non exclusive permettant à la Bibliothèque et Archives Canada de reproduire, publier, archiver, sauvegarder, conserver, transmettre au public par télécommunication ou par l'Internet, prêter, distribuer et vendre des thèses partout dans le monde, à des fins commerciales ou autres, sur support microforme, papier, électronique et/ou autres formats.

L'auteur conserve la propriété du droit d'auteur et des droits moraux qui protègent cette thèse. Ni la thèse ni des extraits substantiels de celle-ci ne doivent être imprimés ou autrement reproduits sans son autorisation.

In compliance with the Canadian Privacy Act some supporting forms may have been removed from this thesis.

Conformément à la loi canadienne sur la protection de la vie privée, quelques formulaires secondaires ont été enlevés de cette thèse.

While these forms may be included in the document page count, their removal does not represent any loss of content from the thesis.

Bien que ces formulaires aient inclus dans la pagination, il n'y aura aucun contenu manquant.


Canada

ABSTRACT

The design and development of a research engine for Homogeneous Charge Compression Ignition (HCCI) combustion was performed. The objectives were; to design and build an experimental apparatus for investigation of parameters affecting control of HCCI burn in engines, to commission the HCCI burn apparatus, to establish HCCI burn of lean fuel/air mixture, and to enable data acquisition of in-cylinder pressure measurements.

A simple design methodology was followed. Three different concepts were presented along with the advantages and disadvantages of each. Concept three was chosen as the best alternative based on functional objective and cost.

Several parameters were identified to affect control of HCCI burn in the literature review. Systems were designed to enable variability of these parameters and study of HCCI burn in a variable compression ratio engine. The criteria and constraints of all the systems of the apparatus were identified. Detailed design drawings and calculations of each system were performed to enable component selection. Testing was performed to verify the functional objectives of each system.

Based on methodology, detailed design, fabrication, testing and verification, the project has met all the objectives. Recommendations for future work were made based on testing.

Dedicated to my Father and Mother.

ACKNOWLEDGEMENTS

I would like to thank my supervisor Dr. Andrzej Sobiesiak, for his guidance, encouragement and allowing me the opportunity to work with one of the finest professors I have ever come to know. Sincere thanks to Dr. Ming Zheng for his inspiration and to Dr. Leo Oriet, and Dr. Jimi Tjong for their time and assistance in the development of this thesis.

This project would not have been possible without the personnel of the Technical Support Center in particular Steve Budinsky and Marc St. Pierre. Their countless hours of expertise and craftsmanship were greatly appreciated. Additional thanks go to Phil Diett, Pat Sequin, Mohsen Battoei, Chunyi Xia, and Jeff Defoe for their contributions and assistance.

The financial support from Auto21 and equipment donations from Allen-Bradley, Kubota Canada and Waffle Electric were also much appreciated.

Finally, special thanks to my parents Viktor and Helen, my siblings Tim and Natalia. Thank you for putting up with my difficult times and for supporting me while I complete one of my dreams.

TABLE OF CONTENTS

ABSTRACT		iii
DEDICATION		iv
ACKNOWLEDGEMENT		v
LIST OF TABLES		ix
LIST OF FIGURES		x
LIST OF ABBREVIATIONS		xiv
LIST OF SYMBOLS		xvii
CHAPTER 1: INTRODUCTION		1
1.1 Motivation		1
1.2 Ethanol as a Fuel		2
1.3 What is HCCI?		3
1.4 Well To Wheel Cost Comparison		4
1.5 Ethanol and HCCI Challenges		5
1.6 Objectives		6
CHAPTER 2: LITERATURE REVIEW – HCCI PARAMETERS		7
2.1 Intake Charge Temperature		7
2.2 Compression Ratio (CR)		8
2.3 Equivalence Ratio		10
2.4 Fuel Effects		12
2.5 Exhaust Gas Recirculation		13
2.6 Practical HCCI Operating Range		15
2.7 Summary		16
CHAPTER 3: RESEARCH APPARATUS CONCEPT DEVELOPMENT		18
3.1 Identification of Need		18
3.2 Background Research		18
3.2.1 <i>Rapid Compression Machine</i>		18
3.2.2 <i>Single Cylinder Research Engines</i>		19
3.2.3 <i>Production Engines Converted for HCCI</i>		20
3.3 Problem Statement		21
3.3.1 <i>Project Methodology and Deliverables</i>		21
3.4 Criteria and Constraints		22
3.4.1 <i>Criteria</i>		22
3.4.2 <i>Constraints</i>		25
3.5 Ideation and Invention		27
3.5.1 <i>Concept One: Rapid Compression Machine</i>		27
3.5.2 <i>Concept Two: Engine with Dynamometer</i>		28
3.5.3 <i>Single Cylinder HCCI Engine with AC Motor and VSD</i>		29
3.6 Selection		31
CHAPTER 4: DETAILED DESIGN		33
4.1 Schematic of Research Engine		33
4.2 Research Engine Selection and Conversion		34
4.2.1 <i>Engine Selection</i>		34
4.2.2 <i>Engine Conversion for HCCI</i>		36
4.2.3 <i>Variable Compression Ratio Options</i>		38

4.3	Drive System Design and Component Selection	41
	4.3.1 Sizing of the AC Motor for Motoring	43
	4.3.2 Feasibility of the AC Motor for Starting	43
	4.3.3 Sizing of the Resistor Banks for Braking of the Drive system	44
	4.3.4 Speed Control Selection	46
	4.3.5 Selection of Engine to AC motor Flexible Coupler	47
4.4	Intake Charge Pre-Heater System Selection	48
	4.4.1 Heater Sizing and Selection	49
	4.4.2 Temperature Controller Selection	50
4.5	Selection of Intake Air Measurement System	51
	4.5.1 Flow Measurement Background	52
	4.5.2 Laminar Flow Element Selection	53
	4.5.3 Transmitter Selection	55
4.6	Intake Piping System Design	55
4.7	EGR System	58
	4.7.1 EGR Piping Leg	59
	4.7.2 MATLAB EGR Program	60
	4.7.3 Exhaust Gas Measurement	62
4.8	Ethanol Fuel System	63
	4.8.1 Fuel Pump Selection	64
	4.8.2 Fuel Tank Selection	65
	4.8.3 Fuel Injector Selection	66
	4.8.4 Fuel Pressure Regulator and Gauge Selection	67
	4.8.5 Fuel Filter Selection	68
	4.8.6 Fuel Fittings and Hose Selection	69
4.9	ECU system	70
4.10	Data Acquisition System	74
	4.10.1 Thermocouple Selection and Location	76
	4.10.2 Pressure Transducer Selection	76
	4.10.3 Charge Amplifier Selection	77
	4.10.4 Differential Pressure to Current Converter	78
	4.10.5 24 Volt Power Supply	79
	4.10.6 Rotary Encoder	79
	4.10.7 DAQ Card	80
	4.10.8 Terminal Box	82
	4.10.9 Connector Box	82
	4.10.10 Personal Computer and Labview Program	83
4.11	Summary	84
CHAPTER 5: FABRICATION AND PROTOTYPING		85
5.1	Apparatus Fixture Prototyping	85
5.2	Drive System Installation	88
5.3	Engine Installation	91
5.4	VCR Secondary Piston Prototyping	93
5.5	Cam Trigger Mechanism Prototyping	98
5.6	Cooling System Installation	102
5.7	Encoder Installation	104
5.8	Intake/EGR Piping System and Heater Fabrication and Installation	105
5.9	Fuel and ECU System Installation	110
5.1	Safety Guarding Installation	113

5.11	Data Acquisition System Development	115
5.12	Summary	120
CHAPTER 6:	TESTING AND VERIFICATION	121
6.1	Engine System Testing	121
6.2	Drive System Testing	122
6.3	Fuel System Testing	125
6.4	ECU System Testing	126
6.5	Intake Piping System Testing	129
6.6	Intake Air Preheater Testing	132
6.7	Data Acquisition System Testing	135
	6.7.1 Thermocouple Verification	137
	6.7.2 Flow rate	138
	6.7.3 In-cylinder Pressure	139
	6.7.4 Crank Angle Encoder	142
	6.7.5 Research Engine System Verification	148
6.8	Summary	148
CHAPTER 7:	CONCLUSIONS AND RECOMMENDATIONS	150
7.1	Conclusions	150
7.2	Recommendations	150
REFERENCES		153
APPENDICES		158
Appendix A:	Engine Specifications and Function	158
Appendix B:	Engine Design Calculations	161
Appendix C:	Drive System Specifications	166
Appendix D:	Drive System Design Calculations	167
Appendix E:	Engine Testing	173
Appendix F:	Intake System Design Calculations	179
Appendix G:	Intake System Specifications	196
Appendix H:	Fuel System Design Calculations	201
Appendix I:	Fuel and ECU System Specification	205
Appendix J:	Data Acquisition System Specifications	207
Appendix K:	Drive System Testing	211
Appendix L:	Fuel and ECU System Testing	215
Appendix M:	Intake System Testing	222
Appendix N:	HCCI Gasoline Combustion Experiments	226
VITA AUCTORIS		245

LIST OF TABLES

Table 1	Well to Wheel comparison of Ethanol, Gasoline and Diesel fuels.	5
Table 2	Summary of HCCI control parameters as found in recent literature publications.	16
Table 3	List of functionality constraints.	26
Table 4	List of durability constraints.	26
Table 5	Legend, Description of ranking system utilized to compare concepts to criteria.	31
Table 6	Concept Selection Matrix	31
Table 7	Kubota D905 Specifications [33].	35
Table 8	Compression ratio and corresponding head gasket thickness required.	38
Table 9	VCR Low CR Secondary piston plunge depth and clearance volume (per cylinder).	40
Table 10	VCR High CR Secondary piston plunge depth and clearance volume (per cylinder basis).	40
Table 11	Variation of AC motor shaft speed (rpm) by varying input frequency with VSD.	47
Table 12	Intake Charge Preheater System legend.	49
Table 13	Intake Air Measurement System legend.	51
Table 14	Summary of pressure loss for longest leg of the system. 3600 RPM, no EGR.	57
Table 15	EGR System legend.	59
Table 16	Summary of Matlab EGR program inputs.	61
Table 17	Summary of MATLAB EGR program simulation at various CO2 concentrations.	61
Table 18	Exhaust Emission Sampling Capability Range for OTC MicroGas Analyzer.	62
Table 19	Ethanol fuel system legend.	63
Table 20	Legend for Figure 38 ECU system.	70
Table 21	Legend for data acquisition system.	74
Table 22	DAQ card limitations compared to encoder sampling rate.	82
Table 23	Summary of VCR secondary piston spacer experiment.	97
Table 24	Emergency braking test results	124
Table 25	Statistical summary of flowmeter data.	138
Table 26	Sample of crank encoder data from combustion experiment.	141
Table 27	Post-processing of corrected sample data-HCCI gasoline experiment 750 RPM.	146
Table 28	Post-processing of corrected sample data-HCCI gasoline experiment 3000 RPM.	147

LIST OF FIGURES

Figure 1:	Increase in stringency of heavy-duty diesel, NO _x and PM emissions regulations.	1
Figure 2:	HCCI is a hybrid of CI and SI engines.	3
Figure 3:	A schematic illustration of the operational window for an HCCI engine.	9
Figure 4:	Equivalence ratio shown as function of load and speed.	10
Figure 5:	Ignition timing map of ethanol for various Lambda and EGR rates.	11
Figure 6:	(a) Combustion duration map (°CA), (b) pressure rise map (bar/°CA).	15
Figure 7:	AVL single cylinder research engine with optical access.	19
Figure 8:	Lund Institute of Technology, Volvo TD100 engine modified to single cylinder HCCI mode with VCR head.	20
Figure 9:	Concept One, rapid compression machine.	28
Figure 10:	(a) 3-cylinder Kubota D905 diesel engine, (b) eddy current dynamometer.	28
Figure 11:	Concept Two: Engine with Dynamometer.	29
Figure 12:	Single-cylinder HCCI engine with AC motor and variable speed drive.	30
Figure 13:	Overall schematic of apparatus.	33
Figure 14:	Kubota D905 base engine, to be converted to single cylinder engine.	35
Figure 15:	Cooling system schematic for Kubota D905.	36
Figure 16:	AutoCAD Template of Kubota D905 head gasket.	39
Figure 17:	Cross-sectional view of Kubota D905 cylinder head pre chamber.	40
Figure 18:	Proposed drive system.	42
Figure 19:	Dynamometer operating quadrants.	42
Figure 20:	Intake charge pre-heater system schematic.	49
Figure 21:	Omega SH-73343, 6kW-240V-25A Intake Air Heater.	50
Figure 22:	Omega CN-i/32 heater controller.	51
Figure 23:	Intake Air Measurement System.	52
Figure 24:	Meriam Laminar Flow Element Model # 50MC2-2.	55
Figure 25:	Intake Piping System Schematic.	56
Figure 26:	Concept Sketch of proposed EGR system.	59
Figure 27:	Brass Gate Valve to be used as EGR valves.	60
Figure 28:	OTC MicroGas Emission Analyzer.	63

Figure 29:	Schematic of ethanol fuel system.	64
Figure 30:	ACCEL model # 310-74701 EFI alcohol compatible fuel pump.	65
Figure 31:	JAZ Pro Cell Model # 547-250-001-01 vertical fuel tank.	66
Figure 32:	Delphi Multec 2 fuel injector model # 2532087.	67
Figure 33:	(a) Mallory Regulator Model 4309, (b) Omega Pressure gauge model # PGS 25L 160.	68
Figure 34:	JAZ fuel filter model 547-836-006-11.	68
Figure 35:	(a) ¼" NPT male to 06 AN male, (b) 06 AN female to 06 AN female coupler, (c) 06 AN swivel hose end, (d) 06 AN to 06 AN union.	69
Figure 36:	(a) Various hose sizes shown from 04 to 010 AN, (b) Multilayered construction hose.	70
Figure 37:	Schematic of the ECU system.	71
Figure 38:	Fully programmable ECU from 034EFI Model Stage 3b.	72
Figure 39:	The 034EFI ECU interface software for monitoring engine performance in real time.	73
Figure 40:	Basic fuel mapping user interface for programming 034 ECU.	73
Figure 41:	Schematic of data acquisition system.	75
Figure 42:	Kistler 5004 dual mode charge amplifier.	78
Figure 43:	Gurley Encoder Output waveform.	80
Figure 44:	Connector box front panel layout.	83
Figure 45:	Front View of the fixture frame.	86
Figure 46:	Top View of fixture frame.	86
Figure 47:	Front View of fixture frame.	87
Figure 48:	End view of fixture frame.	87
Figure 49:	Adjustable levelling feet.	87
Figure 50:	Installation of variable speed drive system.	88
Figure 51:	Allen-Bradley Dynamic Braking/Chopper Module.	89
Figure 52:	Rex Manufacturing Auto-transformer.	90
Figure 53:	Square D 480 Volt, 25 Amp secondary disconnect.	90
Figure 54:	Custom fabricated engine mount bracket.	92
Figure 55:	Custom fabricated upper engine mount.	92
Figure 56:	Coupler for AC motor and Kubota Engine.	93

Figure 57:	Kubota D905 Cylinder head ready for pre-chamber modifications.	94
Figure 58:	(a) VCR secondary piston components, (b) VCR secondary piston side view, (c) View of VCR secondary piston tip.	95
Figure 59:	(a) Tightening of VCR secondary piston, (b) VCR secondary piston installed, (c) View of VCR secondary piston without prechamber cap.	96
Figure 60:	Comparison between OEM, high CR and Low CR prechamber inserts.	96
Figure 61:	(a) Low CR prechamber cap and matching copper spacers, (b) High CR prechamber cap and matching copper spacers.	98
Figure 62:	Cam Trigger Mechanism concept.	100
Figure 63:	(a) Cam Trigger Mechanism, (b) Hall sensor and steel pick-up tab.	101
Figure 64:	Cam trigger mechanism adjustment.	102
Figure 65:	Cooling system installation.	103
Figure 66:	(a) Front view of radiator and mounts, (b) View of custom radiator mounting bracket.	103
Figure 67:	Installation of Gurley 9125 encoder.	104
Figure 68:	Intake/EGR system, hot/galvanized pipe section.	106
Figure 69:	Intake/EGR system, Cold/ABS pipe section.	107
Figure 70:	(a) TPS view of throttle valve, (b) Intake and exhaust flange, (c) Throttle Cable Bracket.	108
Figure 71:	Laminar flow meter and bracket.	109
Figure 72:	Omega SH-73343 intake air heater.	109
Figure 73:	Intake air heater controller.	110
Figure 74:	(a) Fuel tank opening, and return line, (b) Fuel tank, filter, and supply line.	111
Figure 75:	Fuel pressure regulator, gauge, and injector fuel rail.	111
Figure 76:	Fuel pump mounted underneath the top galvanized shelf.	112
Figure 77:	ECU install on firewall of fuel splash tray.	113
Figure 78:	Safety guarding on rotating coupler.	114
Figure 79:	(a) Safety guarding on rotating flywheel, (b) inability to access moving parts.	114
Figure 80:	(a) Safety guarding on rotating pulleys, (b) inability to access moving parts.	115
Figure 81:	Thermocouples installed in appropriate locations.	116
Figure 82:	Quick Connector box.	117
Figure 83:	Labview Data Acquisition PC.	117

Figure 84:	System schematic panel.	118
Figure 85:	Configuration panel.	119
Figure 86:	Required injector scalar for measured engine speeds.	128
Figure 87:	Summary of required injector scalar for all equivalence ratios and engine speeds.	129
Figure 88:	Actual flow rate at various engine speeds.	130
Figure 89:	Actual volumetric efficiency at various engine speeds.	131
Figure 90:	Heater Exit Temperature at various engine speeds.	133
Figure 91:	Heat transferred to air at various engine speeds.	134
Figure 92:	Real-time unprocessed thermocouple data at 775 RPM.	136
Figure 93:	Real-time unprocessed flow meter data at 775 RPM.	137
Figure 94:	Real-time unprocessed in-cylinder pressure data for motoring at 775 RPM.	139
Figure 95:	Real-time processed encoder signal for motoring at 775 RPM.	140
Figure 96:	Pressure versus crank angle degree plot of HCCI gasoline experiment - processed and unprocessed data sample at 750 RPM.	144
Figure 97:	P-V diagram (pressure versus volume diagram) of HCCI gasoline experiment, corrected and uncorrected data sample at 750 RPM.	145
Figure 98:	Log(P) versus Log(V) plot of Gasoline HCCI.	148
Figure 99:	Final HCCI research engine setup.	149

LIST OF ABBREVIATIONS

°C	degrees celsius
883ECU	ECU calibration program
ABS	plastic plumbing material
AC	alternating current
AN	type of connector
AVL	Powertrain Engineering Company
BDC	bottom dead center
BMEP	brake mean effective pressure
BNC	connector type
C	carbon atom
CAD	computer aided design
CDN	Canadian Dollar
cfm	cubic feet per minute
CFR	Corporative Fuels Research Company
CI	compression ignition
CLT	coolant temperature sensor
CN	cetane number
CO	carbon monoxide
CO2	carbon dioxide
CPU	central processor unit
CR	compression ratio
CSA	Canadian Standards Association
D905	Kubota Engine Model
DAQ	data acquisition
DB15	15-pin connector
DB9	9-pin connector
DC	direct current
dyno	dynamometer
ECC	Electrical Code of Canada
ECU	electronic control unit
EFI	electronic fuel injection
EGR	exhaust gas recirculation
EPA	US Environmental Protection Agency
g/s	grams per second
gal	us gallons
GB	gigabytes hard drive storage space
GUI	graphic user interface
H	hydrogen atom

H ₂ O	water molecule
HC	hydrocarbons
HCCI	homogeneous charge compression ignition
HP	horse power
HRR	heat release rate
Hz	hertz
IDI	indirect injection
K	degrees kelvin
kPa	kilopascals
L/s	litres per second
LED	low voltage indicator light
LFE	laminar flow element meter
MAP	manifold absolute pressure sensor
MAT	manifold air temperature
MATLAB	mathematics programming language
MBT	maximum brake torque
N	nitrogen atom
NO ₂	nitrogen dioxide
NO _x	oxides of nitrogen
NPT	national pipe thread
O	oxygen atom
O ₂	oxygen molecule
OEM	original equipment manufacturer
OTC	manufacturer of gas analyzer
PC	personal computer
pC	picocolombs
Phi	equivalence ratio
PM	particulate matter
PV	pressure vs. volume diagram
PVC	poly-vinyl-chloride
RAM	temporary PC memory
RCM	rapid compression machine
RPM	revolutions per minute
Scalar	injector scalar or multiplier
SCRE	single cylinder research engine
SI	spark ignition
T1	air inlet thermocouple
T2	heater thermocouple
T3	mixture thermocouple

T4	exhaust thermocouple
T5	EGR thermocouple
T6	coolant thermocouple
TDC	top dead center
TDI	turbodiesel direct injection
TPS	throttle position sensor
UHC	unburned hydrocarbons
US	United States
VCR	variable compression ratio
VSD	variable speed drive
VVT	variable valve timing
kW	kilowatt
W	watt
MPa	megapascals
ft.lbs	foot pounds
kgf.m	kilograms force meter
mm	millimeter
cm	centimeter
psi	pounds per square inch
scfm	standard cubic feet per minute
L	litres
cu.in	cubic inches
kg	kilograms
lbs	pounds
kJ/kg	kilojoules per kilogram
bar/°CA	bars per degree crank angle
m	meter
in	inches
ft	foot
Hz	cycles per second
J/deg	joules per degree
g/HP-hr	grams per horsepower hour
hr	hour
mA	milli-amperes current
V	volts

LIST OF SYMBOLS

$\%EGR$	percent by volume EGR gas
$^{\circ}CA$	crank angle degrees
C_p	specific heat, constant pressure
d_{cam}	diameter of cam
d_{crank}	diameter of crank
Δp	pressure drop
D_{sp}	secondary piston diameter
ΔT	change in temperature
dV	change in volume
Φ	equivalence ratio
f	frequency
F_{loss}	heat loss factor
F_{os}	oversize factor
$F_{service}$	service factor
G	amplifier gain
J_t	total rotational inertia
λ	air fuel ratio
L_s	piston plunge depth
m	amplifier scalar
M_G	speed ratio
N_{cam}	number of teeth of cam
N_{crank}	number of teeth of crank
nd	safety factor
N_{poles}	number of motor poles
n_R	# of crank revs per power stroke per cylinder
P	power
p	pressure
$P_{absorbed}$	power absorbed
P_{avg}	average power absorbed
P_b	peak break power
p_g	stagnation pressure
P_i	net indicated power per cycle
$p_{incylinder}$	incylinder pressure
plf	loss of function pressure
pt	total pressure
Q	charge signal from kistler
ρ	density
R	resistance

ρ_{air}	density of air
R_{db1}	total dynamic braking resistance
RH	relative humidity
T	temperature
t	time
τ	torque
t_c	cycle time
$T_{coolant}$	coolant temperature
τ_{gross}	gross intermittent torque
T_{inlet}	inlet temperature
τ_{max}	maximum torque
τ_{net}	net continuous torque
τ_{per}	maximum permitted torque
τ_{req}	required torque
τ_{sup}	supplied torque
t_T	total time
U	flow velocity
V_c	clearance volume
V_d	DC bus voltage
V_s	swept volume
V_t	total volume
V_{tank}	tank volume
\dot{V}	volumetric flowrate
$\dot{V}_{calculated}$	calculated flowrate
\dot{N}_{sensor}	sampling rate per channel
$\dot{N}_{required}$	required sampling rate
$N_{datapoints}$	datapoints per degree crank angle
η_v	volumetric efficiency
\dot{m}_a	mass flowrate of air
ω	rotational speed
ω_b	maximum rotational speed
ω_o	minimum rotational speed
$W_{c,i}$	net indicated work per cycle
Q_{HT}	heat transfer rate
γ	ratio of specific heats

1 INTRODUCTION

The purpose of this thesis is to report on the project entitled, "Design of a Research Engine for Homogeneous Charge Compression Ignition (HCCI) Combustion." This thesis will present the motivation for the project, the objectives, methodology, as well as present the details of the design, fabrication, testing and verification of the apparatus.

1.1 Motivation

For the past three decades, engine research and development has been focusing on new technologies and methods for combustion that promise to lower vehicle exhaust emissions and improve fuel economy at part-load conditions.

Since 1974 emissions of particulate matter (PM) and oxides of nitrogen (NO_x) in both Canada and the US have become more stringently regulated as seen in Figure 1. Currently NO_x emissions are 3.353 g/kW-hr (2.5 g/HP-hr), and PM emissions are 0.134 g/kW-hr (0.1 g/HP-hr). Future emission standards for 2007 to 2010 are more stringent. Therefore, research and development will have to focus on new technologies and methods of combustion that promise to lower vehicle exhaust emissions.

Two solutions that promise to improve regulated emissions are: the burning of cleaner, renewable alternative fuels such as ethanol, and HCCI.

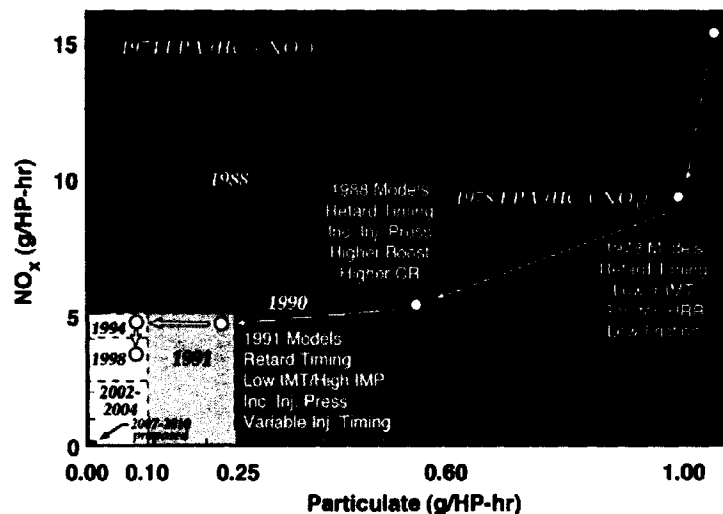


Figure 1: Increase in stringency of heavy-duty diesel, NO_x and PM emissions regulations [1].

1.2 Ethanol as a Fuel

Ethanol has been considered as an automotive fuel for many decades. Infact, when Henry Ford designed the Model T, it was his expectation that ethanol, made from renewable biological resources would be a major automobile fuel [2]. However, gasoline emerged as the dominant transportation fuel in the early twentieth century, because of the ease of operation of gasoline engines with the materials then available for engine construction, and a growing supply of cheaper petroleum from oil field discoveries.

There are two key reasons why gasoline usage has remained the primary fuel for the past century. Firstly, the cost per kilometre of travel is lower than other renewable resources. Secondly, large investments made by both petroleum and auto industries in physical capital, human skills and technology make the entry of a new cost-competitive industry difficult.

The use of ethanol in internal combustion engines has grown in recent years because it offers attractive benefits of reduced exhaust emissions and reduced environmental and human health impact. Due to the finite nature of petroleum reserves, production of ethanol in Canada in the US has been steadily increasing. Since ethanol is produced from plants that harness the power of the sun, ethanol is considered to be a renewable fuel.

With internal combustion engines, the pollutants of major concern are NO_x, unburned hydrocarbons (UHC), carbon monoxide (CO), and PM. Ethanol combustion offers lower NO_x emissions due to its lower flame temperature when compared to petroleum-based fuels. Also the ethanol molecule contains oxygen which promotes better oxidation of the fuel, and results in more complete combustion, thus reducing CO and UHC emissions. However, ethanol emissions are high in formaldehydes.

Formaldehyde has been classified by the EPA as a probable human carcinogen. Formaldehyde in the atmosphere is directly and indirectly a result of gasoline exhaust emissions. Ethanol combustion emissions have a higher rate of direct formaldehyde production compared to gasoline combustion emissions. However, as a result of possible improvements in ethanol-engine and emission-control technology, formaldehyde emissions can be significantly lowered [69].

Formaldehyde emission is a concern due to the low-temperature combustion nature of ethanol HCCI. In general, any engine operating or design parameter which would result in increased temperature of the exhaust or decreased unburnt fuel should encourage formaldehyde oxidation. Oxidizing catalyst using platinum-rhodium substrates have been used to control formaldehyde emissions [70].

1.3 What is HCCI?

Homogeneous charge compression ignition engines employ the following processes:

1. Preparation of the air-fuel mixture in the intake port. This mixture may consist of fuel, air, EGR and preheating.
2. Compression heating of the air-fuel mixture, while mixing continues.
3. Auto-ignition of the mixture in multi-point simultaneous ignition.
4. Combustion of the mixture simultaneously throughout the volume, controlled by chemical reaction rates.

This can be better understood by comparing compression ignition (CI) and spark ignition (SI) engines as seen in Figure 2.

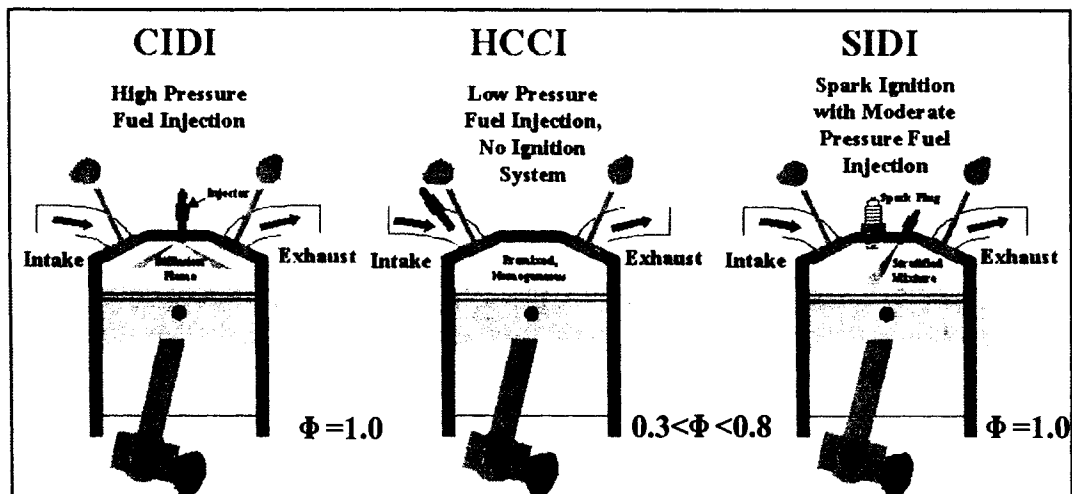


Figure 2: HCCI is a hybrid of CI and SI engines [3].

The combustion process in HCCI engines is fundamentally different from both SI and CI engines. There is no direct means of controlling ignition timing as in SI engines with the presence of a spark or CI engines with direct injection of fuel into the cylinder to control timing.

HCCI engines involve compression heating of the air-fuel mixture to its auto-ignition temperature, which can range anywhere from 700 to 1100K depending on the type of fuel and mixture strength.

The similarities between CI engines and HCCI are such: both have high compression ratios (CR) and both ignite air-fuel mixture by compression heating. CI engines have CR in the range 16-23:1. Similarly, HCCI engines have CR in the range 11-25:1 depending on the fuel.

When comparing SI and HCCI engines, both involve the process of homogeneous mixture preparation in the intake manifold. However, the main difference between SI and HCCI engines is the lack of spark to initiate ignition, and overall lean equivalence ratios (in the range $0.3 < \Phi < 0.8$.) If we compare SI and HCCI combustion for the same equivalence ratio say $\Phi=1.0$, then HCCI would have a much faster heat release rate compared to SI. However, in reality HCCI combustion occurs under much leaner conditions that decrease the heat release rate.

Diesel HCCI compression ratios are typically much lower than conventional CI diesel combustion. Diesel HCCI CR range is between 11 and 15:1 whereas conventional CI diesel CR ranges are between 16 and 23:1. Diesel HCCI has a lower CR range the conventional CI because HCCI is an overall lean mixture, and lean mixtures have higher specific heat ratios (closer to 1.4) than stoichiometric mixtures. Thus, when lean mixtures are compressed the mean temperature will be higher than conventional mixtures which results in a lower autoignition temperature. The thermal efficiency is decreased because of the lower CR, however the thermal efficiency increases due to the lean mixture and the increase in specific heat ratios are closer to 1.4.

Therefore lower compression ratios are employed to expand the operating range of diesel HCCI. The disadvantage of lower compression ratios is a decrease in thermal efficiency of the engine; however the advantage is a reduction in frictional losses.

1.4 Well to Wheel Cost Comparison

A well to wheel analysis was performed comparing our research fuel (ethanol) to gasoline and diesel fuel use. The cost of acquiring ethanol, gasoline and diesel fuels were obtained from the US Department of Energy website for the current year 2005 [71]. This cost was originally normalized on a cost per million Btu basis. This was converted to cost per MJ basis and

multiplied by the calorific heating value of each of the fuels. This resulted in the cost per kilogram fuel basis.

Heywood lists the approximate best brake specific fuel consumption bsfc values for both spark ignition and compression ignition passenger vehicles [64]. The bsfc value for the spark ignition passenger vehicle was multiplied by the air fuel ratio for stoichiometric gasoline combustion (14.7) and divided by the air fuel ratio for stoichiometric ethanol combustion (9.0.) This provides a good estimate for the bsfc of a ethanol spark ignition passenger vehicle of 0.544 g/kW.h. The best bsfc is multiplied by the cost per kg fuel produced to get a comparison of the cost per kilowatt hour of fuel consumed by a standard SI or CI engine, depending on fuel type. The cost per kilowatt hour for the diesel fuel is the lowest at 0.121 US\$/kWh with the ethanol fueled engine having a cost of 0.280 US\$/kWh and the gasoline engine having the highest cost of 0.303 US\$/kWh. This clearly shows that ethanol usage is more cost effective to use than gasoline however not as cost effective as diesel fuel (see Table 1.)

Table 1 Well to Wheel comparison of Ethanol, Gasoline and Diesel fuels.

Fuel	A/F ratio	HHV (MJ/kg)	US\$/MJ	US\$/kg Fuel	Best bsfc (kg/kWh)	Cost per kWh (US\$/kWh)
Ethanol (E85)	9	27.7	0.01855	0.514	0.544	0.280
Gasoline	14.7	44.65	0.01937	0.865	0.350	0.303
Diesel	30	44.3	0.01095	0.485	0.250	0.121

1.5 Ethanol and HCCI Challenges

There are several technical challenges with HCCI combustion, despite the fact that stable HCCI has been demonstrated at selected steady-state conditions [6,7,8,9]. These challenges need to be overcome before HCCI combustion can be applied to production vehicle engines. Research and development is required in the following areas: ignition timing control at various operating condition (speed and load), limiting the rate of heat release at high-load operation, providing smooth operation through rapid transients, achieving cold start, and meeting emission standards. Overcoming these challenges to develop practical HCCI engines will require research of in-cylinder processes, and how these processes can be favourably altered by control strategies. The development and testing of these control strategies will lead to HCCI becoming a practical engine technology.

There are some disadvantages with ethanol as an HCCI fuel. Ethanol has difficulties with auto-ignition, which can lead to problems with cold start. This is due to the cooling effect ethanol has on its surroundings, because of its high latent heat of vaporization (838.3 kJ/kg for ethanol compared to 306.3 kJ/kg for iso-octane) [4]. Additionally, ethanol has a high octane number (109) that prevents auto-ignition from occurring readily. Therefore, ethanol HCCI requires the use of a preheater to promote cold start and improve operating range performance.

HCCI combustion is difficult to control because there is no direct means of control as in SI or CI engines. Pressure versus crank angle or engine torque in SI engines is achieved by spark timing, and in CI engines it is controlled by fuel injection timing. These means are unavailable for HCCI.

1.6 Objectives

The primary objective of this thesis was to develop an experimental apparatus for investigation of parameters affecting control of HCCI combustion.

The following is a list of objectives for the thesis:

- To perform a literature review to identify the parameters affecting control of HCCI with respect to use of ethanol as a fuel.
- To design and fabricate an experimental apparatus for investigation of parameters affecting control of HCCI by following the design process.
- To commission the HCCI research apparatus by performing initial testing, troubleshooting, and verification experiments.
- To establish HCCI burn of lean ethanol/air, and obtain in-cylinder pressure measurements to verify the results.

2 LITERATURE REVIEW – HCCI PARAMETERS

The major challenge for commercialization of HCCI is combustion control in terms of, ignition timing control, and heat release rate control for a variety of speeds and loads. Several methods have been proposed for achieving HCCI engine control for operating conditions required for automotive applications. Control strategies reported in literature have indicated some degree of success. The following are the main HCCI control parameters:

1. Intake charge temperature.
2. Compression ratio (CR).
3. Equivalence ratio (air/fuel composition).
4. Fuel Effects (primary fuel type, and properties.)
5. Exhaust gas recirculation (EGR).

Selected studies on parameters affecting combustion control will be reviewed in these chapters.

2.1 Intake Charge Temperature

The effects of intake charge temperature have been widely reported. Najt and Foster [6] showed that HCCI could be achieved using a SI engine under lean fuelling and elevated inlet charge temperatures (300-500°C). In all cases, intake charge temperature has a strong effect on combustion for HCCI. The effect of increasing intake charge temperature is to advance auto-ignition timing and decrease combustion duration.

Iida and Igarashi [7] investigated the effect of intake charge temperature on n-butane (C_4H_{10}). The results show that by increasing intake charge temperature from 300K, to 325K, to 355K, the heat release rates increased from 20J/deg, to 60J/deg, to 100J/deg respectively. Also the combustion duration decreased as expected from 30, to 20 to 10 degrees respectively, for an increase in intake charge temperature.

Simulation results of ethanol/air HCCI performed by Ng [8] have demonstrated similar findings. Increasing the intake charge temperature will increase the peak in-cylinder temperature, but it is dependent on when ignition occurs. If ignition occurs around top dead center (TDC), then most of the energy will be released during the power stroke. If ignition occurs before TDC, then the effect of increased intake charge temperature is minimized, because the combustion reaction is working

against the piston in the compression stroke. Generally speaking, intake charge temperature can be used to optimize the ignition point, but it must be done correctly to maximize braking torque.

Increased intake charge temperature has also been utilized by Aoyama et al. [9] to extend the lean burn limit (defined by hydrocarbon emissions and combustion efficiency). In other words, a very lean mixture can be ignited more easily if intake-charge preheating is utilized.

2.2 Compression Ratio (CR)

HCCI initiates when the charge temperature reaches its auto-ignition temperature. Therefore, the required inlet charge temperature for MBT combustion timing in HCCI mode is a function of engine compression ratio. Increasing compression ratio can increase the charge temperature during the compression stroke and advance the start of auto-ignition.

Hiraya et al. [10] reported for a gasoline HCCI engine, higher compression ratios allowed lower intake charge temperature, and higher intake density for higher output. Also, higher compression ratio contributes to higher thermal efficiency. However, HCCI enabled by a higher compression ratio will encounter problems due to knock at higher loads with lower octane fuels. Variable compression ratio (VCR) would be a good solution to this problem, since the CR could be increased for lower loads and lower engine speeds and decreased for higher loads and higher engines speeds to decrease the onset of combustion.

Systems that achieve combustion timing control through changes in compression ratio can be divided into two types: Type 1 systems vary combustion chamber geometry, known as variable compression ratio (VCR), and Type 2 system vary the cylinder volume at inlet valve closing, variable valve timing (VVT) [11].

A VCR engine has the potential to achieve satisfactory operation in HCCI mode over a wide range of conditions because the compression ratio can be adjusted as the operating conditions change. However, operating conditions would change quickly and a fast response control system for VCR is yet to be established. Christensen et al. [12, 13, 14, 15, 16, 17] have been carefully investigating compression ratio as an effective means to achieve HCCI combustion control for several years. The VCR engine used in their studies employs a Type 1 system. A secondary piston is installed in the cylinder head whose position can be varied to change the compression ratio [18]. For each test the compression ratio was adjusted to get auto-ignition of the charge

around TDC. The experiments demonstrated the multi-fuel capability of an HCCI engine, and suggested that adjusting the compression ratio fast and correctly could facilitate control of HCCI combustion.

For a given engine system, load will be limited by either saturation of control variables, or by operational constraints. Operational constraints are represented by limitations of NO_x emissions, peak cylinder pressure, and peak pressure-rise rate. Figure 3 below illustrates these constraints. The variation of compression ratio can be used to extend the operational range of HCCI shown below for a given mixture.

A lower CR provides a larger volume for the gas at TDC, which can slow down combustion and lower the peak pressure, but this provides slower expansion after TDC and increases NO_x, CO and UHC emissions, and requires a higher intake charge temperature. With a fixed geometric compression ratio, the effective compression ratio can be adjusted by VVT. An engine could be built with a high geometric compression ratio, and VVT could be used to lower the compression ratio by delaying the closing of the intake valve during the compression stroke. Engines with VVT have the added benefit of retained EGR, which can allow changes in temperature and exhaust residuals to induce HCCI combustion.

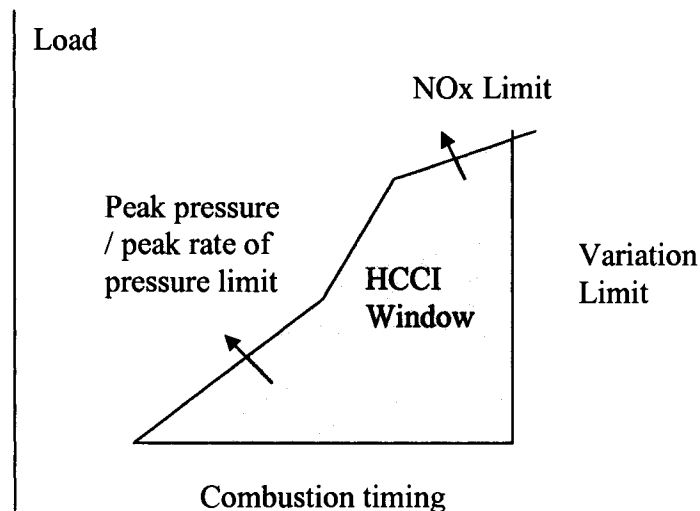


Figure 3: A schematic illustration of the operational window for an HCCI engine [18].

2.3 Equivalence Ratio

Results from a recent experimental study performed by Olsson et al. [19] have demonstrated dependence of brake mean effective pressure (BMEP) on equivalence ratio. The study is particularly important since ethanol was used along with n-heptane as the fuel. Figure 4 plots equivalence ratio versus BMEP for various engine speeds. This curve was derived from Olsson and was converted for equivalence ratio.

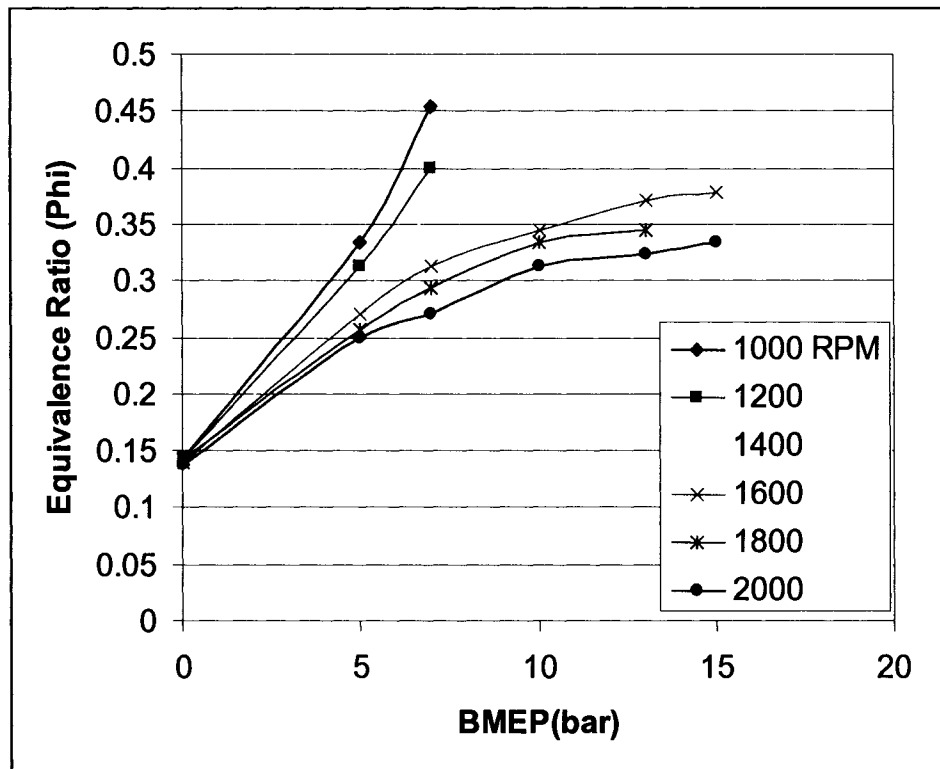


Figure 4: Equivalence ratio shown as function of load and speed [19].

For the highest engine loads the equivalence ratio approaches 0.4 to 0.5. The limiting factors here are maximum cylinder pressure (200 bar), maximum rate of pressure increase (5 bar/°CA), engine noise, and NO_x emissions. All of these factors deteriorate as the mixture gets richer.

For low loads, extremely lean mixtures are used with the equivalence ratio approaching 0.133. The study indicated that these ultra lean mixtures can be used, but the completeness of combustion deteriorates.

Another experimental study conducted by Ladommatos et al. [11] was conducted using a Ricardo Hydra engine. This study determined the satisfactory operating region of several fuels, in

particular the equivalence ratio and EGR rates were investigated for ethanol as an HCCI fuel. In practical terms, this meant recording a set of data points in a region between the richest and leanest equivalence ratios attainable, limited by engine knock (richest), and partial combustion (leanest) respectively.

Ignition timing diagram for ethanol was modified from and is presented in Figure 5.

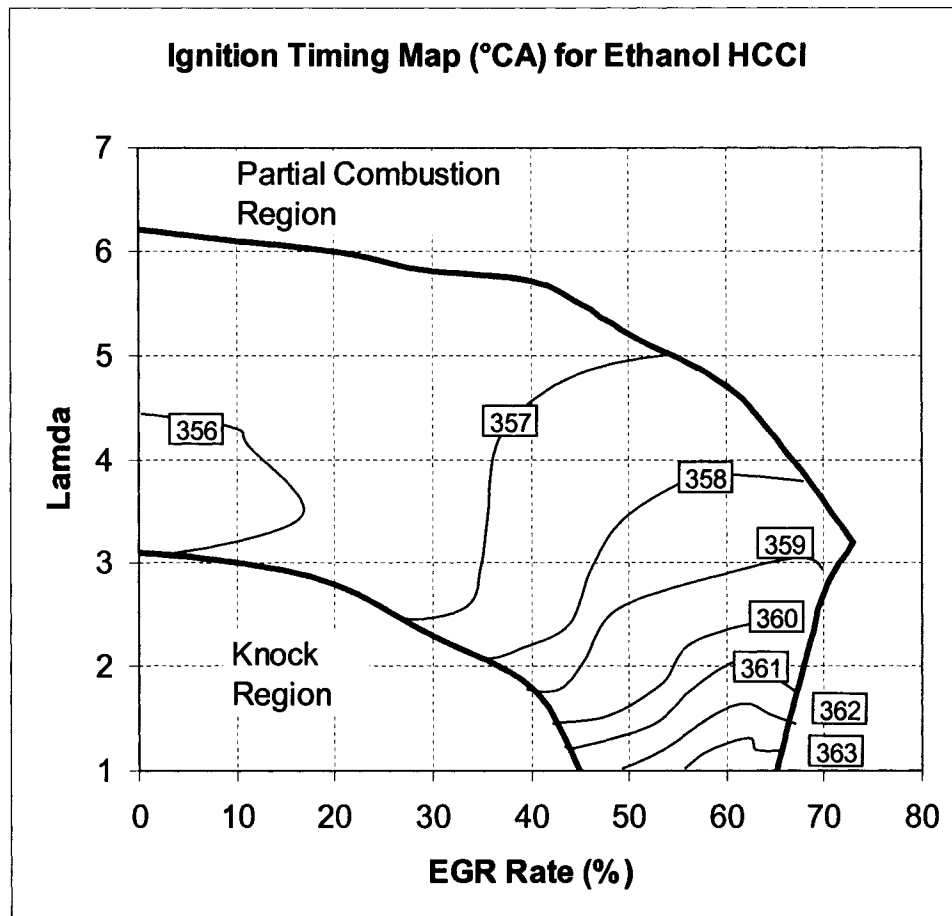


Figure 5: Ignition timing map of ethanol for various Lambda and EGR rates [11].

When the fuelling rate is increased (higher equivalence ratios/lower lambda), combustion rates also increase, eventually leading to unacceptable in-cylinder pressure rise (knock), which can lead to physical damage to the engine.

When the fuelling rate is reduced sufficiently (lower equivalence ratios/higher lambda), the combustion temperature becomes too low to fully oxidize a significant proportion of the fuel. Exhaust CO and unburned HC emissions rise rapidly in this region. At high EGR rates, ignition fails to occur in a small proportion of the cycles due to high concentrations of inert combustion

products in the mixture. Ethanol has the second largest attainable HCCI region next to methanol that has the largest HCCI region. The trends for ethanol ignition timing lie between trends observed for gasoline and methanol. Ethanol ignition timing will show some retardation with increased EGR rates. For all types of fuels tested ignition timings are relatively independent of equivalence ratio at low EGR rates. However, as EGR rate is increased beyond 40 %, ignition timing for gasoline advances under progressively leaner conditions. This is due to the presence of fewer oxygen molecules at higher EGR rates. Inert EGR gas displaces air that contains oxygen. However, for alcohols the oxidation process is less sensitive to the presence of EGR because alcohols already contain a significant portion of oxygen required for combustion.

2.4 Fuel Effects

Fuel selection is perhaps the most important aspect of HCCI engine development. The effect of fuel volatility and auto-ignition characteristics, are important factors for HCCI engine control. Epping et al. [20] demonstrated that a fuel must have a high volatility in order to easily form a homogeneous mixture. Also, fuels with single-stage ignition are less sensitive to changes in speed and load, and are better suited for HCCI, because they can ease the control requirements. The auto-ignition temperature of the fuel is also an important consideration for the optimal selection of an engine compression ratio. With fuel selection for HCCI there is a contradiction.

Selecting a HCCI fuel that is optimal for low loads will limit the range of HCCI operation at high loads. For example, if one proposes to optimize HCCI engine combustion at low loads, a low octane fuel is desired, however for high loads this fuel will exhibit extreme knocking, because of its rapid heat release rate. Additionally, even if one were to employ a dual mode strategy, SI combustion at high loads and HCCI at low loads, a low octane fuel will not prevent SI knocking at high loads. Therefore, there is a contradiction in fuelling strategy when it comes to employing HCCI with a single fuel, and there is no universal fuel that is specific to HCCI operation. The optimal fuel depends on the combustion control strategies and operating conditions [21].

As discussed by Asmus and Zhao [21], some chemical additives have the ability to inhibit or promote the heat release process of auto-ignition. Therefore, HCCI auto-ignition can be controlled by modifying the fuel, in such a way, that it is more chemically reactive or inhibitive by adding an ignition promoter or inhibitor. For a natural gas fuelled HCCI engine, even a small presence of NO_2 present in the charge may advance auto-ignition of HCCI. The use of varying NO_2 addition by injecting chemical fuel additive can be used as a means of controlling HCCI.

By using two fuels with a large reactivity difference it is possible to extend the operation range limits of an HCCI engine. Furutani et al. [22] proposed an approach to combine two different fuels with different octane numbers to enable auto-ignition timing control. The study found that an optimal combination of these two fuels could be determined for each speed and load condition. Also, it is necessary for one fuel to have as high an octane number as possible, and for the other fuel to have as low an octane number as possible. This strategy will enable the widest operating range possible for HCCI using two fuels. A similar study was conducted by Olsson et al. [19] using ethanol and n-heptane. It was found that for static engine operation the performance of the dual fuel system was sufficient, and optimization of MBT timing and low emissions was attainable for a variety of speeds and loads.

2.5 Exhaust Gas Recirculation

EGR is perhaps the most straightforward way of controlling intake charge temperature, and consequently combustion timing and duration. The main problem with EGR control is the response time may be too slow, and difficulties in handling transient conditions.

Control of recycling of burned gases can include both external EGR and internal EGR. External EGR is the more commonly understood method for recycling exhaust gases. Exhaust gases are diverted in the exhaust manifold and brought back to the intake manifold to mix with the incoming air. Internal EGR is more commonly referred to as retained exhaust gas residuals. For HCCI, the use of VVT can be used to re-open the exhaust valve during the intake stroke, thus allowing exhaust gas residuals to return to the combustion chamber and aid in the combustion process [21].

Ladomattos et. al [11] stated that EGR systems are attractive for HCCI engine operation because of three fundamental properties:

1. High temperature residuals aid auto-ignition.
2. Switching from SI to HCCI may be done in one cycle.
3. Degree of residual mixing with fresh charge may be used to control combustion timing and duration.

Figure 6a illustrates the combustion durations trends for ethanol, as modified from the same study as mentioned previously. Unlike ignition trends, combustion duration (or heat release rate) trends

are similar for all the fuels tested. At low EGR rates, combustion duration is mainly dependent on the equivalence ratio. Lean equivalence ratios reduce the heat release rate, and increases the combustion duration. As the EGR rate is increased, duration progressively becomes more dependent on EGR rate.

Trends would indicate that the onset of knock is more dependent on combustion duration than on ignition timing. For all fuels knocking seems to occur when the maximum rate of pressure rise exceeds 5 bar per °CA regardless of charge composition. This result tends to reinforce the view that the occurrence of knock is dependent on heat release rate and not on ignition timing (see Figure 6b). They also found that alcohols have a much higher tolerance for EGR, compared to gasoline fuels.

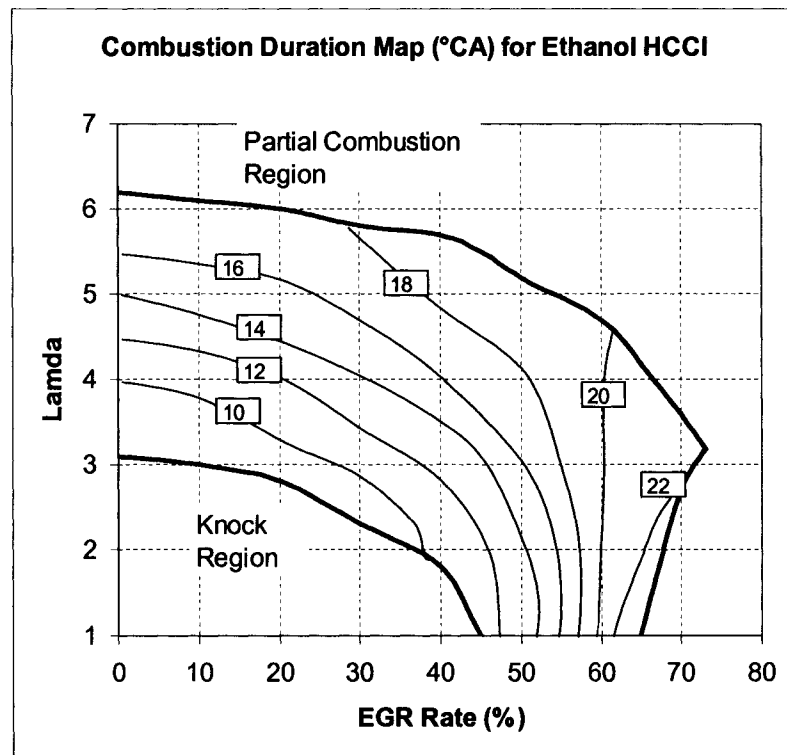


Figure 6(a) Combustion duration map (°CA).

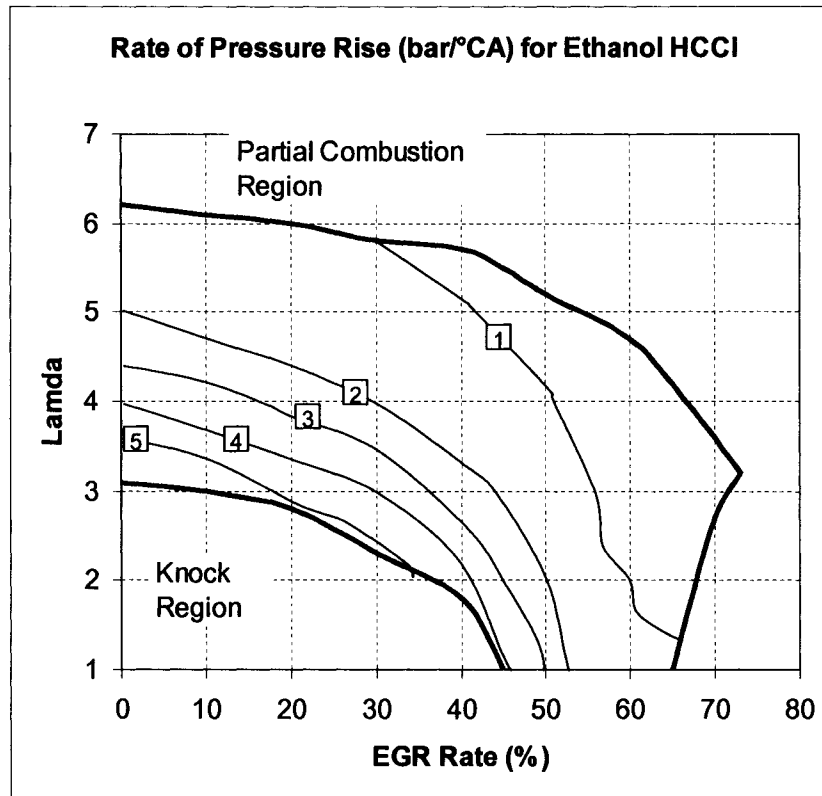


Figure 6: (a) Combustion duration map ($^{\circ}\text{CA}$), (b) pressure rise map ($\text{bar}/^{\circ}\text{CA}$) [11].

2.6 Practical HCCI Operating Range

The practical operational range of HCCI is limited to low loads and low to mid-range engine speeds. Zhou and Asmus [5] reported, at higher loads the combustion rates become excessive and the peak rates of pressure rise are too large resulting in excessive knocking. The combustion rates can be decreased by increasing EGR, using alcohol fuels, water injection and supercharging. All of these methods have shown improvements in operating range extension. Also, SI combustion with a 3-way catalytic converter has better performance than high equivalence ratio gasoline HCCI (0.7 to 0.8), so the NO_x reduction benefit of HCCI is decreased at higher loads. This limits the functional HCCI operating range.

Therefore, it seems the employment of a dual mode strategy would be the recommended course of action. For example, the engine would be used for HCCI at low loads and

switched to SI combustion at a load point where HCCI shows more challenges in combustion control and less benefit when compared to SI combustion. The same dual mode strategy for HCCI can be applied to diesel HCCI engines. For light loads, diesel HCCI can be employed to eliminate aftertreatment devices where low exhaust gas temperature make it difficult to reduce NO_x and PM emission. For high loads the diesel engine will be switched to conventional CI combustion.

2.7 Summary

A summary of the HCCI control parameter trends are listed in Table 2 below. Fuel effects will not be investigated in this project.

Table 2 Summary of HCCI control parameters as found in recent literature publications.

HCCI Control Parameter Action	Resulting Trend (for Ethanol)
Increasing intake charge temperature	<ol style="list-style-type: none"> 1) Advances auto-ignition. 2) Decreases combustion duration. 3) Increases heat release rate (HRR) 4) Extends Lean limit of auto-ignition 5) Temperature range [25-500°C]
Increasing compression ratio	<ol style="list-style-type: none"> 1) Similar as increasing charge temp. 2) Decreases intake charge temperature for auto-ignition. 3) Increases engine knock at high loads. 4) CR range [15 < CR < 25] depending on RPM, load, and Octane #. 5) Increases thermal efficiency. 6) Increases frictional losses.
Varying equivalence ratio (Φ)	<ol style="list-style-type: none"> 1) HCCI Range [Lean $0.14 < \Phi < 0.5$ Rich] 2) Increasing Φ increases load (BMEP) Increases HRR, decreases combustion duration and lowers efficiency. 3) Decreasing Φ decreases load (BMEP) Decreases HRR, increases combustion duration, and increases efficiency.

Fuel Effects	<ol style="list-style-type: none"> 1) Fuel should have high volatility. 2) Optimize low load => low octane fuel 3) Optimize high load =>high octane fuel 4) Additives can control timing 5) Dual fuel strategy to extend range 6) Dual Mode (SI & HCCI) or (CI &HCCI)
Exhaust gas recirculation (EGR)	<ol style="list-style-type: none"> 1) Decreasing EGR, combustion duration depends on Φ . 2) Increasing EGR, increases combustion duration and decreases HRR 3) Ethanol has higher tolerance for EGR than gasoline.

In summary, there are several parameters that affect the control of HCCI burn in an IC engine. Understanding how these parameters impact the point of auto-ignition, the heat release rate and combustion duration will enable us to establish design constraints for our ethanol fuelled HCCI engine. The literature review objective has been performed to identify the parameters affecting control of HCCI with respect to use of ethanol as a fuel.

3 RESEARCH APPARATUS CONCEPT DEVELOPMENT

3.1 Identification of Need

As presented in Section 2, HCCI combustion is attained by controlling; intake charge temperature, EGR rate, compression ratio and equivalence ratio. These parameters are varied to achieve auto-ignition near top-dead-center, control heat release rate and combustion duration. HCCI combustion is difficult to control due to the absence of direct control methods such as spark firing or fuel injection to determine ignition timing as in SI or CI engines. Therefore, investigation of parameters affecting control of ignition timing, and heat release rate are significant for the commercialization of this technology. An experimental apparatus for investigation of all parameters affecting control of HCCI is required to conduct research of this novel combustion phenomenon.

3.2 Background Research

Background research was performed in the literature review to identify the parameters affecting control of HCCI engines. However, this section will identify the types of devices that are currently being used by industry and institutions for investigation of HCCI. Three main categories of apparatus for experimental investigation of HCCI were identified; a rapid compression machine, a single-cylinder research engine, and a production engine converted to run on HCCI.

3.2.1 Rapid Compression Machine

Rapid compression machines (RCM) have been used to study HCCI by several researchers [23, 24]. A rapid compression machine is defined as a device that enables compression of an air fuel mixture to its auto-ignition temperature. The main use for RCM is to study the effect of fuel mixtures on auto-ignition. The RCM has been used for many years to investigate the changes in pressure and ignition properties due to HCCI and other modes of combustion.

The RCM is not a device that can be purchased readily and must be designed and fabricated by the research institution. As a result they are very costly and the quality of the experimental data is highly variable and dependent on the specific characteristics of the RCM. Additionally, the results may not give close correlation to production engine data.

3.2.2 Single Cylinder Research Engines

The single cylinder research engine (SCRE) is a device that is specifically designed for fuels and combustion research. The SCRE can be used in SI and CI modes and also with a variety of fuels. In general, SCRE have variable compression ratios and are ideal for investigation of the knock phenomenon, and auto-ignition of fuels, which also makes them ideal for HCCI research. SCRE can be purchased readily from manufacturers, and they can be fitted with optical combustion chamber access for visual and laser study of combustion. There are three main companies that manufacture single cylinder research engines; AVL, Ricardo and Corporative Fuels Research. Figure 7 shows the AVL optical research engine [25].

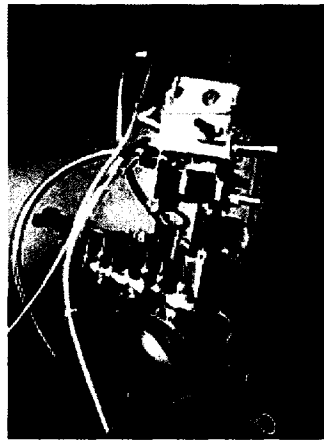


Figure 7: AVL single cylinder research engine with optical access [25].

SCRE have engine geometry similar to production engines, which allows for good prediction of production engine performance. They can be used for the several testing and research activities.

The Ricardo Hydra SCRE can come in several different bore sizes from 65mm to 110mm, and several types of valve actuation methods, including push-rod, overhead cam, and VVT [26].

The Waukesha Engine Corporation manufactures the co-operative fuel research (CFR) engine for testing the octane (RON) and cetane number (CN) of refinery fuels. The CFR engine is an SCRE that employs a VCR design, and was historically used for investigation of knock. This also makes it particularly useful for HCCI research [27].

The main disadvantage of commercially available SCRE is the cost. An SCRE is manufactured in limited quantity and therefore do not enjoy lower manufacturing costs that production engines have due to economies of scale. A quotation provided Waukesha for one of their single cylinder

research engines was for \$125,000 US dollars. This cost does not include the data acquisition system and all other systems that will be required.

3.2.3 Production Engines Converted for HCCI

There are several examples of production engines that were converted to run on HCCI mode.

Researchers at Lund Institute of Technology have converted a six cylinder Volvo heavy duty diesel engine to run on HCCI mode [12]. One of the cylinders has been converted to run on HCCI, and the other five cylinders were motored. This arrangement gives less reliable brake specific values, as the total engine friction is high compared to the output torque from the running cylinder. For this reason only the indicated cylinder results were used in their publication. The running cylinder was equipped with VCR cylinder head, thus allowing the compression ratio to be varied from 10:1 to 28:1 (see Figure 8).

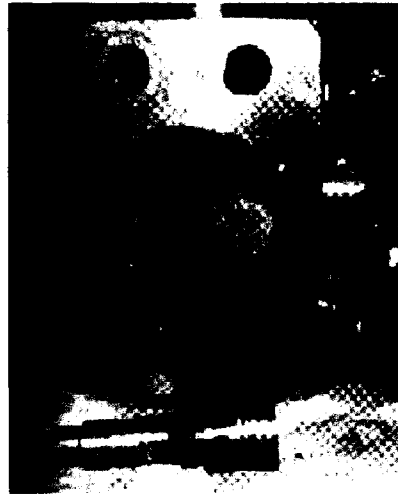


Figure 8: Lund Institute of Technology, Volvo TD100 engine modified to single cylinder HCCI mode with VCR head [12].

The advantages of this design are: the experimental results are in close agreement with production engine results, and variable compression ratio allows for a wide range of fuel experiments. The cost of implementation of this design is reasonable considering that an engine can be donated or purchased readily.

Researchers at Lawrence Livermore National Labs along with researchers at University of California Berkeley have converted a Volkswagen TDI engine to run on HCCI mode [28]. The advantage of this concept is the accurate representation of HCCI in passenger vehicle sized engines and the low cost of this type of engine setup. Volkswagen TDI engines can be purchased

for less than \$5000 dollars. However, the data acquisition system, and other system will have to be purchased and would total an estimated \$40,000 dollars. The experimental work conducted by this collaboration was focused on fundamentals of premixed HCCI combustion and on evaluation of possible techniques for engine operation and control.

In summary, production engines converted to run on HCCI mode are a good option for enabling HCCI mode for experiments. Several examples of production engines converted to run on HCCI have been reported in literature.

3.3 Problem Statement

The problem statement is defined as follows:

To design an experimental apparatus that enables investigation of parameters affecting combustion control of a HCCI engine fuelled with ethanol.

3.3.1 Project Methodology and Deliverables

The methodology employed for this project is as follows:

1. Develop a workable design concept that meets all the criteria and constraints.
2. Develop detailed design schematic drawings for all systems of the apparatus.
3. Perform design calculations for each of the systems of the apparatus.
4. Select components based on design calculations and order the necessary components.
5. Fabricate each system of the apparatus.
6. Test each system and implement improvements.
7. Complete verification experiments to ensure functionality of the apparatus.

The necessary outcomes for the apparatus are:

1. To obtain a functional apparatus that is easy to use and will allow future graduate students the ability to perform HCCI experimental engine research.
2. To have the ability to vary and hold the engine speed with little deviation.
3. To have the ability to acquire in-cylinder pressure measurements, that can be utilized to study the combustion process.

3.4 Criteria and Constraints

Development of design criteria and constraints are both very important steps of the design process. This section will review these points with respect to the design process as applied to the development of our research apparatus.

3.4.1 Criteria

The design criteria for the apparatus are; functionality, durability, manufacturability, cost effectiveness and safety.

3.4.1.1 Functionality

Functionality is defined as the ability of the apparatus to perform its intended mechanical and/or electrical design functions. The question one poses to oneself when considering functionality is;

Does this design perform all necessary design functions?

Determining the design functions is the first and most important step when considering functionality. Based on the literature review, we have identified several functional requirements to perform HCCI combustion research. However, these requirements are actual system requirements that are comprised of both mechanical and electrical components.

Firstly, the ability to vary parameters affecting HCCI combustion control will be required. As mentioned in Chapter 2 these parameters are the following; variable intake air temperature, variable compression ratio, variable equivalence ratio and variable EGR. Additionally, the ability to fix engine speed and dissipate excess power produced will be required

Secondly, the ability of the apparatus to perform data acquisition and measurement functions is also a major criterion. These functions include; high-speed data acquisition for in-cylinder pressure measurements and crank angle degrees, and the ability to perform and display engine performance calculations on in-cylinder pressure data. Additionally, low speed data acquisition and/or measurement will be required for intake air temperature, manifold absolute pressure, coolant temperature, and fuel pressure.

Lastly, a couple of less tangible functionality items are; the ease at which the apparatus can be used during experiments, and the versatility of the apparatus for future research projects.

3.4.1.2 Durability

Durability is defined as the resistance of the design to failure. The question one poses to oneself when considering durability is;

Is this design durable?

Durability can also be defined as the reliability or the robustness of the design. The design of the apparatus should be optimized for robustness. This is achieved by over-sizing critical systems and components and selecting components that are readily available to eliminate downtime. Design with durability in mind will eliminate breakage of costly components and ensure piece-of-mind.

3.4.1.3 Manufacturability

The definition of manufacturability is the ease of which the design can be fabricated. The question one poses to oneself when considering manufacturability is;

Is this design easy to manufacture?

Often designs that are optimized for ease of fabrication typically use off-the-shelf components, such as; standard size construction materials such as standard steel tubing for fixture structure or use of standard fastener sizes. Use of purchased components instead of fabricating all components will minimize the overall machine shop labour hours and ultimately cost required to fabricate the apparatus. Additionally, the capabilities of the machine shop must be taken into account when selecting a design concept as elimination of outsourcing will reduce cost and time.

3.4.1.4 Cost Effectiveness

Cost effectiveness is quite simply the minimization of cost associated with a design concept. The question one poses to oneself when considering cost effectiveness is;

Will this design be less than or meet budgetary constraints?

There are several design concepts that meet or exceed all other criteria, and are often the ideal design solution. However the cost of design and fabrication exceeds the allowable budget and this fact alone eliminates the design from future consideration. Techniques for reducing cost at the design concept phase are selection of standardized components and selecting the simplest design that meets all criteria. Often the simplest design concept is the most likely to succeed and meet budgetary constraints. This involves purchasing components as opposed to fabricating.

3.4.1.5 Safety

The definition of safety is; the state of being certain that adverse effects will not be caused by some agent under defined conditions. The question one poses to himself when considering safety is;

Is this design safe for use?

It can also be thought of as the degree of safety of the design as a complete system.

Adverse effects that are caused by machine devices are; short-term bodily injury such as, burns, cuts, contusions, electrocution. The sources of these short-term injuries are; from reciprocating parts, pinch points, projectile metal debris, heat sources, sharp edges, and electric power wires and components. Although these are termed short-term bodily injuries since they occur and are visible instantly, this does not imply that the injuries sustained by these means are for a short-term, but often the injuries are severe and result in long term effects.

Long-term injuries usually are not evident immediately upon exposure. Injuries such as nervous system damage or other physical injuries that result from exposure to hazardous materials while operating the device should be avoided when possible. These materials could be a hydrocarbon fuel such as gasoline and ethanol, exhaust products, or carcinogenic materials such as asbestos. Most safety concerns regarding a design concept can be remedied by conforming to health and safety regulations.

Care must be taken in the design of the device to prevent, and inform the operator of the potential dangers of using ethanol and experiment HCCI combustion. Unpredictable combustion events and motor run-off must be controlled. Use alcohol fuels such as ethanol of particular concern, since the flame is not easily detected in daylight, and could lead to serious injuries if proper precautions are not taken.

3.4.2 Constraints

Now that the criteria have been determined it is important to summarize the constraints on the apparatus. This section will review constraints on all the criteria mentioned above.

The most significant criterion for our apparatus is functionality. Table 3 lists the constraints on functionality. This list will be consulted when designing the apparatus along with its various systems.

The constraint of durability is difficult to quantify, but can be best addressed through common sense and experience when selecting components, and sizing systems. However there are certain factors of safety that can give us a degree of durability for critical systems. Table 4 lists the constraints for durability.

The constraints for manufacturability are mainly subject to the limitation of the capabilities of the machine shop. Therefore, for each system of the apparatus the technician should be consulted early in the design process to address concerns and limitations that the machine shop may have.

The main constraint for cost effectiveness is our project budget which is a maximum of \$35,000. To keep costs low it is important to utilize industry contacts, on-campus technical experts, and off-the-shelf components.

Safety constraints on the apparatus are mostly based on common sense and experience.

There are certain health and safety regulations that the University of Windsor has for laboratories and research apparatuses, which are governed by the Electrical Code of Canada (ECC), and the Canadian Safety Association (CSA) Standards. In particular the fuel storage limit on the device should not exceed 5 liters of flammable liquid [29].

Table 3 List of functionality constraints.

Functionality	Constrained Parameter	Constraint Range
HCCI Control	Intake Air Temperature	T_{inlet} , 0 to 300 °C
	Compression Ratio	CR, 15 to 25:1
	Equivalence Ratio	Φ , 0.0 to 1.0
	Exhaust Gas Recirculation	EGR, 0 to 80%
Engine Control	Cycle Time, (Engine Speed)	0 to 3600 RPM
	Cycle Time Deviation	Less than 1% of max.
	Power Dissipation	$P_{absorbed}$, 0 to 10 HP
	Coolant Temperature	$T_{coolant}$, 60 to 90 °C
	Intake Valve Timing	Suitable for HCCI
Fuel System	Fuel Pressure	2 to 5 bar, Nom. 3.1 bar
	Ethanol Compatibility	Components must be non-reactive with alcohols and gasoline.
EGR	% EGR Measurement	Capability required.
Data Acquisition System	Labview User Interface	Logical layout, easy to use.
	Data Acquisition Speed	1/10 th °CA at 2000 RPM
	In-Cylinder Pressure	Highly sensitive & accurate
	Crank Angle Encoder	Resolution, >1/10 th °CA
	Intake Air Thermocouple	-10 to 500 °C
	Intake Air Pressure sensor	1 to 2.5 bar
	Coolant Thermocouple	-10 to 200°C

Table 4 List of durability constraints.

Durability	Constrained Parameter	Constraint Range
Fixture	Structural Steel Fixture	Adequate sizing components selected
	Vibration Control	Minimize vibration
Engine	Combustion Chamber	Pressure, 0 to 200 bar
	Overall	Output Power, <= 25 hp
Subsystem Components	Various	Of high quality and durability

Data Acquisition System	Program Design	Prevent crashing, easy to use. Logical organization of GUI.
-------------------------	----------------	---

Additionally, all moving parts should be enclosed with safety cage, to prevent human access while in operation. A certified electrician in accordance with ECC will perform the high-voltage electrical wiring. The device shall also be subject to an inspection by a CSA inspector. All other low voltage wiring shall be wired in a safe manner and enclosed in wiring loom where possible. The fuel pump shall have its own power off switch to cut fuel to the apparatus. The engine shall be able to stop from and engine speed of 3600 RPM to 0 RPM within 16 seconds in the case of emergency. The apparatus shall be constructed of materials that are not combustible [29].

3.5 Ideation and Invention

The purpose of this section is to develop the design concepts. In the background research section 3.2, three options were identified for an HCCI experimental apparatus. In this section we will compare two of these concepts namely; rapid compression machines and production engine conversions, as well as introduce a third concept for our HCCI apparatus.

3.5.1 Concept One: Rapid Compression Machine

Rapid compression machine is a device that performs a compression and expansion process in an optical combustion chamber. Similar to a single cylinder engine except only compression is performed. A typical example of a RCM, shown in Figure 9, uses a pneumatic or hydraulic cylinder would to drive the combustion piston upwards. This would compress the mixture and initiate auto-ignition of the homogeneous mixture.

The advantage of Concept One is that it can be customized for any desired application, since all the components are designed and fabricated by the researcher. However the disadvantages of this concept are numerous; potentially high manufacturing costs, excessive design and fabrication time required and questionable durability. Additionally the device can only perform one cycle at a time due to its design, also quality of results is questionable, and it is also not an accurate representation of a real engine since previous cycle effects are not taken into account.

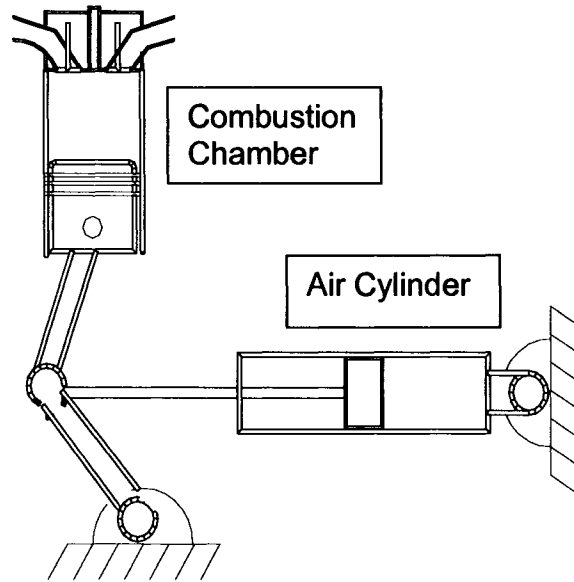


Figure 9: Concept One, rapid compression machine.

3.5.2 Concept Two: Engine with Dynamometer

The second concept studied was an engine with a dynamometer. This concept consists of a 3-cylinder Kubota D905 diesel production engine as the base engine (see Figure 10a), and a Land and Sea #200 eddy current brake as the dynamometer (see Figure 10b).



Figure 10: (a) 3-cylinder Kubota D905 diesel engine, (b) eddy current dynamometer [30].

To simplify and stabilize the operation of this concept, only one of the cylinders is to be converted to run on HCCI mode with ethanol as the fuel, whereas the other two cylinders would be fueled with the original equipment manufacturer (OEM) diesel system (see Figure 11.)

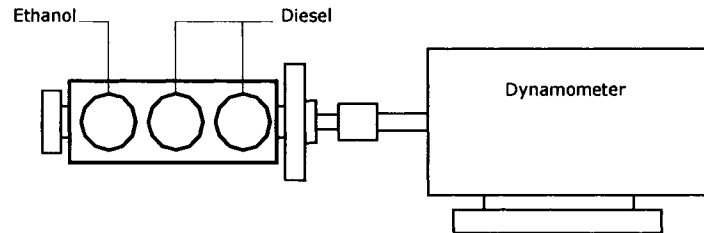


Figure 11: Concept Two: Engine with Dynamometer.

The appropriate dynamometer was sized and quoted to cost \$14,245 USD [31]. The dynamometer will dissipate power and hold the engine at fixed speed.

The advantages of Concept Two are as follows: easy to manufacture, (since all major components can be purchased,) safe and proven design, and the concept has the capability to realize the entire engine cycle. Also, Concept Two allows for the accurate representation of HCCI on an actual production engine, which means that the experimental results obtained will be of higher quality than with RCM.

There are some disadvantages of Concept Two. A water brake dynamometer cannot be used, since they have difficulty holding engine fixed at lower RPM. Research has shown that water brake dynamometers are better suited to higher RPM engines. An eddy-current dynamometer would be better suited to sustaining lower RPM; however the cost is substantially approximately \$20000 CDN. Also ensuring HCCI timing is in correct synchronization with diesel combustion timing in other two cylinders could prove to be difficult.

3.5.3 Single Cylinder HCCI Engine with AC Motor and VSD

Concept Three consists of a Kubota D905 engine converted to single cylinder HCCI research engine. It uses an AC motor with a variable speed drive (VSD) to motor the engine at the desired speed (see Figure 12).

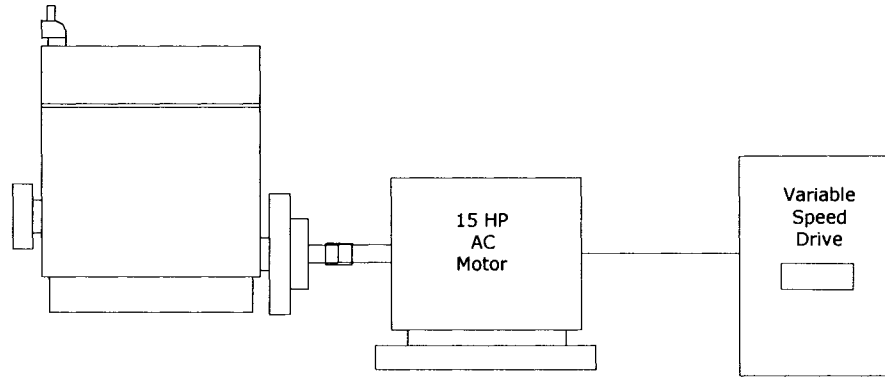


Figure 12: Single-cylinder HCCI engine with AC motor and variable speed drive.

One cylinder is enabled for HCCI experiments, whereas the other two would be disabled. The power developed by one cylinder would not be sufficient enough to warrant the use of a dynamometer. The VSD system would have an additional resistor brake to dissipate engine power and act as an engine brake. VSD is used to vary the frequency supplied to the AC motor, which alters the AC motor speed, and can fix the engine speed to the desired RPM.

The advantages of this concept are: ease of manufacture, safety and durability. All components can be purchased, which reduces fabrication time. The AC motor with VSD can hold a fixed RPM and the addition of resistor bank can dissipate up to 20 HP.

The main disadvantage of this concept is the high cost. A VSD costs \$12000, and a chopper/resistor bank costs \$5000, plus \$2000 for an AC motor totaling \$19000 CDN. Although this is less than our budgetary limit this leaves only \$16000 for the engine and all other systems and fabrication.

The solution was to contact Alen Bradley and ask if they could provide any assistance with the purchase of the VSD. Alen Bradley said they would donate a VSD that would suit our application (saving \$12000). Also Waffles Electric agreed to donate an AC motor (saving \$2000). However, we still needed to purchase the resistor/chopper bank, engine and all other systems along with fabrication costs.

3.6 Selection

A ranking system, shown in Table 5, was utilized to compare the three concepts and to provide a rationale for the selection of the concept for further development. All three of the concepts were compared against the selection criteria and the results are presented in Table 6.

Table 5 Legend, Description of ranking system utilized to compare concepts to criteria.

















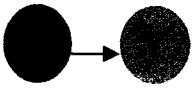

Legend	 Red light	 Yellow light	 Green light
	-cannot proceed -not feasible	-proceed with caution	-proceed -feasible

Table 6 Concept Selection Matrix

Concept	Functionality	Durability	Manufacturability	Cost Effectiveness	Safety
One RCM					
Two Engine w/Dyno					
Three Engine AC w/VSD					

For the criteria of functionality both Concept Two and Three would enable accurate representation of combustion in a production engine and therefore received a “green light” ranking. Whereas Concept One RCM would not be able to provide a realistic representation of a production engine, however could simulate the compression process easily. Therefore Concept One was given a “red light” rating.

For the criteria of durability, both Concept Two and Three received a “green light” rating on the basis of robustness, because a production diesel engine would be utilized as the combustion

apparatus. The Kubota D905E production diesel engine is already designed to handle high compression ratios (22:1) similar to what would be required for an HCCI engine and therefore would be a reasonable choice for this application. On the other hand, Concept One will require design and fabrication of the combustion chamber. This is a difficult endeavour and perhaps out of scope for a Master's project. This combustion chamber would have to withstand the pressures experienced in an HCCI engine close to 150 bar [12]. The design of such a combustion chamber requires expertise in several different areas. This knowledge is lacking in our research group, and therefore it would be wise to opt to purchase a proven, existing design, such as a production diesel engine chosen for Concept Two and Three. Therefore, Concept One is seen as feasible yet difficult and as such received a "yellow light" ranking.

For the criteria of manufacturability, Concept Two and Three utilize off-the-shelf components and as such reduce the fabrication time and costs required, whereas Concept One requires fabrication of all components. Fabrication costs are hard to predict for this type of design, and any minor setbacks can quickly turn into serious problems with excessively high costs and delays. Therefore, Concept One was ranked as "red light" because of the high uncertainty of manufacturing feasibility and expenses.

For the criteria of cost effectiveness, Concept One received a ranking of "yellow light" due to the uncertain manufacturing costs expected. Concept Two (engine with dyno) was also given a "red light" because the high cost of an eddy current dynamometer (quoted at \$20000). Also Concept Three (engine with VSD) was originally ranked a "yellow light" because the high cost of the VSD (quoted at \$12000), but because of a generous equipment donation from Alen Bradley and Waffles Electric, we were able to change the ranking to "green light".

For the criteria of safety, all designs would employ safety measures to prevent injury to the operator of the apparatus, and ensure compliance with health and safety regulations. Since these safety aspects could be designed into each design without much difficulty, all the concepts received a "green light" ranking. Therefore, on the basis of all the criteria and rankings Concept Three (engine with AC motor and variable speed drive), was selected as the most feasible design concept. A detailed design of this concept will be described in Section 4 of this report.

4 DETAILED DESIGN

In this section, the development of the detailed design for the research engine is reported. This section shows the schematics, determines, and solves the critical design element for each major system, along with performing component selection. Minor systems will also be identified and components for these systems are selected.

4.1 Schematic of Research Engine

To develop the initial concept schematic of our research engine it was necessary to consider the criteria and constraints mentioned in Chapter 3. Concept Three outlined a production engine, namely the Kubota D905 and an AC motor with VSD. These two sub-systems are considered to be the foundation to which all other systems are sized and fitted accordingly. Figure 13 illustrates the initial concept schematic.

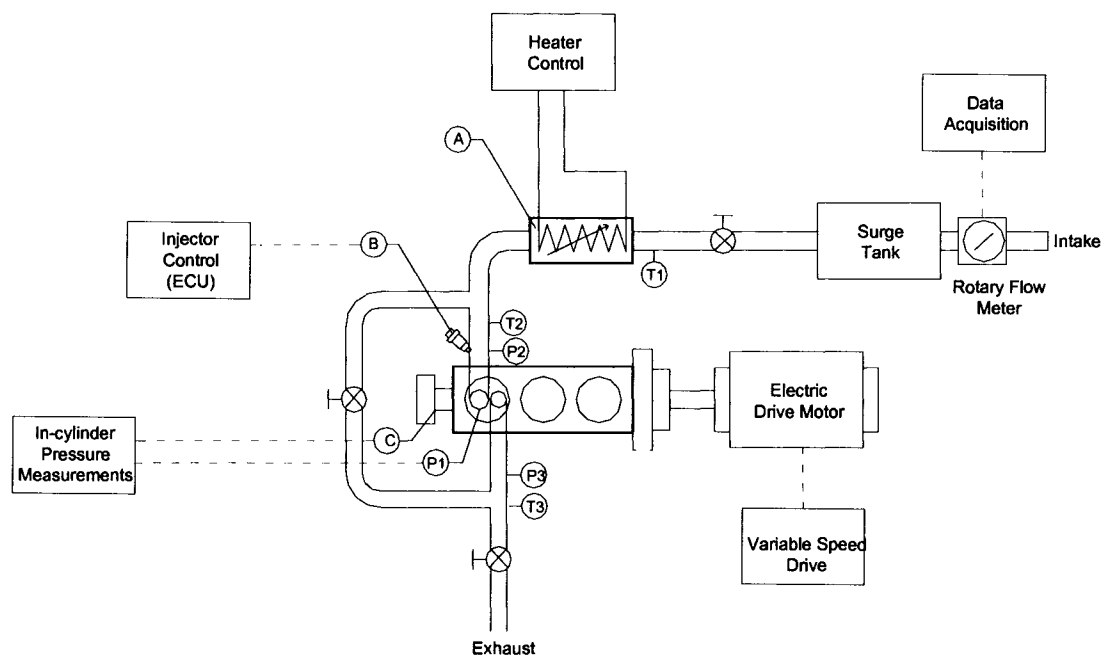


Figure 13: Overall schematic of apparatus.

Note the various other sub-systems in the schematic. The ethanol fuelling system (B) is comprised of a delivery and control system. The intake charge heater system (A) also contains the heater control system. The EGR system is comprised of the EGR valve and EGR measurement system. These three systems were developed and incorporated into the design of the intake system. The ECU system along with the data acquisition system (DAQ) was also selected and

developed. The DAQ system has the capability of providing in-cylinder pressure measurements, air flow measurements, as well as crank shaft encoder reading and several temperature thermocouples located at various points of interest.

4.2 Research Engine Selection and Conversion

In this section, the research engine will be selected and design for conversion to an HCCI engine will be performed.

4.2.1 Engine Selection

The starting point of our design is selecting a suitable base engine. Our objective for the base engine is to provide a durable, functional, low cost and safe engine for performing HCCI combustion experiments.

Listed below are the two major design constraints for the research engine:

1. To keep size and cost down, the engine shall have less than 18.6 kW (25 HP) of output power.
2. Engine shall have a combustion chamber design pressure not exceeding 18 MPa (180 bar).

The selection the base engine has satisfied these constraints. The Kubota D905 is a 3-cylinder engine that has 18.5 kW (24.8 HP) at 3600 RPM and 5.5 kgf.m (42 ft.lbs) of torque at 2400 RPM when fuelled with diesel [32]. The specifications are summarized in Table 7, while full details are available in Appendix A. This engine is commonly found in Kubota lawn trackers and was designed for reliability, durability and fuel efficiency. Since the engine has less than 25 HP in gross output power the first constraint has been met.

To meet the chamber design pressure constraint we require some assumptions and insight into the problem. The Kubota D905 has a compression ratio of 22 to 1. The factory specification for a compression pressure is 3233.6 kPa [33]. The combustion pressure was estimated to be fifty percent of the compression pressure 1616.8 kPa. Adding 1616.8 to 3233.6 results in a total pressure (p_t) 4850.5 kPa on the system. The total pressure is then multiplied by the factor of safety to get the loss of function pressure (p_{lf}) or design pressure. See Appendix B.2 for further detail.

Table 7 Kubota D905 Specifications [33].

Engine Type	Vertical 4-cycle liquid cooled diesel
Number of cylinders	3
Bore & Stroke [mm (in)]	72.0 X 73.6 (2.83 X 2.90)
Total Displacement [L (cu.in)]	0.898 (54.8)
Output Power Net Continuous [kW (HP)]	13.0 (17.4) @ 3000 rpm 15.2 (20.4) @ 3600 rpm
No load high idling speed	3800
No load low idling speed	800
Direction of Rotation	Counter-clockwise (from flywheel side)
Dry Weight [kg (lbs)]	110.0 (242.5)

The factor of safety is determined from Shigley and Mischke [34] to be between 3.0 and 4.0 for uncertain loads, uncertain stress and uncertain environment but with better known materials, such as in our case. It was assumed that Kubota uses a factor of safety (n_d) of 4.0, since this is the upper value for the range. Using the Philon Factor of Safety Method given by the following equation:

$$p_{lf} = n_d \times p_t, \quad \text{Equation 1}$$

Loss of function pressure (p_{lf}) is calculated to be 19402 kPa or 194.2 bar. Since this is greater than our chamber design pressure (180 bar) it can be concluded that the Kubota D905 engine has met the constraint for chamber design pressure, and is sufficient for our purposes. Figure 14 shows the Kubota D905 as the base engine for our HCCI research apparatus. The Kubota D905 was purchased with a discount from Kubota Canada.



Figure 14: Kubota D905 base engine, to be converted to single cylinder engine.

4.2.2 Engine Conversion for HCCI

Conversion of the Kubota D905 engine to single cylinder operation required some major and minor modifications. Listed below are the two major design constraints for the research engine:

1. Engine shall have the ability to maintain the operating temperature of 75°C.
2. Engine shall have variable compression ratio 15 to 25:1.

The cooling system consists of the following components; radiator, water pump, suction fan, thermostat, cylinder head and cylinder block as shown in Figure 15 below. The cooling system functions in the following manner. At temperatures lower than 71 °C, the thermostat is closed and the coolant circulates in the engine through the water return pipe without running to the radiator. When the temperature of the coolant exceeds 71 °C the thermostat begins to open and the cooling water is sent to the radiator.

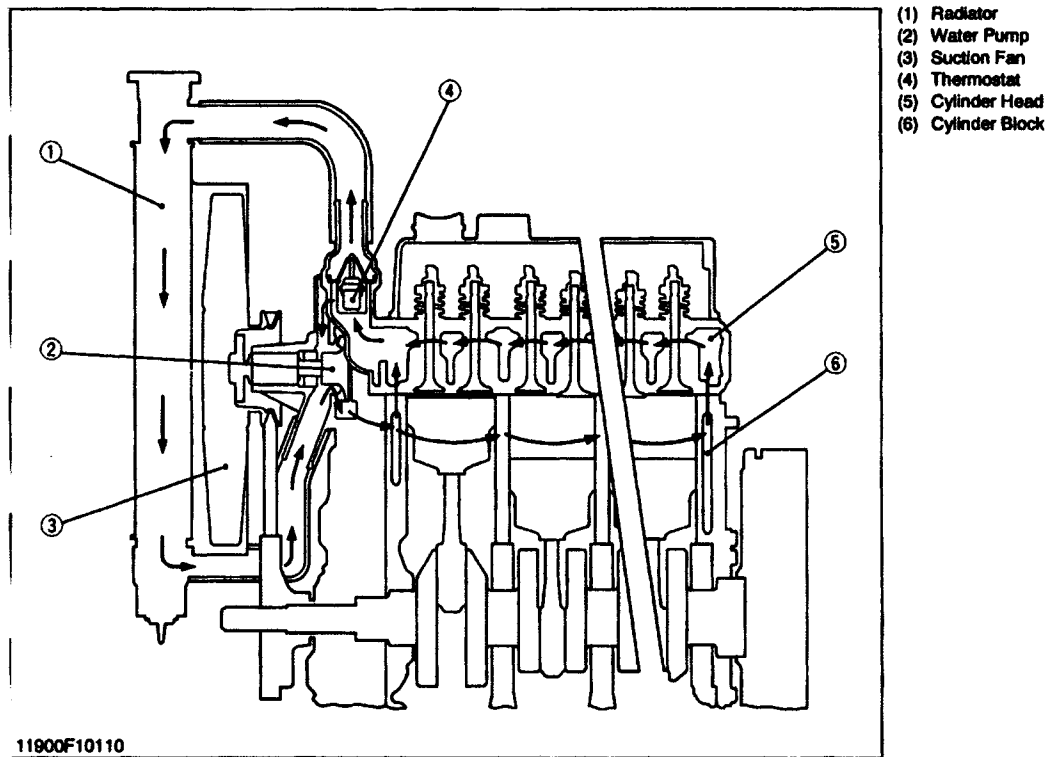


Figure 15: Cooling system schematic for Kubota D905 [33].

This hot coolant flows to the radiator and is subsequently cooled to below 71 °C and returns to the bottom of the engine and flows through the cylinder head to absorb heat again [33].

The cooling system attempts to maintain the engine coolant temperature within a factory determined design range, for example 71 to 90 °C (Appendix B.3). This meets our design constraint of having the engine operating temperature at 75 °C.

This temperature range shall be suitable for HCCI operation but is yet to be determined for our specific setup. However, the proposed design calls for only one cylinder to be enabled as the test cylinder for combustion, thus our cooling system will most likely have a greater capacity for heat dissipation than it will require. Furthermore, the cooling system will have some difficulty getting to the desired operating temperature of 75 °C, since there is less heat being transferred from the combustion chamber to the cooling system.

The proposed solution required assembly of the cooling system as Kubota had proposed in Figure 15 except the suction fan (3) needed to be removed and mounted at the front of the engine and replaced with a stand alone floor fan. The purpose of the suction fan was to draw air across the radiator fins (1) and hence cool the engine. This fan is connected to the water pump flange and powered by the crankshaft pulley. Therefore, the fan speed or cooling rate is proportional to the speed of the engine. Removal of the suction fan limits the amount of heat that can be removed from the cooling system. During testing, if the engine requires additional heat removal, the floor fan can be turned on to accommodate this.

For our engine heat is only being generated from one cylinder and thus will take longer for the engine to reach operating temperature of 75 °C. Therefore, an engine block heater shall be installed in the engine block. Kubota supplied a 1200 W engine block heater that is used in mainly in cold weather climates. The engine block heater is plugged into a standard 120 V wall outlet to maintain the engine coolant temperature warm enough to enable faster more reliable cold starting.

To facilitate ease of use, it is desirable to reach the operating temperature from room temperature as quickly as possible, or at least estimate the amount of time required to reach operating temperature. A calculation was performed to estimate the warm up time, assuming the system is at room temperature of 18°C, and a fixed coolant volume of 4.73 L, and contains a 50/50 mixture of ethylene glycol and water solution with a specific heat of 3.338 kJ / kg.K [35]. The result indicated that it would take approximately 110 seconds to warm up the coolant engine from room temperature to operating temperature. See Appendix B.4 for further detail.

4.2.3 Variable Compression Ratio Options

As mentioned earlier, there are several methods for attaining variable compression ratio. However, at this stage, the base engine for our apparatus has already been specified and only two methods are available to us. Both options involve varying the clearance volume of the combustion chamber. The first option is variation of head gasket thickness, and the second option is variation of clearance volume with secondary piston.

The first option employed the Kubota D905 cylinder head with some modifications, and required the machining of 5 different thickness copper head gaskets. Decreasing the clearance volume of the cylinder increases the compression ratio of the engine. So for a compression ratio of 15 we have a gasket thickness of 3.04 mm and for a CR of 25 we have a thickness of 0.853 mm, (see Table 8 for a summary.) Detailed calculations are presented in Appendix B.5, and B.6.

Table 8 Compression ratio and corresponding head gasket thickness required.

CR	Thickness (mm)	Thickness (inch)
15	3.041	0.120
17	2.384	0.094
20	1.659	0.065
23	1.290	0.051
25	0.853	0.034

The compression of the head gasket material was not taken into account in the calculation of the head gasket thickness as it was assumed to be not significant factor. Figure 16 illustrates the template of the head gasket for the Kubota D905 engine. The AutoCAD template file could be emailed to Gasket Works [36]. Gasket Works could laser cut the desired gasket using our AutoCAD template file. The procedure for changing the compression ratio would be as follows; the cylinder head of the engine is removed and the new head gasket is installed, after which the cylinder head is replaced and tightened according to specifications listed in Appendix A.5.

Option 1 would be easier to implement since the factory cylinder head could be used, with little or no modification. The head gaskets could be rather easily fabricated. However, the replacement of the head gaskets could prove to be inconvenient. Option 2 for varying compression ratio is to modify the Kubota D905 cylinder by installing a secondary piston. The position of the secondary

piston is variable and thus the compression ratio of the engine could be changed with little effort and no removal of the cylinder head.

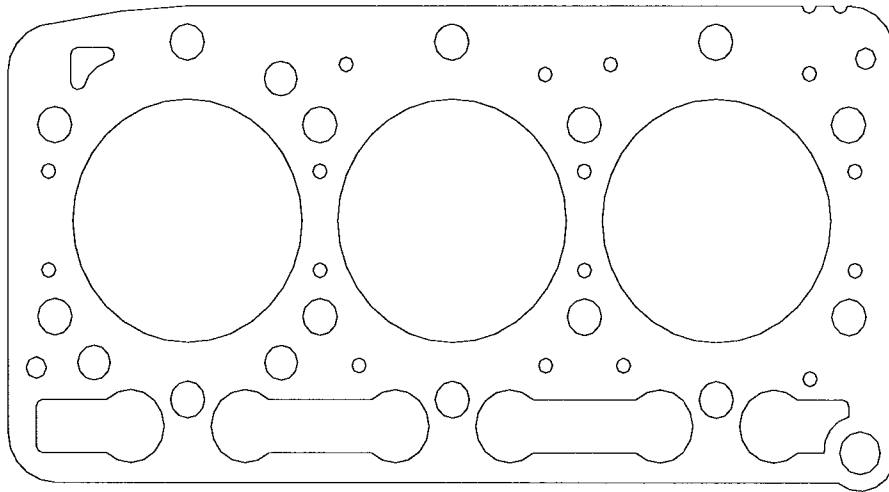


Figure 16: AutoCAD Template of Kubota D905 head gasket.

This type of cylinder head was already illustrated in Figure 8 of the background research section 3.2.3. The realization of Option 2 will require fabrication of the secondary piston and some modifications to the cylinder head.

The Kubota D905 engine is an indirect injection (IDI) type engine. An IDI engine is known for injection of fuel into a small pre-chamber in the cylinder head before it is drawn into the main combustion chamber. Figure 17 illustrates the cross section of the pre-chamber assembly for the Kubota D905 cylinder head.

For Option 2 the fuel injector (4) would be removed and replaced with a secondary piston and the glow plug (5) would be removed and replaced with a machined plug. The position of the secondary piston could be varied with spacers, and this would vary the compression ratio. The diameter of the secondary piston (D_{sp}) is 1.732 cm and is equal to the diameter of the fuel injector. The fuel injector bore would have to be machined all the way through to accommodate the travel of the secondary piston. The volume of the pre-chamber was measured before the injector and glow plug were removed and found to be 9 cm^3 (shown in Table 9). This volume is suitable for higher compression ratios 22 to 25:1, however for lower compression ratios the cylinder head pre-chamber would have to be machined to allow for an increase in clearance volume from 9 cm^3 to 16.1 cm^3 (shown in Table 8).

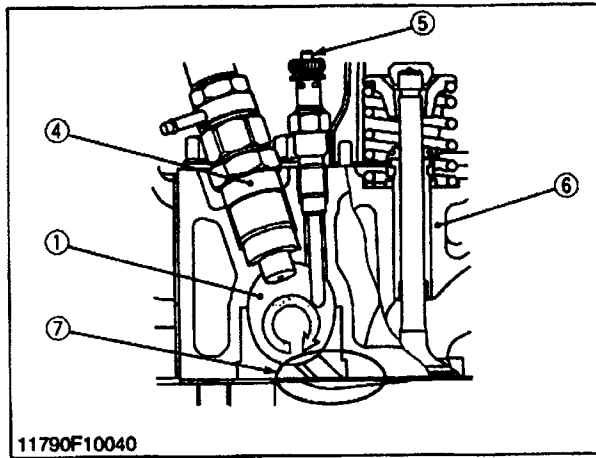


Figure 17: Cross-sectional view of Kubota D905 cylinder head pre chamber [33].

Compression ratio on a single cylinder basis is defined as:

$$CR = \frac{V_t}{V_c} = \frac{(V_c + V_s)}{V_c}, \quad \text{Equation 2}$$

Where the total volume (V_t) is the volume above the piston when the piston is at BDC and the clearance volume (V_c) is the volume above the piston at when the piston is at TDC [37].

Appendix B.7 contains further details of the calculations, and Table 9 and 10 summarize the results.

Table 9 VCR Low CR Secondary piston plunge depth and clearance volume (per cylinder).

Compression Ratio (CR):1	Clearance Volume (V_c) [cm^3]	Piston Plunge (L_s) [cm]
15	21.38	0.000
17	18.71	1.134
19	16.63	2.017

Table 10 VCR High CR Secondary piston plunge depth and clearance volume (per cylinder basis).

Compression Ratio (CR) :1	Clearance Volume (V_c) [cm^3]	Piston Plunge (L_s) [cm]
22	14.25	0.000
25	12.47	0.756

Option 2 was chosen over Option 1 for variation of the CR. The main reason for this decision was cost, as machining of the copper head gaskets was estimated to be more expensive than the machining of the secondary piston. Also, the time required to change the head gasket will be longer than the time required for the secondary piston spacer.

The Kubota D905 engine required conversion from three-cylinder diesel to a single cylinder test engine to study HCCI mode of combustion. To accomplish the conversion two cylinders were disabled from firing. This was accomplished by removal of the intake and exhaust valves from the disabled chambers, as well as removal of the corresponding pushrods for these valves. This allowed the two disabled combustion chambers to “breathe” without combustion, and any of the corresponding forces. Additionally, the cylinder head required installation of an in-cylinder pressure transducer. The pressure transducer is integrated with the secondary piston of the VCR mechanism. The prototype of the secondary piston with pressure transducer will be discussed in further detail in Section 5.

In conclusion, the selection and conversion of the Kubota D905 engine for single cylinder operation has met all design constraints.

4.3 Drive System Design and Component Selection

The development of the drive system is a significant portion of the project. The drive system is the physical means by which we can motor our Kubota single cylinder research engine. The objective for the drive system is to provide a durable, functional and safe drive and braking system.

Listed below are the four major constraints for the drive system of our apparatus:

1. Drive system shall be able to motor the engine as well as dissipate up to a maximum of 7.46 kW (10 HP).
2. Drive system shall be able to motor our base engine at a fixed RPM between (0-3600 RPM) with less than 1% variation.
3. The coupling shafts and coupler shall have a factor of safety of 4.5.

A schematic of the proposed system is shown in Figure 18. To meet the first constraint, correct sizing of the AC motor is required. The AC motor is required to develop torque as well as absorb

torque. Figure 19 illustrates the four quadrants in which a dynamometer may be required to operate. Most engine testing takes place in the first quadrant if we consider the engine running anticlockwise when viewed from the flywheel end (as is the case for the Kubota D905). In the first quadrant the engine is running and the dynamometer will be absorbing torque only.

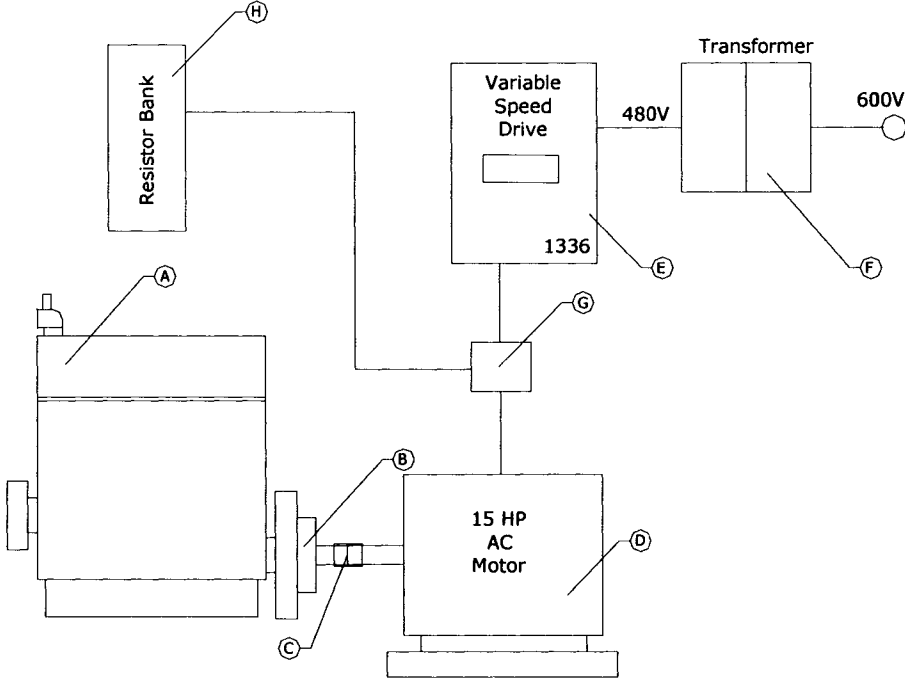


Figure 18: Proposed drive system.

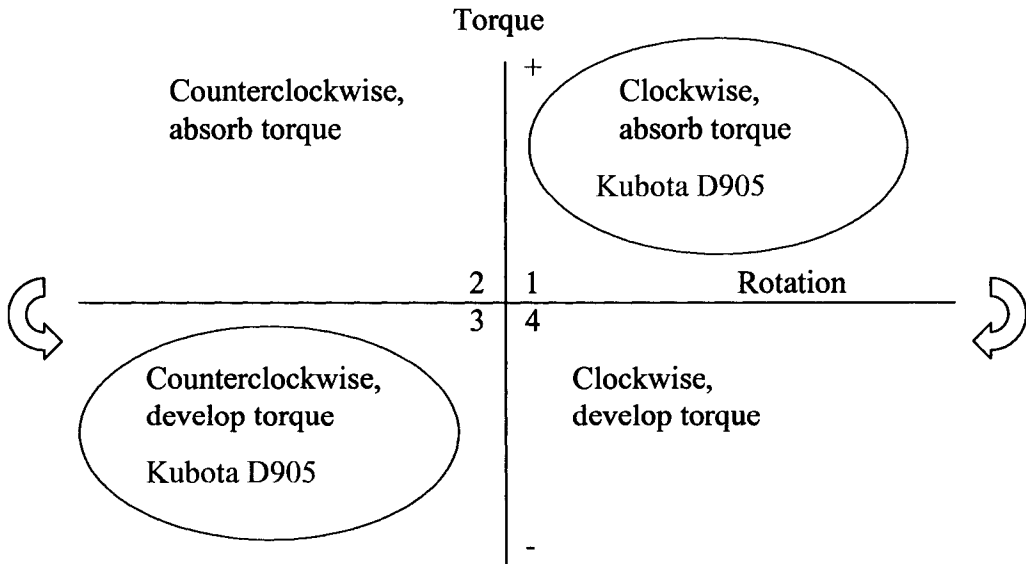


Figure 19: Dynamometer operating quadrants [38].

For this design, a dynamometer is required that can both absorb torque in the clockwise direction (quadrant 1) and also develop torque in the counter-clockwise direction (quadrant 3) [38]. A regular water-brake or hydraulic dynamometer cannot perform both of these functions. AC or DC machines are the only two choices available when operating in the third or fourth quadrants, as is the case in our setup.

4.3.1 Sizing of the AC Motor for Motoring

Motoring of an engine is defined as the rotation of the research engine without the occurrence of combustion. The combustion chamber is sealed and is being prepared for fuel and air mixture. The Kubota D905 has a maximum gross intermittent torque (τ_{gross}) of 5.5 kgf.m (42 ft-lbs) at 2200 RPM (see Appendix A.1 for motor details.) Plint and Martyr [38] suggest that the amount of motoring torque required (τ_{req}) to rotate an engine seldom exceeds 30 percent at steady state operation and that this motoring torque is directly related to the friction losses of the engine. Thus, the amount of torque required (τ_{req}) from the electric motor to drive the Kubota engine is 30 percent of 5.5 kgf.m (42 ft-lbs) which equals 1.65 kgf.m (12.6 ft-lbs), (the detailed calculations are available in Appendix D.1.) Therefore an electric motor that can supply greater than 1.65 kgf.m 12.6 ft-lbs of torque will be adequate for motoring of the Kubota D905. Review of several electric motors indicated that the best alternative for this design is an AC motor. The main reason was availability of second-hand AC motors, and the relatively small cost and size when compared to a DC motor.

The subject AC motor is manufactured by Emerson Electric and is a US Motors model H15E1D. The US Motors model H15E1D can supply a torque (τ_{sup}) at 3.07 kgf.m (22.2 ft-lbs), (see Appendix C.1 for AC motor specifications.) Since the supplied torque is greater than the required torque, the H15E1D would sufficiently meet the functionality constraint for motoring.

4.3.2 Feasibility of the AC Motor for Starting

In order to verify the feasibility of the H15E1D AC motor for starting torque, an approximation of the required flywheel torque to turn the Kubota engine over needs to be determined. The existing OEM Kubota starter has more than adequate starting torque (by default) for starting operation of all three cylinders of the Kubota D905 Engine. A calculation based on the existing starter performance can be used to determine the torque required on the flywheel. Kubota Canada supplied the starter performance data for a 1.4 kW Kubota starter. An estimate of performance of the 1 kW starter was conducted by interpolating specifications for a 1.4 kW Kubota starter (see

Appendix D.3 for detailed calculations). The starting torque required to start the engine is 10.5 kgfm (75.953 ft-lbs,) for three-cylinder operation. Since one cylinder of our engine is under compression dividing by three to get a rough estimate of starting torque yields 3.50 kgf.m (25.32 ft-lbs), which is the required starting torque for one cylinder.

The maximum amount of motoring torque that the H15E1D AC motor can provide is 3.07 kgf.m (22.2 ft-lbs). Since, the estimated starting torque of the single-cylinder operation Kubota is 3.50 kgf.m (25.32 ft-lbs) the AC motor cannot provide enough torque on its own for starting. This could have been grounds for eliminating the H15E1D AC motor for use with our engine, since the AC motor has insufficient torque for starting (turning over the engine under compression). However, the H15E1D AC motor has sufficient torque for motoring once it is turned over, and only needed assistance during starting. The 1 kW Kubota starter motor was utilized to assist the AC motor in starting the Kubota Engine. This provided the required torque for starting the Kubota engine. Once the Kubota engine is started (by the starter) and is undergoing motoring by the AC Motor the starter motor can be disengaged. At this point the single cylinder engine will be motored (with compression) solely by the AC motor. And the HCCI experiments can commence.

Therefore, with assistance of 1 kW starter motor, the US Motors H15E1D can satisfactorily meet the design constraints.

4.3.3 Sizing of the Resistor Banks for Braking of the Drive system

The H15E1D AC motor, by itself, cannot act as an engine brake for the single-cylinder Kubota D905. However with the addition of the chopper module and resistor bank, the excess torque produced by the Kubota D905 can be absorbed and dissipated by means of a resistor bank. To dissipate power, a chopper module is installed between the VSD and the AC motor (see Figure 18.) When the research engine begins to develop power this transmits back to the AC motor, and begins to induce reverse-current in the motor windings. (Basically, the AC electric motor begins to act as an AC generator, which is harmful to our circuit.) At this point the chopper module will interrupt the electrical connection from the VSD controller to the resistor bank, where the excess electrical power can be dissipated. This serves the purpose of braking the research engine as well as protecting the VSD from back-current induced damage.

The resistor bank is sized by determining both the total resistance value (R_{db1}) and the power absorption capacity (P_{avg}). The governing dynamics of the system involve dissipation of the rotational energy at 3600 RPM to a full stop (0 RPM).

The H15E1D AC motor and the Kubota D905 engine are coupled together and have a total rotational inertia (J_T) of 1.852 kg-m², (see Appendix D.2 for detailed calculations.) A typical cycle was developed that represents a high load factor on the resistor banks. The engine is accelerated to its maximum 3600 RPM in 4 seconds, followed by motoring the engine for 30 seconds, and then decelerating from maximum RPM 16 seconds. The total cycle time is 50 seconds.

As mention earlier, the maximum rated speed of the system is 3600 RPM and must be decelerated to 0 rpm in 16 seconds to meet the design constraint. The necessary values are determined and the peak braking power (P_b) is calculated using the following equation obtained from Alen Bradley sizing chart [39]:

$$P_b = \frac{J_T[\omega_b(\omega_b - \omega_o)]}{(t_3 - t_2)}, \quad \text{Equation 3}$$

Where:

J_T is the total rotational inertia of the system (1.822 kg-m²).

ω_b is the maximum speed (3600 RPM).

ω_o is the minimum speed (0 RPM).

t_3-t_2 is the deceleration time (16 seconds).

The peak braking power was calculated to be 16.455 kW. The rated power for the AC Motor is 15 HP or 11.19 kW. The peak braking power should be less than 1.5 times the rated power of the AC motor. This is to prevent current overloads on the system. Note that 1.5 multiplied by 11.10 kW equals 16.785 kW, and our peak braking power is slightly less than this at 16.455 kW. The average braking power (P_{avg}) that must be dissipated by the resistor is calculated using:

$$P_{avg} = \left[\frac{(t_3 - t_2)}{t_4} \right] \times \frac{P_b}{2} \times \left[\frac{(\omega_b - \omega_o)}{\omega_b} \right], \quad \text{Equation 4}$$

Note that the average braking power 2.633 kW is less than the peak braking power 16.455 kW.

The maximum braking resistance value (R_{db1}) is calculated using the following equation:

$$R_{db1} = \frac{0.9 \times (V_d)^2}{P_b}, \quad \text{Equation 5}$$

Where,

R_{db1} = Maximum allowable value for the dynamic braking resistor (W).

V_d = DC bus voltage, the chopper module regulates to 750 VDC.

P_b = Peak braking power calculated in earlier (W).

The resistance value is calculated to be 30.76 Ω . Therefore, the selection of the dynamic braking resistance value should be less than $R_{db1} = 30.76 \Omega$. A value greater than 30.76 Ω will trip the DC bus over-voltage.

A resistor was selected from IPC Resistors Inc. that meets the following constraints:

1. A resistance value that is less than the value calculated (R_{db1}) = 30.76 Ω .
2. A power value greater than the average power value calculated $P_{avg} = 2633$ W.

The IPC resistor bank model # DB445-11A-GALV has a resistance of 23 Ω which is less than R_{db1} and dissipation power of 11.125 kW which is greater than P_{avg} . Further details regarding the resistor bank are available in Appendix C.7. In summary, the IPC resistor is satisfactory for performing the required braking function for the HCCI research engine.

4.3.4 Speed Control Selection

The Allen Bradley 1336 variable speed drive is the device that will enable variation of the speed of the AC Motor and hence the Kubota Engine. The H15E1D AC motor is designed to run at a fixed speed of 3600 RPM at an input power line frequency of 60 Hz. However, AC motors such as this are often used in conjunction with VSD in industry and are durable enough to handle output speed variation. Therefore, a VSD is required to vary the input line frequency that will result in variation of shaft speed. The following equation is used to determine the speed of the AC motor output shaft:

$$\text{Speed} = \frac{120 \times f}{N_{poles}}, \quad \text{Equation 6}$$

The AC motor has two motor poles (N_{poles}), therefore if we vary the frequency from (0 to 60 Hz) in increments of 10 Hz we can see how the speed of the AC motor changes (see Table 11 below.) The selection of the Alen Bradley VSD enables output shaft speed variation that is acceptable for speed control of the Kubota research engine.

Table 11 Variation of AC motor shaft speed (rpm) by varying input frequency with VSD.

Frequency (Hz)	Shaft Speed (RPM)
0	0
10	600
20	1200
30	1800
40	2400
50	3000
60	3600

4.3.5 Selection of Engine to AC motor Flexible Coupler

Initial selection is based on the maximum rated torque of the engine with consideration given to the type of engine and number of cylinders, dynamometer characteristics and inertia. Plint and Martyr [38] suggest a simple method for sizing engine/dynamometer couplings as well as several other considerations such as safety, vibration, and alignment. This method is presented in Appendix D.4 and D.6 in full detail, and summarized below.

Kubota D905 has a maximum net rated continuous torque (τ_{net}) of 4.4 kgf.m (30 ft-lbs) at 2200 RPM. From Plint and Martyr Table 8.4, the service factors ($F_{service}$) are listed for a wide range of engine and dynamometer types. For this application the service factor is 4.5. The maximum rated torque multiplied by the service factor must not exceed the maximum permitted torque (τ_{per}) of the coupler as shown in the following:

$$\tau_{per} = F_{service} \times \tau_{net}, \quad \text{Equation 7}$$

$$\tau_{per} = 4.5 \times 4.4 \text{kgf.m} = 20.25 \text{kgf.m}$$

The maximum torque (τ_{max}) of the McMaster-Carr coupler # 6507K7 from Appendix C.6 is 1800 in-lbs or 20.7 kgf.m. Since, $\tau_{max} \geq \tau_{per}$, the coupler should be adequate to handle the torque from the motor. The torque on the coupler during emergency braking was also calculated and is presented in Appendix D.6. Care should be taking when performing emergency braking as the

coupler is the weak link in the system. In summary, the AC motor, VSD, resistor bank and chopper, and coupler, selected for the drive system have met or exceeded the design constraints, and ensures reliable and safe operation.

4.4 Intake Charge Pre-Heater System Selection

The design objective for the intake charge pre-heater is to provide adequate supply of heat for the research engine to enable experiments. The design constraints on the pre-heater are:

1. To provide enough heat to the intake air for one cylinder of a Kubota D905 engine to raise intake air temperature from 0 to 300 °C.
2. To enable accurate control of the heater.

The heater control system senses the charge temperature in the intake duct after fuel injection but just before the intake valve and then adjusts the heater to maintain the desired set point temperature. This ensures that the charge temperature or the temperature of the air and fuel mixture will have compensated for the vaporization losses of mixing ethanol with air. A design concept sketch is presented in Figure 20 and the legend is presented below in Table 12.

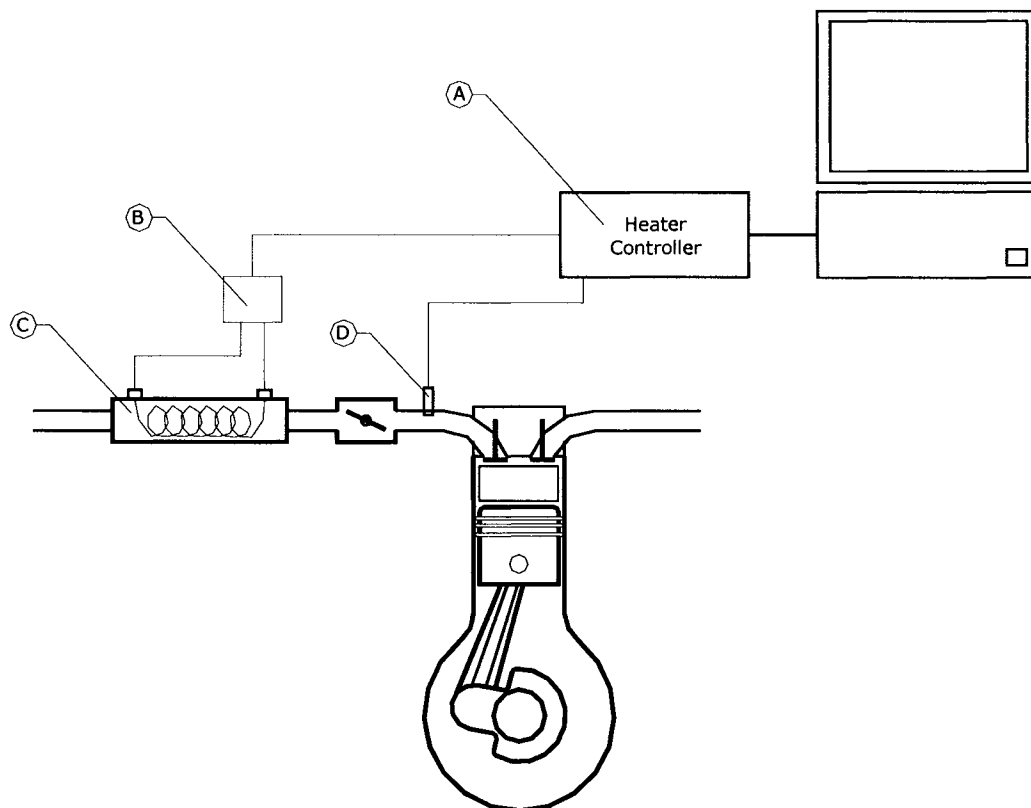


Figure 20: Intake charge pre-heater system schematic.

Table 12 Intake Charge Preheater System legend.

Item	Description
A	Heater Controller
B	Relay
C	Heater
D	Thermocouple

The intake charge pre-heater system is comprised of a heater element, a switching relay, a digital controller, a thermocouple (located close to the intake valve), and capability for data communications with a personal computer.

4.4.1 Heater Sizing and Selection

The electric heater sizing is based on the air flow rate of one cylinder of a Kubota D905 at 3600 RPM, plus intake heat losses (F_{loss}) estimated to be 40%. Also the heater was oversized (F_{os}) by 10% to compensate for any electrical losses not accounted for. The equation below was used to determine the electric power of the heater in kilowatts (kW):

$$\dot{W}_e = F_{loss} \times F_{os} \times \rho_{air} \times \dot{V} \times C_p \times \Delta T, \quad \text{Equation 8}$$

Where \dot{V} is the volumetric flowrate in [m^3/s], ρ_{air} is the average air density, and C_p is the averaged specific heat of air for the range $\Delta T = T_2 - T_1 = 300^\circ C$. The detailed calculations are presented in Appendix F.1 to F.3.

Based on calculations presented in Appendix F, the electric power requirement (\dot{W}_e) was determined to be 5.4 kW. The Omega SH-73343 was selected because it had a power rating of 6 kW and had a lower voltage requirement at 240 V compared to the 480 V model, making it a safer device to operate.

The Omega SH-73343 (shown in Figure 21) has a cross-flow heating element selected to minimize flow resistance, as well as an over-temperature circuit for heater element burnout protection. When operated correctly it has a useful life of 5000 hours. It has a practical flow rate range of up to 94.4 L/s with internal temperatures up to $700^\circ C$. The heating element is nickel-chrome plated and insulated by ceramic beads on a stainless steel support frame.

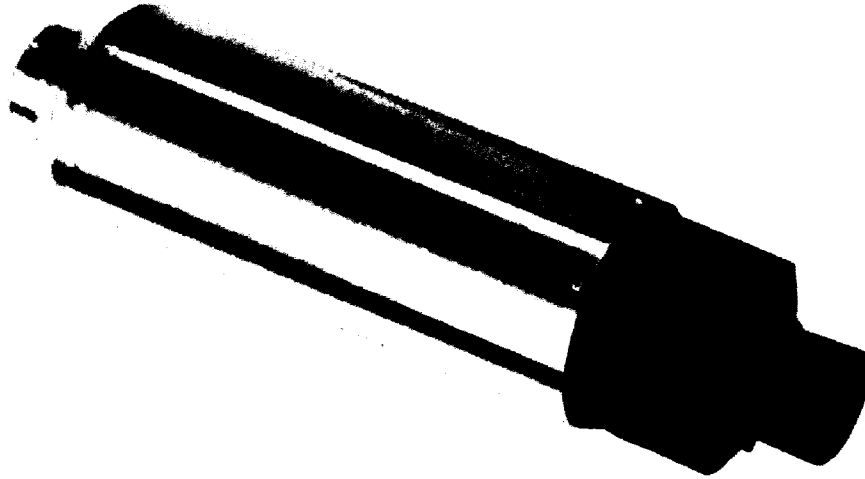


Figure 21: Omega SH-73343, 6kW-240V-25A Intake Air Heater [40].

4.4.2 Temperature Controller Selection

The temperature controller selected is an Omega CNi/32 with digital display. This controller was recommended by both Mr. Patrick Seguin of University of Windsor and Joel Thivierge of Omega Canada for this application.

The controller reads the thermocouple input, compares it against the set point value for temperature and adjusts the output voltage appropriately to the relay. The relay either turns on or off the heating element depending on the controller signal (ON for heating, OFF for cooling).

Figure 22 illustrates the CNi/32 controller.



Figure 22: Omega CN-i/32 heater controller [41].

The relay selected is a solid-state type relay that has a maximum current load capacity of 25 A. The thermocouple selected is a K-type thermocouple that has operating range (-17 to 650 °C). This range should be sufficient for the expected operating conditions of the heater system. The thermocouple should be placed as close to the intake valve as possible so that the heater can get a

true reading for the charge temperature entering the engine, and can compensate for the heat losses of the intake system.

The heater controller and relay will have to be mounted in a CSA approved enclosure, and connected to the heater itself. In summary, the Omega CNI/32 controller will meet the constraints and will provide safe and accurate control of the Omega SH-73343 heater.

4.5 Selection of Intake Air Measurement System

The main objective for this section is to select an accurate and reliable system for measurement and data acquisition of intake air for the research engine. The intake air measurement system shall enable experiments for both single cylinder operation and three-cylinder operation of the Kubota D905.

The design constraints on the flow meter are:

1. To select a flow meter that will be able to measure accurately, and reliably the intake air for three cylinders of a Kubota D905 engine at 3600 RPM.
2. The flow meter measurements shall provide a signal that is compatible with a data acquisition system.

Figure 23 illustrates the flow meter schematic and Table 13 lists the components. The intake air measurement system shown consists of the airflow measurement device, transmitter, surge tank and data acquisition system.

Table 13 Intake Air Measurement System legend.

Item	Description
A	Transmitter
B	Flow Meter
C	Surge Tank

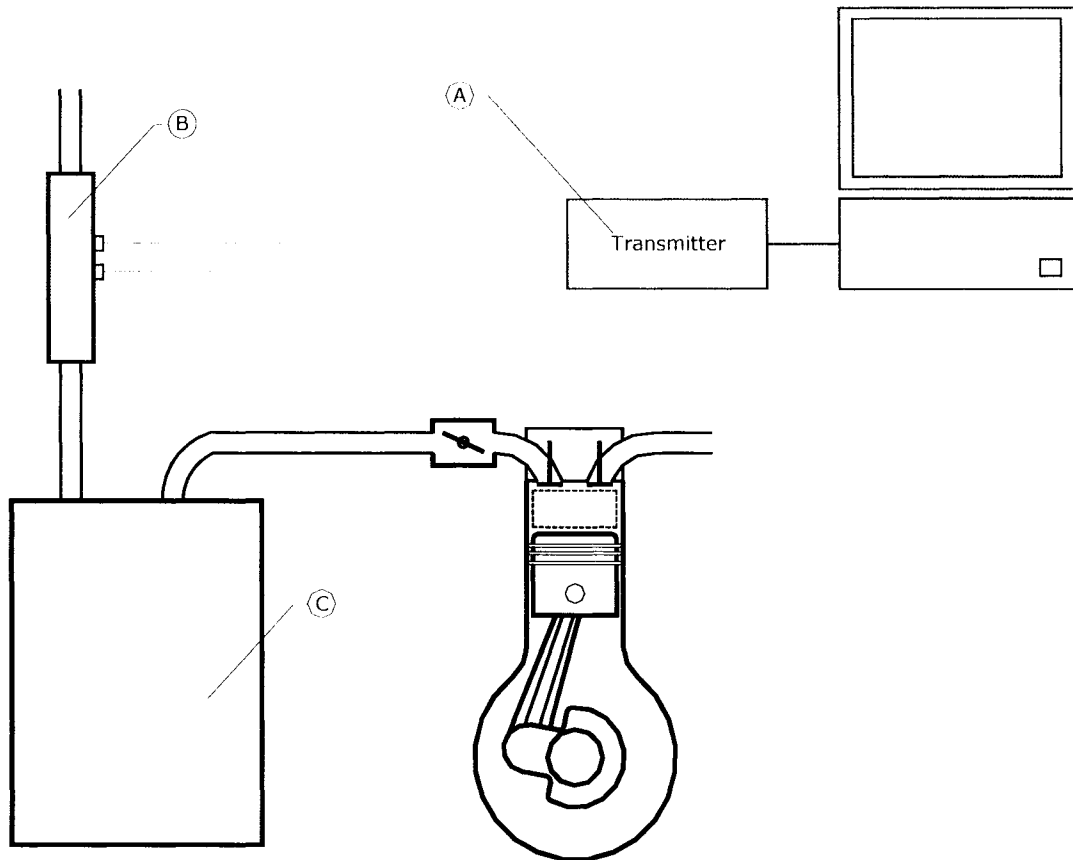


Figure 23: Intake Air Measurement System.

4.5.1 Flow Measurement Background

According to Plint and Martyr [38] there are three main methods of airflow measurement for an engine; orifice meter, corona (hot) wire, and viscous flow.

The orifice meter method is the simplest method and involves drawing air through a sharp edge orifice through an airbox and into the engine. The pressure drop (Δp) across the orifice is measured across the orifice by means of a manometer and the velocity (U) is calculated by:

$$U = \sqrt{\frac{2\Delta p}{\rho_{air}}}, \quad \text{Equation 9}$$

Where ρ_{air} is the density of air.

The Corona Wire or hot wire is more technically known as the Lucas-Dawe air mass flow meter. Its operation depends on a sensing the current discharge from an electric wire running through

airflow. The discharge from an electrode located on the centerline axis of the duct through which the air is flowing is measured. An increasing airflow diminishes the passage of ion current from the corona wire to collector electrodes located on the duct wall. This gives rise to an imbalance of current flow that is proportional to the airflow rate. This measurement method has the advantage of a quick response to flow changes, ideal for transient conditions.

The viscous flow air meter is the most widely used alternative to the orifice method for measuring airflow. The measuring orifice is replaced by an element consisting of a large number of small passages, generally in triangular form. The flow through these passages is mostly laminar, which results in the pressure drop being proportional to velocity of flow, rather than to its square. A viscous flow air meter was selected for this project because of its accuracy, availability and cost savings compared to orifice flow meter and corona wire.

4.5.2 Laminar Flow Element Selection

The most common industry units for flow rate are cubic feet per minute or (cfm) however L/s are the appropriate SI units that will be used in this thesis. Often the flow rate value is referenced to base condition to compensate for temperature and pressure of the gas compared to standard temperature and pressure (101.3 kPa absolute and 21.1°C) [10]. This is denoted by units of standard cubic feet per minute or (scfm) or in our case std. L/s. Note the std. L/s equals L/s at standard temperature and pressure.

The flow rate of air drawn by three cylinders of the Kubota D905 engine was calculated in Appendix F.4. The same quantities calculated in Appendix F.1, F.2, F.3 are also used in Appendix F.4 except the flow rate is representative of all three cylinders as opposed to just a single cylinder. The reason for the over-sizing of the laminar flow element (LFE) is to allow for future research to be performed on the entire engine, whereas the heater would only be required for single cylinder operation.

The volumetric flow rate ($\dot{V}_{calculated}$) or air consumption of the engine is calculated by using the following equations obtained from Heywood [37]:

$$\dot{V}_{calculated} = \eta_v \frac{V_s}{t_c}, \quad \text{Equation 10}$$

Where:

η_v = volumetric efficiency of the Kubota D905 assumed =1.0.

V_s = is the swept volume of the engine or displaced volume = 898 cm³

t_c = cycle time which is defined by the equation:

$$t_c = \frac{N}{120}, \text{ where } N = \text{engine speed in RPM.}$$

For an engine speed of 3600 RPM, the volumetric flow rate of air through the LFE was calculated to be 26.94 std. L/s (see Appendix F.3, F.4, F.5 for detailed calculations.) Since the flow is at standard condition, the LFE can be selected directly from the capacity chart given in Appendix G.3.

There are two LFE that have a flow rate range covering the expected flow rate of our Kubota D905 engine. The 50MC2-2 was selected because it had a slightly larger range from 0 to 47.18 L/s (0-100 scfm) and has hose end attachments that will be easier to incorporate with the proposed research engine. Figure 24 illustrates the Meriam 50MC2-2. Note the 10 mm hose end fittings on the top of the flow meter. These fittings supply the differential pressure that is read by a transmitter. The transmitter is a sensor that measures differential pressure and outputs a corresponding analog signal. Therefore, the Meriam 50MC2-2 was determined to have met the design constraints for the intake air measurement system.

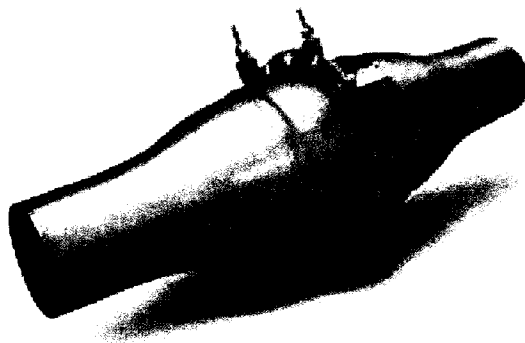


Figure 24: Meriam Laminar Flow Element Model # 50MC2-2 [42].

4.5.3 Transmitter Selection

A transmitter was recommended by Paul Derisi of Peacock Inc. to work with the Meriam 50MC2-2 flow meter. The transmitter is manufactured by Honeywell Inc. and is denoted as Model # STD904. The transmitter senses the differential pressure developed by the LFE, and produces an analog signal varying from 4 to 20 mA. The 4-20 mA signal can be easily read by a data acquisition system. See Appendix G.6 for further details or consult the manual available from Honeywell Inc. [44].

In summary, the Meriam LFE along with the Honeywell transmitter has met the design constraints and will provide accurate and reliable flow rate measurements for the research engine.

4.6 Intake Piping System Design

The design objective for the intake piping system is to provide an effective means of flowing air into the engine, exhaust gases out of the engine and providing a means to attain exhaust gas recirculation (EGR). A schematic of the proposed intake piping system is presented in Figure 25.

The constraints for the intake design include the following:

1. Use of standardized components to reduce cost and manufacturing time.
2. Use of materials that are resistant to high temperatures, and corrosion.
3. Minimize flow resistance by selecting appropriate components.

The intake piping system employs standard galvanized steel piping components (after the heater element) and plastic ABS piping components (before the heater). These were selected to meet the constraints for use of standard components, save manufacturing costs, and to improve the safety of the design.

Galvanized steel piping is also resistant to melting at elevated temperatures. The melting temperature of steel is dependent on its carbon content. Steel piping components are manufactured using mild 1040 steel, and then are galvanized to prevent corrosion. According to Askeland, mild plain-carbon 1040 steel has 0.40 % carbon content and a corresponding melting temperature of 723 °C [45]. This is greater than the desired maximum temperature of the heater at 300 °C. Therefore; the galvanized piping should be an adequate material for use with the heater. (See Appendix F.8 for further details).

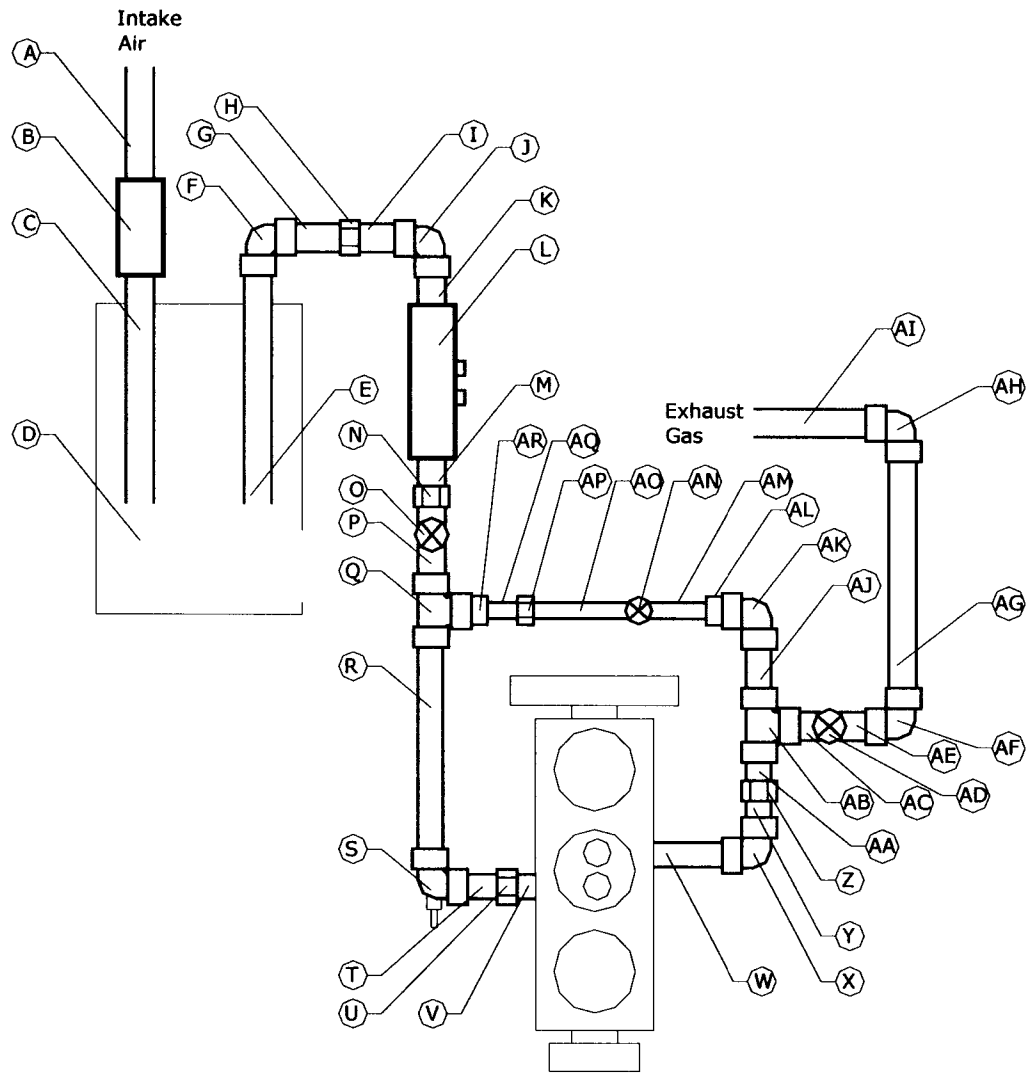


Figure 25: Intake Piping System Schematic.

Resistance to elevated temperature is not a concern upstream of the heater. Therefore plastic ABS piping components are better suited, because they are easy to assemble and are less costly. The melting point of ABS plastic is 80-125 °C. These piping elements will be fitted together to provide the desired function. The diameter of the piping will be 3.75 cm (1.5") for the intake and exhaust and 2.54 cm (1") for the EGR pipe. This diameter was chosen to minimize resistance to flow in the intake and exhaust.

The Intake Piping Flow Resistance Excel program was developed to analyze the piping system. The details of this excel program are available in Appendices F.8 through F.12. The purpose of

this program is to determine the pressure loss associated with the intake piping system for various engine speeds, EGR and exhaust valve positions, and heater temperatures.

The program prompts the user to input engine specifications, properties of air, EGR and exhaust valve position, and engine speed (as seen in Appendix F.9). The program assumes steady flow through all piping and also assumes that the engine acts as a steady-flow pumping device.

A trial was performed to investigate the pressure loss of the longest leg of the intake piping system (Appendix F.10.) This is defined in Figure 25 as the intake leg (A to Q to V) plus the exhaust leg (W to AB to AI). The EGR leg, (AB to Q), was disabled by closing the EGR valve (AN), and the exhaust valve (AD) was fully opened. This trial was done to estimate the pressure loss of the system at the engine speed of 3600 RPM. Summary of the results of the program are listed in Table 14.

Table 14 Summary of pressure loss for longest leg of the system. 3600 RPM, no EGR.

Piping Leg	Description	Summary of Pressure Loss (kPa)
A to Q	Intake to first tee	0.309
Q to V	First tee to engine	0.111
W to AB	Engine to second tee	0.0996
AB to AI	Exhaust system	0.236
AB to Q	EGR	No flow

The total flow loss for the longest leg of the intake piping system is 0.755 kPa. The pressure gain of the engine relative to the intake/exhaust system is on average 1.031 kPa at 3600 RPM. It is evident that the engine on average has a greater gain than the losses if the system. Therefore, the losses developed by the piping system will not be detrimental to the performance of the engine.

In summary, the intake piping system has met all constraints and the intake piping system program has been developed for future analysis of the piping system at other engine speeds and conditions.

4.7 EGR System

The design objective for the EGR system is to provide an effective means of recirculating exhaust gases back to the intake system. The amount or percentage of EGR that is recirculated needs to have a direct means of control and measurement. A schematic of the proposed EGR system is presented in Figure 28. A list of the components of the EGR system is presented in Table 15 below.

The design constraints for the EGR system are:

1. To provide an effective means of recirculation and control.
2. To provides a means of measurement of EGR gas present in the intake manifold.
3. To provides a means of logging data for EGR.

The EGR system employs 25.4 mm (1in) standard galvanized steel piping components for the EGR leg (AB to Q) as shown earlier in Figure 25. Both the exhaust valve [B], and the EGR control valve [A] are brass gate valves as shown in Figure 27 below. Brass gate valves were selected to meet the constraints for use of standard components and to save manufacturing costs.

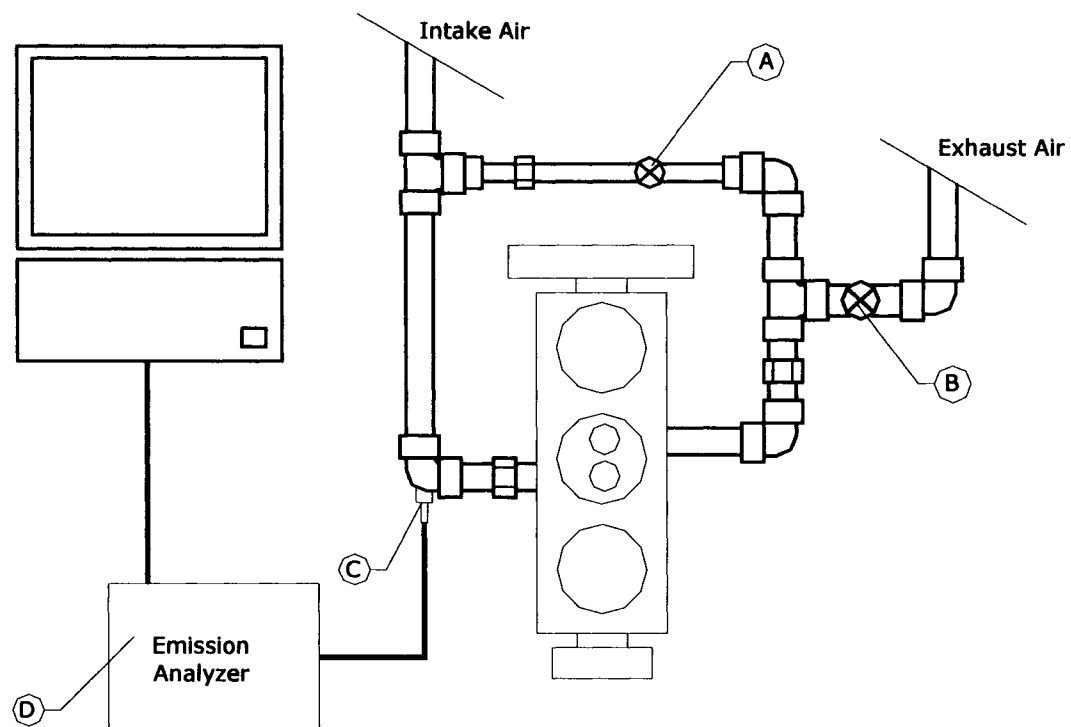


Figure 26: Concept Sketch of proposed EGR system.

Table 15 EGR System legend.

Item	Description
A	25.4 mm (1") EGR Gate Valve
B	38.1 mm (1.5") Exhaust Gate Valve
C	EGR Probe
D	OTC Emission Analyzer

4.7.1 EGR Piping Leg

The brass gate valves shown in Figure 27 are very common components with female NPT ends such as would be found in most plumbing systems. The exhaust gate valve (B) will be used to generate backpressure for the engine and assist with EGR gas flow through the 25.4 mm diameter EGR leg to the 38.1 mm diameter intake pipe. The generation of backpressure in this manner can be used to create sufficient pressure for high EGR flow rates, or even 100 %EGR. The 25.4 mm gate valve in the EGR line will be used to adjust the EGR flow rate. The reason for the reduced size of the EGR leg is to increase the velocity of the EGR gas that will result in quicker response and decrease cooling of the EGR gas. Both valves are adjusted manually which will suffice for steady state operation. The gate valve handle is marked to give a reference, so that one can count the number of turns relative to fully closed. The number of turns is entered into the EGR program to help determine the pressure losses of the system. The number of turns can be correlated to EGR percentage based on engine RPM, but verification experiments will need to be completed in order to attain this. Therefore, the proposed design will enable an effective means of recirculation and control of EGR gas.



Figure 27: Brass Gate Valve to be used as EGR valves.

4.7.2 MATLAB EGR Program

For determining the EGR mass fraction, a method was developed that require measurement of CO₂ concentration in the intake manifold slightly before the intake valve and then calculating the EGR percentage in the intake. The gases produced from combustion of hydrocarbons are water (H₂O), CO₂, CO, NO_x, HC and O₂. These gases can be sampled in the exhaust leg to determine, and verify the equivalence ratio of the air fuel mixture. Additionally, these gases are brought into the intake in varying concentration by means of the EGR leg. The EGR gas mixes with the intake gases to form a reactants mixture.

The Matlab EGR program was developed by Arthur and Defoe [46]. The Matlab EGR program was utilized for determining EGR mass fraction based on CO₂ mass fraction in the intake leg. Full Details of the Matlab EGR program including: inputs, outputs, and the MATLAB M-file are listed in Appendices F.13, F.14, and F.15.

The Matlab EGR program inputs are; relative humidity, ambient air pressure, saturation pressure of water, mass flow rate of intake air, volume fraction of CO₂ (from emission analyzer), composition of fuel (number of atoms of C, H, O, N), composition of additives (number of atoms of C, H, O, N), mole fraction of fuel and additives, and equivalence ratio. Table 16 below, summarizes the inputs utilized for the simulation trial of the program.

It is to be noted that this method does not take into account residual combustion gases present in the combustion chamber of the engine after a combustion event occurs, and would result in a slight error, but in general the Matlab EGR program should be acceptable for the purposes of this report.

The output of the Matlab EGR program is mass percentage of EGR (m_EGR_percent) or in other words, the percentage of mass entering the cylinder that is EGR. A simulation was run of the program for several different EGR fractions present in the intake and the results are summarized in Table 17 below. The results of this simulation should be verified with an experiment; however this step does at least prove functionality of the Matlab EGR program as a method for calculating percent EGR.

Table 16 Summary of Matlab EGR program inputs.

Inputs	Quantity (units)										
Relative Humidity (RH)	0.75										
Ambient Pressure (p)	101.325 (kPa)										
Saturation Pressure of Water (p _g) @ 25°C	3.169 (kPa)										
Mass flow rate of air entering intake before EGR mixing (m _{dot} _air) @ 4000 RPM	0.01279 (kg/s)										
Mole/volume fraction of CO ₂ from the emission analyzer (N_CO2)	Variable (%)										
Fuel Composition (fuel) for ethanol	<table style="margin-left: auto; margin-right: auto;"> <tr> <td></td> <td>C</td> <td>H</td> <td>O</td> <td>N</td> </tr> <tr> <td>fuel =</td> <td>[2</td> <td>6</td> <td>1</td> <td>0]</td> </tr> </table>		C	H	O	N	fuel =	[2	6	1	0]
	C	H	O	N							
fuel =	[2	6	1	0]							
Additive Composition (adds)	<table style="margin-left: auto; margin-right: auto;"> <tr> <td></td> <td>C</td> <td>H</td> <td>O</td> <td>N</td> </tr> <tr> <td>adds =</td> <td>[0</td> <td>0</td> <td>0</td> <td>0]</td> </tr> </table>		C	H	O	N	adds =	[0	0	0	0]
	C	H	O	N							
adds =	[0	0	0	0]							
Mole fraction of fuel (a)	1.0										
Mole fraction of additives (b)	0.0										
Equivalence Ratio (equiv)	0.4										

Table 17 Summary of MATLAB EGR program simulation at various CO₂ concentrations.

Mole/volume fraction of CO₂ (%)	% EGR
0.05	9.7
1.0	18.4
1.5	27.8
2.0	37.4
2.5	47.0
3.0	56.8
3.5	66.8
4.0	77.0
4.5	87.3
5.0	97.7

4.7.3 Exhaust Gas Measurement

The OTC MicroGas Analyzer shown in Figure 28 is a portable gas analysis unit that measures and graphs the levels of CO, CO₂, HC, NO_x, and O₂ present in the exhaust of internal combustion engines. Data for each of the five gases plus the AFR are displayed and graphed on a single screen for side by side analysis and review of each gas. The user guide contains detailed information regarding the setup, gas analysis, calibration and maintenance procedures, and troubleshooting procedures. The user guide is available on the OTC website [47]. See Appendix G.7 for a summary of the functional capability of the emission analyzer. The sampling range of the exhaust emissions is listed in Table 18 below.

Table 18 Exhaust Emission Sampling Capability Range for OTC MicroGas Analyzer.

Exhaust Emissions	Measurement Range (units)
Hydrocarbons (HC)	0 – 30,000 ppm
Carbon Monoxide (CO)	0 - 15 %
Oxides of Nitrogen (NOx)	0 –5000 ppm
Carbon Dioxide (CO ₂)	0 – 20%
Oxygen (O ₂)	0 - 25 %



Figure 28: OTC MicroGas Emission Analyzer.

These ranges should be sufficient for HCCI operation of ethanol. The OTC MicroGas analyzer will measure the concentration of the various gases in the intake manifold. The concentration of CO₂ will be of interest and can be saved on the memory of the analyzer and later downloaded

from the analyzer to the data acquisition computer for analysis. The Matlab EGR program is an effective means of calculating the percent EGR and therefore satisfies the third constraint.

In summary, the proposed design of the EGR system will satisfy all three design constraints. A MATLAB EGR program has been developed for use in conjunction with the gas analyzer to determine the percentage EGR present in the intake manifold.

4.8 Ethanol Fuel System

The design objective of the ethanol fuel system is to provide a safe and functional means of delivering ethanol to the engine. The following is a list of constraints for the fuel system:

1. The fuel system shall be able to supply fuel to the engine for at least a minimum flow rate of 1.69 g/s.
2. The design should limit fuel storage to a maximum of 5 L.
3. System pressure range shall be within 200 kPa to 500 kPa, and nominal operating fuel pressure shall be 310 kPa.
4. Resort to purchasing components instead of fabrication.
5. All components shall be compatible with alcohol fuels.

Figure 29 illustrates a schematic of the fuel system and all its components that include the following; fuel tank, fuel pump, filter, pressure regulator, injector, fuel rail, main and return fuel lines and fittings. Table 19 lists the legend for the ethanol fuel system shown in Figure 29.

Table 19 Ethanol fuel system legend.

Item	Description
A	Fuel pressure regulator
B	Fuel injector
C	Custom fuel rail for single injector
D	Main fuel line with fittings
E	Return fuel line with fittings
F	Fuel filter
G	Fuel pump
H	Fuel tank
I	Ethanol fuel

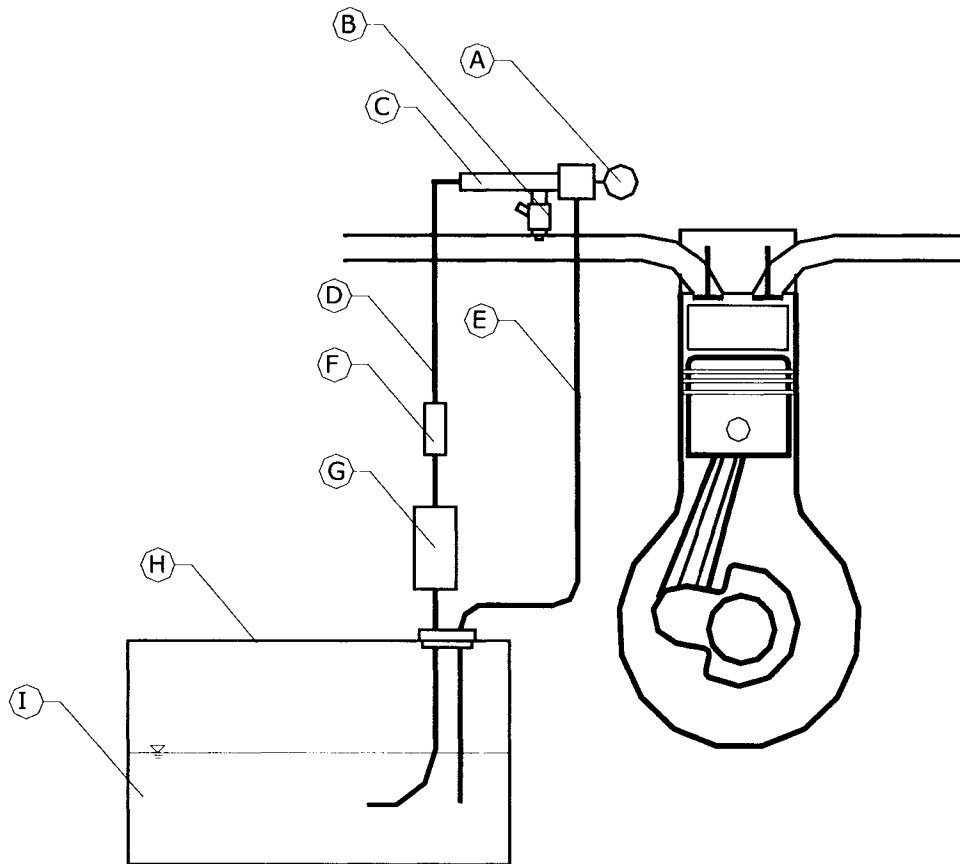


Figure 29: Schematic of ethanol fuel system.

Alcohol compatibility is the most significant issue when it comes to selecting fuel system components. Certain automotive plastics used in fuel pumps of the past expand, when exposed to alcohol for a prolonged period of time, therefore attention to alcohol compatibility of all components is the most important constraint.

4.8.1 Fuel Pump Selection

A catalogue search was performed to find a fuel pump with alcohol compatibility, and lower flow rates. The selection was limited because most alcohol fuel pumps are designed for high performance alcohol dragsters, which require higher fuel flow rates than what is needed for this application. The Accel Model 310-74701 electronic fuel injection (EFI) fuel pump was selected because it was the smallest commercially available fuel pump that was compatible with alcohol (see Figure 30.) The fuel pump is required to provide enough fuel flow to supply three cylinders of the Kubota D905 engine at 3600 RPM and with the equivalence ratio equal to 1.0. Appendix H.1 provides further detail regarding these design calculations.

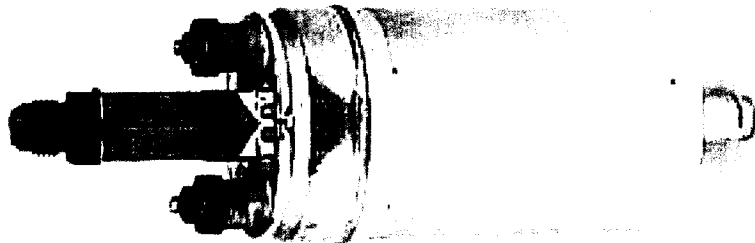


Figure 30: ACCEL model # 310-74701 EFI alcohol compatible fuel pump.

The required fuel mass flow rate under these conditions is 4.68 kg/s or the volumetric flow rate is 0.00593 L/s. The Accel fuel pump has a rated volumetric flow rate of 0.0274 L/s at 310 kPa. Therefore, the fuel pump is more than adequate for supply fuel to our system, and in fact is oversized by a factor of 4.6. Although this is substantially oversized, the compatibility with alcohol and the availability of the pump were the two major factors that resulted in selection of the Accel fuel pump. Therefore, the Accel Model 310-74701 fuel pump adequately satisfies the first constraint.

4.8.2 Fuel Tank Selection

University of Windsor Health and Safety Regulations state that storage of a Class 1-A substance is permitted outside of a flammable mixture storage cabinet, but limited to no more than 5L [48]. Ethanol is considered a Class 1-A substance, so therefore the fuel tank capacity can be no larger than 5 L.

The Jaz Pro Cell 547-250-001-01 vertical fuel tank was selected and is shown in Figure 31. It has dimensions of 15.2cm by 15.2cm by 30.4cm and is compatible with alcohol fuels and also with the fuel pump selected earlier. The volume capacity (V_{tank}) of the fuel tank is 1 gal or 3.78 L. Since this is less than the Health and Safety limit of 5 L the tank size was acceptable for use with the fuel system. Also the Jaz fuel tank is easily available through Performance Parts Plus of Windsor.

Therefore, the JAZ fuel tank will meet the design constraints of alcohol compatibility, storage capacity, and use of readily available components (see Appendix H.3 and I.1).

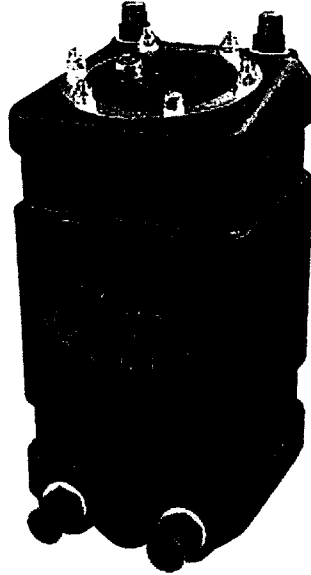


Figure 31: JAZ Pro Cell Model # 547-250-001-01 vertical fuel tank.

4.8.3 Fuel Injector Selection

There are several fuel injector suppliers along with several types of fuel injectors available. Delphi Automotive is an OEM that manufactures a line of ethanol compatible injectors for the North American automakers. Delphi injectors are available in several different sizes, and flow rates to suit the needs of the automakers, and a comprehensive list of them is available on their website (see reference [49]).

To select an appropriate injector the fuel flow rate for one cylinder operation is required. A design calculation was performed to determine the fuel flow rate to be 1.56g/s and is available in Appendix H. Therefore the fuel injector should have a flow rate greater than 1.56 g/s in order to compensate for losses and to meet the design constraint. The dynamic flow rate of Delphi # 2532087 injector from Appendix I.3 is listed as 2.18 g/s [49]. The Delphi # 2532087 is shown in Figure 32 and is a highly reliable and durable injector used in the Chevrolet Silverado, among other vehicles.

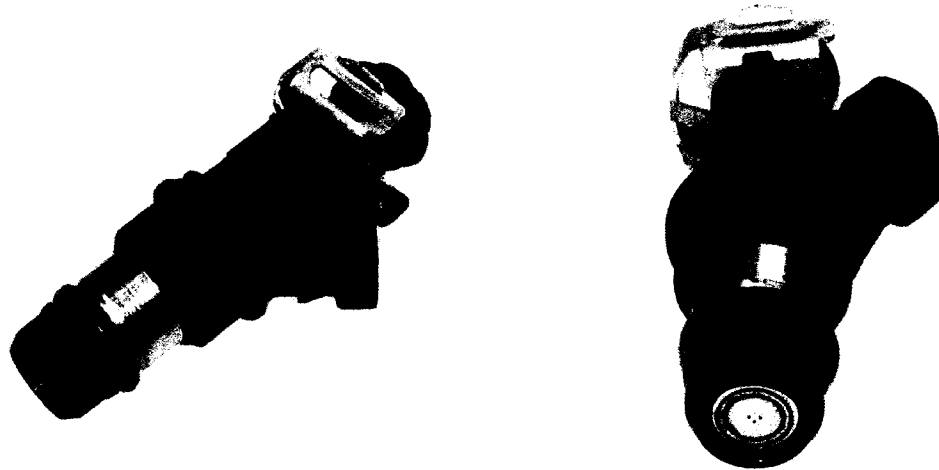


Figure 32: Delphi Multec 2 fuel injector model # 2532087 [49].

The Delphi # 2532087 is readily available and is compatible with alcohol fuels. Since the flow rate of the injector is greater than the required flow rate of the engine, the Delphi Multec 2 has met the design constraints.

4.8.4 Fuel Pressure Regulator and Gauge Selection

The selection of the pressure regulator requires that it is compatible with the fuel pump and tank selected earlier. Also the regulator will have to be able to vary the system pressure between 200 kPa to 500 kPa. The nominal system pressure for the fuel pump and for the injector selected is 310 kPa. The Mallory regulator model 4309, shown in Figure 33a, is fully adjustable with a pressure range 207 to 689 kPa. This regulator is also compatible with alcohol fuels and is easily connected to the rest of the system with 6.34 mm (0.25 in) NPT female connections.

See Appendix H.5 and Appendix I.4 for further details. The Mallory pressure regulator meets the design constraints of the fuel system. The selection of the pressure gauge was a fairly simple task. The first constraint was alcohol compatibility, and the second constraint was gauge pressure range. The Omega Model PGS 25L 160, shown in Figure 33b, has a pressure range of 0 to 1103 kPa. This pressure range is adequate to read our regulator pressure range 207 to 689 kPa. Also, the pressure gauge is both gasoline and alcohol compatible. Therefore, the Omega Pressure gauge meets the design constraints of the fuel system.

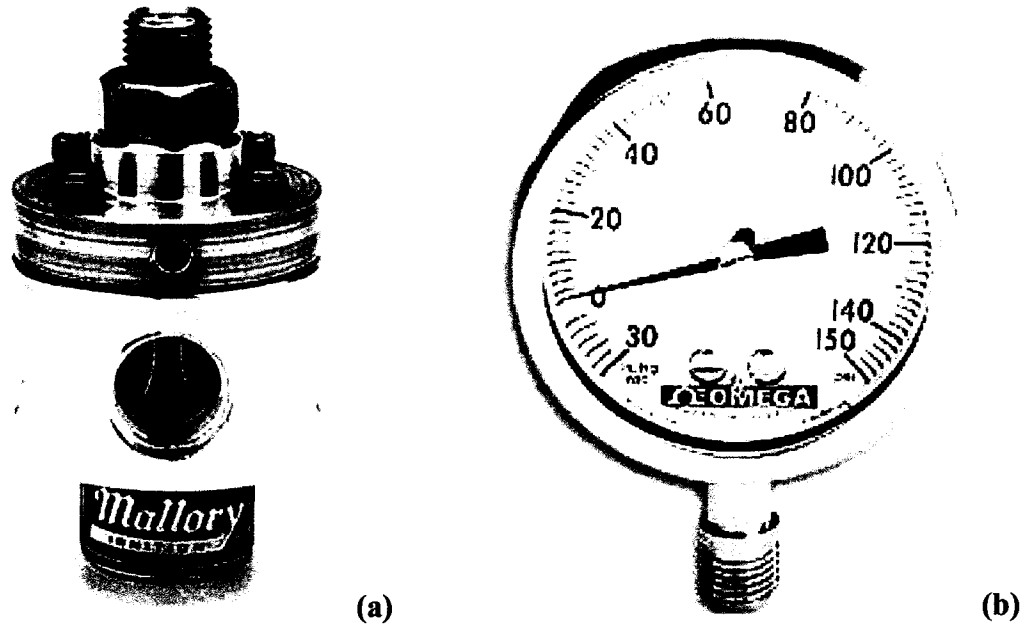


Figure 33: (a) Mallory Regulator Model 4309, (b) Omega Pressure gauge model # PGS 25L 160 [50].

4.8.5 Fuel Filter Selection

Selecting the fuel filter was also a simple task. The fuel filter had to be compatible with alcohol and also have 06 AN connections. Figure 34 shows several fuel filters from JAZ. The JAZ fuel filter model # 547-836-006-11 meets the design constraints and is also manufactured anodized blue aluminum. This fuel filter is also compatible with the fuel pump and fuel tank selected earlier and is suited for 06 AN connections.

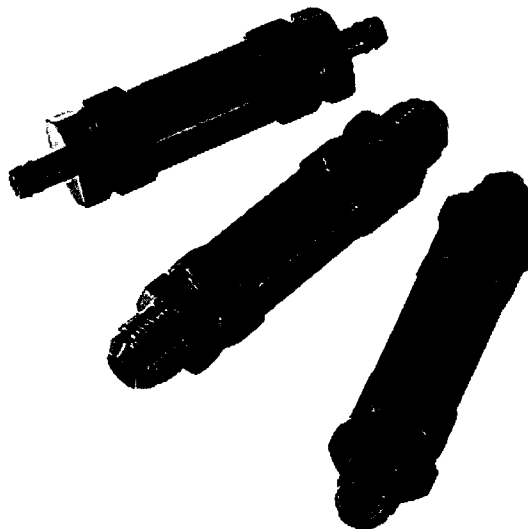


Figure 34: JAZ fuel filter model 547-836-006-11 [50].

4.8.6 Fuel Fittings and Hose Selection.

Aeroquip manufactures a line of products that consist of connectors and hoses and are used mainly for custom high performance automotive fuel systems. These fittings are available in several sizes depending on the applications, and are finished in anodized blue aluminum for anti-corrosion and alcohol compatibility. The fuel system will use the following connectors shown in Figure 35.

Aeroquip also manufactures stainless steel braided hose, with elastomer inner tube, partial stainless inner wire, and full stainless outer wire braid. This hose is alcohol compatible and has a temperature range from -49 °C to 150 °C. This hose was selected for use with our fuel system, (see Figure 37.)

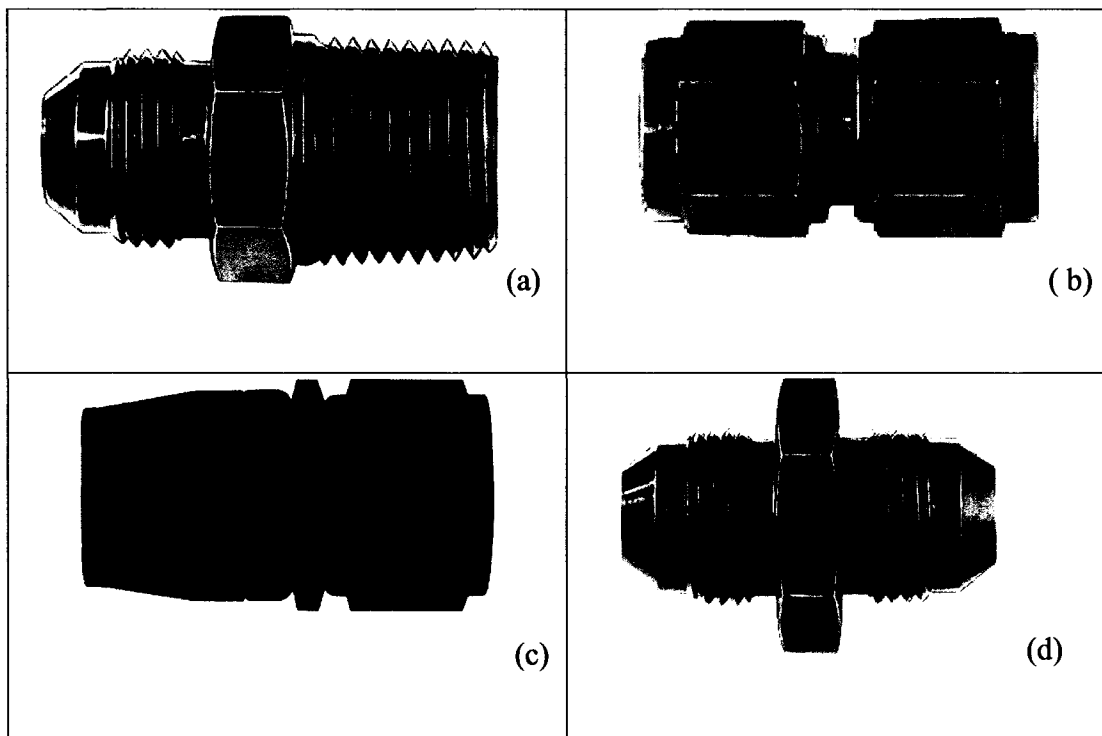


Figure 35: (a) 1/4" NPT male to 06 AN male, (b) 06 AN female to 06 AN female coupler, (c) 06 AN swivel hose end, (d) 06 AN to 06 AN union [50].

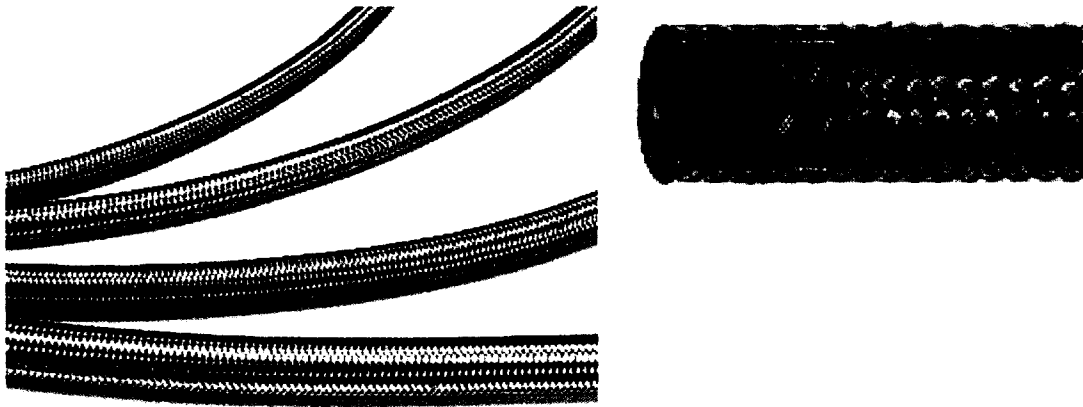


Figure 36: (a) Various hose sizes shown from 04 to 010 AN, (b) Multilayered construction hose [50].

Therefore, both the connectors and the hose have met the design constraints for use with the fuel system. The proposed fuel system satisfied all design constraints and ensures safe and reliable operation of the research engine.

4.9 ECU system

The design objective of the engine control unit (ECU) system is to provide a direct means of controlling the fuel injector. The design constraints are listed below:

1. The ECU shall have an interface with a personal computer such that the equivalence ratio (0.0 to 1.0) and other pertinent parameters can be varied.
2. The ECU system shall be comprised of commercially available products.
3. The ECU system shall be easy to implement and easy to use.

The schematic of the ECU system is presented in Figure 37 and a legend for the ECU system is displayed in Table 20 below.

Table 20 Legend for Figure 38 ECU system.

Item letter in Figure 38	Description
A	Electronic Control Unit
B	Intake air temp sensor
C	Manifold Absolute pressure
D	Throttle valve with TPS sensor
E	Mass air flow sensor
F	Coolant temp sensor
G	Cam trigger sensor
H	Cam trigger mechanism

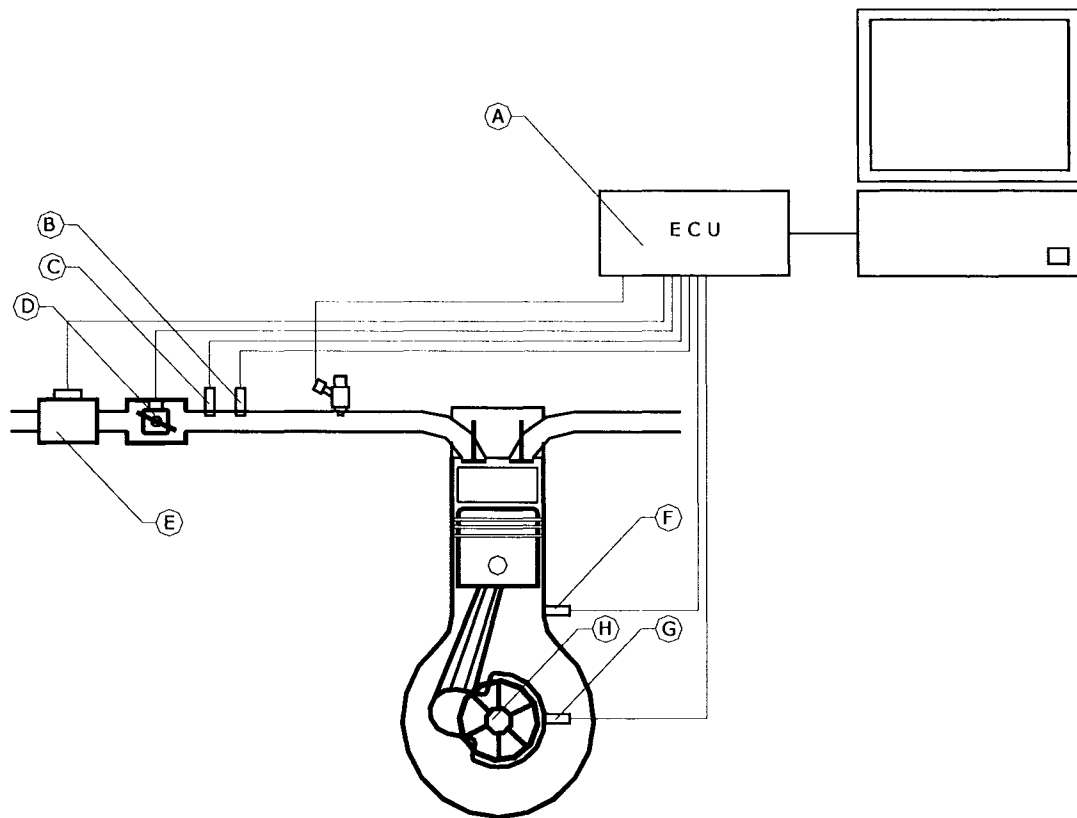


Figure 37: Schematic of the ECU system.

The proposed ECU system is fully programmable ECU with a programmable fuel map. The ECU chosen for our apparatus was purchased from 034EFI, known as 034 ECU Model # Stage 3b, and is shown in Figure 38. 034EFI developed a fully programmable ECU that is used by automotive performance enthusiasts who desire greater fuel tuning capability.

The 034ECU was ideal for our application because of the many features and programmability. The 034ECU features a high-speed microprocessor controller along with specialized control circuitry, which allow for simple but effective fuel and ignition control system. However, since HCCI does not require a spark ignition system, only the fuel controller of the ECU will be utilized.

The ECU uses the speed density method for fuel calculation. The ECU gets trigger information from the hall sender or a timing wheel, and injects fuel with a pulse width that is proportional to engine load and speed. The ECU determines engine load and speed by inputs from the throttle position sensor and manifold pressure. The 034 ECU uses several other sensors in order to

precisely control any engine. Additionally, all parameters are variable and therefore the ECU can be adapted to run on any engine.

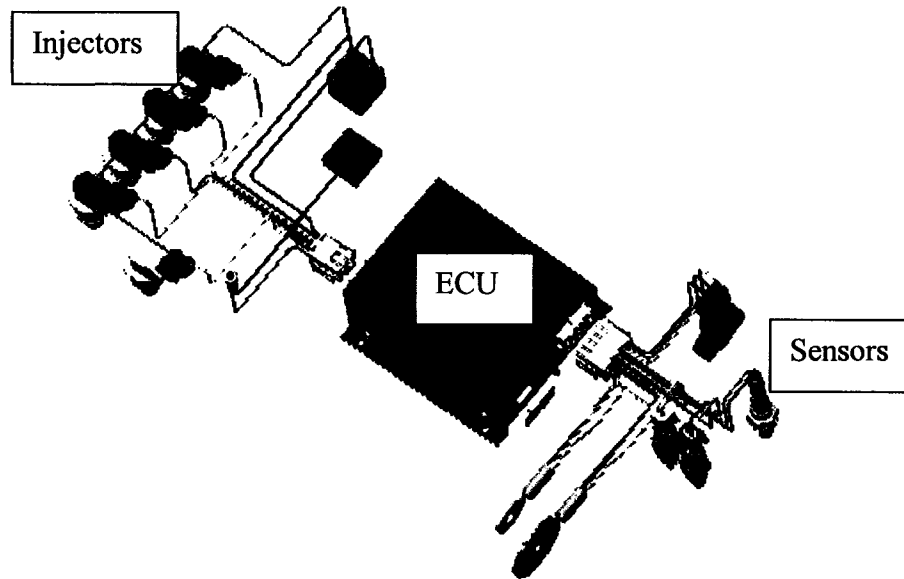


Figure 38: Fully programmable ECU from 034EFI Model Stage 3b [51].

The 034 ECU comes with PC based user interface that allows the user to program all parameters and sensors in an efficient manner. Also the software allows the user to monitor the performance of the engine in real time (see Figure 39), and program the fuel map (Figure 41.) Since the ECU is a commercially available product, it satisfies the second design constraint of the system.

The equivalence ratio value for each RPM and throttle position is normally set to 1.0, since the 034ECU is designed for stoichiometric operation of gasoline spark ignition. These values can be modified from 0.0 to more than 1.0 by the user quite easily and therefore satisfies the first constraint of the system. Secondly, since the software interface is easy to use, the 034ECU satisfies the third constraint as well. Therefore since the 034ECU satisfies all three design constraints, it is a good selection for use with the research engine.

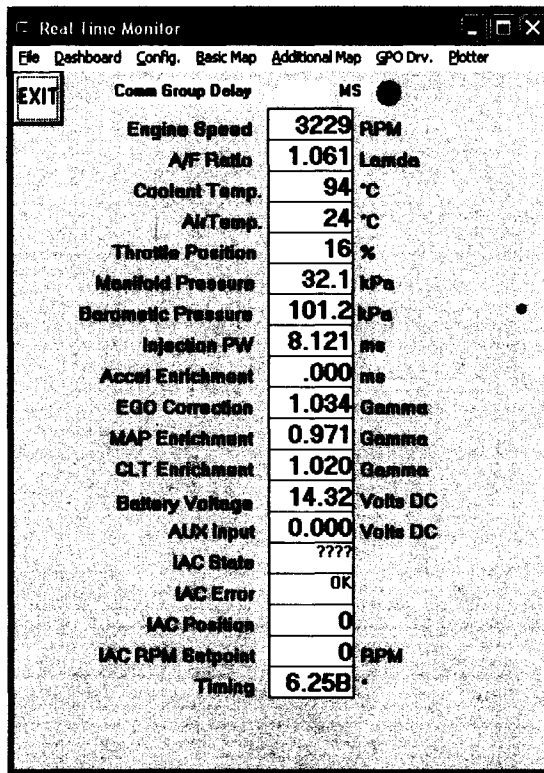


Figure 39: The 034EFI ECU interface software for monitoring engine performance in real time [51].

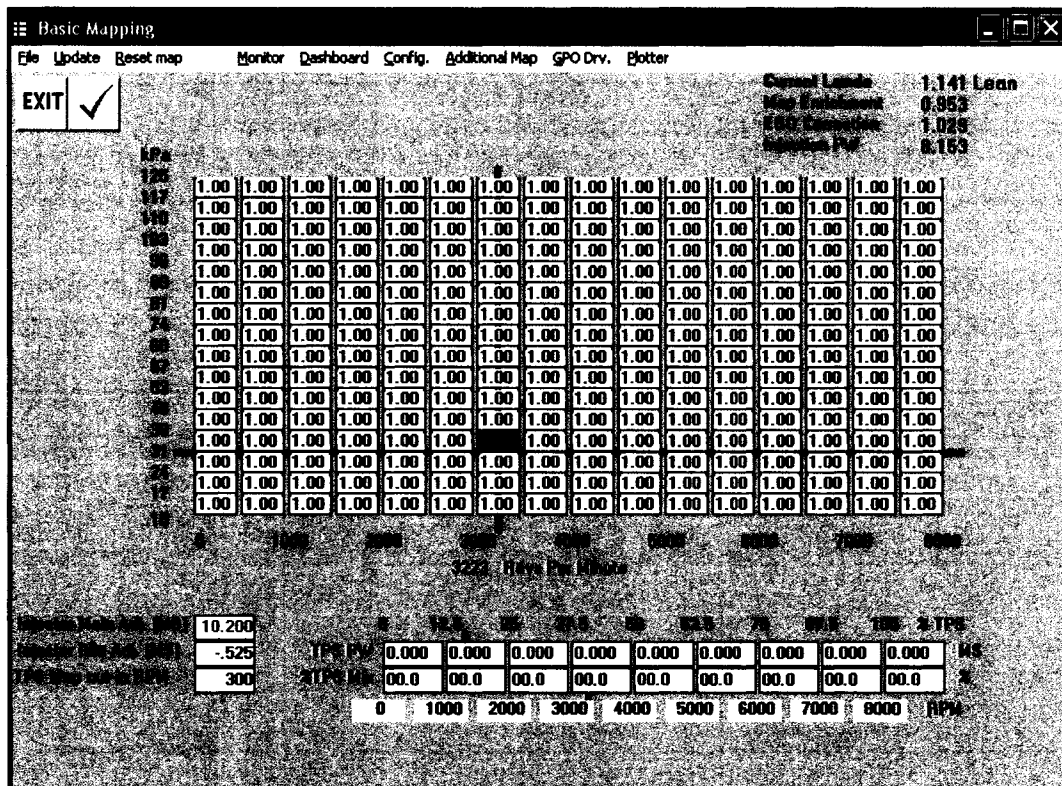


Figure 40: Basic fuel mapping user interface for programming 034 ECU [51].

4.10 Data Acquisition System

Data acquisition is the process of gathering information in an automated fashion from analog and digital measurement sources such as sensors and devices under test. Data acquisition uses a combination of PC-based measurement hardware and software to provide a flexible, user-defined measurement system [53].

The design objective of the DAQ system is to provide a direct means of measurement of the temperature, airflow, crank angle, and in-cylinder pressure. The design selection constraints are listed below:

1. The data acquisition system shall have software graphic user interface (GUI) with a personal computer such all the measurements can be monitored and acquired.
2. The data acquisition system shall be comprised of commercially available components.
3. Functional requirement of the DAQ system accuracy of 1/10 °CA at 2000 RPM.

The schematic of the data acquisition system is presented in Figure 41, and the legend is presented in Table 21.

Table 21 Legend for data acquisition system.

Item letter in Figure 42	Description
A	T1 Intake Air Thermocouple
B	Meriam Laminar Flow Element
C	T2 Heater Thermocouple
D	T3 Mixture Thermocouple
E	In-cylinder pressure transducer
F	Crank Encoder
G	T4 Exhaust Thermocouple
H	T5 EGR Thermocouple
I	T6 Coolant Thermocouple
J	Kistler Charge Amplifier
K	LFE Transmitter
L	24 Volt Power Supply
M	Data Acquisition Card
N	Terminal Box
O	Quick Connector Box

The DAQ system hardware along with functional group is comprised of several sensors. Six Omega K-type thermocouples are used for temperature measurement of the intake, heater, fuel

mixture, exhaust, EGR, and engine coolant. A Kistler 6052A pressure transducer is used for combustion event measurement.

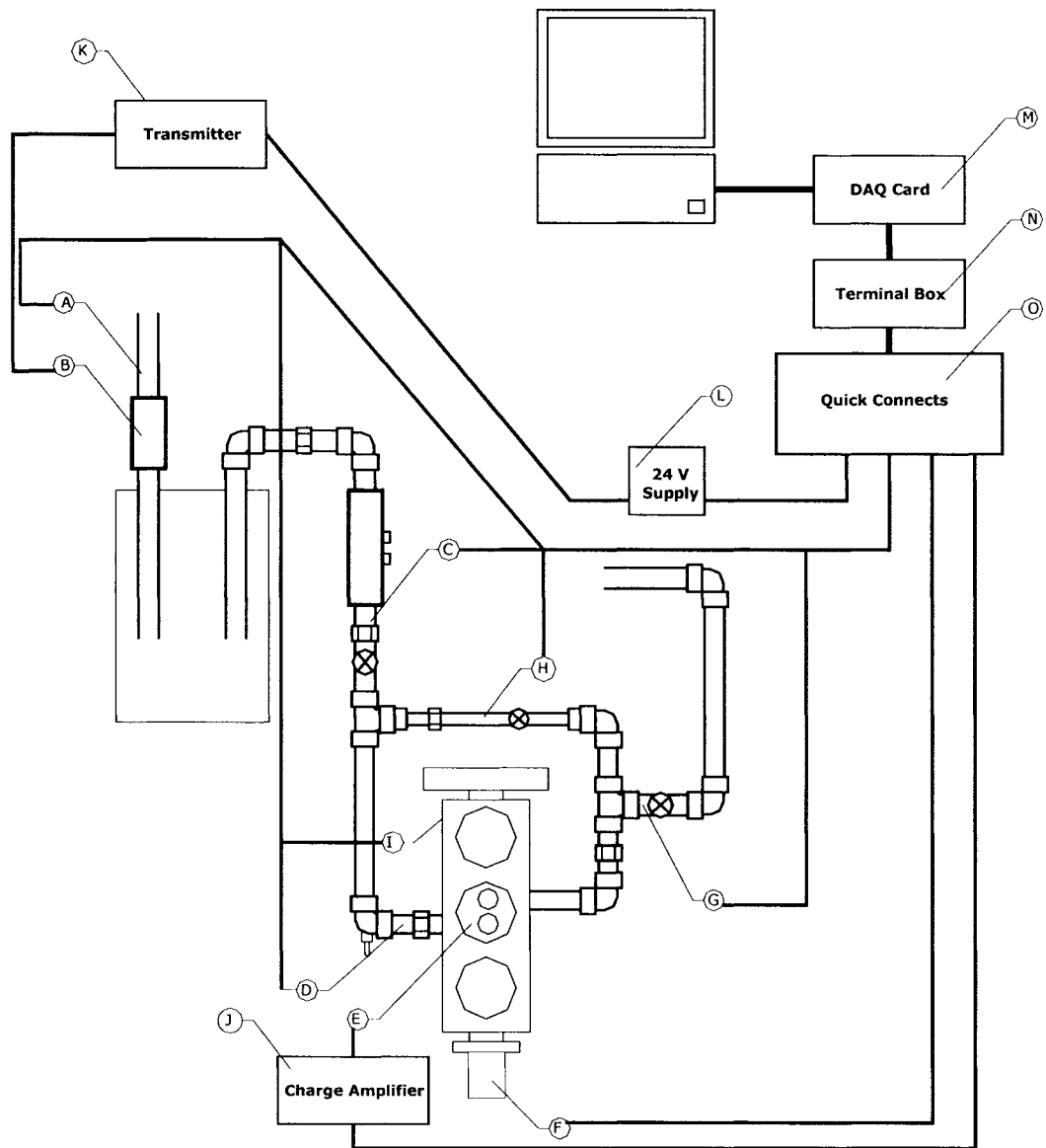


Figure 41: Schematic of data acquisition system.

A Kistler 5004 charge amplifier is used pressure transducer signal amplification. A Meriam 50MC2-2 laminar flow meter is used for intake air measurement. Honeywell ST3000 differential pressure to current converter is used for intake air measurement.

A 24 V power supply is used to power the Honeywell ST3000. Gurley rotary encoder is used for crank angle measurement. A custom fabricated connector box is used to provide a quick connect

interface for all the sensor connections and a National Instruments SCB-10 terminal box is housed inside. The connector box is connected via cable to a National Instruments PCI-6071-E data acquisition card. A 3.0 MHz Dell personal computer is used as the user interface. Further details of the data acquisition system are available in Appendix J.

A summary of the each device selected as it pertains to the data acquisition system as well as its intended purpose in controlling the HCCI engine was modified with permission from Defoe [52].

4.10.1 Thermocouple Selection and Location

The thermocouples selected were Omega K-type thermocouple probes with quick disconnect. These thermocouples are the most popular calibration and are well suited for measuring air and liquid mixtures in temperature range from -270 to 1372 °C, more than adequate for this application. The Omega K-Type thermocouples are of high quality and low cost and feature nylon connectors that are rated for temperatures up to 220 °C. The probes are available in diameters as small as 0.25 mm (0.010 in) and as large as to 3.0 mm (0.125 in). Therefore, these thermocouple probes are ideal for this research engine and meet the selection criteria.

The six thermocouples selected are part of the DAQ system and are show in Figure 41. Thermocouple T1 is located at the beginning of the intake (A) and measures the intake air temperature. Thermocouple T2 is located just after the charge pre-heater (C) and is used to determine the temperature increase after the pre-heater. Thermocouple T3 is located at the end of the intake manifold (D), just before the intake valve and is used to determine the charge temperature just before the mixture enters the engine. Thermocouple T4 is located in the exhaust (G), and is used to monitor the temperature of the combustion products exiting the active cylinder. Thermocouple T5 is in the EGR pipe (H) and is used to determine the temperature of the gases entering the intake manifold. And lastly thermocouple T6 is set into the cylinder head at (I), and is used to monitor the coolant temperature.

4.10.2 Pressure Transducer Selection

The in-cylinder pressure transducer is a wall-mounted Kistler 6052A1. According to Kistler it is the most accurate non-cooled transducer for in-cylinder pressure available on the market. The Kistler 6052A1 was selected because of its availability, reliability and accuracy.

The sensing element of the transducer is inserted into a hole drilled into the secondary piston located in the cylinder head and is the pressure sensing tip is exposed to the combustion chamber. The pressure sensing tip of the transducer face is to be 4mm from the combustion chamber wall. The element is cooled by heat transfer to the cylinder head water-jacket in order to reduce the effect of thermal shock.

The pressure transducer outputs a charge (Q) proportional to the gauge pressure (p_{cylinder}) according to the following formula:

$$Q = m \cdot p_{\text{cylinder}}, \quad \text{Equation 11}$$

Where $m = 19.2 \text{ pC/bar}$ [23]. See Appendix J.6 for calibration certificate.

This transducer is designed to operate in the pressure range from 0 to 250 bar suitable for HCCI chamber pressures. Kistler pressure transducers are known as the industry standard for in-cylinder pressure measurement, and are widely used by major automakers, research labs, and universities for accurate data collection. Specifications are available in Appendix J.3 and J.5.

4.10.3 Charge Amplifier Selection

The Kistler 5004 Charge Amplifier is necessary component that accompanies the Kistler 6052A1 pressure transducer. The Kistler Charge Amplifier converts the charge signal output from the Kistler pressure transducer to a voltage signal that is easily read by the data acquisition (DAQ) card, (see Figure 42.)

There are two selector knobs that control the settings of the amplifier: one specifies the sensitivity of the input device in picocoulombs per mechanical unit (pC/bar); the other specifies the output gain of the amplifier in mechanical units per Volt (bar/Volt). Since the DAQ card can handle signals only up to 5 Volts, and the expected maximum pressure to be measured is 100 bar, the required gain (G) setting is determined by the equation:

$$G = \frac{100 \text{ bar}}{5 \text{ V}} = 20 \frac{\text{bar}}{\text{V}}, \quad \text{Equation 12}$$

Charge amplifier specifications are listed in Appendix J.3.

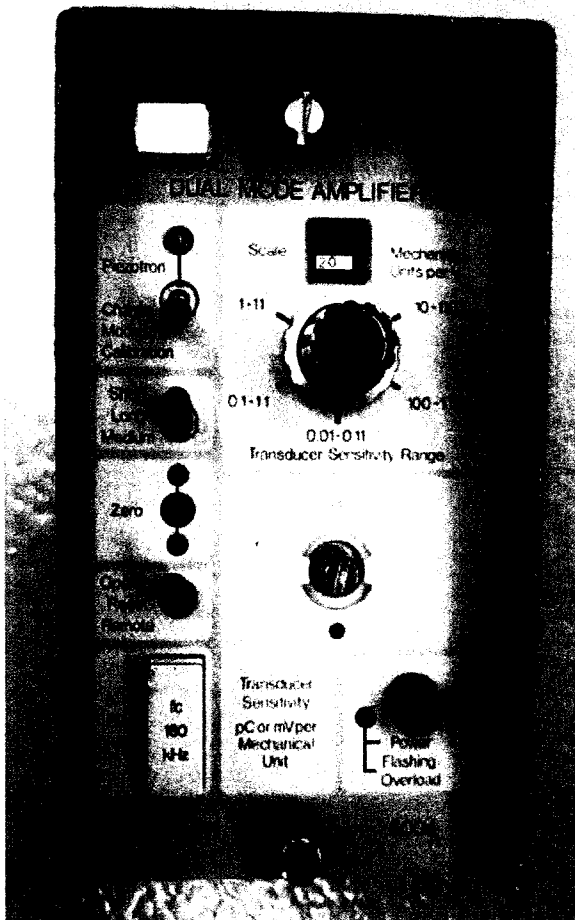


Figure 42: Kistler 5004 dual mode charge amplifier.

4.10.4 Differential Pressure to Current Converter

The Meriam 50MC2-2 laminar flowmeter selected earlier in Section 4.5.2 is used to measure the volumetric flow rate of the air entering the intake system. The flow rate is significant for determining the amount of fuel to inject to obtain the desired mixture equivalence ratio. The flow rate \dot{V} (cfm) and differential pressure Δp measured by the meter are related by the quadratic function:

$$\dot{V} \text{ (CFM)} = 12.6268 \cdot \Delta p - 0.0173314 \cdot \Delta p^2, \quad \text{Equation 13}$$

Where Δp is inches of H₂O.

The meter can accurately measure flowrates of up to 100 cfm which corresponds to a differential pressure of 254 mm (10in) of H₂O, see certificate of calibration in Appendix G.5.

The Honeywell ST 3000 Smart Transmitter, selected in Section 4.5.3, converts the differential pressure output from the flow meter into an electric current that can be read by the DAQ card. The transmitter converts the differential pressure range of 0 to 10 inH₂O to the current range of 4 to 20 mA, linearly as shown in the equation:

$$\Delta p = 625 \cdot I - 2.5, \quad \text{Equation 14}$$

where I is current in amperes.

Thus, after substitution into the equation above the final conversion from current amperage to flow rate [cfm] is given by:

$$\dot{V} = [-6770.07813 \cdot I^2 + 7945.91063 \cdot I - 31.67532], \quad \text{Equation 15}$$

Conversion to units of L/s is given by:

$$\dot{V} = 0.4719 * [-6770.07813 \cdot I^2 + 7945.91063 \cdot I - 31.67532], \quad \text{Equation 16}$$

for the range of I from 0.004 to 0.020A.

4.10.5 24 Volt Power Supply

The 24 Volt power supply was obtained to provide the Honeywell ST 3000 with correct and adequate electrical power. The supply will be connected in parallel between the transmitter and a shunt resistor, with a resistance of R = 350 Ω. The resistor is necessary to ensure that the transmitter is not overloaded with current. The selection of this power supply was a simple task, and was purely based on functionality, and cost effectiveness.

4.10.6 Rotary Encoder

A rotary encoder is an optical digital device that outputs square-wave pulses with a period equal in length to 1/10 of a degree or higher depending on the requirements. A rotary encoder is required to provide means of reference for our in-cylinder pressure data, and temperature data. There are several encoders on the market for this application, but the Gurley model 9125S was selected because of its durability, accuracy, and cost effectiveness.

The Gurley encoder has three output channels that go to the DAQ card from the encoder [53]. Two channels, namely channels A and B, output a square wave every single 1/10 of a °CA that the encoder rotates. These two signals are 180° out of phase with each other. The third output

signal, named Index H, also outputs this square wave, however it only outputs one pulse every full revolution of the encoder, see Figure 43 for further details.

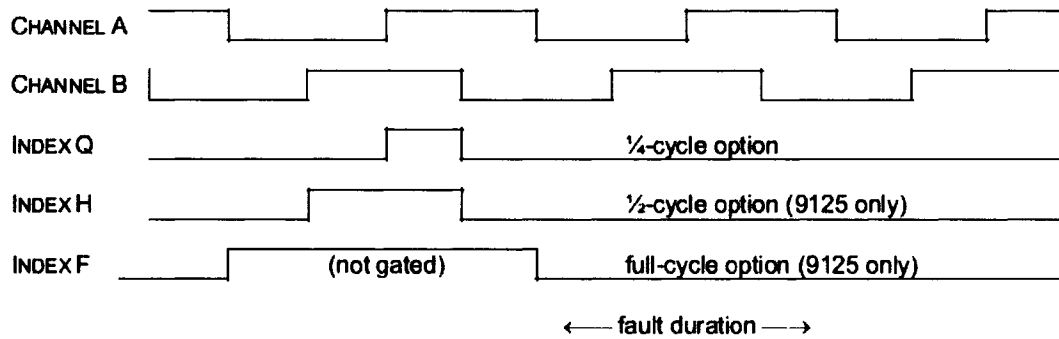


Figure 43: Gurley Encoder Output waveform [53].

Notice that Channel A and B are 180 degrees out of phase and the Index H only occurs once every revolution. This signal is matched with the test cylinder of the engine to correspond with TDC and is the reference or 0 °CA.

Therefore, the Gurley Model 9125S meets the design selection constraint for the data acquisition system, since it is cost effective, durable and accurate.

4.10.7 DAQ Card

A data acquisition (DAQ) card is a hardware electronic device that allows the computer to interface with sensors that sense the physical phenomenon, such as temperature and pressure. For our system a high speed data acquisition card is required to be able to acquire pressure data of the combustion event.

The National Instruments PCI-6071-E card was selected for this application, because it can acquire data at a maximum rate of 1.25 mega-samples per second [54]. Appendix J.6 has further details.

The nine signals that the DAQ card must read for the current data acquisition task are: six thermocouples, pressure transducer, flowmeter, and encoder Index signal. Thus the available sampling rate (\dot{N}_{sensor}) per channel is determined using the following equation (see Appendix J.7 for detailed calculations):

$$\dot{N}_{sensor} = \frac{\dot{N}_{card}}{N_{sensors}}, \quad \text{Equation 17}$$

$$\dot{N}_{sensor} = \frac{1.25 \times 10^9 \text{ samples / sec}}{9},$$

$$\dot{N}_{sensor} = 138,888.8 \text{ samples / sec},$$

Since there is a switching delay between channels, a maximum rate of approximately 90% of this value so \dot{N}_{sensor} becomes 125,000 samples/sec. Recall that the functional requirement of the DAQ system is an accuracy of 1/10 °CA at 2000 RPM. The required sampling rate ($\dot{N}_{required}$) for this is determined from the following equation:

$$\dot{N}_{required} = \omega \cdot N_{datapoints} = 33.3 \cdot 3600 = 120,000 \frac{\text{samples}}{\text{sec}} \quad \text{Equation 18}$$

Where $N_{datapoints}$ is the number of data points per crank angle degrees.

$$N_{datapoints} = 10 \frac{\text{pts}}{\text{CAD}} \cdot 360 \frac{\text{CAD}}{\text{rot}} = 3600$$

and ω is the angular engine speed calculated from the following,

$$\omega = 2000 \text{ rpm} \cdot \frac{1 \text{ min}}{60 \text{ s}} = 33.3 \frac{\text{rot}}{\text{s}},$$

Thus, the required sampling rate $\dot{N}_{required}$ is less than the \dot{N}_{sensor} available sampling rate.

The maximum sampling rate of the DAQ card is 125000 samples per second. The encoder rate is determined by the angular velocity of the crankshaft for a given engine speed multiplied by the # of encoder ticks per revolution which is 3600. At 2084 RPM the encoder rate exceeds the maximum sampling rate of the DAQ card. Therefore, achieving data acquisition at engine speeds higher than 2000 RPM is not technically possible with the current DAQ card. It should be noted out that the DAQ card selection was completed by a previous student. Therefore, the National Instruments PCI-6071-E DAQ has fulfilled the resolution requirement for up to 2000 RPM, however is not able to provide sampling at a higher engines speeds (see Table 22.)

Table 22 DAQ card limitations compared to encoder sampling rate.

Engine (RPM)	Angular Speed rot/s	Encoder rate samples/sec
0	0	0
250	4.166667	15000
500	8.333333	30000
750	12.5	45000
1000	16.66667	60000
1250	20.83333	75000
1500	25	90000
1750	29.16667	105000
2000	33.33333	120000

4.10.8 Terminal Box

The National Instruments SCB-100 terminal box is the connection between the sensors and the DAQ card. The circuit board in this box contains connections for 100 pins. The board features analog and digital channels, as well as support for external counters. It has an on-board temperature sensor that can be used as cold-junction compensation for any thermocouples wired to the board [54]. Appendix J.8 lists all connected pins, the DAQ channel associated with the pin, and what device is connected to each pin. The National Instruments SCB-100 terminal box makes connecting sensors easy and reliable.

4.10.9 Connector Box

Mr. Patrick Seguin fabricated the connector box to make connecting and disconnecting devices from the terminal box easy. It is made of steel sheets and the front panel has the layout shown in Figure 44. The pressure transducer (via the charge amplifier) is connected to the BNC 1 input, and the flow meter (via the transmitter) is connected to the BNC 2 input. The encoder is connected via the DB 15 connector. The thermocouple connectors are connected in a straightforward manner (T1 to T6.) The LED illuminates when the encoder Index signal is transmitting the ON value, that is, the engine is at TDC. This can be used when manually

rotating the crankshaft to verify that the synchronization of the encoder index H signal and the TDC of the test cylinder with is attained and functioning correctly.

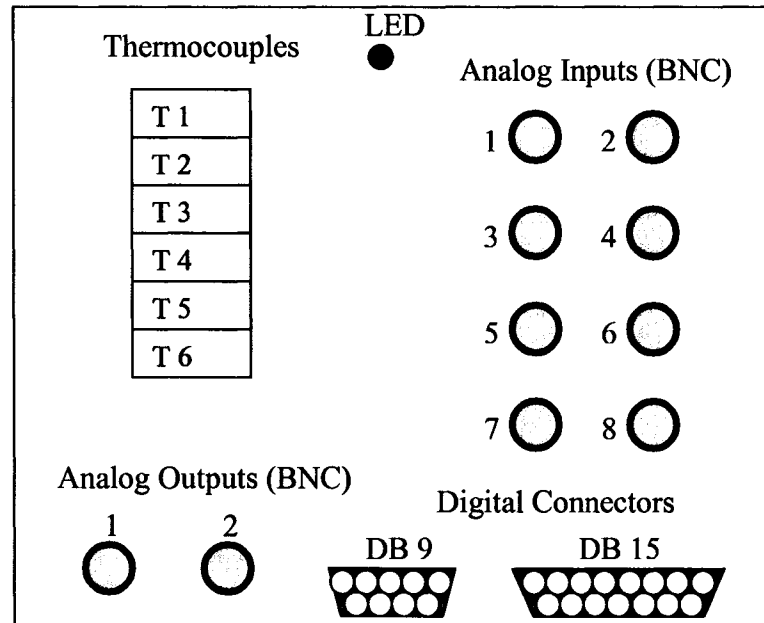


Figure 44: Connector box front panel layout.

The outputs from the connectors go to the National Instruments SCB-100 terminal box that is located inside the connector box. The connector box makes it quick and easy for all the sensors to be connected and disconnected. Also, the box was purchased from Electrozaad Ltd. and is a low cost commercially available product.

4.10.10 Personal Computer and Labview Program

The personal computer (PC) along with the Labview data acquisition software is the user interface for the research engine. The PC used has an Intel Pentium 4 3.0 GHz processor with 1 GB of RAM and 120 GB hard drive running Microsoft Windows XP and Labview 7.1. The PC enables the data acquisition criteria to be met. With the PC and data acquisition system the user is able to monitor the status of the temperatures and engine speed, as well as the in-cylinder pressure on a cycle-by-cycle basis. The DAQ system also allows the user to monitor the airflow, and has the option of controlling the intake air heater remotely.

Labview 7.1 software was used to develop the data acquisition program along with the GUI. This program will be used to control the channels from the DAQ card for acquiring data, the sampling rate, as well as nearly every other configurable setting related to the system.

The components of the DAQ system were selected to meet the constraints of the system. All components were commercially available, the graphic user interface developed in Labview is easy to use, and a DAQ card was selected to meet the constraint for sampling rate. For further details of the Labview program and the user interface consult Defoe [52].

4.11 Summary

In summary, all the systems of the HCCI research engine have met design constraints and should provide functional, safe and reliable service for the combustion lab.

5 FABRICATION AND PROTOTYPING

The purpose of this section is to detail the fabrication and prototyping phase of the research engine project. This section discusses fabrication details in chronological order. These details include the following; prototype development, design methods, fabrications materials and methods, any difficulties, and final product description.

5.1 Apparatus Fixture Prototyping

The objective of the apparatus fixture is to provide the structural skeleton for which all the other components of the apparatus can be mounted. The apparatus fixture design must provide a solid mounting point for the research engine and the AC motor. The design of the fixture must also provide adequate space for the VSD, resistor bank, transformer, fuel system, cooling system, and the intake/EGR systems.

The fixture designs were produced using AutoCAD and are presented in Figures 45 and 46. In both figures the units of measure are in inches to simplify fabrication. The fixture table height of 88.9cm (35 in) was selected to provide easy access to the systems of the research engine that require the most adjustment (ie; intake and fuel systems.) The width and length were limited by the 1.52 x 2.133 m (5 x 7 ft) bolster plate. Consideration was also given to frame materials and sizes. The heaviest components namely the Kubota engine and AC motor are supported by a rectangular steel frame constructed of 5.04 x 5.04 cm (2 x 2 in) rectangular steel tubing. The lighter components are supported on 2.54 x 2.54 cm (1 x 1 in) rectangular steel tubing. Welding and fabrication was performed by Marc St. Pierre according to ASTM standards to ensure structural rigidity and alignment [56].

Photographs of the final apparatus fixture design are presented in Figures 47, 48 and 49. Adjustable fixture feet were designed to have the ability to accept castors and also to rigidly mount the fixture to the bolster plate (Figure 49). The castors enable the fixture to be rolled around the machine shop during the fabrication phase and also made it easier to transport to the combustion lab. Once the final position was determined the fixture was secured with levelling fasteners to the bolster plate to provide added stability.

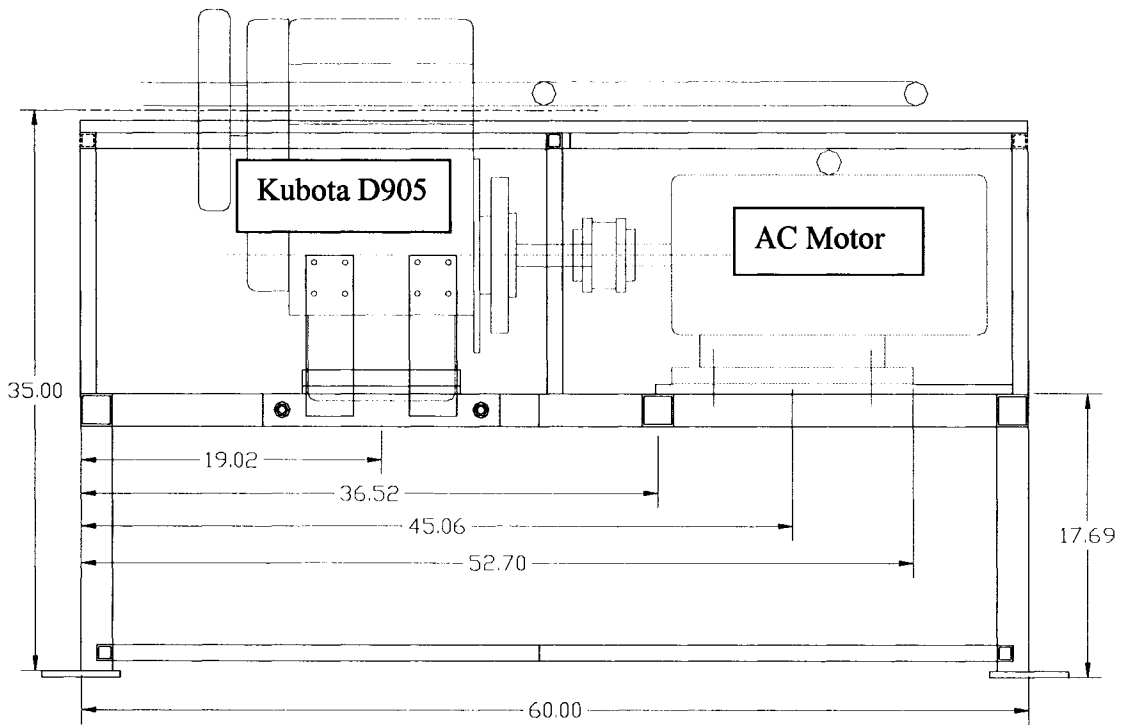


Figure 45: Front View of the fixture frame.

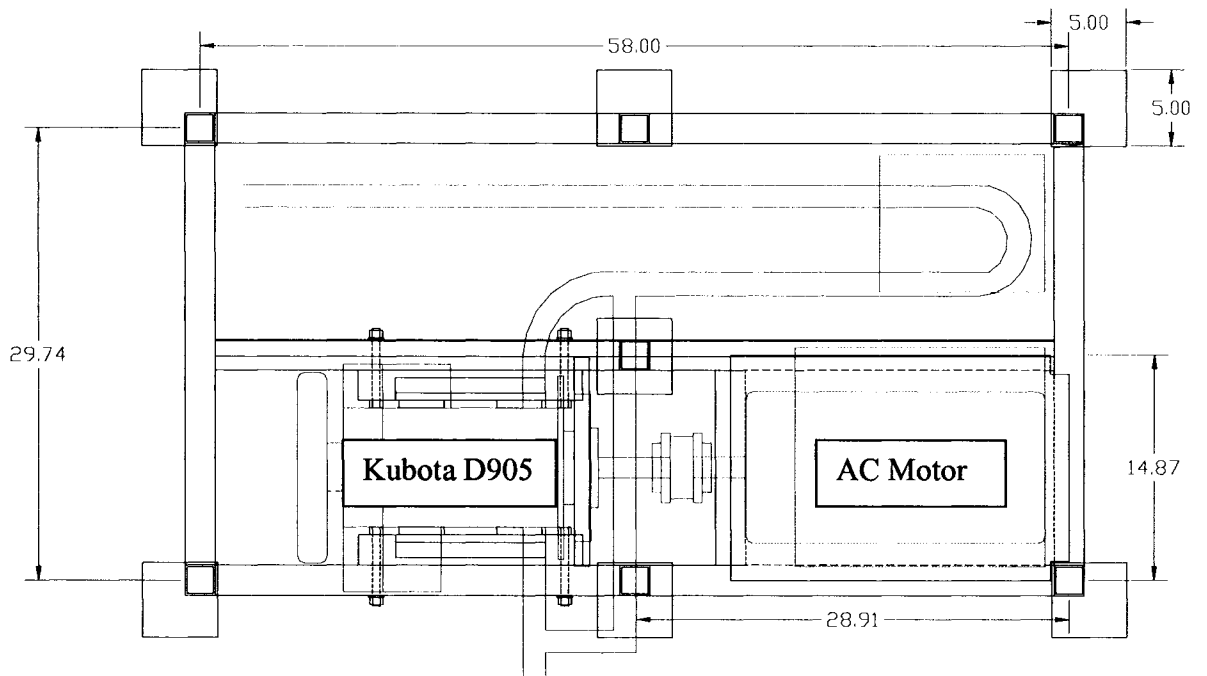


Figure 46: Top View of fixture frame.

Galvanized sheet metal was utilized both as the top shelf and as the lower shelf. This material was chosen for its anti-oxidation properties and cost effectiveness compared to stainless steel (see Figure 47). An additional center beam frame support was added to help stabilize and distribute the load of the engine and AC motor to the ground, shown if Figure 48.

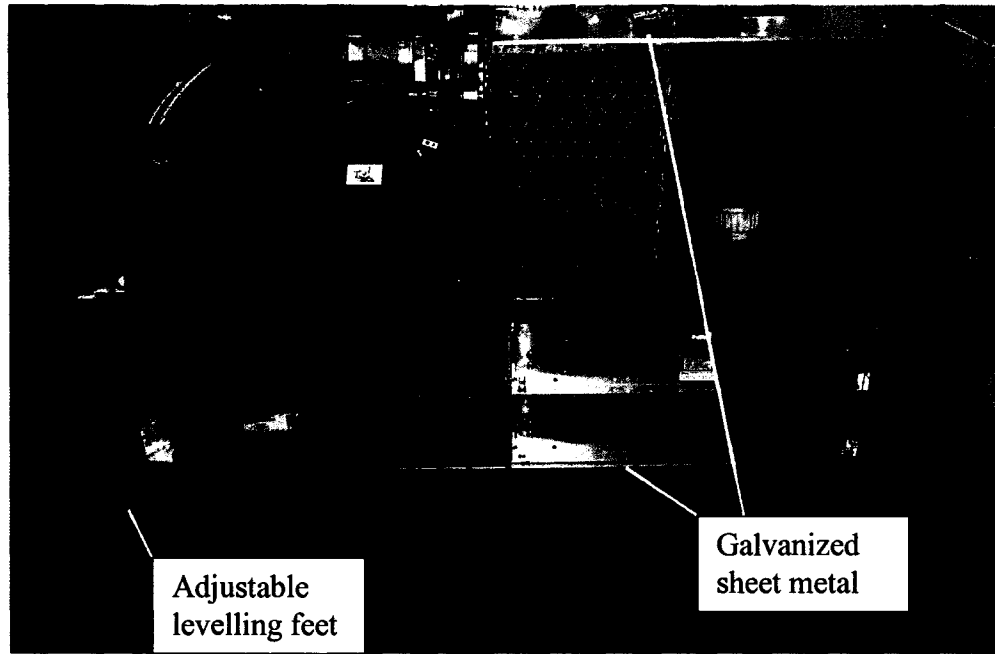


Figure 47: Front View of fixture frame.



Figure 48: End view of fixture frame.



Figure 49: Adjustable levelling feet.

5.2 Drive System Installation

The installation of the drive system was a significant portion of the project. The major components of the drive system are; VSD, AC motor, resistor bank, chopper module, disconnect and transformer and are shown below in Figure 50. All the components of the drive system were installed by Marc St. Pierre of Technical Services [56]. The electrical wiring of the drive system was performed by Tricon Ltd. and electrical component selection was advised by Phil Diett of Physical Plant and Dave Dumachelle of Electrozaad [57, 58].

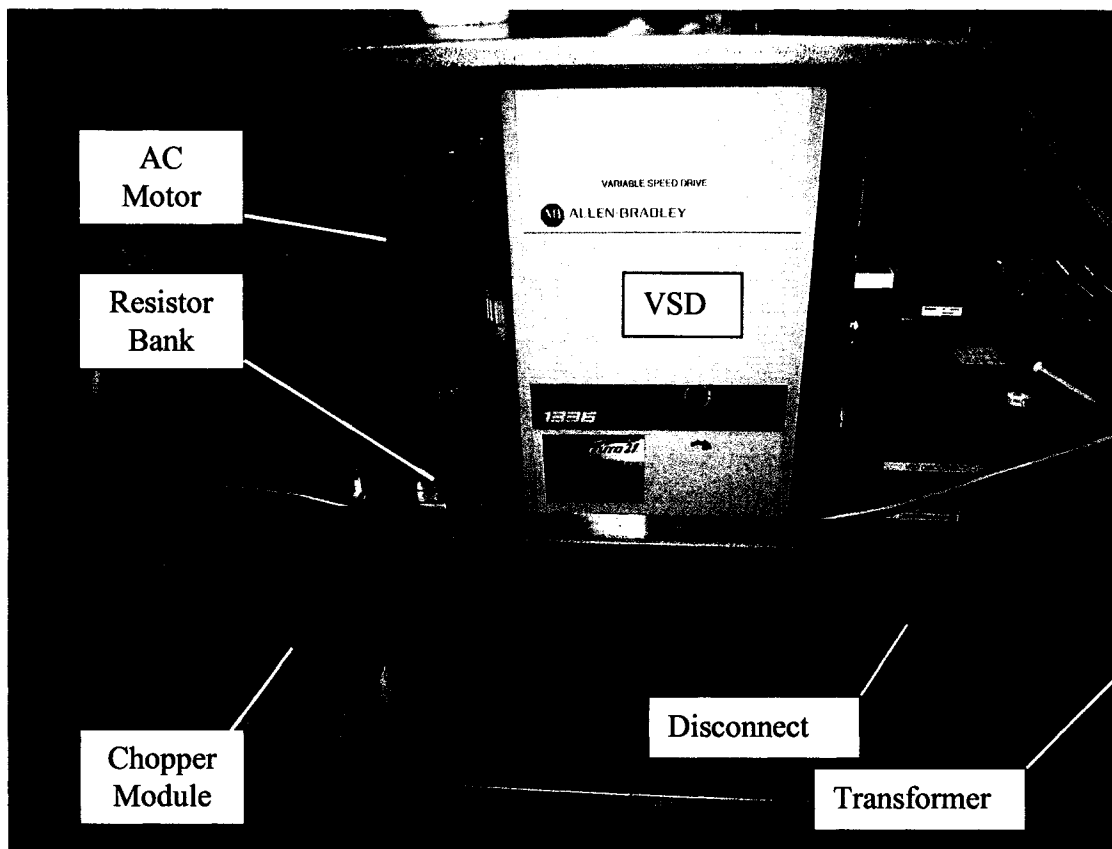


Figure 50: Installation of variable speed drive system.

The VSD was installed in a convenient upright position located in the middle of the of the apparatus fixture. Sufficient clearance was ensured between the VSD and the fixture to ensure access to the service panel. Dave Dumachelle made recommendations based on the VSD installation requirements [58]. These requirements suggest that the VSD be located within 10 feet of the AC motor and resistor bank. In its current location the VSD installation meets that requirement.

The AC motor was mounted directly to the apparatus fixture frame with its own mounts. The surface of these mounts was machined to ensure the AC motor was square and level with respect to the fixture frame. The resistor bank was mounted in the space below the AC motor. The resistor bank location needed to be in close proximity to the chopper module and the AC motor, therefore this was determined to be an ideal location.

The chopper module installation requirements suggest that the distance from both the VSD and resistor bank be minimized or within 5 feet [58]. This was achieved by mounting the chopper module in the location shown in Figure 51. A cover plate was fabricated to cover the exposed connectors and prevent electrical shock.

A Rex Manufacturing auto-transformer was selected with the assistance of Phil Diett (see Figure 52).



Figure 51: Allen-Bradley Dynamic Braking/Chopper Module.

The step-down auto-transformer (shown in Figure 52) decreases the supply voltage from 600 V to 480 V. The VSD, AC motor and chopper module are all rated to operate at 480 V. Two disconnects were required for the drive system. The main power disconnect is located on the north-east wall in the combustion lab and features 600 V, 15 A fuses.



Figure 52: Rex Manufacturing Auto-transformer.

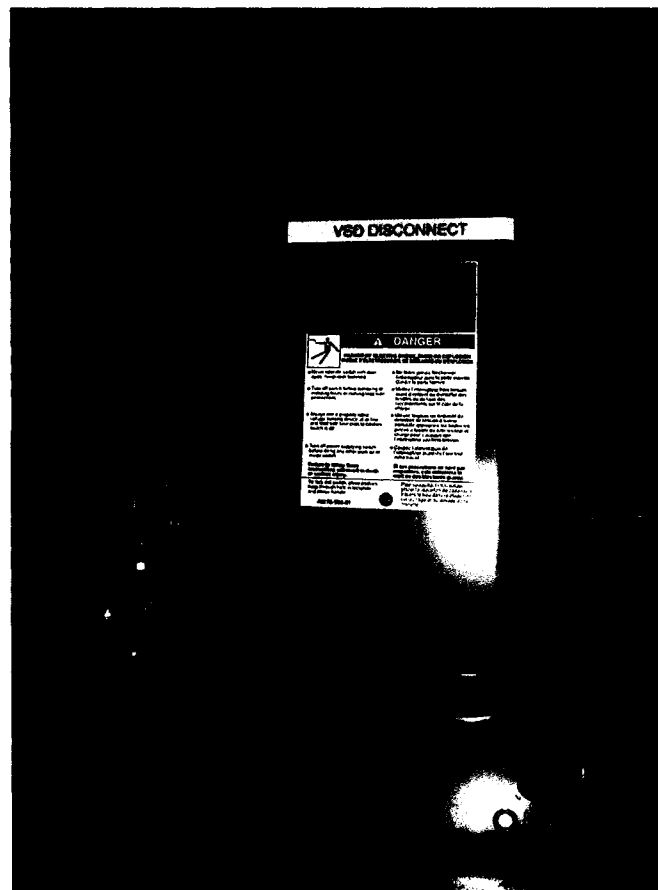


Figure 53: Square D 480 Volt, 25 Amp secondary disconnect.

The secondary disconnect (Figure 53) is located between the Rex auto-transformer and the VSD. The function of the secondary disconnect is to isolate the VSD from the main power, especially during energizing of the auto-transformer. The secondary disconnect features 480 V breakers with 25 A fast-response fuses.

5.3 Engine Installation

The installation of the engine required custom support fabrication and alignment of the output shaft to the AC motor output shaft. All of the fabrication was performed by Marc St.Pierre and this required some prototype design work on his part [56]. Marc St.Pierre was pivotal in determining the best concepts, and also able to execute them very well.

The conversion of the Kubota engine to a single cylinder engine required several modifications. Identification and removal of unnecessary components on the Kubota engine was performed. The valves and pushrods of the two unused cylinders were removed. This has the benefit of reducing friction losses on the engine however does create a slight unbalance for the engine. The injector pump was removed to reduce friction losses and also since diesel fuel injection is not required. Also the alternator was removed and is replaced by generic automotive battery charger that can use 115 V electrical service.

To countermeasure the unbalance issue of the modified engine, rubberized engine mounts were used with a custom engine mount bracket. Two custom fitted rubberized engine mount brackets were fabricated by Marc St.Pierre to help isolate the vibration and support the engine at the base [56]. The left engine mount is presented in Figure 54 below. The engine mount brackets are made out of rubber, and the support was fabricated using various sections of steel fitted and welded together. This engine mount bracket is easily removable and can be modified to accept different engine models if desired. Additionally, to align the engine output shaft with the AC motor shaft a third engine mount bracket was fabricated. This mount is also rubberized and has an adjustment to help align the engine to the AC motor. The third engine mount is shown in Figure 55. A stabilizer bar was also fabricated and installed to the fixture. This bar is rotated in place and is used to secure the engine while the upper engine mount is being removed or adjusted.

The engine and the AC motor are coupled together using the stub shaft and coupler shown in Figure 56. Two set screws were fastened in each hole and coated with Loctite sealer to prevent them from loosening during the severe vibration and high rotational speeds.

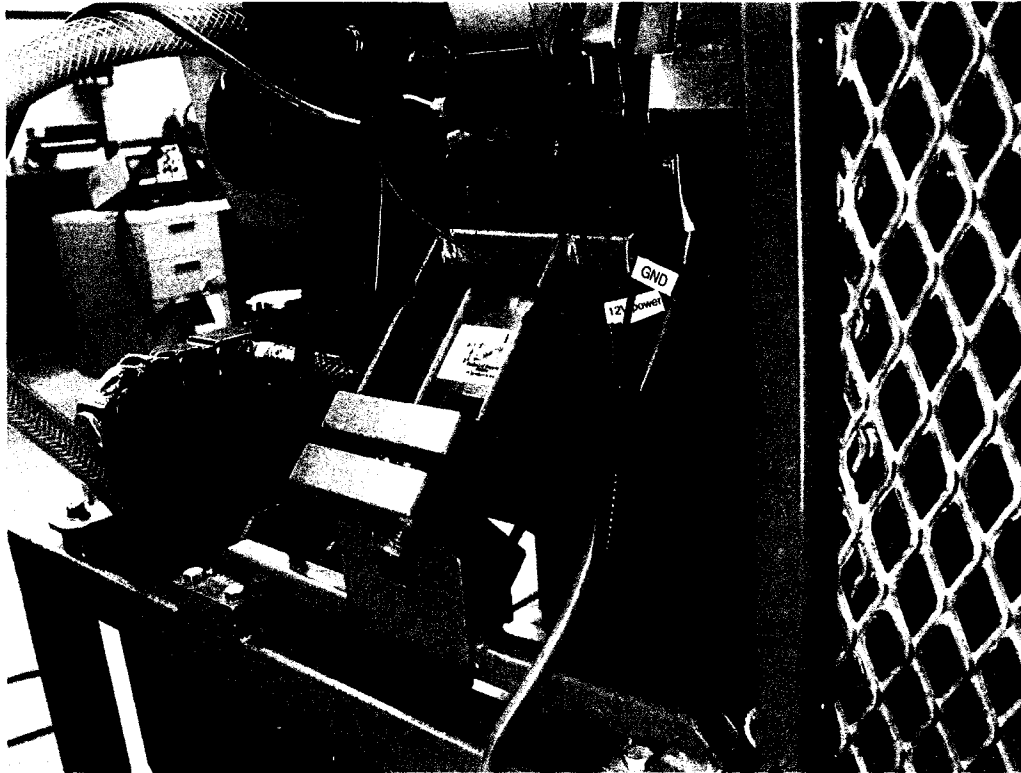


Figure 54: Custom fabricated engine mount bracket.

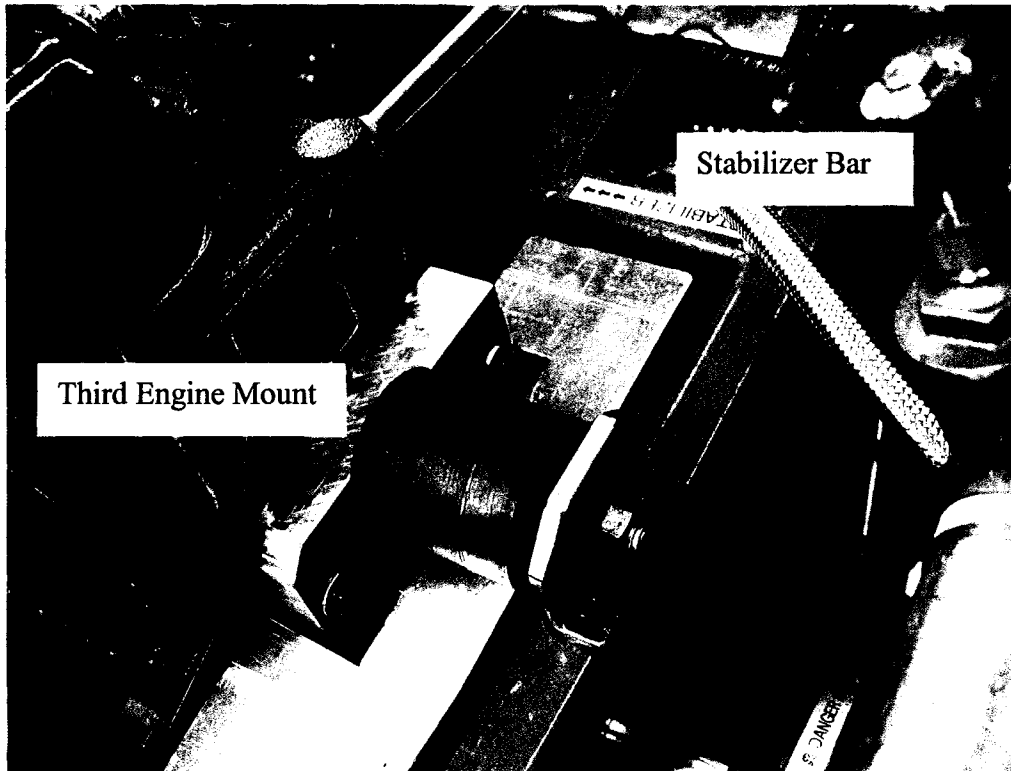


Figure 55: Custom fabricated upper engine mount.

The stub shaft was purchased directly from Kubota and was installed and torqued down to 40 ft-lbs using a torque wrench. Both shafts were aligned using a run-out indicator to ensure correct alignment. However, while the engine is being operated, the vibrations will result in a slight misalignment of the shafts. This out of alignment will be taken up by the rubberized spacer insert.

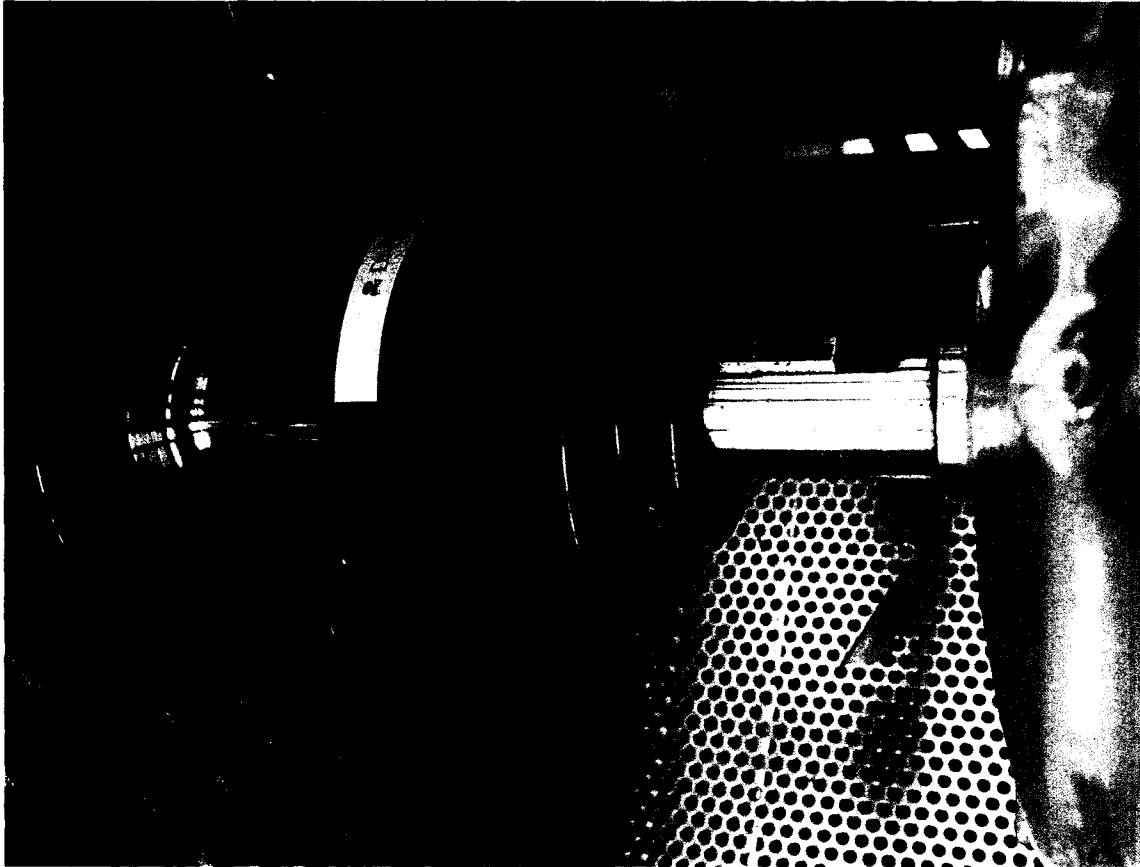


Figure 56: Coupler for AC motor and Kubota Engine.

5.4 VCR Secondary Piston Prototyping

The prototyping of the VCR secondary piston required custom fabrication and trial and error to develop the final product. All of the fabrication was performed by Marc St.Pierre [56]. The VCR secondary piston concept required fabrication of a secondary piston that can vary position relative to the cylinder head and hence vary the clearance volume and compression ratio. Additionally, the VCR secondary must have adequate sealing to ensure that no combustion chamber leakage occurs. By inspection of the bottom of the Kubota cylinder head in Figure 57, the prechamber is clearly visible. The original prechamber cap was removed for inspection, and the remaining two

original prechambers are visible. The threaded hole that accepts the original diesel fuel injector is also visible in this figure.

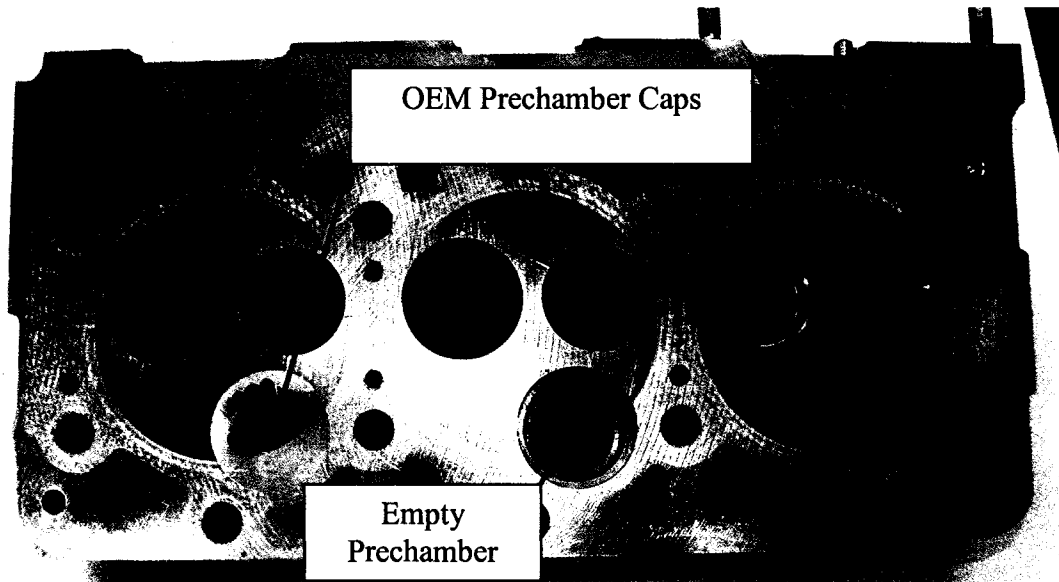


Figure 57: Kubota D905 Cylinder head ready for pre-chamber modifications.

It was determined that by making a piston with the same diameter as the fuel injector (1.732 cm) and with the same thread pattern, the existing hole could be used, and only a slight modification would have to be made to the cylinder head (boring it through.) The position of the VCR secondary piston could be varied by simply threading the piston in and out of this hole; threading in decreases the CR, and threading out increases the CR. It was already shown in Chapter 4, and Appendix B.7 that two prechamber caps installed separately will be needed to achieve the required compression ratio range of (15 to 25:1).

Figure 58a illustrates a copper spacer that will be used in conjunction with the VCR secondary piston. The copper spacers have two functions. Firstly, to provide adequate spacing to achieve the desired prechamber volume, and secondly to create a seal between the VCR piston, threads, and the cylinder head. The sealing surface on the cylinder head was machined flat to ensure a clean, tight seal.

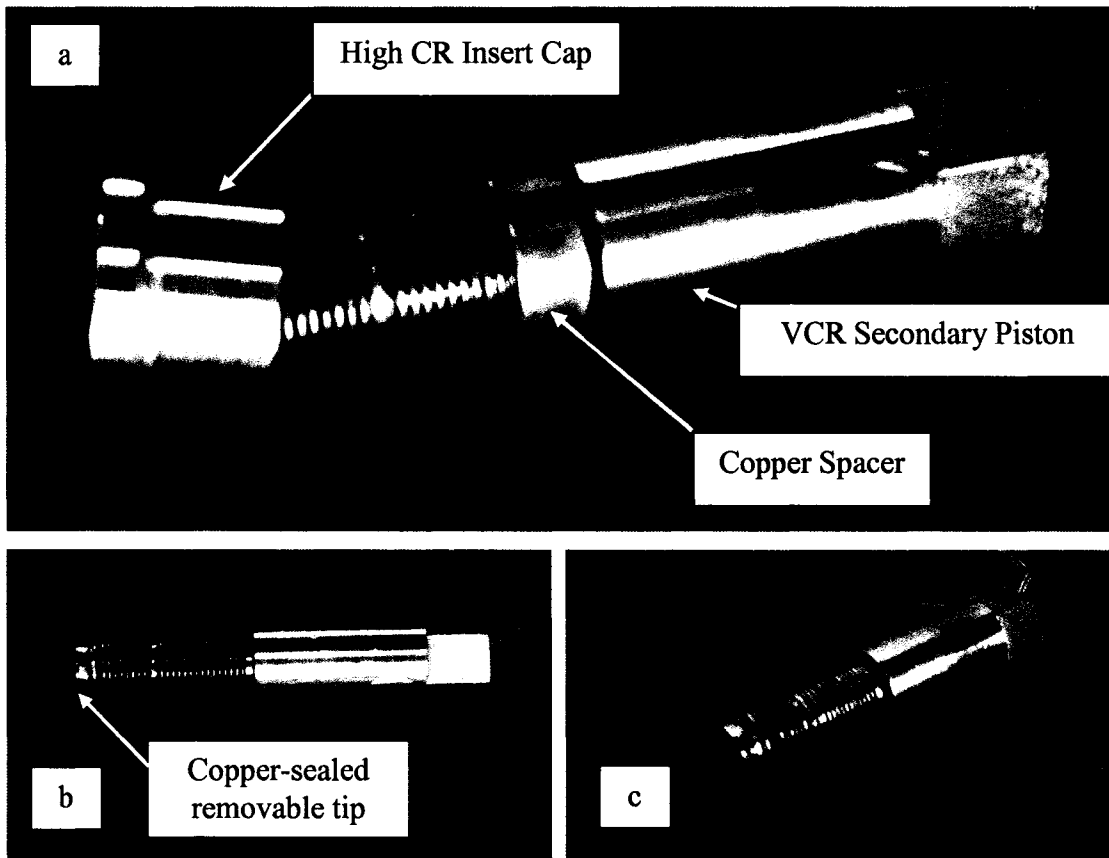


Figure 58: (a) VCR secondary piston components, (b) VCR secondary piston side view, (c) View of VCR secondary piston tip.

Shown in Figure 58b and 58c is the view of the tip of the VCR secondary piston. This custom tip contains the Kistler 6052 pressure transducer installed according to manufacturer specifications (recessed 4mm). The custom tip is removable and the tight seal is achieved with compression of the copper washer by extreme tightening.

Figure 59a illustrates the installation of the assembled VCR secondary piston along with copper spacer. The VCR is turned by hand until it reaches the bottom. It is then tightened by a torque wrench to 50 ft-lbs. The prechamber view of the VCR secondary piston is visible in both Figure 59c without a prechamber insert cap, and in Figure 59d with the Low CR prechamber insert cap. The prechambers were machined using high grade steel and are machined to a press fit tolerance. Once the prechamber insert cap is placed in the correct location as shown in Figure 59d, it is press fit and machined flat using a cylinder head grinder.

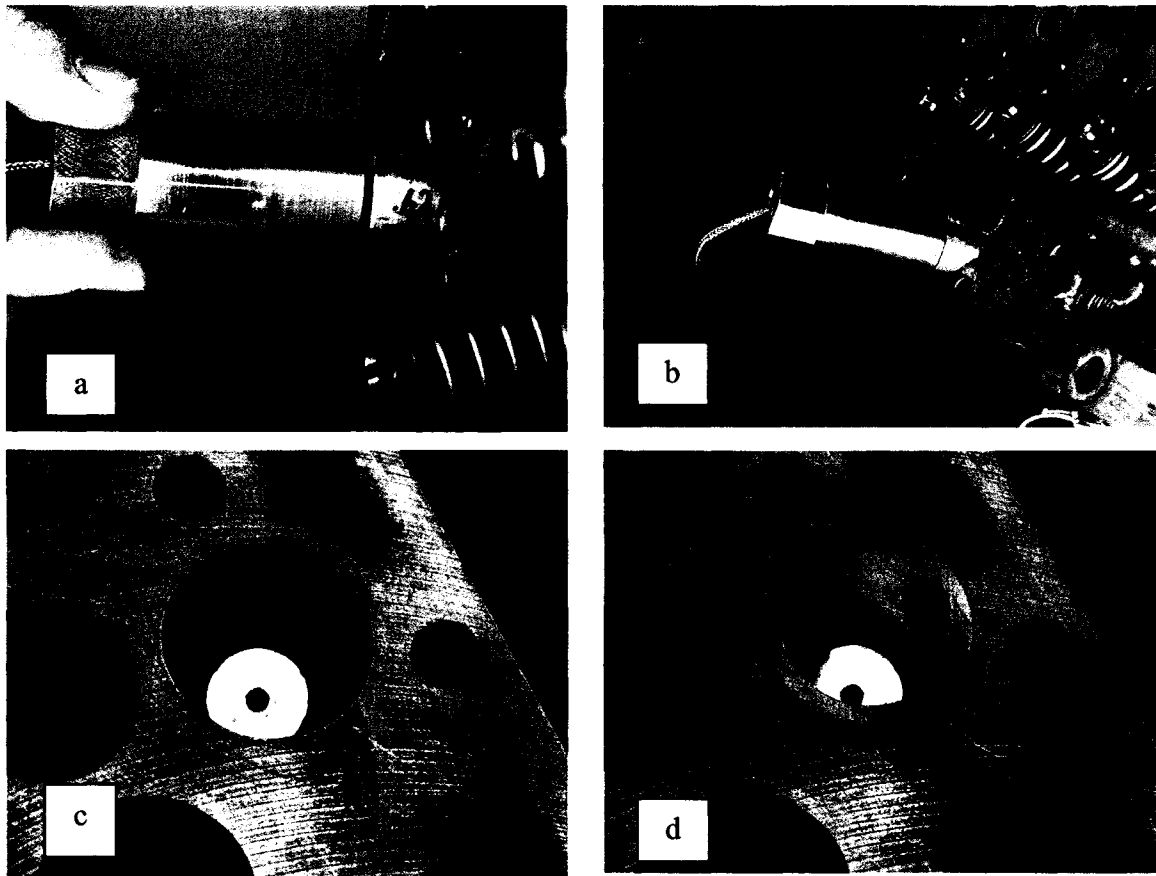


Figure 59: (a) Tightening of VCR secondary piston, (b) VCR secondary piston installed, (c) View of VCR secondary piston without prechamber cap, (d) Low CR prechamber cap ready to be press fit.

Figure 60 below illustrates a comparison between the original (OEM), high CR, and low CR prechamber insert caps.

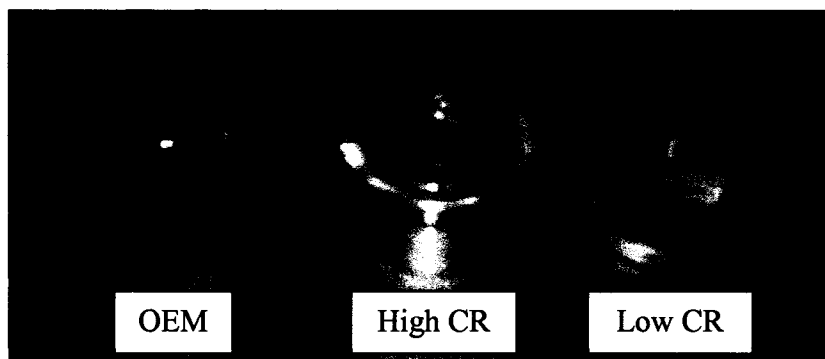


Figure 60: Comparison between OEM, high CR and Low CR prechamber inserts.

Although the shape of the combustion chamber appears to be slightly irregular, the desired effect of varying the CR was achieved and verified by volume measurements.

The volume measurement experiment was performed to determine the length of the copper spacers and is presented in Appendix E. The objective of the experiment was to verify the VCR design calculations and to determine the actual spacer length required to obtain the necessary pre-chamber volume. The calculated prechamber volume for each compression ratio is the desired volume to be achieved in the actual prechamber. This is achieved by adjusting the spacer length.

The experiment setup utilized a titration burette and acetone to measure the actual prechamber volume very accurately. The experimental setup and procedure are listed in Appendix E.3 and E.4 respectively.

A summary of the results of the experiment are presented in Table 23 below. Table 23 organizes the results by; compression ratio, number of trials required, calculated prechamber volume, spacer length installed, and measured actual prechamber volume.

Table 23 Summary of VCR secondary piston spacer experiment.

CR	Number of Trials	Calculated Prechamber Volume (cc)	Spacer Length (inches)	Actual Prechamber Volume (cc)
25	2	7.22	0.23	7.2
22	3	9.0	0.447	9.05
19	2	11.38	0.3	11.5
17	1	13.45	0.62	13.45
15	2	16.13	0.95	16.2

Figure 61 illustrates the prototype copper spacers. Their lengths were determined by experiment (further detail is available in Appendix E.) Figure 61a shows the Low CR set that allows for varying compression ratio from 15, 17, and 19:1.

Notice that the prechamber insert cap is flat, and will not protrude as much into the prechamber, thus giving the increased clearance volume more suitable to lower CR's.

Figure 61b illustrates the high CR prechamber insert cap with copper spacers for 22, and 25:1. It is possible to achieve CR higher than 25, even 28, by machining a shorter copper spacer. However the upper CR limit is restricted by the maximum plunge depth of the secondary piston, which in turn is limited by internal clearance of the prechamber, (between the prechamber insert cap and the tip of the VCR secondary piston.)



Figure 61: (a) Low CR prechamber cap and matching copper spacers, (b) High CR prechamber cap and matching copper spacers.

5.5 Cam Trigger Mechanism Prototyping

The cam trigger mechanism was developed to provide the ECU with a trigger signal to be used to determine the timing of the fuel injector. The trigger signal is in-phase with the rotational speed of the cam shaft, and most EFI engines have an injector trigger wheel with multiple timing points around the trigger wheel. However, the Kubota D905 engine does not have the luxury of this

feature, since it uses an injector pump, and therefore a cam trigger mechanism will have to be developed.

The prototype of the cam trigger mechanism involved the selection of an appropriate timing gear. The concept shown in Figure 62 required using the front crank pulley (A) as a driver shaft and fabricating a spindle to accept a timing gear, and then running a timing belt to another timing gear (C). The angular velocity of the camshaft is half the speed of the crankshaft, therefore the speed ratio (M_G) is 1:2. From Shigley and Mische [62] we have:

$$M_G = \frac{N_{crank}}{N_{cam}} = \frac{d_{crank}}{d_{cam}}, \quad \text{Equation 19}$$

Where N_{crank} and N_{cam} are the speed of the crank and cam respectively, and d_{crank} and d_{cam} are the diameters of the crank and cam respectively. Therefore, the diameter of the cam is equal to twice the diameter of the crank, $d_{cam} = 2d_{crank}$, and the selection of timing gear will have to reflect this. A 15 tooth timing gear was selected for the driver gear to be mounted on the crankshaft pulley. Therefore a 30 tooth timing gear will be required for the cam trigger.

The trigger signal is provided by a hall sensor, and a steel pick-up tab, shown in Figure 63a and 63b. For every revolution of the camshaft the intake valve opens once and hence the injector is triggered for one injection. The tension of the timing belt can be adjusted by means of the adjustment plate and bolt. The adjustment plate pivots about the base point (D) and is secured by the securing bolt (E).

The position of the Hall sensor can be varied three ways as shown in Figure 64. The spacing between the Hall sensor and the pick-up tab can be varied and the angle of pick-up can be varied by loosening and clamping the trigger position adjuster, and the final position can be also be fine-tuning using the screws.

The timing gears were purchased from McMaster-Carr, and all other components were fabricated using mild steel, or aluminum. The mechanism is easy to setup and use, and provides an accurate timing signal. However, a glitch in the signal was noticed when trial operation of the trigger was attempted. Further investigation and discussion with 034EFI revealed that the 883ECU program is expecting more signals per revolution than this design is supplying. A redesign of the trigger

mechanism should be made. A 36 tooth trigger wheel with 1 space left blank would provide the necessary signal profile to eliminate the signal glitch. A trigger wheel similar to the one found on OEM engines could be incorporated or used as an example.

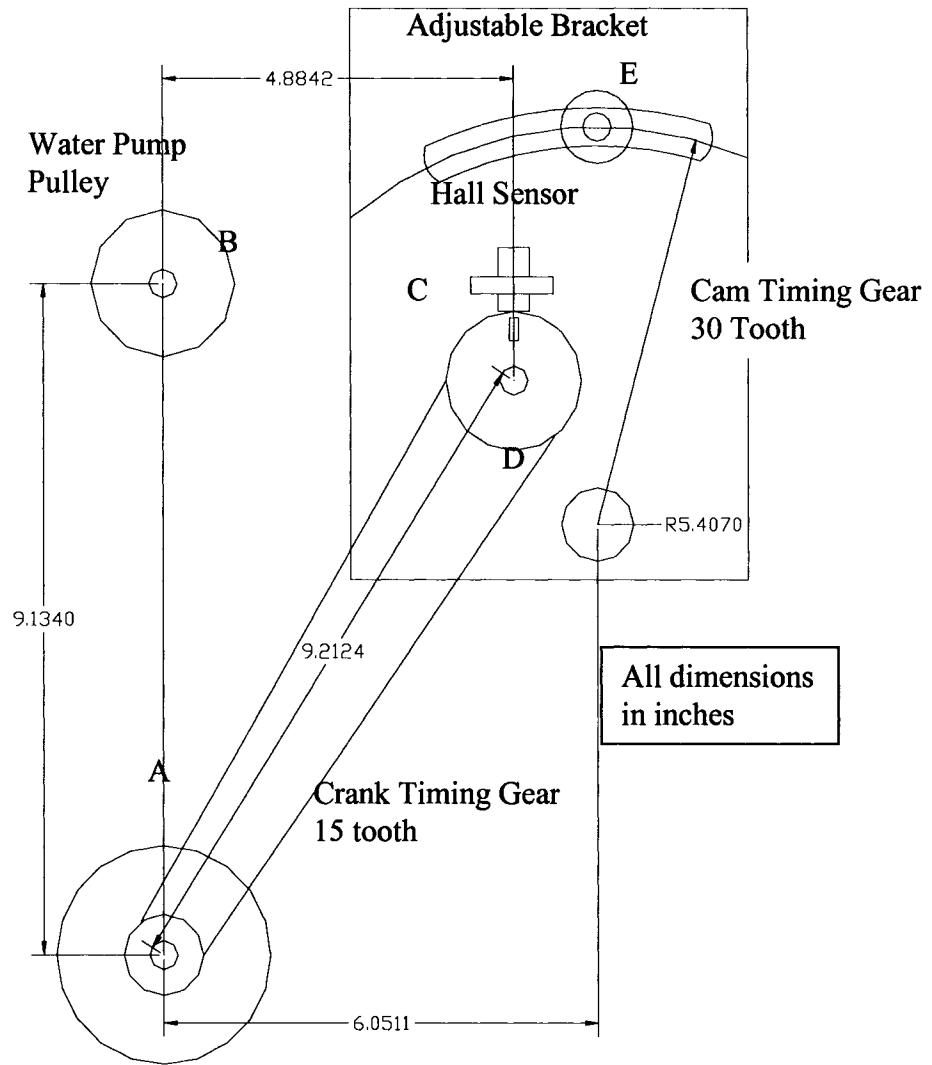


Figure 62: Cam Trigger Mechanism concept.

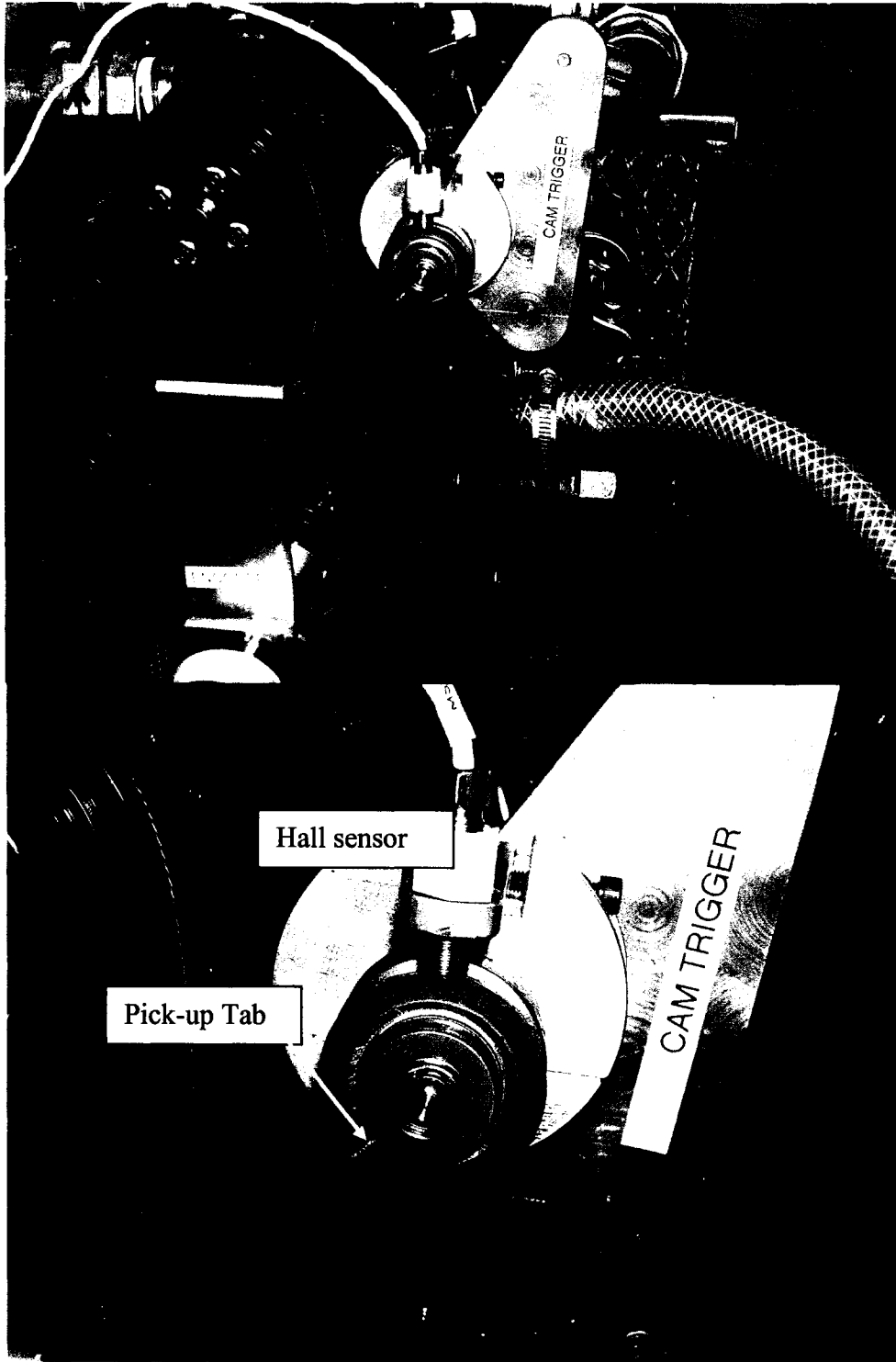


Figure 63: (a) Cam Trigger Mechanism, (b) Hall sensor and steel pick-up tab.

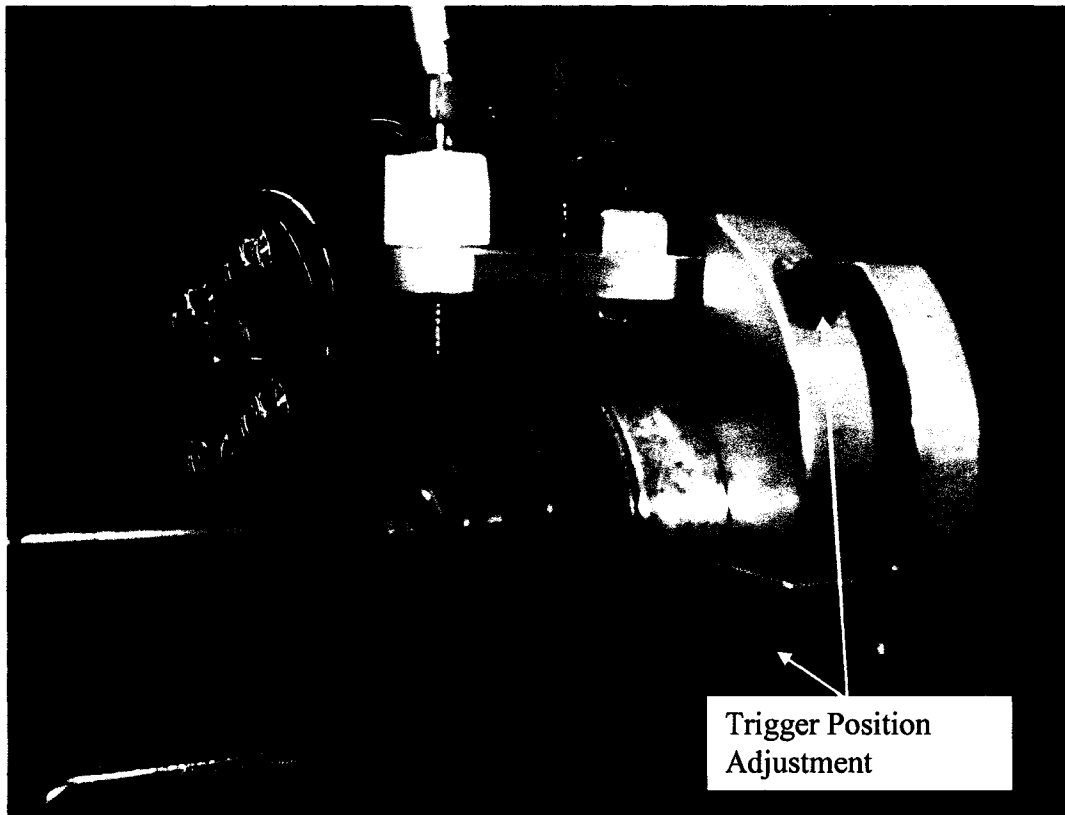


Figure 64: Cam trigger mechanism adjustment.

5.6 Cooling System Installation

The cooling system was a relatively simple system to implement. Section 4.2.2 already discussed in detail the major components of the cooling system and their functions. Further detail is presented in Appendix A.5 and A.6. For this section, the installation of the radiator is the major task that is discussed.

The requirements for the installation of the radiator are as follows:

1. The radiator must be installed in close proximity of the engine, to minimize hose length.
2. The radiator must be easy to install and remove, and the installation should enable easy access to radiator cap.

Figure 65 is a photo of the completed installation of the radiator. The radiator is located in close proximity to the engine, and minimizes the hose length. The hose selected is a 2.54 cm (1 in) reinforced poly-vinyl chloride (PVC) clear hose and makes the coolant level easily visible. Regular stainless steel hose clamps were used to appropriately secure the hose ends to both the engine and

the radiator. The original thermostat was left unchanged and the cooling fan was removed to allow the engine to build up heat quicker. Figure 66a and 66b show further details of the custom radiator brackets. These bracket feature anti-vibration rubberized mounts, to prevent vibration transfer from the engine frame to the radiator. The custom mounting brackets can be easily removed by loosening the fasteners.

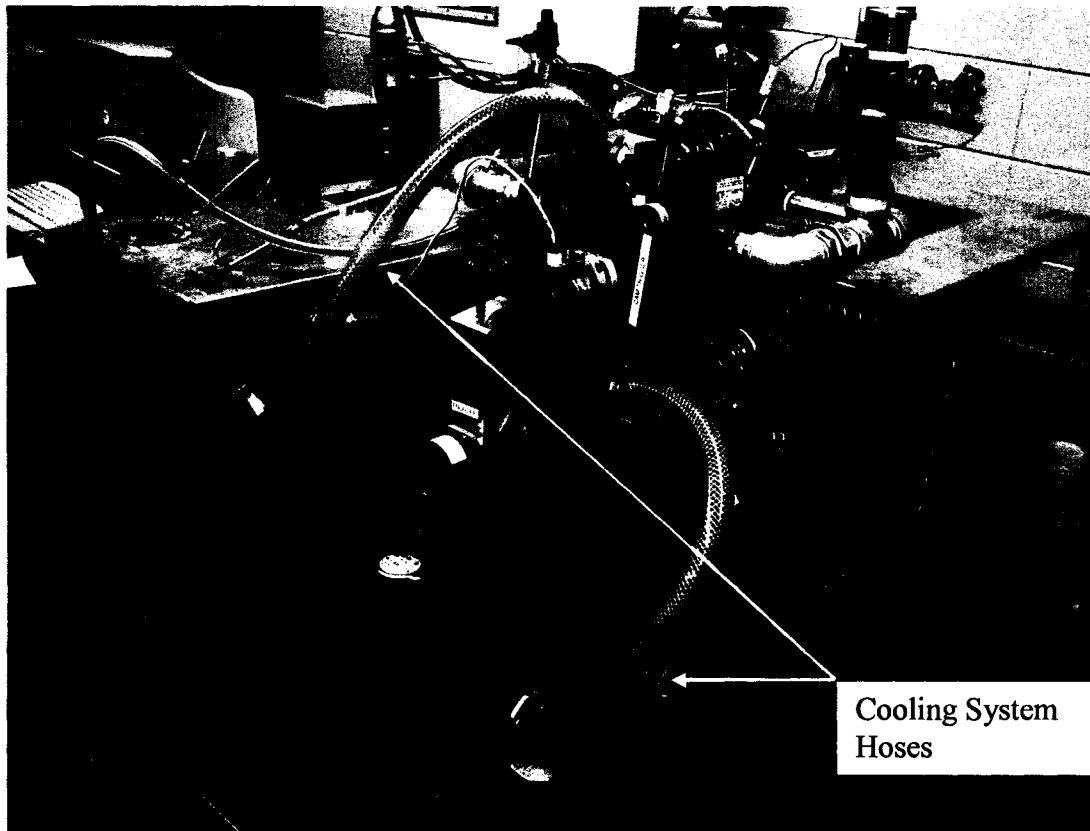


Figure 65: Cooling system installation.

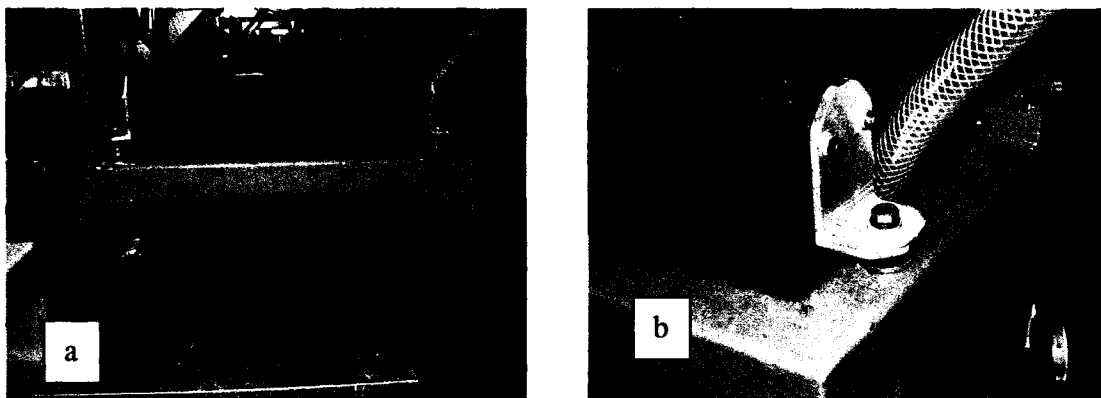


Figure 66: (a) Front view of radiator and mounts, (b) View of custom radiator mounting bracket.

5.7 Encoder Installation

The installation of the crank angle encoder had to meet two requirements.

1. The encoder input shaft must be coupled to the crank shaft pulley.
2. The mounting bracket must be rigidly attached to the engine block.

Figure 67 illustrates how the installation of the crank angle encoder was accomplished.

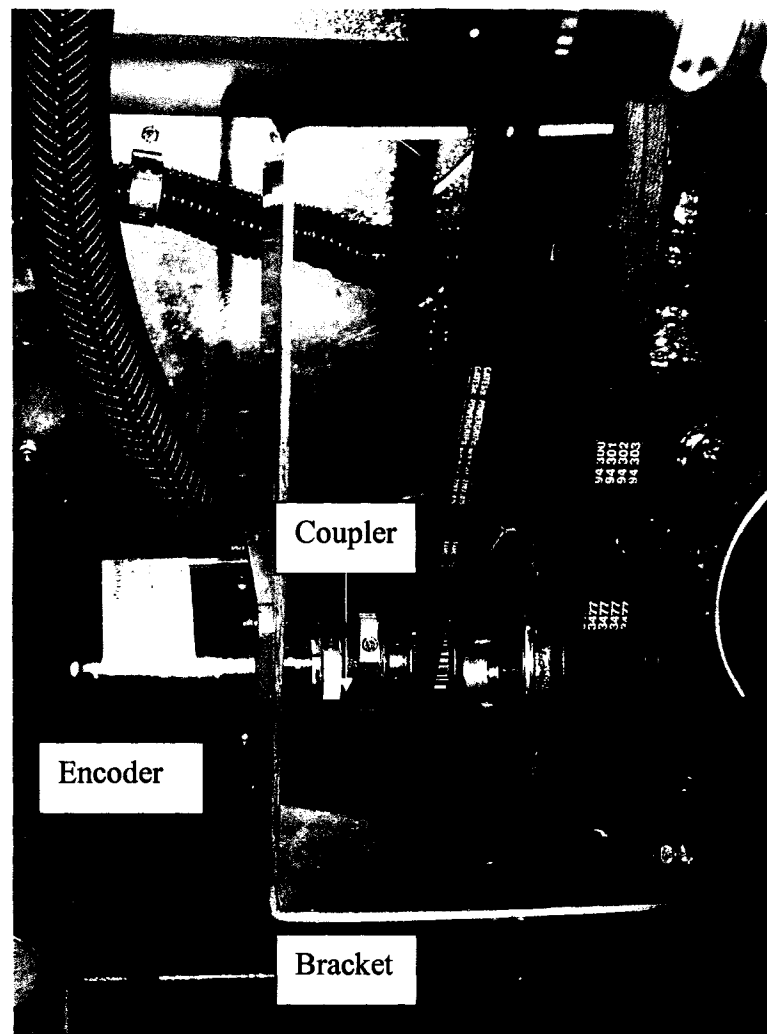


Figure 67: Installation of Gurley 9125 encoder.

The bracket was fabricated using aluminum sheet because of its lightweight and anti-corrosion properties. Note the rigid attachment of the mounting bracket to the engine block. The flexible coupler was provided by the Gurley Encoders and was installed according to their recommendations. The encoder index signal was synchronized to the exact TDC position of cylinder two (research cylinder) of the engine.

5.8 Intake/EGR Piping System and Heater Fabrication

The fabrication of the Intake/EGR piping system was completed using off-the-shelf components as prescribed in Chapter 4. The Intake/EGR piping system is divided into two sections; hot/galvanized piping section and cold/ABS piping section. These sections are separated by the intake air heater.

Figure 68 illustrates the hot/galvanized piping section and Figure 69 illustrates the cold/ABS piping section. Notice the direction of flow indicated by the orange arrows. All the components of the hot/galvanized piping section were purchased from a local plumbing supplier. They were measured and cut to the correct length using a cut-off saw. Most of the components were pre-threaded, which made them easy to assemble, however there were a few pipe lengths that needed to be threaded manually with a 3.81 cm (1.5in) NPT Pipe thread die and threading machine. Prior to assembly, Teflon tape sealer was applied to the threads to ease assembly and to provide an airtight seal.

A prototype throttle valve and two prototype flanges were fabricated and are shown in Figure 70a, 70b and 70c. The flange (shown in Figure 70b) was fabricated using a galvanized steel pipe that was press fit into a flange plate. The flange plate provides a flat surface for a gasket to seal the intake and exhaust with the cylinder head. The throttle valve shown in Figure 70a was also fabricated using a galvanized steel pipe. A custom fitted throttle plate was machined and mounted to a pivot shaft that runs through the pipe and into the aluminum housing. The pivot shaft is supported by small bearings on either end. A throttle position sensor is mounted on one end of the housing (Figure 70a) and a throttle cable bracket is mounted on the opposite end (Figure 70c.) The throttle cable is used to set the position of the throttle valve, and was fabricated using a simple lawnmower cable.

The cold/ABS piping components were all purchased from a local plumbing supplier. The assembly of these components was very simple, and only required the use of a hacksaw, and the ABS adhesive. The piping was cut to length and pre-assembled to test fit, and was glued together using a special adhesive. Rubber couplers were installed to minimize the transmission of engine vibration and to ease assembly. The surge tank was developed using a 40 gallon drum. This reduced cost substantially, and provides enough surge volume to dampen the pressure pulsations prior to the flow meter.

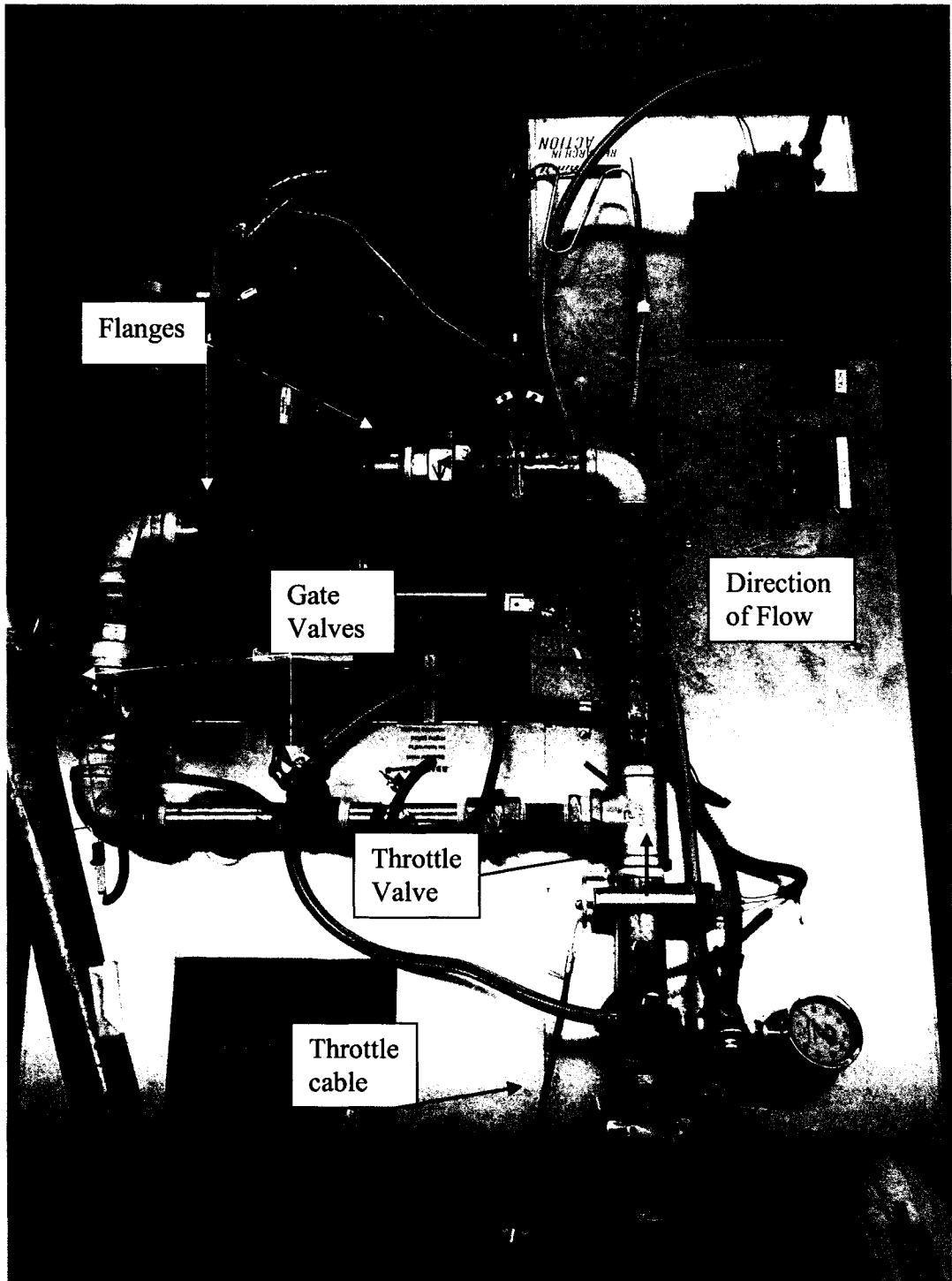


Figure 68: Intake/EGR system, hot/galvanized pipe section.

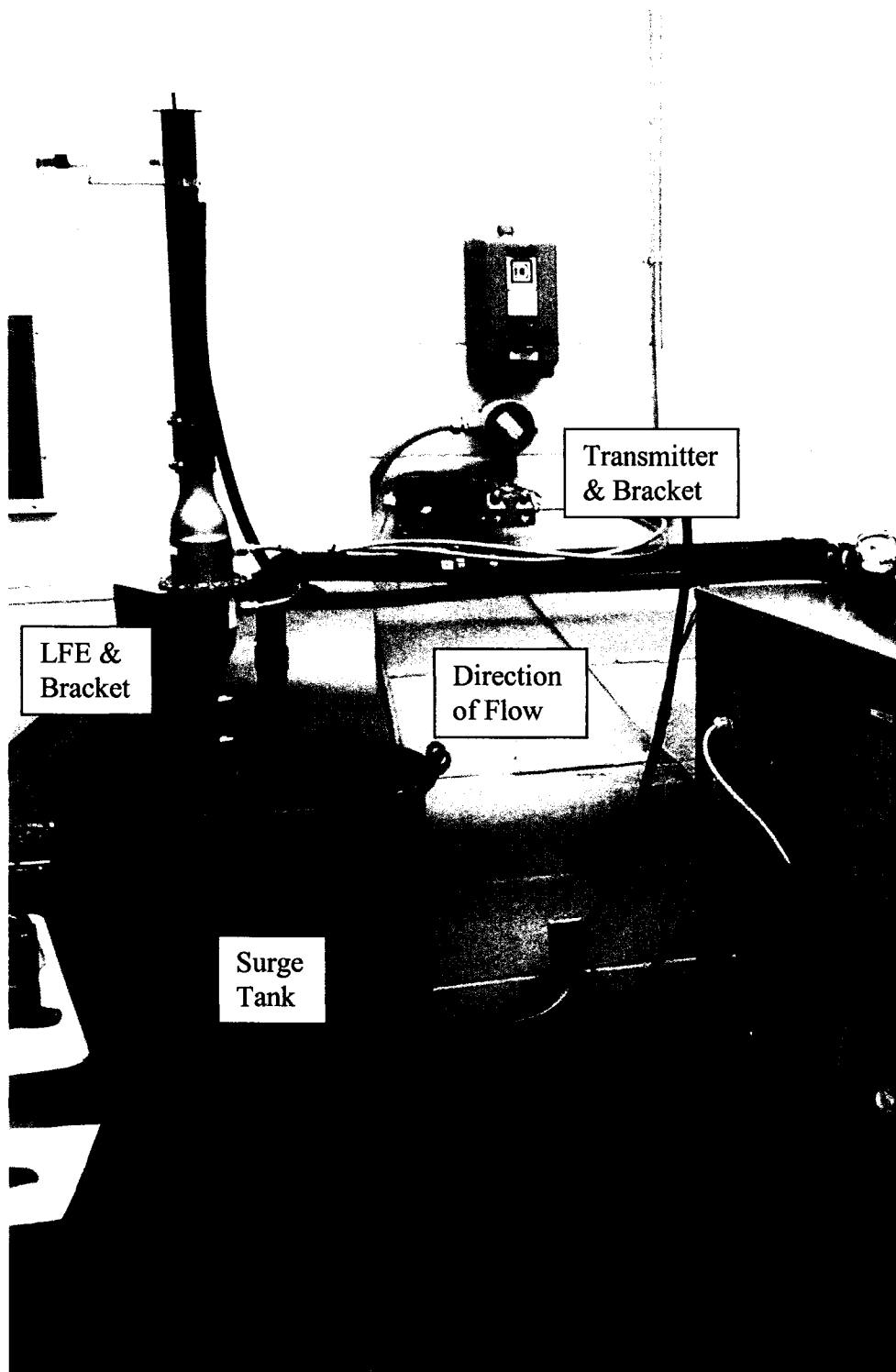


Figure 69: Intake/EGR system, Cold/ABS pipe section.

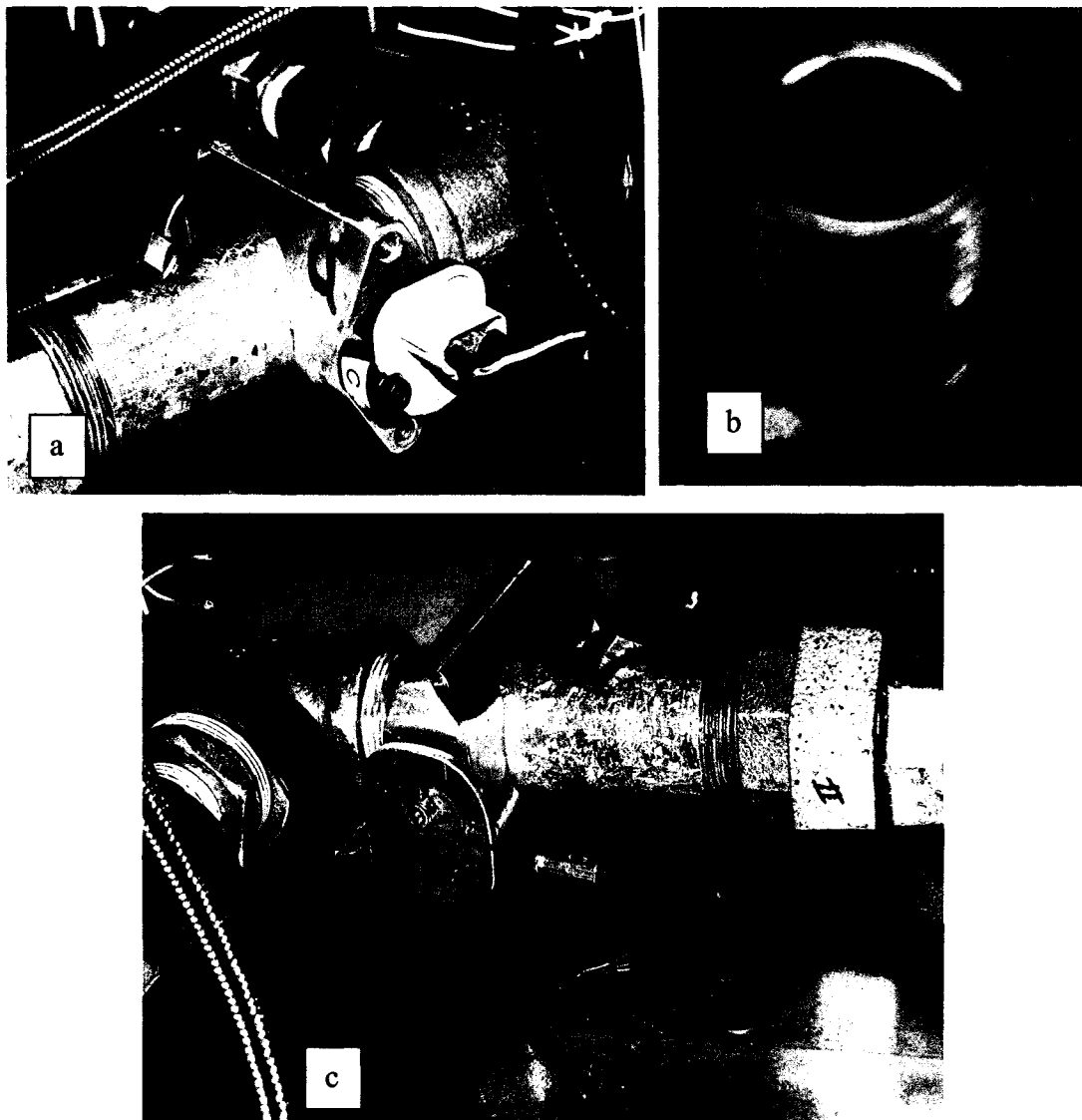


Figure 70: (a) TPS view of throttle valve, (b) Intake and exhaust flange, (c) Throttle Cable Bracket.

The flow meter was mounted to the top of the surge tank using a custom aluminum bracket (shown in Figure 71.) The transmitter was mounted to the concrete block wall using the bracket included with the transmitter and concrete fasteners.

The intake air heater was installed between the hot/galvanized piping and the cold/ABS intake piping. The direction of flow is indicated in Figure 72.

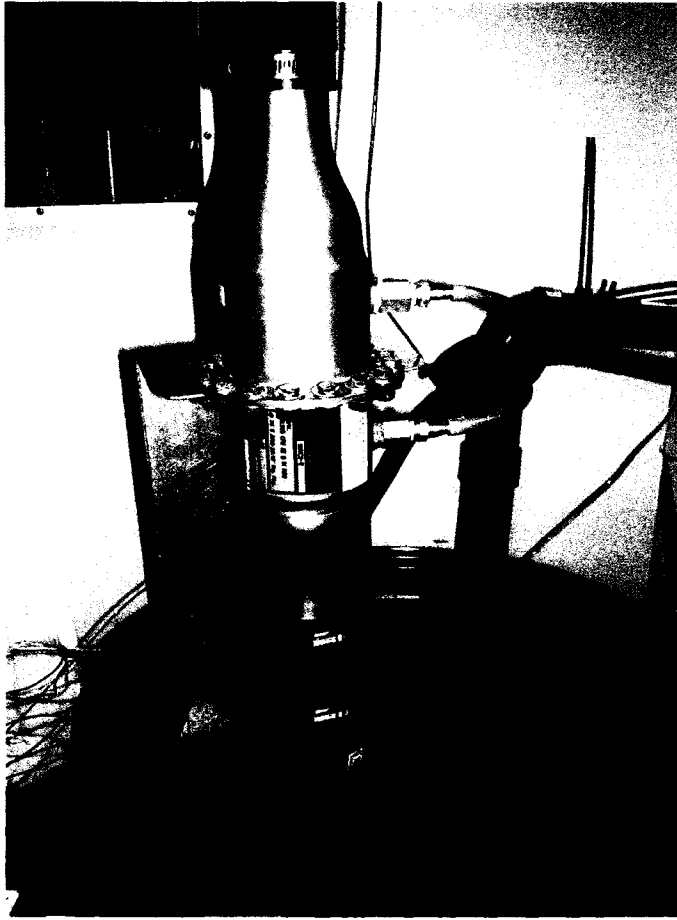


Figure 71: Laminar flow meter and bracket.

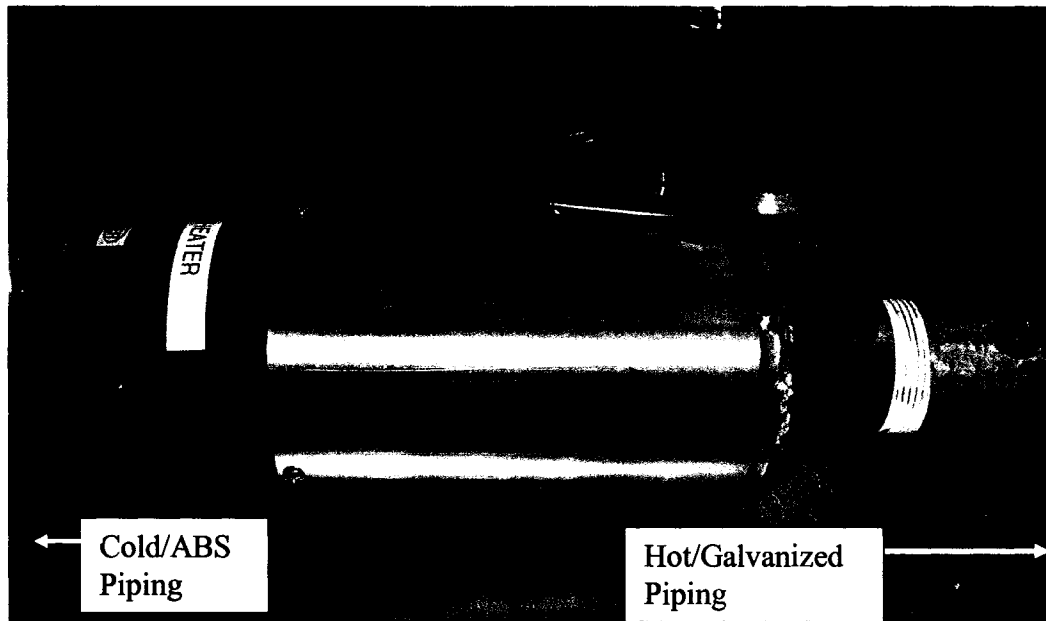


Figure 72: Omega SH-73343 intake air heater.

Figure 73 shows the electrical enclosure that houses the heater controller and wiring. The enclosure was purchased from ElectroZad Ltd and the CNI/32 heater controller from Omega was installed and setup by Pat Seguin [61].

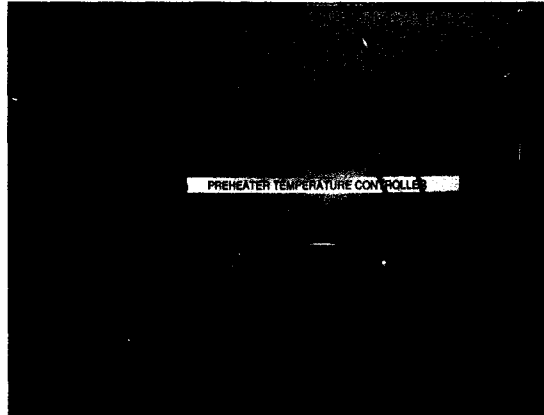


Figure 73: Intake air heater controller.

5.9 Fuel and ECU System Installation

The installation of the fuel and ECU systems were completed in a timely manner. As mentioned earlier, all the components of the fuel system are off-the-shelf items, however some fabrication and fitting was required to install the fuel system.

Firstly, the fuel tank needed to be installed in the top plate; therefore a 10 cm diameter hole was cut out of the galvanized steel and six bolt holes were drilled for the fuel tank fasteners. The return line and the fuel cap is shown in Figure 74a and the feed line, fuel tank and fuel filter are shown in Figure 74b. The fuel lines were difficult to cut to length because the outside stainless steel sheathing is made from braided wire, and is very difficult to cut a clean edge. A clean straight edge is necessary to install the hose end fittings, therefore a technique was devised to overcome this problem. The braided lines were taped in the area to be cut with special packing tape, and a hacksaw was used to cut the hose. This eliminated the frayed ends, and made it a lot easier to install. The fuel gauge, pressure regulator and injector fuel rail is shown in Figure 75.

The fuel gauge and regulator were easily assembled and tightened with wrenches, and light anti-seize lubrication. The injector fuel rail was fabricated using off-the-shelf brass fittings that were machined to accept the injector and create a tight seal.

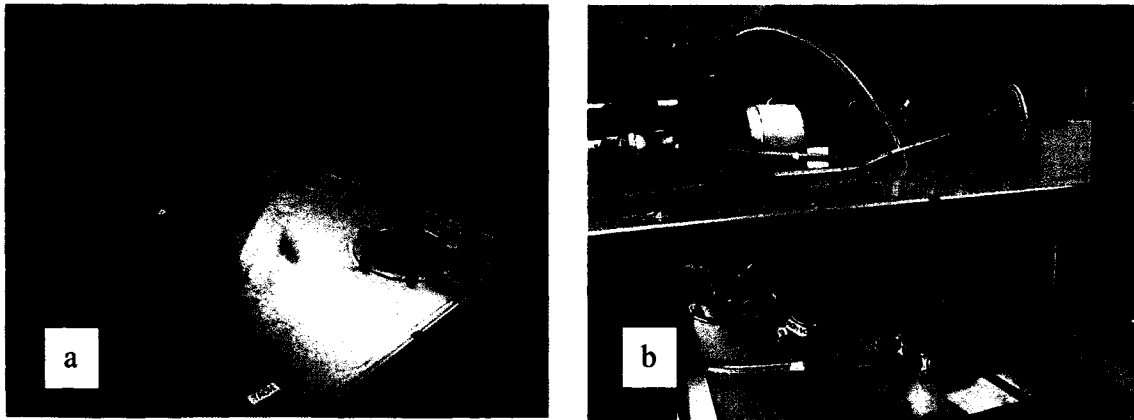


Figure 74: (a) Fuel tank opening, and return line, (b) Fuel tank, filter, and supply line.

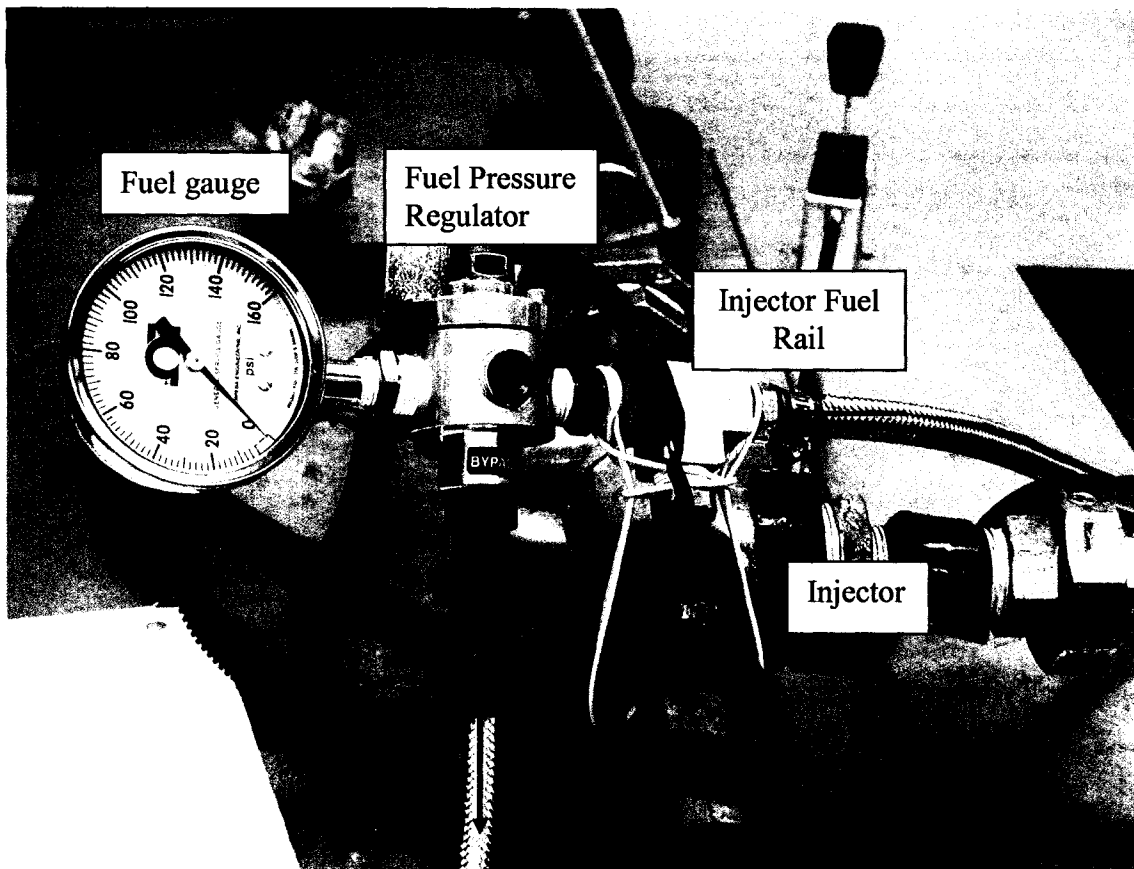


Figure 75: Fuel pressure regulator, gauge, and injector fuel rail.

When the fuel system was pressurized, it had a tendency to want to come apart at the injector seal, therefore a retaining wire was fashioned to secure the assembly to the intake manifold. A potential future improvement would be to fabricate a small sheet metal bracket to hold the brass fittings on both sides of the injector together.

The fuel pump (shown in Figure 76) was mounted to the underside of the galvanized steel table top. This proved to be an ideal location since the fuel pump was out of the way yet easily accessible for maintenance purposes.

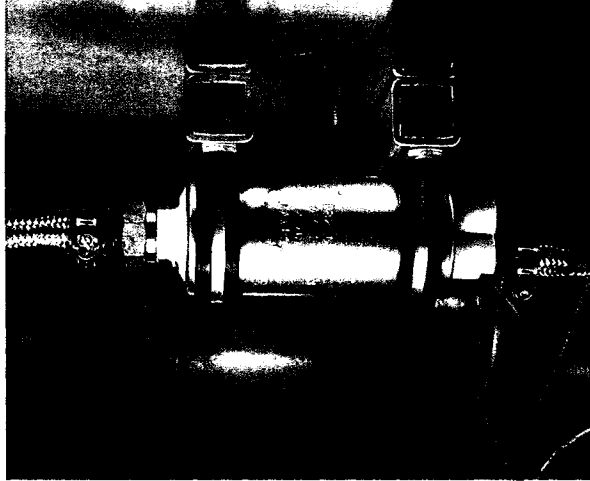


Figure 76: Fuel pump mounted underneath the top galvanized shelf.

To protect the electrical power system from accidental spills of combustible mixtures a fuel splash tray was installed to enclose the fuel system from four sides. The fuel splash tray along with the ECU is shown in Figure 77.

The ECU was mounted on the firewall of the fuel splash tray. This was determined to be an ideal location since it was in close proximity to the engine and easily accessible for modifications. The ECU system required several sensors to be installed on the engine. These sensors include; throttle position sensor, coolant temperature, intake air temperature, manifold absolute pressure, and hall sensor. The appropriate location for each of these sensors was identified and the sensors were quite easily installed.

The wiring harness was fabricated using the supplied wiring diagram, coloured wires and wire stripper. Each wire was installed in the harness using the appropriate colour and additionally labelling was attached for easy identification. The wires were routed in protective plastic wiring loom.

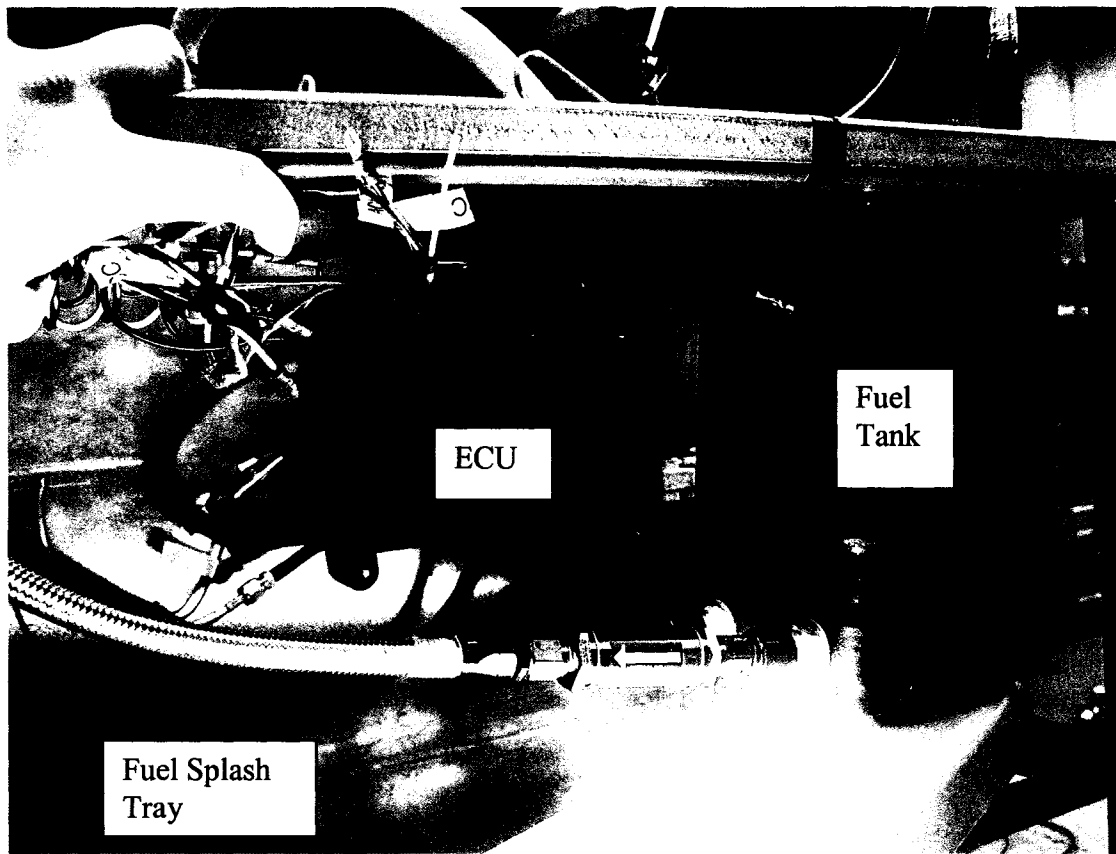


Figure 77: ECU install on firewall of fuel splash tray.

5.10 Safety Guarding Installation

Safety guarding was installed to eliminate accessibility to dangerous mechanical components. The three major areas of concern were; the rotating coupler, the rotating flywheel and the rotating pulleys.

Figure 78 shows the guarding installed to cover the rotating coupler assembly. The guarding was fabricated using expanding galvanized steel grating. This grating is used extensively in industry for outdoor applications, and as a result is relatively cheap compared to plexiglass or stainless steel grating materials and was recommended by Steve Budinsky [60]. The guarding is easy to remove for maintenance accessibility. Figure 79a and 79b shows the safety guarding installed to prevent access to the rotating flywheel. The cover is fabricated out of aluminum sheet metal and was made using tin shears and a sheet metal brake. It is easily removable, and was fitted to provide just enough space to prevent metal-to-metal contact from vibration. The safety guarding was fabricated using aluminum sheet metal, tin shears, sheet metal brake and a TIG welder.

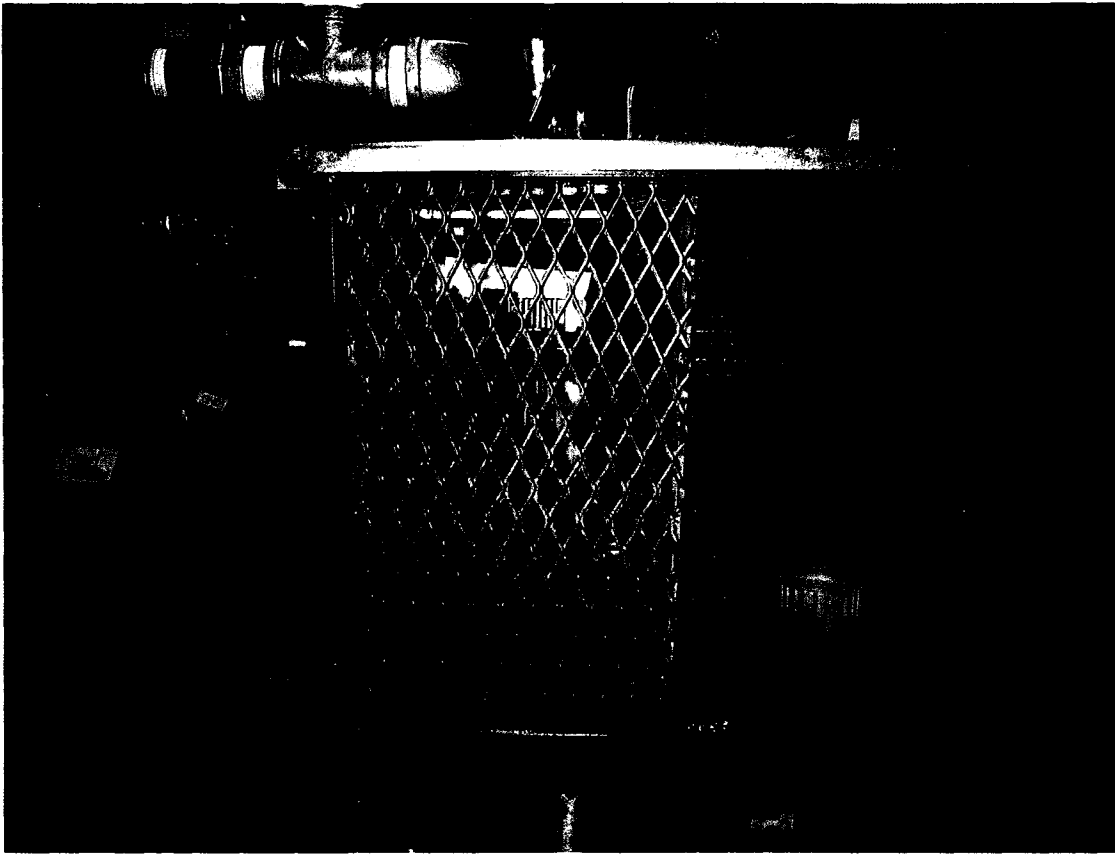


Figure 78: Safety guarding on rotating coupler.

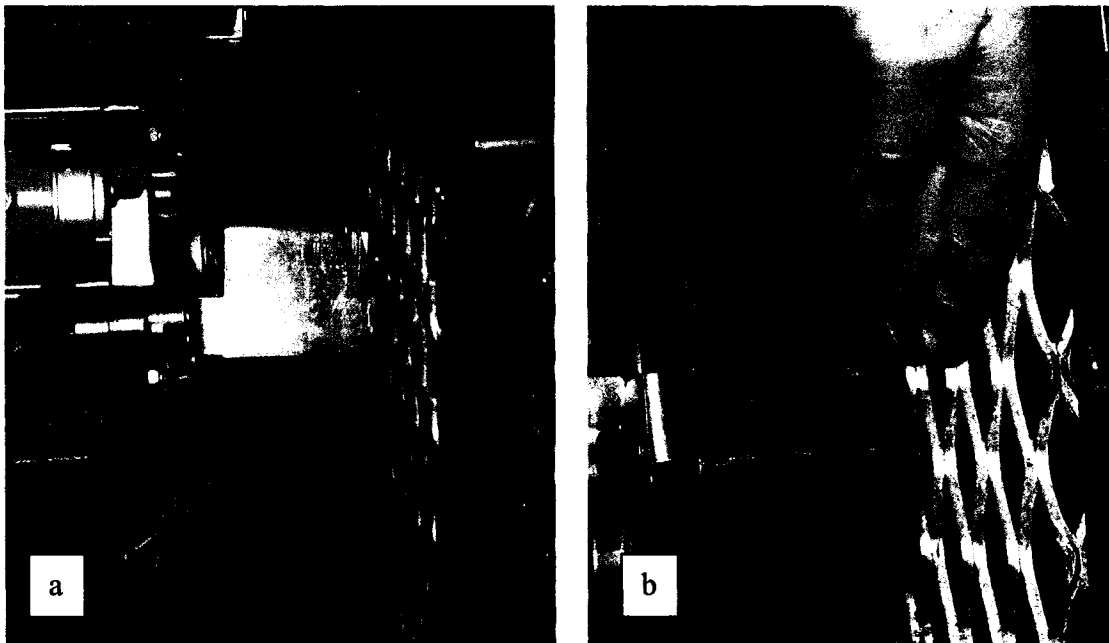


Figure 79: (a) Safety guarding on rotating flywheel, (b) inability to access moving parts.

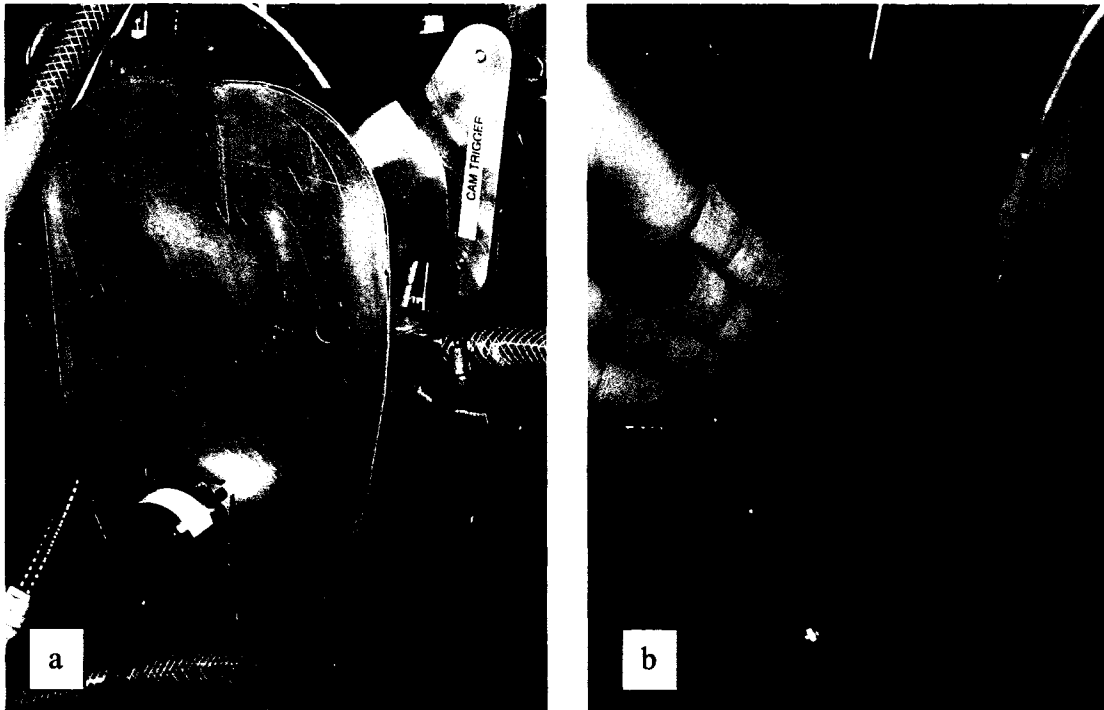


Figure 80: (a) Safety guarding on rotating pulleys, (b) inability to access moving parts.

Figure 80a and 80b illustrate the safety guarding installed on the front cover of the engine. This guarding was designed to prevent access to pinch points between the crankshaft pulley and water pump pulley and v-belt. Also the cam trigger gears and timing belt are also covered to protect from injury. Notice in Figure 80b the inability to access the pinch points.

In summary, all the areas of risk for injury were identified and safety guarding was fabricated and installed to protect the operator of the apparatus from injury.

5.11 Data Acquisition System Development

The DAQ system required the installation of; six thermocouples, in-cylinder pressure transducer, laminar flow meter, and the rotary digital encoder.

The thermocouples were all installed in their appropriate locations as shown in Figure 81. Each thermocouple installed required a special plug adapter. This plug adapter required a 3/8" hole to be drilled and tapped so that it could be threaded into the piping. The plug adapters have a hole through the center where the thermocouple passes through. This adapter also locks and seals the thermocouples in position.

All of the thermocouples were very thin (1.58 mm) and long (127 mm) and as a result would tend to “flop around” quite vigorously while the engine is running. Therefore, custom support brackets were fabricated to prevent damage and stabilize them.

The fully assembled and installed quick connector box is shown in Figure 82. All the relevant sensors are plugged in to their appropriate location. The PC was setup alongside the apparatus and connected to the quick connect box and to the ECU (see Figure 83.)

Labview 7.1 was installed on the PC and used to develop the custom data acquisition user interface, and post processing programs. Further detail is available in Chapter Six.

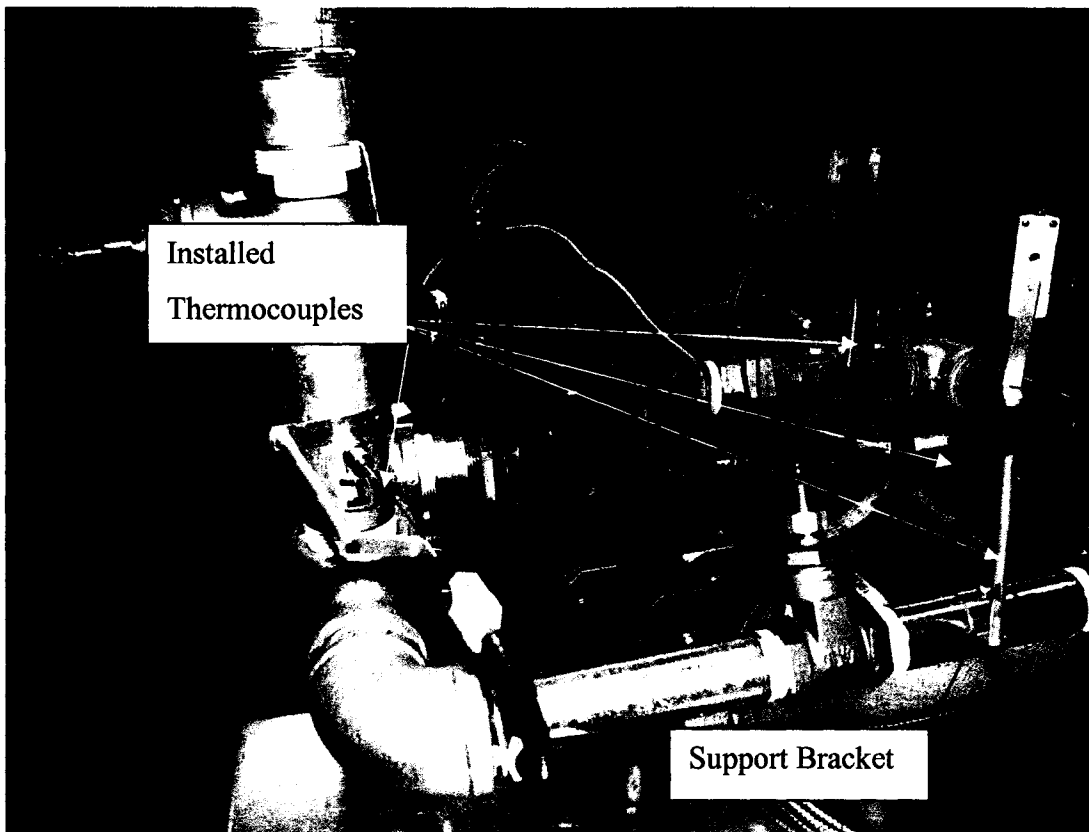


Figure 81: Thermocouples installed in appropriate locations.

The installation of the Gurley encoder was already shown in Figure 67 and the laminar flowmeter and transmitter were shown in Figure 69. The encoder was wired directly to the quick connector box 0.5 in plastic conduit. The flowmeter was plumbed to the differential pressure transmitter with 0.25 in plastic hose. The transmitter was connected to the quick connect box with a special cable, and was shielded by flexible conduit.

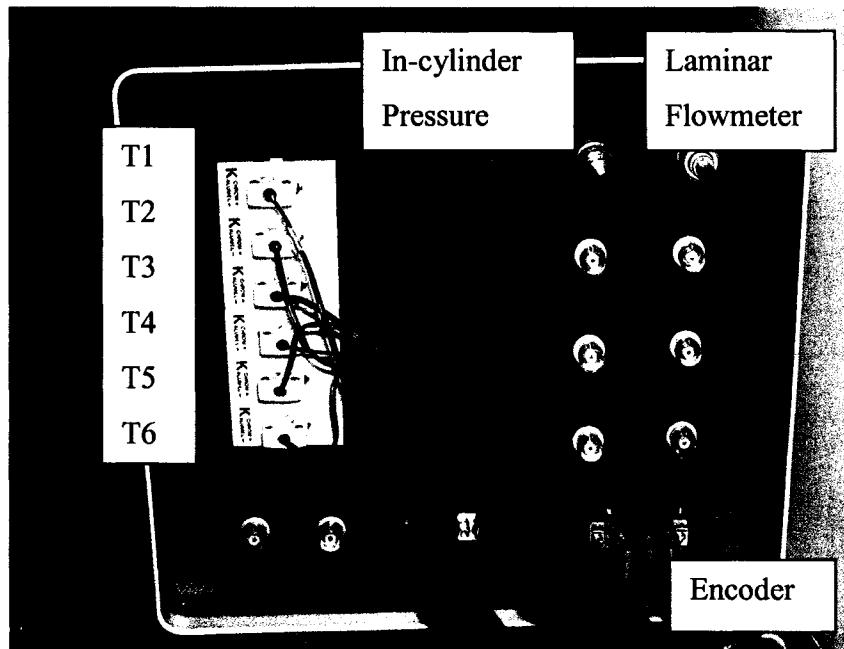


Figure 82: Quick Connector box.

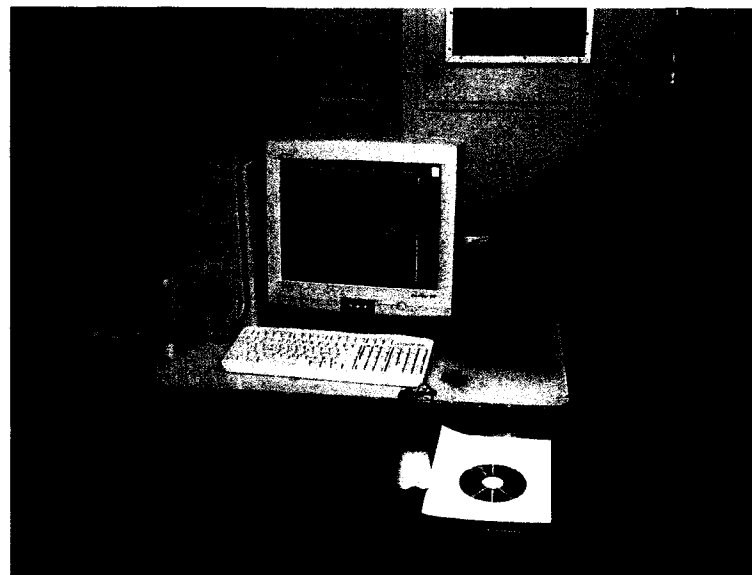


Figure 83: Labview Data Acquisition PC.

The Research Engine Data Acquisition System is the main virtual instrument (VI) developed for both sensor monitoring and low-rate data acquisition. The GUI was jointly developed with the help of Jeff Defoe, a 3rd year undergraduate student [63]. The GUI contains five main panels: system schematic, configuration, temperature, flowrate, and pressure. These panels allow the user to observe at-a-glance or in-depth information on all sensor data.

Figure 84 shows the system schematic panel and it contains a summary of the vital information from sensor data: temperatures, flowrate, combustion event occurrence, and engine speed. This is all presented via the intuitive graphical representation shown below. This panel is most useful to have displayed while running the engine to track the status of the system during operation. The configuration panel, shown in Figure 85, allows the user to modify several performance settings for the software. These settings include; data recording, buffer size, sampling rate, number of samples, amplifier setup, trigger pressure, and flowmeter setup.

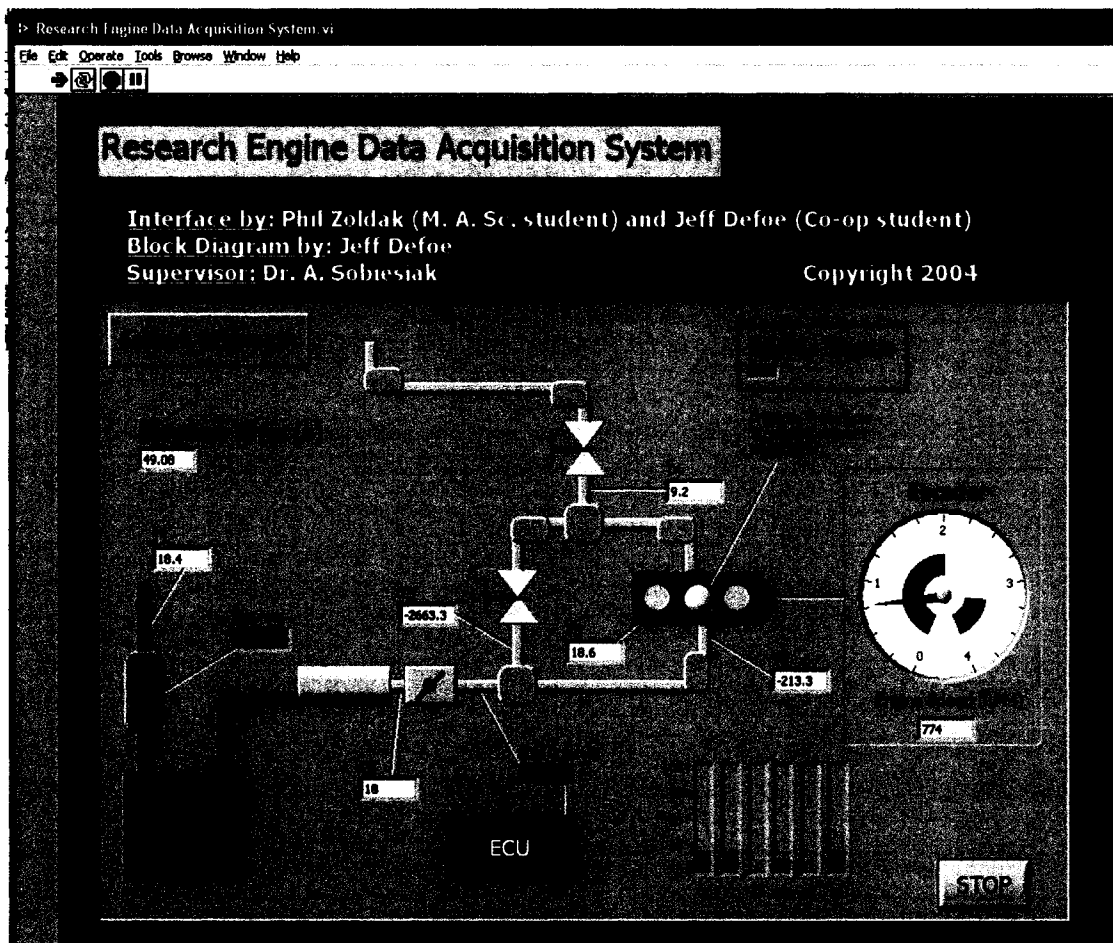


Figure 84: System schematic panel.

The data-recording feature lets the user choose the length of sampling duration (by stopwatch) and whether or not to save data to a file. At times the user will just want to monitor the status of the engine while some change is being made, or perhaps be waiting for steady operating state. Once the user is ready to record a sample of data he/she can select record and the data shown in the graphs will be saved to file. A typical length of sampling time should be no longer than 10 seconds.

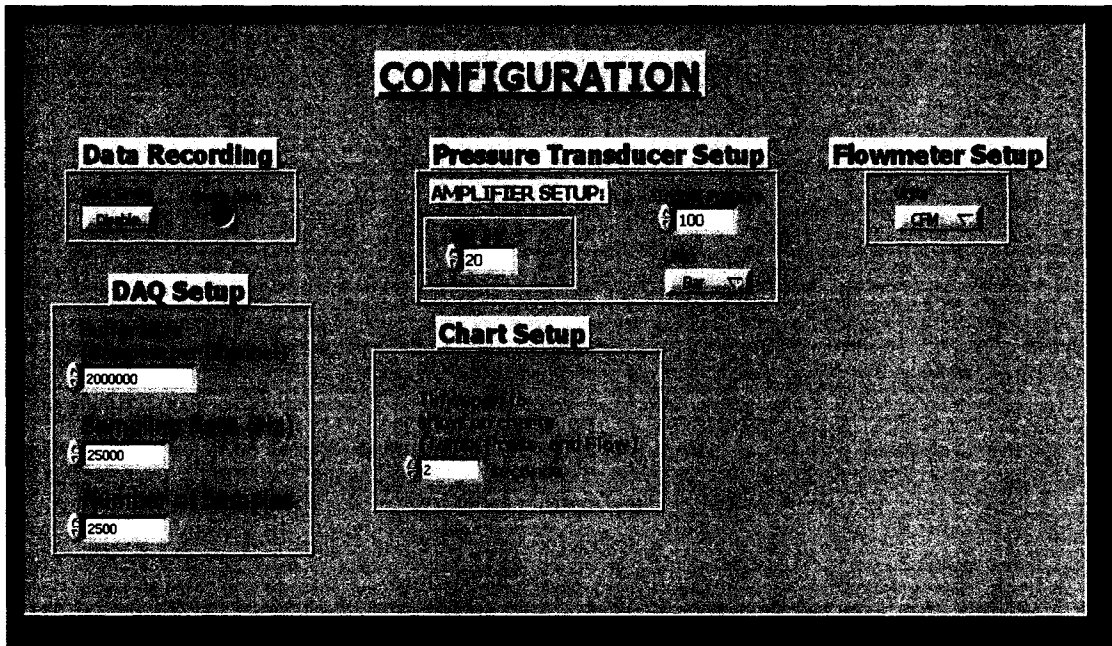


Figure 85: Configuration panel.

The buffer size is used to select memory allocated for the buffer memory. The size of the buffer should be large enough to accommodate for the data that is being sampled. A higher value indicates more memory usage for the buffer. This means that a higher sampling rate can also be used, however the duration of the sampling event decreases. Typically the buffer size of no more than 2 million data points is the maximum the system can tolerate.

The sampling rate feature enables the user to select the number of samples per channel to acquire per second. The higher the value, the more CPU-intensive the data acquisition will be. Typically a sampling rate of 25000 samples per channel per second, will give more than enough accuracy for most experiments under 2000 RPM. If higher engines speeds are desired than a higher sampling rate is required, and therefore a shorter sampling duration will have to be used.

The number of samples features enables the user to choose the number of samples to acquire before updating the graphical displays and/or writing them to disk. 10 % of the sampling rate is ideal to get smoothly updating visual displays without consuming too much CPU power

The amplifier setup feature ensures that the program amplifier settings are matched with the values on the Kistler 5004 charge amplifier. This ensures that the calibration curve for the pressure transducer is accurate in the program. The user reads the values of the charge amplifier and inputs them in the amplifier gain section. The amplifier gain is normally set to 50 bar/V, but higher cylinder pressures will require adjustments.

The trigger pressure feature enables the user to select the minimum pressure for the combustion event notification light to come on in the Summary Panel. The GUI also lets the user select the units for all pressure outputs (bar, psi, and kPa.).

The flowmeter setup feature allows the user to select the units for all flowrate outputs. The temperature, flowmeter, and in-cylinder pressure panels will be presented in Chapter Six.

5.12 Summary

The fabrication of the research engine along with all of its systems and components was completed in a timely manner. A prototype VCR secondary piston was developed that enables variable compression ratio. The fuel system was installed that facilitates accurate fuel metering by means of an ECU and software. The intake air system, preheater system, and LFE enable accurate control and measurement of both air flow and temperature. The drive system enables accurate control of engine speed and provides adequate torque absorption. The frame structure provides a rigid support structure for the entire apparatus. The safety guarding provides protection from all rotating objects and prevents the user from accidental injury. The data acquisition system provides both monitoring, measurement and recording capabilities of important parameters.

6 Testing and Verification

Upon completion of the design and fabrication phase of the project, a series of tests were performed to validate the functionality of each of the systems of the research engine. These tests were necessary to ensure that all systems of the apparatus were working correctly. This section includes the following; testing and verification procedures, results and any difficulties encountered.

6.1 Engine System Testing

Engine system testing was performed to verify function of the engine prior to combustion experiments. A leak test was performed on the cylinder head prechamber prior to assembly, and a compression test was performed on the engine after assembly.

The leak test was performed on the prechamber and fully assembled VCR secondary piston to test the integrity of the VCR seal. A suction cup was purchased and installed on the suction line of a vacuum tester. The vacuum tester was used to draw a vacuum on the prechamber. The suction cup creates a tight seal around the opening of the prechamber from the combustion chamber side of the cylinder head.

The leak test was performed several times and the procedure and results are presented in Appendix E.7 through E.10. Initially, the leak test revealed that the VCR assembly had severe leakage, however it was not apparent what part of the assembly was leaking. The main seal by the copper spacer and the plug seal were determined to be secure. The leak was isolated and found to be occurring at the copper washer around the tip of VCR secondary piston. Further tightening and compression of the copper washer was attained using Teflon tape wrapped around the threads and the copper washer. The Teflon tape provided a slick surface and enabled the threads to be tightened further and hence allowing greater deformation of the washer and a tighter seal. As a result, the prechamber was able to hold the maximum capable vacuum at 90 kPa.

The compression test was performed on the engine once it was fully assembled. A diesel compression tester was purchased from Snap-On Tools that was well suited for compression testing up to 6894 kPa (1000 psi). A custom glow plug adapter was fabricated and threaded into

the glow plug hole in the cylinder head. This adapter enabled the compression tester to be connected to the prechamber (see Appendix E.11 to E.14 for further details.)

The first compression test resulted in no compression detected in the engine. This was of great concern as the prechamber had already been verified to hold the maximum vacuum possible. The cylinder head was removed and inspected, and it was determined there were two possible sources of compression leakage. The first source was determined to be the lack of flatness of the cylinder head. A straight edge was used to identify that the cylinder head surface was not perfectly flat. This would cause an improper seal with the cylinder head gasket and hence substantial leakage. The second source of leakage was determined to be from the valve seat. The valve seat is located at the interface between the valve and the cylinder head. Valve seat leakage could cause substantial leakage since the valves would not close completely and hence the compression pressure would be completely lost. The cylinder head was sent to Couvillion Automotive Machine Shop to have the cylinder head ground flat and the valve seats ground and lapped. These processes ensure the cylinder head is perfectly flat giving a tight and even seal with the head gasket, and ensured the valves close completely. Also, since the valve seats were ground flat, some material was removed from the seat and therefore the valve spring tension would be lower since the spring tension is a function of length, and the length increased from the seat grinding. Therefore, a shim was fabricated using 0.00254 cm sheet stock and installed under the affected valve springs. This shim takes up the slack that was removed as a result of the valve grinding, and restores the spring tension to its originally specification.

The second compression test (CR=22:1) resulted in 2861 kPa (415 psi) compression with the engine cold, and 3103 kPa (450 psi) compression was measured after the engine was motored for half an hour and warmed to 40 °C. Therefore, it was verified that the modified Kubota engine with the VCR secondary piston installed had no leakage and a compression pressure of 3103 kPa.

6.2 Drive System Testing

Drive system testing was performed to verify the function of the VSD prior to combustion experiments. Motoring tests were performed both with and without the Kubota engine coupled to the AC motor. Emergency braking tests were also performed to verify the ability of the drive system to stop during an emergency situation.

The first motoring test was performed without the Kubota engine coupled to the AC motor. This test involved turning the AC motor without any load, and was performed to verify the functionality of the AC motor and the VSD. The test was done to ensure that the system was able to start, stop and run at different speeds. The procedure and results for this test are listed in Appendix K.3 and K.6. The test proved that the system was able to attain a shaft speed of 530 to 3535 RPM with a corresponding input frequency of 9.0 to 60.0 Hz. The system ran perfectly without significant evidence of vibration, or any other electrical problem.

The second motoring test was performed with the Kubota engine coupled to the AC motor. This test was performed to verify the functionality of the drive system while the Kubota engine was being motored. The test ensured that the system was able to start, brake the engine and run at different speed. As mentioned previously, the AC motor would require assistance from the starter motor to overcome the starting torque of the Kubota engine. Therefore, the starter was connected to 12 volt power and a switch to enable use of the starter. The procedure and results for this test are listed in Appendix K.4 and K.7.

The results showed that the drive system was unable to start the engine without the assistance of the starter. However, with the starter engaged shortly, the starting torque of the Kubota engine was overcome and at that point the drive system would begin to rotate the engine under its own power. The minimum shaft speed of the drive system was determined to be 707 RPM or 12.0 Hz. Lower speeds were attempted but the vibration of the engine at those speeds was too severe. The drive system was able to rotate the Kubota engine from 707 to 3004 RPM, with a corresponding input frequency of 12.0 to 51.0 Hz. Certain shaft speeds induced greater vibrations in the apparatus than others and this was noted in the observation portion of the results in Appendix K.7. The system functioned well at all shaft speeds, however in general the noise level became greater as the shaft speed was increased. The test was stopped at 3004 RPM (51 Hz) due to excessive noise and vibration of the engine, although the drive system seemed capable of continuing to maximum speed (3535 RPM.) The vibration was induced by both vertical and yaw vibrations of the engine on the engine mounts. These two modes would transfer vibrations from the engine through the engine mounts, and through the intake manifold to the apparatus fixture.

The majority of the noise from vibration seems to be emanating from the following sources; coupler misalignment due to engine oscillations and sheet metal and exhaust pipe vibrations. The fabrication and installation of a larger flywheel will help reduce engine oscillations and help

stabilize the rotational motion of the coupler interface. This should reduce the source of noise from the coupler. The sheet metal vibrations can be reduced by installation of rubberized padding between the sheet metal interfaces with the fixture frame. This will help insulate against vibration transfer. Rubberized mounts were installed between the intake manifold and the sheet metal top to help with this problem. The exhaust pipe vibration can be reduced by installation of a stabilizer bar to provide support to the exhaust pipe.

The third test was performed to verify the functionality of the drive system in the case of emergency braking the Kubota engine. This test was performed to ensure that the braking system was able to stop in an emergency situation at various different engine speeds.

The procedure and results for this test are listed in Appendix K.5 and K.8. The results showed that the braking system was able to stop the engine from all speeds in a timely manner. At speeds less than 1178 RPM (20.0 Hz) the braking system was able to stop the engine by using the internal resistor of the VSD in less than 0.5 seconds. For speeds greater than 1200 to 3000 RPM the braking system was able to stop the engine using the resistor bank in 2 seconds or less. Table 24 lists the summary of the emergency braking results.

Table 24 Emergency braking test results

Input Frequency (Hz)	Desired Speed (RPM)	Stopping Time (sec)
12	707.00	½ sec
15	883.75	½ sec
20	1178.33	½ sec
25	1472.92	1 sec
30	1767.50	1 sec
35	2062.08	1.5 sec
40	2356.67	1.5 sec
45	2651.25	2 sec
50	2945.83	2 sec

The braking system was not verified for braking function above 3000 RPM due to the excessive noise and vibration that developed at those speeds.

Therefore, it was verified that the drive system was able to motor the Kubota engine, and also the braking system was able to emergency stop the engine at 3000 RPM in less than 2 seconds. However, the vibration and noise of the system are significant to hinder the full operation range of the system therefore effective countermeasures will need to be developed in order to minimize these concerns.

6.3 Fuel System Testing

Simple functional tests were performed on the fuel system to verify the required function of all the components of the system.

A visual inspection of the fuel system was performed to ensure all the components were assembled correctly and no leaks were present. All the fittings were connected properly and tightened. The fuel pump was connected to the 12 V battery by means of a switch. Two litres of ethanol fuel was poured in the fuel tank and a visual inspection was performed to ensure no leaks occurred. The fuel pump was turned on briefly to check operation and then was turned on for 30 seconds to check flow and pressure. Initially, no fuel pressure was registered on the fuel gauge. The regulator adjustment screw was tightened and adjusted at which point the pressure was registered to shoot up to over 690 kPa (100 psi). The fuel pressure was adjusted until the gauge reading was 310 kPa (45 psi), and was locked into place. The gauge was observed to be quite erratic with the oscillating around 310 kPa +/- 34 kPa . This is most likely due to the turbulence of the fuel flow moving through the regulator causing the regulator spring to experience oscillations. This could be improved by using a smaller fuel pump or increasing the line distance between the fuel pump and the regulator.

The fuel injector was also briefly tested to verify its function. Power (5 V) was supplied to the injector by means of a power supply and switch. The fuel injector was turned on for a 5 second interval, and the spray atomization of fuel was observed. The fuel injector had a tendency to want to separate from the mount fitting due to the pressure. A bracket should be fabricated and installed to prevent this from happening.

In summary, all the components of the fuel system were observed to function properly but the injector mount requires fabrication of a bracket to ensure no leaks. A smaller fuel pump would improve system accuracy, and help reduce turbulence.

6.4 ECU System Testing

The purpose of the ECU is to receive and process sensors outputs that read the current state of the engine, and output a corresponding injector pulse width based on calculations performed on those sensors. Therefore, two types of tests were performed on the ECU system to verify operation; simple functional tests and injector scalar calibration.

Simple functional tests were performed on the ECU system to verify the function of all the components of the system. The ECU was installed according to the manufacturer's recommendations. All the sensors were connected and tested accordingly. The results of the sensors functional test and procedure are listed in Appendix L.6 and L.7.

The TPS sensor output was found to vary with throttle opening from 1 to 75 %. However, the TPS sensor maximum reading was at 75 % and corresponded to a fully open throttle valve. This is not a concern, but needs to be taken into account when programming the ECU. The air temperature sensor (MAT) functioned correctly for temperature ranges -10 °C to 100 °C. Higher temperatures, as would be expected with use of the heater, could melt the plastic material of the MAT sensors. Therefore, it is not recommended to use the MAT for intake temperatures greater than 100 °C, and the sensor should be removed from the intake when temperatures go beyond this point. The coolant temperature sensor (CLT) also functioned correctly for temperatures in the range 0 – 90 °C. Subzero temperatures were not tested but it is believed that the sensor would behave accurately at temperatures lower than -25 °C. The manifold absolute pressure sensor (MAP) functioned properly as expected. The MAP was able to read manifold pressure accurately in the range of 95 to 105 kPa. The battery voltage indicator was verified with a voltmeter, and it was determined that it read the voltage accurately. The hall-effect sensor responded to cam trigger signal from the cam trigger mechanism. However, there was a glitch with the cam trigger mechanism. The trigger signal would periodically read a higher engine speed than is actually occurring. It is believed that this glitch is caused by the overly simplified cam trigger mechanism. If the cam trigger wheel had 35 teeth and one space, (as in most automotive engines) instead of 1 tooth, this glitch would be eliminated.

Injector scalar calibration was performed to determine the scalar value for the injector at different equivalence ratios and engine speeds, and also to verify the function of the ECU and all its components. The procedure and results of the scalar calibration can be found in Appendix L.8 through L.13. Injector calibration experiments were performed for engine speeds of 670, 1000,

1500 and 2000 RPM. The throttle position was set for 65 % for all the injector calibration tests. For these test the TPS sensor was fixed to establish a baseline. (Increasing TPS percentage will increase the pulse-width of the injector and deliver more fuel.) Two litres of ethanol were added to the fuel tank, the weigh scale was zeroed with a plastic bucket, the 883ECU program was loaded and the ECU was turned on.

The experiment requires the use of the spreadsheet Fuel System Design Calcs2.xls and the 883ECU program. The basic mapping window of the 883ECU is utilized. By trial and error the injector scalar value was determined and adjusted until the value displayed in the 883ECU program for pulse width matched the value calculated in the spreadsheet. The scalar value is entered into the spreadsheet as the initial guess scalar. At this point the engine was motored at the desired engine speed and the fuel pump and injector were turned on. A stopwatch was used to ensure the injector operated and sprayed into the plastic container for 4 minutes. Then the injector and pump were turned off and the plastic bucket was weighed, giving the mass of the fuel in grams. The mass of fuel was entered into the spreadsheet under initial fuel mass. The program calculated the ratio between the theoretical mass of fuel and initial mass of fuel, and this ratio was multiplied by the initial guess scalar to determine the required scalar. The required scalar value was entered into the basic mapping window and the test was repeated again. The final mass of fuel was entered into the spreadsheet and compared to the theoretical amount of fuel. The results for each engine speed are presented in Figure 86.

The lowest engine speed (625 RPM) is the farthest off from the other grouping. This suggests that for low engines speeds the ECU may be out of range. The next three engines speeds (1000, 1500, and 2000 RPM), are more closely grouped together. This suggests that the ECU functioned more accurately in this range.

The results also indicate that as the engine speed is decreased the required scalar value also decreased. This was not expected, since injector scalar varies the pulse width of the injector, and pulse width should be independent of engine speed. The expected line should have been a linear line for all engine speeds and should show a linear dependence between equivalence ratio and scalar value. The equation of this line would be:

$$\text{Scalar} = 25.695\Phi + .2054.$$

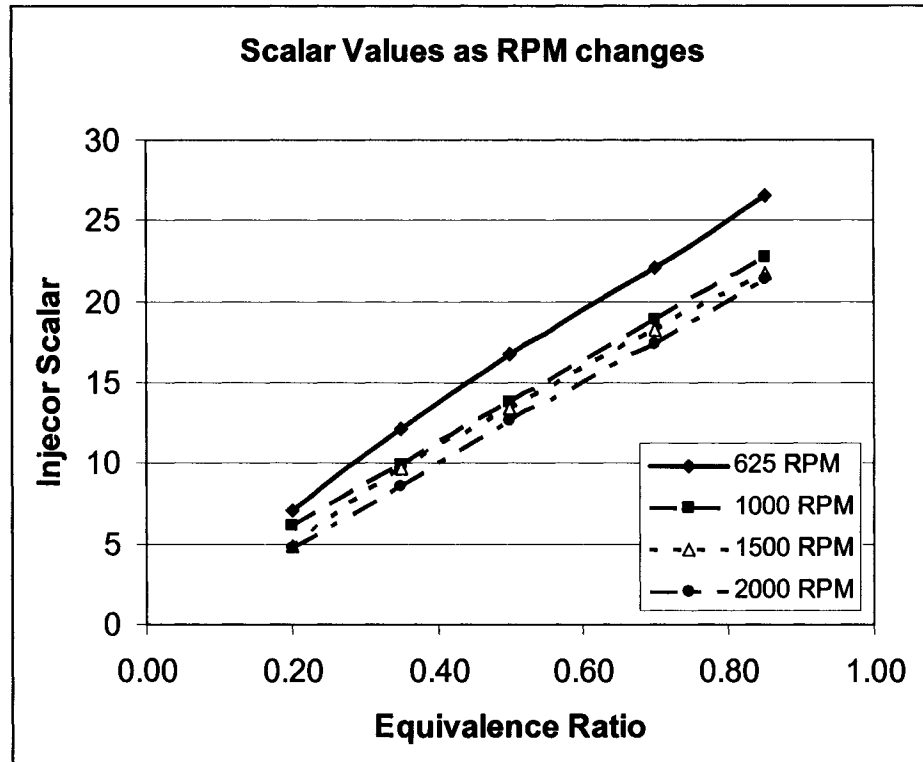


Figure 86: Required injector scalar for measured engine speeds.

Figure 87 is based on the raw data located in Appendix L.8 through L.12 and is summarized in Appendix L.13. The raw data extrapolated to obtain the curves for higher engine speeds 2500 and 3000 RPM.

Figure 87 displays the injector scalar results along the y-axis, and can conveniently be used by the research engine operator. By selecting the desired engine speed across the x-axis, and by selecting the desired equivalence ratio, the operator can determine the required scalar to be inputted into the basic mapping window of the 883ECU program. The main disadvantage of this method is that the calibration process is lengthy and each fuel type will require its own set of calibration experiments. Also this method was performed independently of the air flow meter. The injector scalar calibration should be performed in conjunction with the flow meter, since the throttle position and engine speed affect the injector pulse width and ultimately the scalar value.

Nonetheless, the ECU system was verified to function correctly and provide accurate fuel metering. An injector scalar summary was created to make it convenient for the user to determine the injector scalar for ethanol, and this method can be extended to other HCCI fuels such as gasoline. Further calibration experiments should be conducted using the airflow meter.

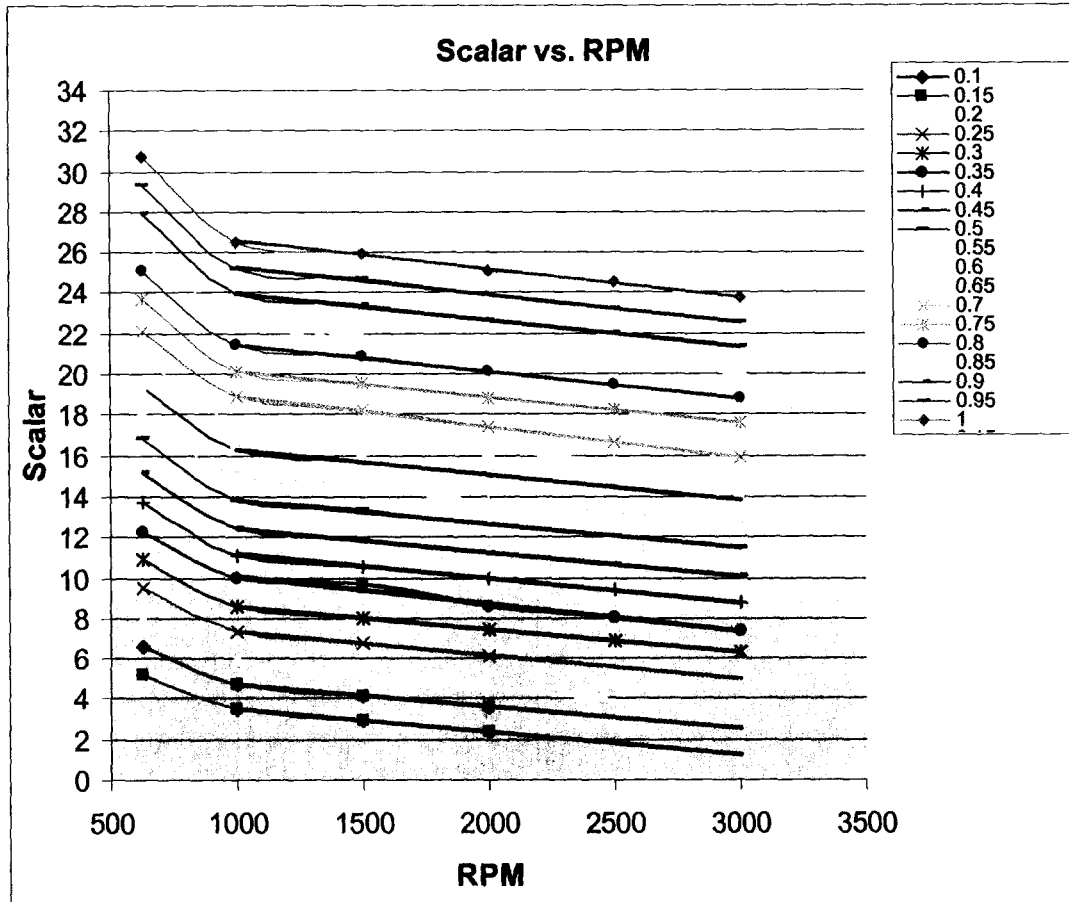


Figure 87: Summary of required injector scalar for all equivalence ratios and engine speeds.

6.5 Intake Piping System Testing

The intake piping system was tested by performing air flow experiments using the laminar flow meter at room temperature (20°C). Simple functional tests were performed on the system to verify the function of all the components of the system. The results of the intake system test and procedure are listed in Appendix M.

All the components of the intake system were tightened and secured. The VSD was turned on to prompt the system. The 24 Volt power supply was turned on to activate the transmitter and the laminar flow meter. The PC was turned on and both Labview and 883ECU were loaded. The 883ECU program was used to ensure the throttle position sensor was set to 70 % fully open throttle. The Research Engine Data Acquisition System program was run and the flow rate versus time curve was observed. Initially, at no engine speed, the laminar flow meter had a flow offset reading of -0.38 L/s. This value is subtracted from the flow rate values at other engine speeds to

obtain the actual corrected flow rate reading. The results from the experiment are presented in Figure 88 below.

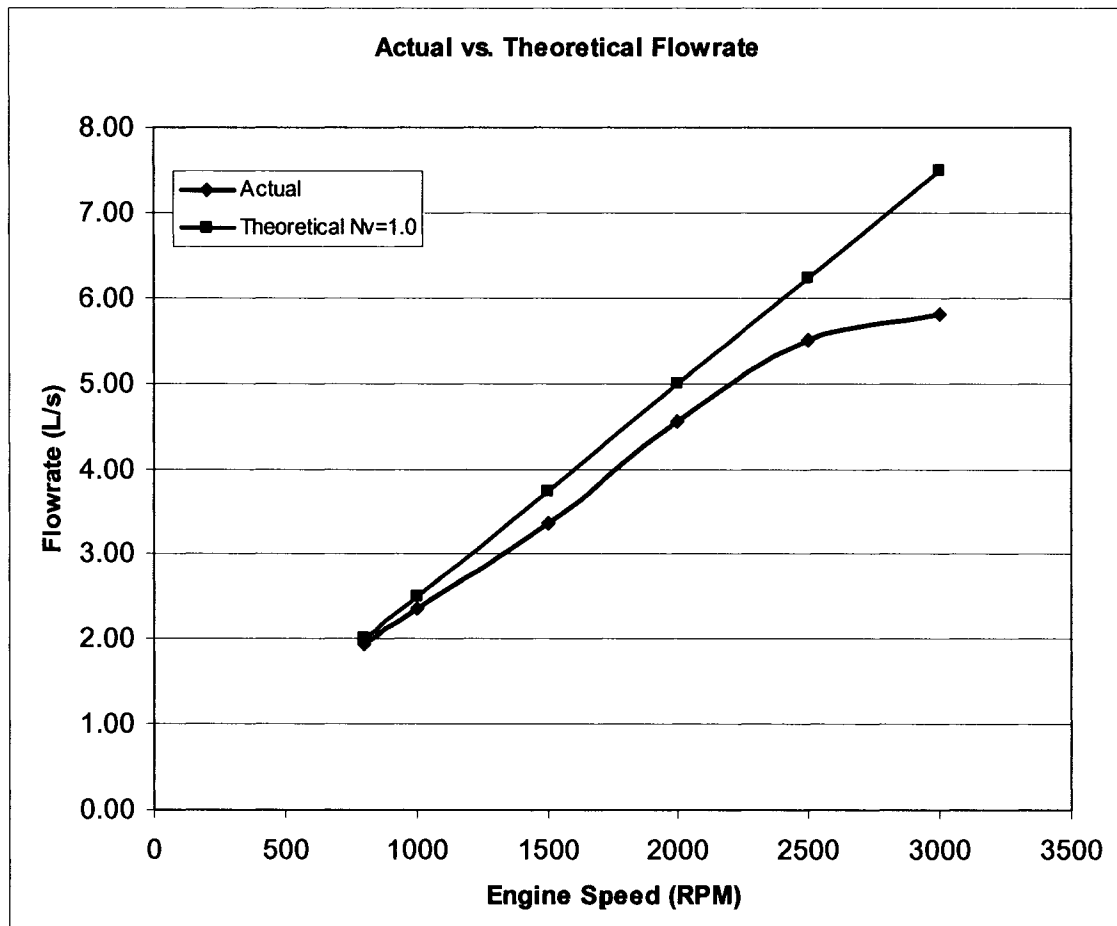


Figure 88: Actual flow rate at various engine speeds.

The VSD was turned on and the engine was run for 20 minutes to warm up the lubricating fluids in the engine. The engine speed was set to each of the following values for approximately 1 minute while the flow meter readings were recorded; 800, 1000, 1500, 2000, 2500 and 3000 RPM respectively. Both the theoretical and actual flow rate results with respect to engine speed are presented in Figure 88.

The theoretical flowrate was calculated by assuming the volumetric efficiency (η_v) to be =1.0 (details are shown in F.4). The actual flowrate was determined from the measurements made during the experiment with a correction factor applied to them. Note the linear line of the theoretical results for the engine, compared to the polynomial shaped line for the actual flow rate results. The experimental results for intake flowrate show fairly good agreement with

theoretically calculated results. The deviation of the actual flow rate compared to the theoretical flow rate tends to increase as engine speed increase. This is expected, since the long 3 m length of the intake system will create a stronger resistance to flow at higher engine speeds than a shorter system. This is also confirmed in Figure 89, which shows the volumetric efficiency versus engine speed.

The following equation obtained from Heywood [64] was used to calculate actual volumetric efficiency.

$$\eta_v = \frac{2\dot{m}_a}{\rho_{air} V_d N}, \quad \text{Equation 20}$$

At 800 RPM the volumetric efficiency is greater than 95 % and decreases slightly as the engine speed increases to 1500 RPM. Between 1500 and 2300 RPM, the volumetric efficiency is 90 %.

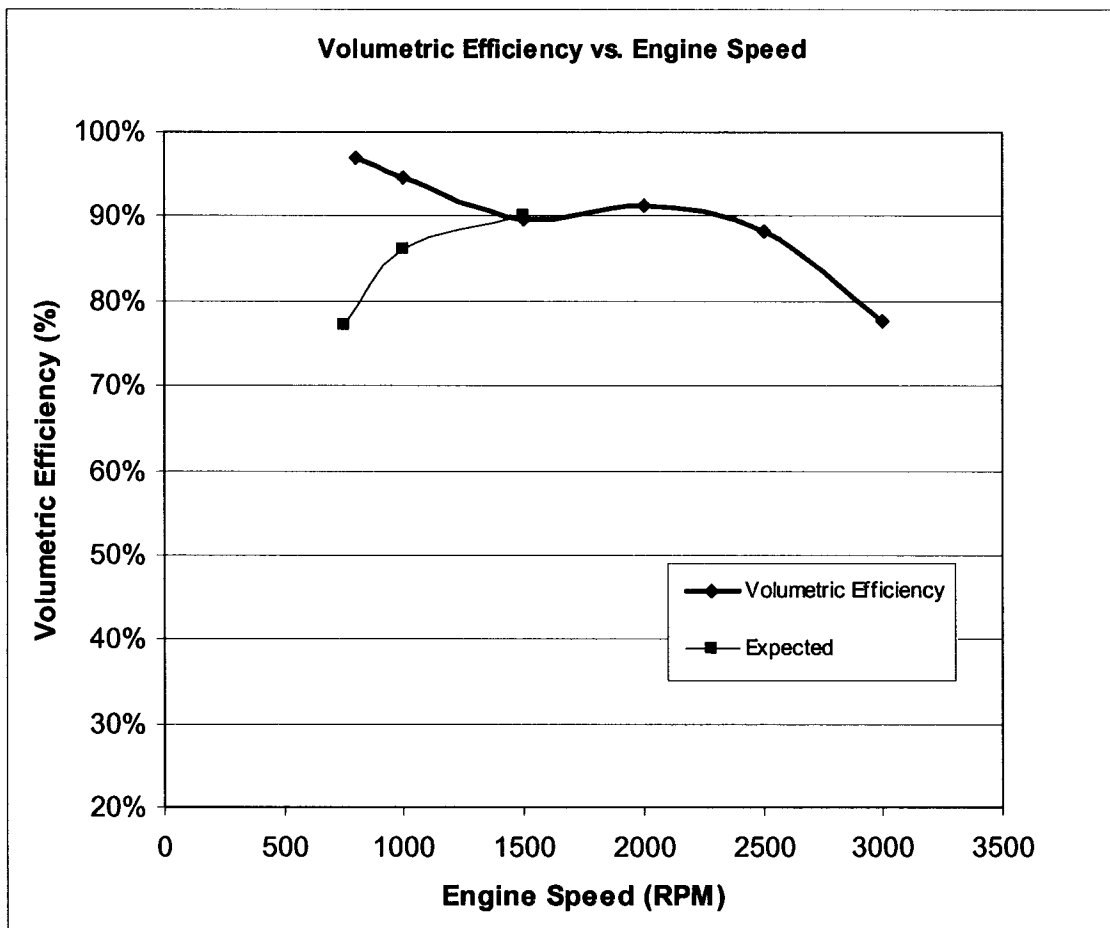


Figure 89: Actual volumetric efficiency at various engine speeds.

Increasing the engine speed to 2500 RPM the volumetric efficiency decreases until to less than 80 % at 3000 RPM. These volumetric efficiencies are considered to be acceptable based on Heywood [64]. Improvements can be made by decreasing the intake piping run length, since this is significantly longer than production OEM length. This will increase the volumetric efficiency at higher engine speeds.

At 800 and 1000 RPM the actual volumetric efficiencies were higher than expected. The volumetric efficiencies were expected to be less than 90% at low engine speed. The expected volumetric efficiency should look more like the expected values shown in Figure 89.

This experiment verifies that the intake piping system and air flow meter functioned correctly. However, further improvements can be made to improve the volumetric efficiency of the engine. The air flow meter produced results that were accurate and useful in verifying the functionality of the intake system.

6.6 Intake Air Preheater Testing

The intake air preheater system was tested by performing air heating experiments. The results of the intake air preheater system test and procedure are listed in Appendix M.

All the components of the intake system were tightened and secured and the VSD was turned on to begin motoring. The 240 V disconnect was turned on and the heater controller was connected and turned on. The PC was turned on and 883ECU was loaded, to ensure the throttle position sensor was set to fully open (70 %). The intake air temperature sensor was removed to prevent burn-up. Heater tape was wrapped around the intake manifold to assist in bringing the intake manifold up to the desired temperature. Insulation was also wrapped around the heater tape to keep the heat on the intake pipe. Refer to schematic of the intake system in Figure 25 for more details.

Two batches of experiments were performed. The first experiment utilized the heater tape without insulation and the second experiment utilized the heater tape with insulation.

For Experiment One, heater tape was installed on the intake system. The heater controller set-point was set to the desired temperatures of 50 and 100 °C. The controller compared the set-point value to the thermocouple value located closest to the intake valve. Approximately 20 minutes

ramp time was allotted for the system to reach thermal equilibrium. Thermal equilibrium was reached once no significant changes were observed in the heater exit temperature. The heater exit temperature was recorded along with the heater tape percentage setting. The heater exit temperature was measured using a 1.588 mm K-type thermocouple with an Omega digital readout. The results are displayed in Figure 90 and listed in Appendix M.7.

Experiment Two utilized the same procedure as Experiment One except the intake piping was wrapped with reflective insulation to minimize radiative losses. For comparison, the 100 °C set-point temperature was re-run and the results are also displayed in Figure 90. The results for 100 °C set-point show a decrease of approximately 30 °C in heater exit temperature for Experiment Two with the addition of insulation. This was a great improvement and based on these results it is recommended that heater tape be used on the intake piping system for all future experiments. The decrease in heater exit temperature with the addition of insulation for 100 °C set-point indicated reduced heat loss of the intake piping system. Therefore, the remaining experiments are conducted using insulation to reduce heat loss. As the set-point temperature was increased to 150 °C, the maximum heater exit temperature reached 201 °C at 1500 RPM. This maximum is amplified as the set-point temperature was increased to 200 °C while the heater exit temperature reached 315 °C.

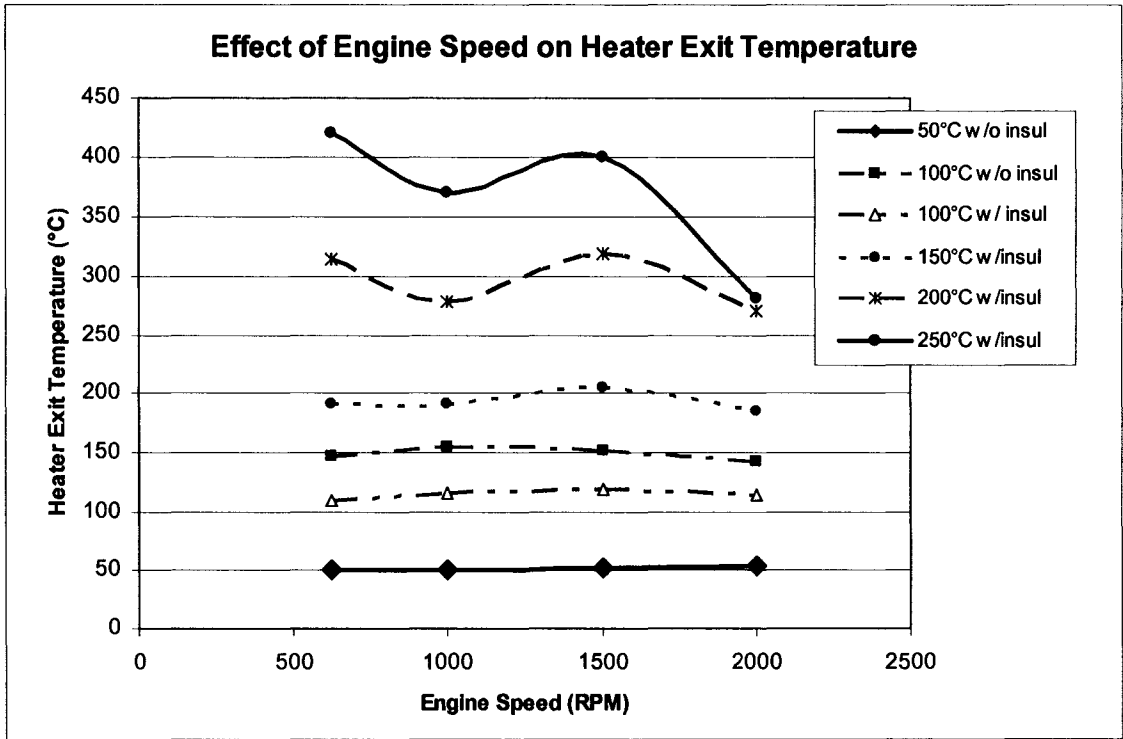


Figure 90: Heater Exit Temperature at various engine speeds.

The increase in heater exit temperature can be attributed to increased flow resistance or a decrease in flow efficiency at 1500 RPM. This was confirmed in Figure 89 with the drop in volumetric efficiency to 90% at 1500 RPM.

Figure 91 displays the calculated heat transfer rate of the intake air heater to the air at various engine speeds. The heat transfer rate was calculated by using the following equation from the First Law of Thermodynamics [35].

$$Q_{HT} = \dot{m}_a C_p \Delta T, \quad \text{Equation 21}$$

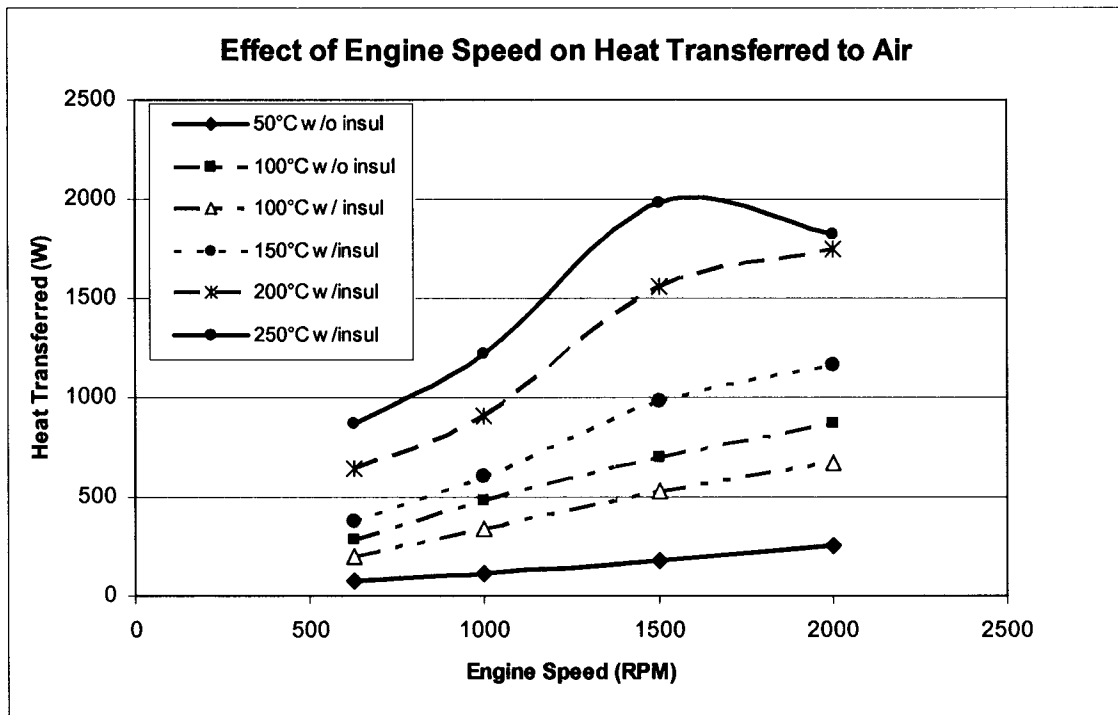


Figure 91: Heat transferred to air at various engine speeds.

The non-linear increase in heat transfer rate required for the 200 °C set-point at 1500 RPM is clear in this figure. The non-linear behaviour is most likely due to the reduced volumetric efficiency at higher engine speeds. Figure 91 also illustrated 200 kW heat transfer rate improvement for 100 °C with insulation compared to without insulation.

Upon attempting to raise the set-point temperature to 250°C similar yet more pronounced trends for 650, 1000, and 1500 RPM were observed. At 650 RPM, as the volumetric efficiency decreases the heater exit temperature increases. At 1000 RPM, the flow resistance decreases, as a

result the heater exit temperature also decreases to 370°C. Then at 1500 RPM, the flow resistance increases and corresponds to an increase in exit temperature to 400°C.

This experiment indicated that the intake air preheater did function correctly up until 250 °C set-point was selected. A replacement heater element will have to be obtained and the experiments will have to be completed with use of the laminar flow meter to provide more accurate data of air flow and prevent heater failure.

6.7 Data Acquisition System Testing

The data acquisition system was verified by performing a motoring experiment and acquiring data using the Labview program. This involved obtaining screen captures of each of the system panels in the Research Engine Data Acquisition System program. The screen captures were obtained while the engine was motoring at 750 RPM, with no fuel injected, and hence no combustion events occurring. The data files were obtained during combustion experiments and post-processing was performed. Statistical analysis was performed on the data and tabulated. The screen captures are shown, and the statistical summary is presented in the following sub-sections.

6.7.1 Thermocouple Verification

The thermocouple signals were verified by screen capture of the display screen and by data acquisition tabulated in Appendix N. The temperature panel display screen (shown in Figure 95) shows a real-time readout of the data from all six thermocouple channels simultaneously.

The thermocouple wires were routed with insulated conduit to minimize electric field noise from the AC motor. When the AC motor was not operated, the thermocouples were tested using a portable omega thermocouple reader. The reader can plug into each thermocouple separately and provides accurate measurement of the temperature at that location. These values were compared to the values obtained using the data acquisition system and appeared to be stable and consistent with expected values.

When the AC motor was started, the field noise from the rotor and stator interfered with the thermocouple signals significantly. This can be seen in Figure 92.

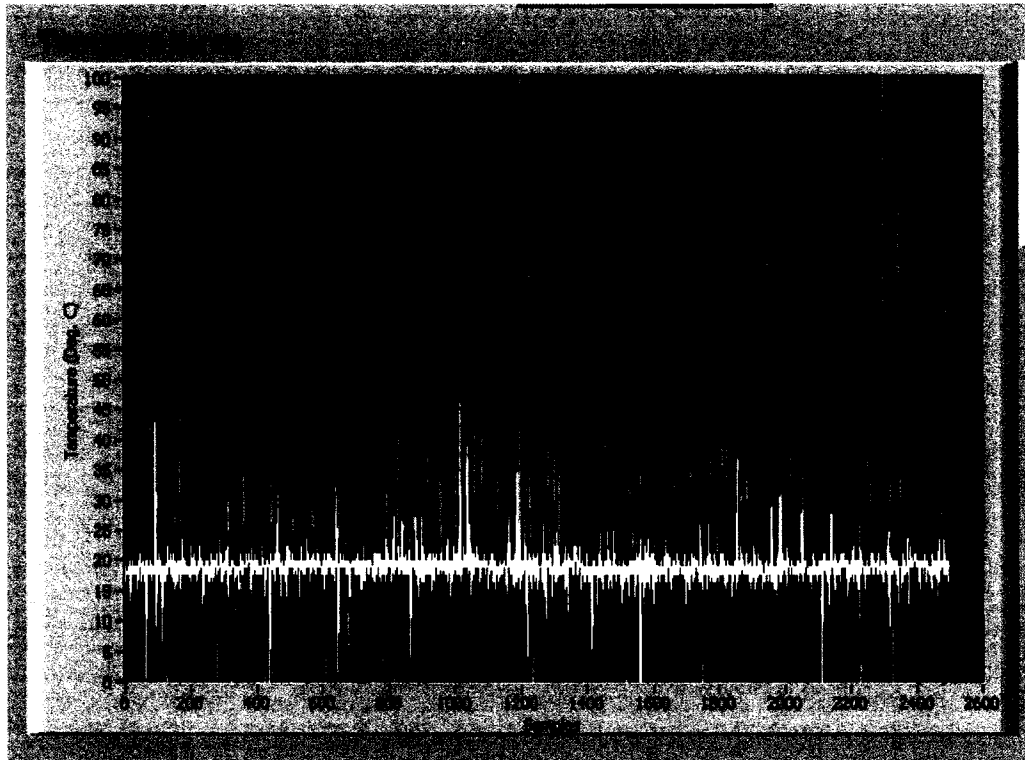


Figure 92: Real-time unprocessed thermocouple data at 775 RPM.

The signal interference was concluded to be coming from strong magnetic field generated by the AC motor, since the thermocouple were initially reading correctly. Thermocouple signals are weak low voltage signals, and therefore are subject to interference from strong magnetic fields such as is present around an AC motor. This magnetic field can penetrate through insulating conduit through the thermocouple wire sheath and interfere with the signal traveling from the thermocouple to the DAQ. Also, since grounded type thermocouples were used they could receive electrical interference from the fixture frame itself since all the Drive system components were mounted to the frame.

To remedy the heavy noise interference present with the current thermocouple DAQ system a National Instruments 6 channel low-pass filter and amplifier should be installed. This device will both clean and boost the signal and will eliminate the noise and provide accurate readings. The grounded K-type thermocouples used should be replaced with ungrounded K-type thermocouples. This will isolate the low voltage thermocouple signal from the high voltage noise present in the fixture frame.

Overall the thermocouple and the data acquisition system did function to a certain extent. However, some thermocouple readings were inaccurate due to severe noise interference. A

filter/amplifier should be purchased to eliminate the noise, and ungrounded thermocouples should be installed in all locations.

6.7.2 Flow rate

The flow rate signal was verified by screen capture of the display screen and by data acquisition tabulated in Appendix N. The flow rate panel display screen (shown in Figure 93) shows a real-time readout of the Meriam laminar flow meter via the Honeywell transmitter. The flow meter function was already verified earlier, however this section pertains to the verification of the flow meter signal.

The flow rate panel contains the real-time output of the flow meter. As mentioned earlier, the flow meter has an offset value of -0.38 L/s at no flow. This value must be subtracted from the raw flow rate reading in order to obtain the actual value.

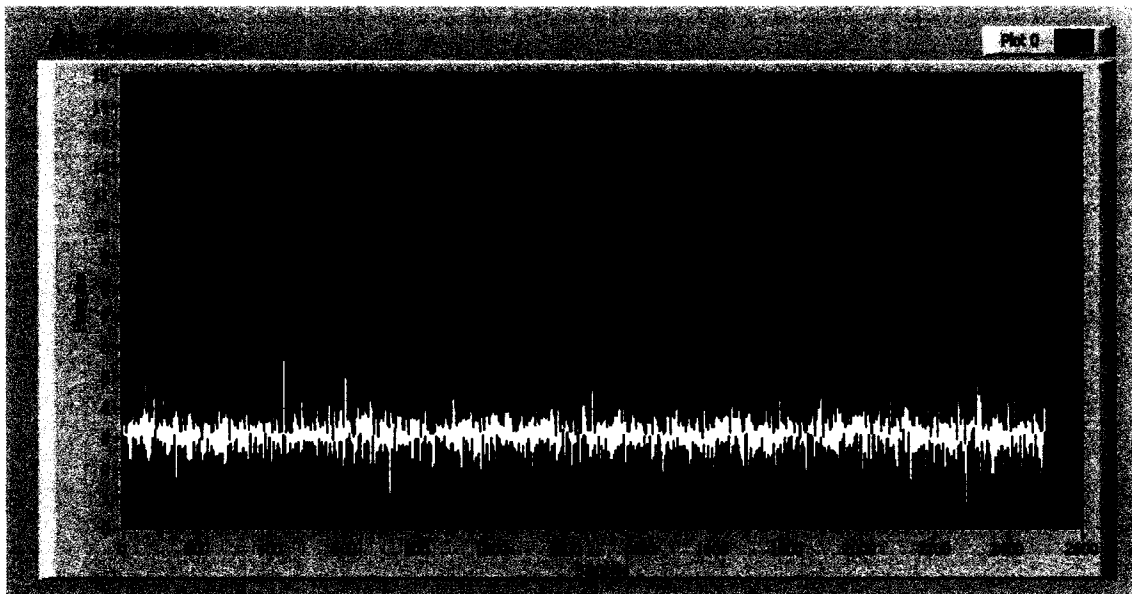


Figure 93: Real-time unprocessed flow meter data at 775 RPM.

The signal reading from Figure 93 is 3.0 cfm or 1.41 L/s. A statistical summary of this data is displayed in Table 25 below. The corrected median value of the flow rate for an engine speed of 775 RPM is 1.79 L/s. This is in close agreement with the corrected mean value of 1.788 L/s. The standard deviation of the data is 0.1724 L/s.

The flow meter signal is considered to be quite accurate. Trouble free data can be expected from this system for many years to come. One possible improvement would be to recalibrate the range

of the transmitter to be between 0 and 14 L/s (0 to 30 cfm), instead of the currently set range of 0 to 47 L/s (0 to 100 cfm).

Table 25 Statistical summary of flowmeter data.

	Raw Flowrate Data(L/s)	Corrected Flowrate Data (cfm)
median	1.4166	1.79413
mean	1.41096	1.788429
stdev	0.172367	0.172367

This would improve accuracy over the expected flow range of the engine. Recall originally the flow meter was calibrated for the flow rate of all 3 cylinders to ensure further expansion capacity.

6.7.3 In-cylinder Pressure

The in-cylinder pressure transducer signal was verified by screen capture of the display screen and by data acquisition tabulated in Appendix N. The display screen (shown in Figure 94) shows a real-time readout of the Kistler 6052A pressure transducer installed in the VCR secondary piston. As mention earlier, the pressure transducer produces a charge signal that is converted to voltage using the Kistler 5004 amplifier. The function of the in-cylinder pressure transducer was verified by performing a motoring experiment at 775 RPM.

The pressure panel of the Research Engine Data Acquisition System program displays the real-time output of the pressure transducer and monitors the peak pressure over each cycle. For this case, the engine speed is at 775 RPM and no fuel is being injected into the engine. The raw peak pressure is 8300 kPa (83 bar), and is displayed in the small display window in the bottom right corner of the graph. Notice the -700 kPa offset of the pressure curve near the origin of the x-axis.

The offset value is subtracted to all data points on the pressure curve to obtain the actual corrected pressure values. Therefore, the corrected peak pressure becomes 9000 kPa. Also notice the uniform sinusoidal shape of the curve. This shape is consistent with motoring piston engines found in Heywood and represents both compression and expansion without combustion [64]. This valued was compared to the calculated peak pressure shown in Appendix E.16 for an isentropic compression. The compression ratio of the engine during this experiment was 25:1. The ratio of specific heats for air is $\gamma = 1.4$. Using the MAP sensor reading we can determine the initial pressure in the manifold. This was found to be 8951 kPa or (89.51 bar).

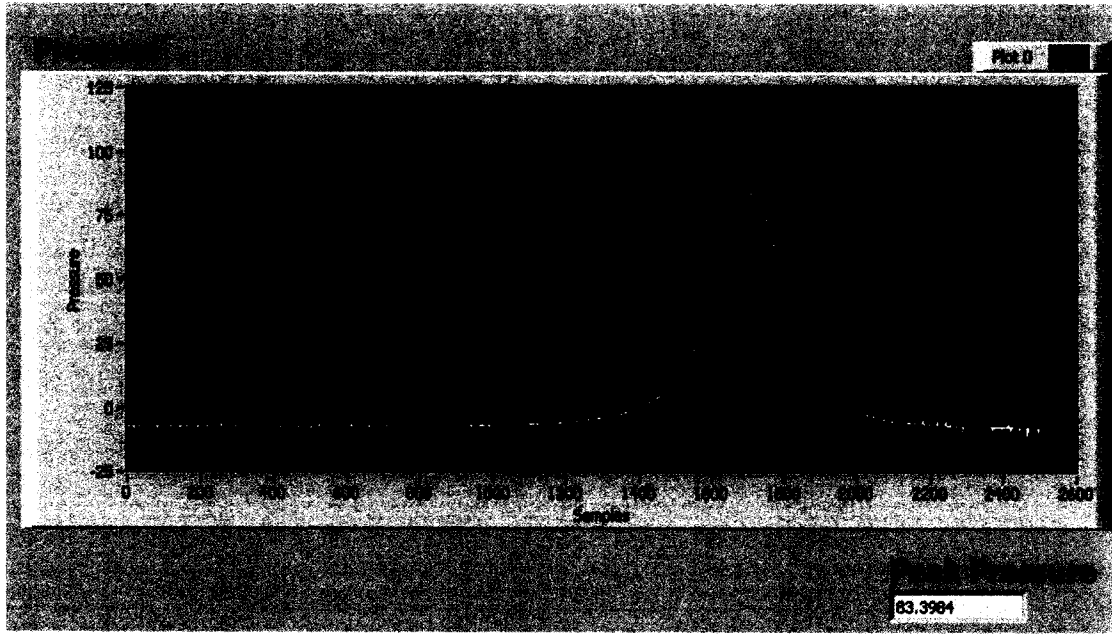


Figure 94: Real-time unprocessed in-cylinder pressure data for motoring at 775 RPM.

Using the following equation derived from isentropic compression we get:

$$p_2 = p_1 \times CR^\gamma, \quad \text{Equation 22}$$

$$p_2 = .988 \times 25^{1.4} = 89.51 \text{ bar or } 8951 \text{ kPa.}$$

The calculated peak pressure was show to be 8951 kPa or (89.51 bar). This is consistent with the pressure transducer measurement of 9000 kPa (90 bar), and verifies the function of the data acquisition system for reading and displaying the in-cylinder pressure signal and also verifies the compression pressure of the engine.

6.7.4 Crank Angle Encoder

The crank angle encoder signal was verified by screen capture of the display screen and by data acquisition tabulated in Appendix N. The display screen (shown in Figure 95) shows a real-time readout of the engine speed as determined from the crank encoder. As mention earlier, the crank encoder provides two signals; an index signal, and an encoder signal. The index signal provides a reference for rotation counting and can be used to determine crank shaft speed. The encoder signal provides the actual position of the encoder in 3600 increments per one rotation. The function of the crank angle encoder was verified by performing a motoring experiment and screen capture of the encoder gauge at 775 RPM, shown below. A combustion experiment with data

acquisition was also performed and the results will be presented. A sample of the encoder data from the combustion experiment is tabulated in Table 26.

The first column entitled “Index” refers to index H of the encoder. As mention earlier the index signal provides a rotational reference for the encoder. The index sample signal is primarily “0” until the index point on the encoder is reached and at that point the signal changes to “1”. The sample data indicated that the index signal is occurring and is picked up by the data acquisition system. The index signal is used by both of the other two columns of data; engine speed (RPM), and crank angle degrees (°CA).

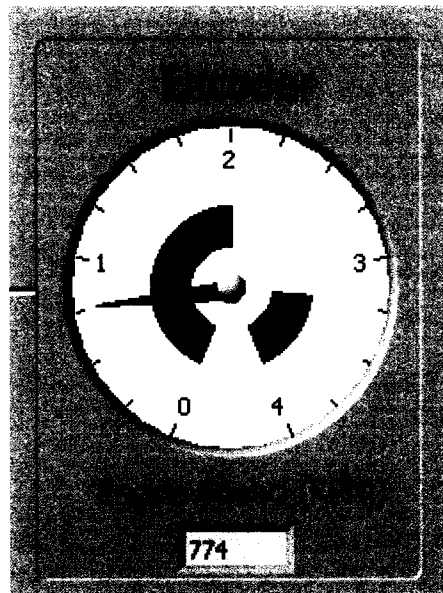


Figure 95: Real-time processed encoder signal for motoring at 775 RPM.

The crank angle degree data is acquired from channel A of the encoder and is the result of an incremental counter. The crank angle degree data range is from 0.00 to 360.00 CA degrees. Channel A is an absolute incremental counter and count to infinity had the index signal not be used to reset the counter.

The engine speed (RPM) is calculated in the following manner. The acquisition rate is used to determine elapsed time between each reading from any channel. This can be determined from total time t_T (s) = 1 / rate (Hz). Then, simply counting the number of data points between subsequent “high” values from the encoder gives the total time for a single rotation. The inverse of this value is the rotational speed of the engine ω (rot/s) = 1 / t_T .

Table 26 Sample of crank encoder data from combustion experiment.

Index	RPM	CA
0	405.359772	359.675720
0	405.359772	359.716248
0	405.359772	359.756775
0	405.359772	359.797333
0	405.359772	359.837860
0	405.359772	359.878387
0	405.359772	359.918915
0	405.359772	359.959473
1	836.431213	0
0	836.431213	0.083643
0	836.431213	0.167286
0	836.431213	0.250929
0	836.431213	0.334572
0	836.431213	0.418216
0	836.431213	0.501859
0	836.431213	0.585502
0	836.431213	0.669145
0	836.431213	0.752788

Multiplying this value by 60, transforms it into the engine speed in RPM. This process can be repeated for each cycle of the encoder to get a new rpm value for each rotation of the crankshaft [68]. The data sample for engine speed in column two seems to indicate there is a problem with this calculation in the program. The data indicates that the engine speed jumps from 405 RPM to 836 RPM in a split second which is physically impossible. Therefore, there must be a glitch in the calculation that requires further investigating and troubleshooting to solve.

This data set verifies the function of both channel A and Index H signals of the crank encoder. The encoder increments correctly and the index signal is correctly acquired. However, the calculation to determine engine speed in RPM appears to have a problem and requires further investigation.

6.7.5 Research Engine System Verification

Verification of the research engine as an entire system required conducting HCCI combustion experiments. One of the main objectives of this project was to obtain in-cylinder pressure measurements of HCCI burn of lean ethanol/air mixture. This was not possible since intake air preheater had failed during its verification experiment.

However, HCCI burn of lean gasoline/air mixtures was possible without pre-heating the intake air because gasoline has a lower octane number and hence lower resistance to auto-ignition, which is the initiating mechanism to attain HCCI burn.

Therefore, low octane number gasoline was chosen to be the test fuel and HCCI combustion experiments were performed on the research engine. The results and procedure of the HCCI combustion experiments are listed in Appendix N.

All the components of the intake system were tightened and secured and the VSD was turned on to begin motoring. The PC was turned on and 883ECU program and Research Engine Data Acquisition System programs were loaded. The throttle position sensor was set at 70 % throttle opening and the engine was motored without fuel for 30 minutes to build up heat in the engine block. Heater tape was wrapped around the intake manifold to assist in bringing the intake manifold up to the desired temperature. The intake air heater was replaced with a plastic ABS straight pipe. Injector scalar calibration experiments were performed for gasoline to obtain the injector scalar summary for 750 RPM.

Once the engine coolant temperature had reached 30 to 40°C and all safety precautions were taken, fuel injection of gasoline was started. Initially, fuel was injected to produce lean equivalence ratios (0.3 to 0.5), but HCCI was not attained because the engine was still too cold and the fuel mixture far too lean. Fuel was then injected to produce equivalence ratios (0.8 to 0.85) and auto-ignition and HCCI burn was attained. When auto-ignition began the engine began to knock severely and the injector had to be shut off to prevent engine damage. This was due to severe HCCI knock and engine run-off, which was reported in literature to occur with high equivalence ratios and with gasoline.

A starting strategy was developed that was effective in producing repeatable HCCI initiation. The strategy was to initially fuel the engine with a richer mixture to attain HCCI combustion and then

lean it out quickly to 0.6 once combustion was attained. As the engine coolant temperature was increased from 40 to 60 to 70 °C, the equivalence ratio could be leaned out even further to 0.3 and even 0.25. This had the effect of slowing down the combustion and retarding auto-ignition timing. Increasing equivalence ratio would advance auto-ignition timing and increase the onset of knocking. Increasing engine speed would cause a halt in HCCI, and equivalence ratio would have to be increased in order to initiate HCCI combustion again. The onset of knocking occurred quicker at higher engine speeds.

The drive/braking system was able to both motor the engine before HCCI occurred and provide braking while HCCI combustion was occurring. Before fuel injection would begin the drive system would be set to run the engine at 750 RPM, then once HCCI was attained the engine speed reached closer to 800 to 825 RPM. The drive system prevented the engine from running away, and provided adequate braking during HCCI combustion experiments. The resistor banks were not utilized during the experiments since the internal resistor of the VSD seemed to provide an adequate amount of braking. Experiments will be needed to verify the capability of the resistor bank braking system.

During HCCI combustion, the engine created strong vibrations, which seemed to be caused by the imbalance forces present during combustion. The vibrations could be reduced by developing a larger flywheel to smooth out the imbalance forces. Perhaps an alternative method of running all three cylinders on HCCI simultaneously or two on diesel and one on HCCI could eliminate the majority of the vibrations present.

The results of the HCCI gasoline combustion experiments are presented in Appendix N. Post-processing of the data was performed in the following manner. The raw data was surveyed and a representative sample of HCCI gasoline combustion was determined. Two graphs were constructed, namely Figure 96 and Figure 97 shown below.

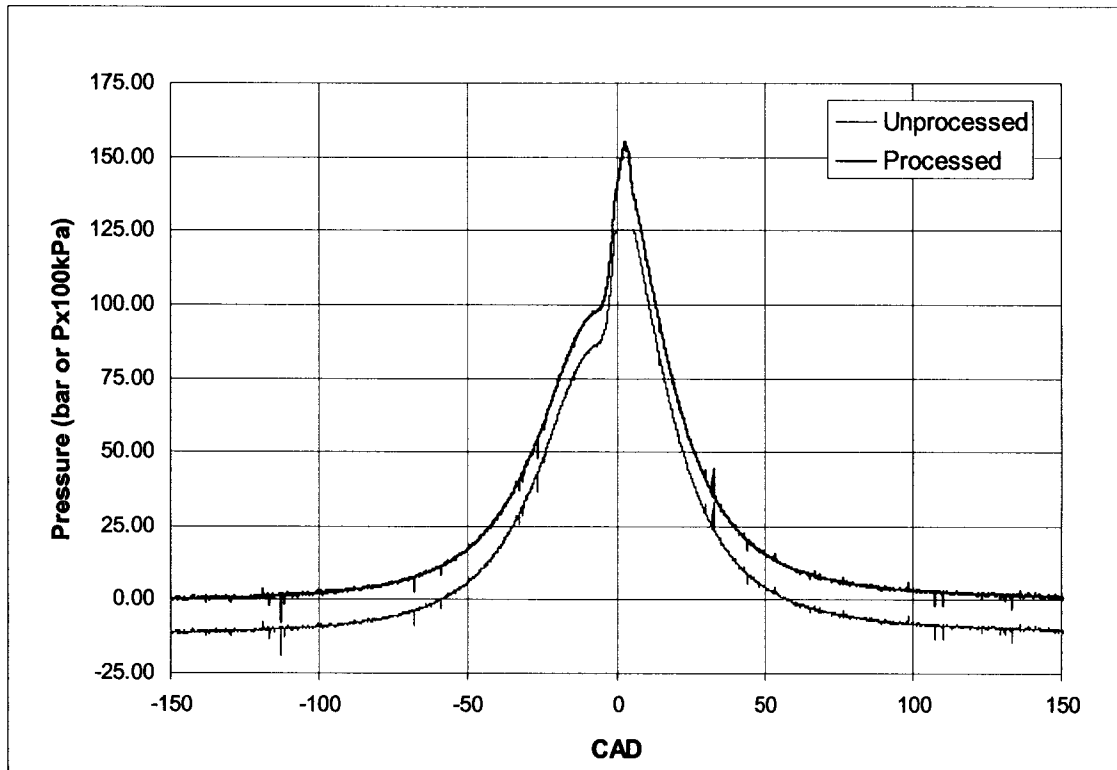


Figure 96: Pressure versus crank angle degree plot of HCCI gasoline experiment - processed and unprocessed data sample at 750 RPM.

Figure 96 represents a plot of the pressure versus crank angle degree for both processed and unprocessed data sample. The unprocessed or raw data sample (pink colour) is the actual output waveform from the in-cylinder pressure transducer as acquired by the data acquisition system. Notice the -1000 kPa (10 bar) offset from the origin, and the flat peak pressure curve. The -1000 kPa offset was corrected by subtracting this value from the rest of the data set. This has the effect of shifting the entire data sample up 1000 kPa, giving in a more accurate representation as shown in the processed data sample (blue). Also notice the start of auto-ignition occurring at roughly 2 to 5 degrees after top dead center. This is consistent with auto-ignition timing found in Christensen et al. [69].

The flat peak pressure curve was an unexpected feature of the raw data. It was attributed to the saturation of the data acquisition system at the higher pressures values. This can be corrected by adjusting the gain on the amplifier to extend the operating range of eliminate the flat peak pressure curve. The processed data sample was constructed extrapolating both positive and negative slopes and rounding the peak. This resulted in a curve that displays the peak pressure of

15500 kPa (155 bar). Although, this peak reconstruction is not 100 % accurate it does give an adequate representation of the actual shape of the HCCI peak pressure curve.

The pressure volume or PV diagram (shown in Figure 97) was constructed by plotting the change in pressure against the change in volume. Similar to Figure 96 both unprocessed and processed data series are presented to illustrate the comparison between the data set. The lower curve represents compression of the air fuel mixture and the upper curve represents expansion of the combustion products. The PV diagram is a very useful tool in analyzing in-cylinder combustion events. Notice the -1000 kPa offset of the unprocessed data compared to the processed data and the reconstructed peak pressure curve. The area under the curve of the PV diagram represents the work associated with the compression and expansion of the piston by the gases inside the cylinder. The work to compress the gases is considered negative work by the gases, and the work done by the gases to expand the piston is considered positive work. By subtracting the compression work from the expansion work you obtain the net indicated work for the cycle.

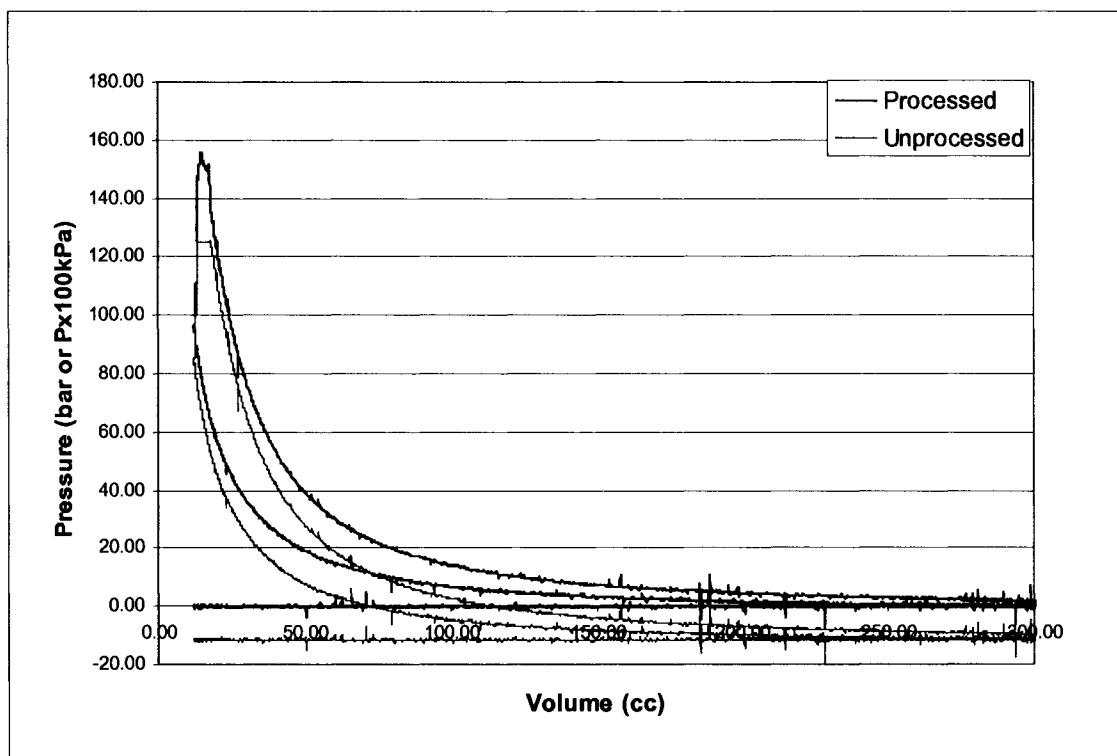


Figure 97: P-V diagram (pressure versus volume diagram) of HCCI gasoline experiment, corrected and uncorrected data sample at 750 RPM.

Heywood provides thorough discussion and list mathematical definitions for calculating work and power from P-V diagram data sets [64]. The difference in area under the compression and expansion curves is representative of the gross indicated work per cycle and is defined as:

$$W_{c,i} = \oint p dv , \quad \text{Equation 23}$$

Given in units of [N-m], Where p is the pressure in bar and dv is the change volume in cubic centimetres (cc). This definite integral was solved using Simpson's Rule and further details are provided in Appendix N. The indicated power (P_i) per cylinder is obtained using the following:

$$P_i = \frac{W_{c,i} N}{n_R} , \quad \text{Equation 24}$$

Given in units of [W], where N is the number of revolutions per second, and n_R is the number of crank revolutions for each power stroke per cylinder. For four stroke cycles, n_R equals 2. This power is also more commonly known as the gross indicated output per cylinder.

The results of integration of the area under the P-V diagram curve, for both compression and expansion strokes of the sample cycle, are presented in Table 27.

Table 27 Post-processing of corrected sample data-HCCI gasoline experiment 750 RPM.

Engine Speed	750	RPM
Compression Work	341.43	Nm
Expansion Work	393.77	Nm
Gross Indicated Work	52.35	Nm
Gross Indicated Power	327.16	W
Gross Indicated Power	0.44	HP

The loss or compression work for the sample cycle is 341.43 Nm. The gain or expansion work for the sample cycle is 393.8 Nm. Therefore, the gross indicated work for the cycle is the difference and is 52.35 Nm. The gross indicated power of the cycle is 327 W or 0.44 HP. This power is quite small considering the factory Kubota D905 can produce 18 HP with all three cylinders, but this is a preliminary proof of concept experiment, and only a single cylinder is operating at low engine speed. The amount of compression work appears to be too high when compared to the expansion work. This is a result of auto-ignition occurring after TDC, and optimization of combustion

timing closer to TDC would reduce the compression work and improve the gross indicated work of the cycle.

A calculation was performed using the same gross indicated work, however multiplying by 3 to estimate indicated power for three cylinder and using engine speed of 3000 RPM. The results of this calculation are tabulated in Table 28. Now we see that the gross indicated power of the engine is 3.98 kW or 5.27 HP, which is closer to a useful value than determined earlier. With further testing and fine-tuning, it is possible to attain higher gross indicated work per cylinder and therefore higher engine power.

Table 28 Post-processing of corrected sample data-HCCI gasoline experiment 3000 RPM.

Engine Speed	3000	RPM
Compression Work	341.4	Nm
Expansion Work	393.8	Nm
Gross Indicated Work	52.35	Nm
Gross Indicated Power	3926	W
Gross Indicated Power	5.27	HP

The EGR system verification experiment should have been performed at this stage, since combustion gases are needed in order to divert a portion to the intake and measure with the emission analyzer. However, only basic EGR and exhaust valve operation was verified. The use of the OTC emission analyzer was not tested in conjunction with combustion experiments. The reason for this was the presence of a fault code during power up of the analyzer that prevented the unit from functioning properly. Once this fault is cleared and the necessary repair is made, the emission analyzer and EGR system can be verified.

Figure 98 shows the $\log(P)$ versus $\log(V)$ plot determined from the processed data used in Figures 96, and 97. The polytropic exponents of both the compression and expansion strokes were calculated by measuring the slopes of the lines in the graph. For compression the polytropic exponent is 1.31 and for expansion the polytropic exponent is 1.34. According to Heywood, the value for polytropic exponents for compression and expansion processes of conventional fuels should be 1.3 +/- 0.5 for compression, and 1.33 +/- 0.5 for expansion [4]. The $\log(P)$ versus $\log(V)$ plot shows good agreement with Heywood's specification. However, the plot also shows a slight curvature in the polytropic values for both the compression and expansion strokes. This

indicates that the thermal cycling effects on the pressure transducer are present and have a slight affect. This could be improved by relocating the pressure transducer to the glow plug hole, where more cooling to the cylinder head is present.

Therefore, the HCCI gasoline combustion experiments verified the functionality of all the systems of the research engine except the EGR and Heater systems.

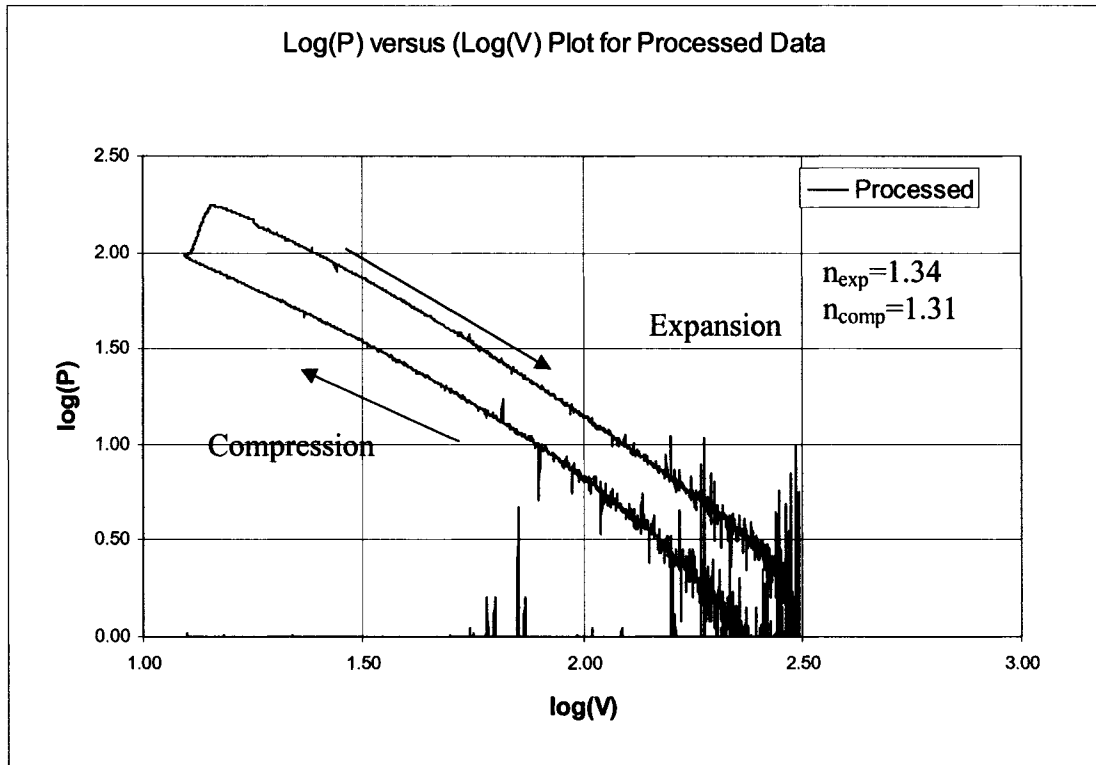


Figure 98: Log(P) versus Log(V) plot of Gasoline HCCI.

6.8 Summary

In summary, the following systems of the research engine were verified by experiment.

- Engine system was verified by compression test, cylinder head leak test, and combustion chamber leak test.
- Drive/braking system was verified by motoring and emergency braking test.
- Fuel system was verified by leak test, pressure regulator function test
- ECU system was verified by sensor function test using the PC.
- Intake system was verified by air flow meter tests.
- Heater system was verified by intake air heater tests, failure occurred at high temperature.

- Data Acquisition, thermocouples, in-cylinder pressure, crank encoder, air flow data signals, were verified by screen captures and signal sampling.
- Research engine system was verified by HCCI combustion experiments of lean gasoline/air mixtures

The following two objectives for the project were achieved:

- Commissioning the HCCI burn apparatus by performing initial testing, troubleshooting, and verification experiments.
- Establishing HCCI burn of lean gasoline/air mixture, and obtain in-cylinder pressure measurements to verify the results. HCCI burn of lean ethanol/air mixture was not achieved due to failure of intake air heater during testing.



Figure 99: Final HCCI research engine setup.

7 CONCLUSIONS AND RECOMMENDATIONS

7.1 Conclusions

Overall the design and development of the research engine project was successful in achieving its criteria and constraints and has met the following objectives;

1. A literature review was performed identify the parameters affecting control of HCCI with respect to use of ethanol as a fuel.
2. An experimental apparatus was designed, and fabricated for investigation of parameters affecting control of HCCI.
3. The design process methodology was followed to ensure tasks were completed and documented correctly.
4. The HCCI research apparatus was commissioned by performing initial testing, troubleshooting, and verification experiments.
5. HCCI combustion of lean ethanol/air was not achieved due to heater system failure, however HCCI combustion of lean gasoline/air was achieved and verified by means of in-cylinder pressure measurements.

7.2 Recommendations

From initial tests, it is recommended that the research engine be utilized as a tool for further development and understanding of the parameters affecting HCCI combustion properties such as timing, heat release rate, and combustion duration. Further investigation into HCCI fuels such as biodiesel would also be beneficial. At present the research engine is able to fulfill its objectives and provide temperature, air flowrate, engine speed, and in-cylinder pressure measurements. As with any process or machine, future enhancements will be suggest by new graduate students These modifications should be considered thoroughly, and investigated to see what impact they have on the initial objectives of the apparatus. The following recommendations are made with the intention to provide useful information to guide subsequent students, technicians and researchers in the appropriate direction.

The fixture frame had significant sources of noise exhibited under testing. These noises can be reduced by installing anti-vibration padding between any surface contact point of components.

To reduce vibration with the engine, a larger flywheel could be designed and fabricated that will dampened the angular accelerations. Also, the other two cylinders could be enabled and fuelled with diesel fuel using the original diesel injector pump or perhaps retrofitting a common rail system. Therefore the engine could run on all three cylinders and this would most likely reduce the imbalance of the engine.

The VCR secondary piston could be improved by development of a hydraulic actuated secondary piston and custom fabricated cylinder head. This concept would allow the compression ratio to be varied, while the engine is running and would enable advance VCR and HCCI research.

The accuracy of the fuel system could be improved by reducing the size of both the fuel injector and the fuel pump. The fuel injector should be reduced to 4.5 kg fuel/hour, and a smaller fuel pump should also be obtained (18.1 kg fuel/hour.) This would enable a higher level of precision with the fuel metering. Future ECU calibration experiments should be performed using the laminar flow meter. This will provide a higher level of accuracy.

Further verification experiments will need to be performed on the intake air preheater using the laminar flow meter while the engine is running. Caution must be taken to ensure air flow through the heater is not drastically changed, and vibrations are reduced.

For the data acquisition system the thermocouples will have to be replaced with ungrounded 1.5875 mm K-Type. National Instruments thermocouple low-pass filter and amplifier would also be recommended to eliminate harsh AC motor magnetic field interference. Also, the heater and equivalence ratio readings must be incorporated into the Research Engine Data Acquisition System program.

The braking absorption capacity needs to be quantified by means of a combustion experiment using the resistor banks and the chopper module. A current meter should be installed on the 480 V line between the AC motor and the Chopper in order to determine the current while the engine is producing torque during HCCI combustion experiments. Current meters can be attained from ElectroZad Ltd in Windsor or any electrical supply store.

The verification of the EGR system needs to be performed by experiment while HCCI combustion is occurring. The emission analyzer requires clearing of fault codes and then it can be

used to acquire percent volume CO₂ data. This data can be entered into the MATLAB EGR program to determine percent EGR. The influence of EGR on HCCI combustion can then be studied.

A detailed set of HCCI combustion experiments should be performed. They would provide invaluable information on the effect of parameters affecting HCCI control. These experiments would be performed at several different engine speeds (750, 1000, 1250, 1500, 1750, 2000, 2250, 2500, and 3000 RPM) by keeping the engine speed constant and varying one parameter at a time. The intake charge set-point temperature should be varied from 50, 100, 150, and 200 °C to study the effect. The EGR rate should be varied from 0 to 80 % to study the effect of EGR. The equivalence ratio should also be varied from 0.25 to 0.8. The compression ratio should be varied from 15 to 25:1 to study the effect of VCR. Post-processing should be performed and the effect of the control parameters on ignition timing, heat release rate and combustion duration would be determined. These experimental results could be compared with results obtained from previous research and compared with results from previously conducted simulations.

REFERENCES

1. US Environmental Protection Agency – Heavy Trucks, Buses and Engines (n.d), date accessed April 15th, 2004, from “<http://www.epa.gov/otaq/diesel.htm#regs>”
2. Canadian Renewal Fuels Association (n.d), date accessed January 15th, 2003, from “<http://www.greenfuels.org/ethanol/index.htm>.”
3. U.S. Department of Energy, “Homogeneous Charge Compression Ignition (HCCI) Technology-A Report to the U.S. Congress,” April 2001.
4. Cengel, Y., Boles, M., “Thermodynamics, An Engineering Approach, 3rd Edition,” McGraw-Hill, Table A-1, pp. 898, 1998.
5. Norton, R.L., “Design of Machinery, 2nd Edition” Chapter 1, Section 1.5, McGraw-Hill, 2001.
6. Najt, P.M., and Foster, D.E., “Compression-Ignited Homogeneous Charge Combustion”, SAE Paper 830264, 1983.
7. Iida, N., Igarashi, T., “Auto-Ignition and Combustion of n-Butane and DME/Air Mixtures in a Homogeneous Charge Compression Ignition Engine,” SAE Paper 2000-01-1832, 2000.
8. Ng, C., “The Effect of Fuel/Air Equivalence Ratio, Starting Temperature, EGR and Reforming on HCCI Combustion,” University of Toronto-Proposal, 2002.
9. Aoyama, T., Hattori, Y., Mizuta, J., Sato, Y., “An Experimental Study on Premixed-Charge Compression Ignition Gasoline Engine,” SAE Paper 960081, 1996.
10. Hiraya K. et al., “A study on gasoline fuelled compression ignition engine ~ a trial of operation region expansion,” SAE Paper 2002-01-0416, 2002.
11. Ladommatos, N., Zhao, H., Oakley, A., “Dilution Effects on the Controlled Auto-Ignition (CAI) Combustion of Hydrocarbon and Alcohol Fuels,” SAE Paper 2001-01-3606, 2001.
12. Christensen, M., et. al, “Supercharged Homogeneous Charge Compression Ignition,” SAE Paper 980787, 1998.
13. Christensen, M. et al., “Homogeneous Charge Compression Ignition (HCCI) using Iso-octane, ethanol and natural gas-a comparison with spark ignition operation”, SAE Paper 972874, 1997.
14. Christensen, M. et al., “Influence of mixture quality on homogeneous charge compression ignition,” SAE Paper 982454, 1998.
15. Christensen, M. et al., “Demonstrating the multi-fuel capability of a homogeneous charge compression ignition engine with variable compression ratio,” SAE Paper 1999-01-3679, 1999.

16. Christensen, M. et al., "Homogeneous charge compression ignition with water injection," SAE Paper 1999-01-0182, 1999.
17. Christensen, M., Johansson, B., "Supercharged homogeneous charge compression ignition (HCCI) with exhaust gas recirculation and pilot fuel," SAE Paper 2000-01-1835, 2000.
18. Olsson, J., Tunestal, P., Johansson, B., "Compression Ratio Influence on Maximum Load of a Natural Gas Fueled HCCI Engine," SAE Paper 2002-01-0111, 2002.
19. Olsson, J., Tunestal, P., Haraldsson, G., Johansson, B., "A Turbo Charged Dual Fuel HCCI Engine," SAE Paper 2001-01-1896, 2001.
20. Epping, K., Aceves, S., Bechtold, R., Dec, J., "The potential of HCCI combustion for high efficiency and low emissions," SAE Paper 2002-01-1923, 2002.
21. Asmus, T., Zhou, F., "Homogeneous Charge Compression Ignition (HCCI) Engines-Key Research and Development Issues," PT-94 Society of Automotive Engineers, Chp.4, 2003.
22. Furutani, M. et al., "An investigation into the effect of fuel composition on HCCI combustion characteristics," Proceedings of Comodia '98. pp. 173-177, 1998.
23. Chemistry Department, University of Ireland, Galway, (n.d), date accessed August, 12th, 2003, "<http://www.nuigalway.ie/chem/combust.htm>."
24. Nolan, S., Cardiff School of Engineering, date accessed August 10, 2003, "<http://www.ucc.ie/research/hmrc/SWERF/conferences/IST/Papers%20and%20Slides/SINEAD~1.pdf>."
25. AVL Ltd. (n.d.), date accessed October 18th, 2003, from "<http://tec.avl.com>."
26. Ricardo and Cussons (n.d.), date accessed October 18th, 2003, from "<http://www.cussons.co.uk>."
27. Waukesha Engines Corporation (n.d), date accessed October 25th, 2003, from "<http://www.waukeshaengine.com/internet/businessunits/waukesha/pages/applications/products/fueltesting/flf2.cfm?r=973&numPageID=378>."
28. University of California at Berkeley (n.d), date accessed October 18th, 2003, from "<http://www.me.berkeley.edu/cal/HCCI>."
29. Canadian Safety Standards Association (n.d), date accessed October 25, 2003, from "<http://www.csa.ca/default.asp?language=English>."
30. Land and Sea Inc. (n.d), date accessed June 20, 2003, from "<http://www.land-and-sea.com/eddy-current-dynamometer/eddy-current-dynamometer.htm>."
31. Quotation #0020959, "200 Eddy Current Absorber 96v - \$14,245 US," Land and Sea Inc, June, 2003.
32. Kubota Canada Ltd, date accessed November 10th, 2003, from "http://www.css-club.net/kubota_catalog/pdf/Super_Five.pdf."

33. Kubota Corporation (n.a), "Kubota Workshop Manual 9789701642," May 1996.
34. Shigley J., Mischke C., "Mechanical Engineering Design, 6th Edition," McGraw-Hill, 2001. pp. 23 -25.
35. Cengel, Boles, "Thermodynamics: An Engineering Approach," McGraw-Hill, 1998.
36. Gasket Works USA (n.d), date accessed November 25, 2004, from "<http://www.headgasket.com/whoweare.html>."
37. Heywood, J.B., "Internal Combustion Engine Fundamentals," McGraw-Hill, various pages, 1988.
38. Plint, M., Martyr, A., "Engine Testing – Theory and Practice, 2nd Edition," Society of Automotive Engineers, 1999. pp. 127-135.
39. Rockwell Automation – Drives and Service Support/Resistor Sizing (n.d), date accessed January 20, 2005, from "<http://www.ab.com/support/abdrives/peripherals/brakes/rsizing.html>."
40. Omega International (n.d), date accessed December 2004, "http://www.omega.com/pptst/SH_HEATER.html."
41. Omega International (n.d), date accessed December 2004, "http://www.omega.com/ppt/pptsc.asp?ref=CNI_Series&nav."
42. Meriam Process Technologies (n.d), date accessed December 20, 2004, from, "<http://www.meriam.com/products/default.asp?m=3&d=62&p=14>."
43. Plint, M., Martyr, A., "Engine Testing – Theory and Practice, 2nd Edition," Society of Automotive Engineers, 1999. pp. 183-219.
44. Installation Guide, "ST3000 Smart Transmitter Release 300 and SFC Smart Field Communicator Model STS103, Installation Guide," 34-ST-33-39, Honeywell Inc., July, 2000.
45. Askeland, D.R., "The Science and Engineering of Materials," Third Edition, Chapman & Hall, London, UK., 1996.
46. Defoe, J.D., Arthur, D.M., "Matlab M-file used to calculate EGR fraction based on fuel and air flow rates, relative humidity and dry CO2 molar fraction in intake manifold," Modified by Defoe, J.D. for use with all fuels and additives, University of Windsor, University of Alberta, 2003, 2004.
47. OTC Corporation - MicroGas Analyzer User Guide, date accessed September 10th, 2004, from, "http://www.otctools.com/newcatalog/products/162_man.pdf."
48. McGinlay, J., "Personal Discussions – Regarding Fuel Storage," Occupational Health & Safety Department, University of Windsor. (519) 253-3000 ext. 4521, January 2005.

49. Delphi Automotive -Photos and Technical information (n.d), date accessed November 10th, 2004, from “[http://go2.delphi.com/default.asp?Language=English.](http://go2.delphi.com/default.asp?Language=English)”
50. Jegs Corporation (n.d), date accessed September 8th, 2004, from, “[http://www.jegs.com/cgi-bin/ncommerce3/CategoryDisplay?cgmenbr=361&cgrfnbr=639.](http://www.jegs.com/cgi-bin/ncommerce3/CategoryDisplay?cgmenbr=361&cgrfnbr=639)”
51. 034EFI Ltd, date accessed May 20th, 2003, from “[http://www.034efi.com/034ECUSTGII.html.](http://www.034efi.com/034ECUSTGII.html)”
52. Defoe, J. “Data Acquisition System for HCCI Research Engine Design and Implementation,” Work Term Report, University of Windsor, December 2004.
53. Gurley Precision Instruments - Specifications Sheet (n.d), obtained June 20, 2004, “ 9X25 Rotary Incremental Encoder”
54. National Instruments Ltd, date accessed November 20th, 2004, from “[http://www.ni.com/dataacquisition/whatis.htm.](http://www.ni.com/dataacquisition/whatis.htm)”
55. Kistler Instruments Inc., “Kistler Calibration Certificate,” Appendix J.5.
56. Personal Conversations, Marc St. Pierre, Technical Services, University of Windsor, December 2002 to January 2005.
57. Personal Conversations, Phil Diett, Physical Plant, University of Windsor, December 2002 to September. 2004.
58. Personal Conversations, Dave Dumachelle, Electroxad Ltd. Windsor, April 2004 –September, 2004.
59. Personal Conversations, David Doyscher, Tricon Ltd. Windsor, March 2004-Sept 2004.
60. Personal Conversations, Steve Budinsky, Technical Services, University of Windsor, December 2002 to January 2005.
61. Personal Conversations, Pat Seguin, Faculty of Engineering, University of Windsor, December 2002 to January 2005.
62. Shigley J., Mischke C., “Mechanical Engineering Design, 6th Edition,” McGraw-Hill, 2001. pp. 876,1051.
63. Defoe, J. “Data Acquisition System for HCCI Research Engine Design and Implementation,” Work Term Report, University of Windsor, December 2004.
64. Heywood, J.B., “Internal Combustion Engine Fundamentals,” McGraw-Hill, 1988, pp. 212-220. 28,47-48, 58, 385.
65. Email Conversations, Arsene Philogene, Omega Service Dept., Omega Newport Montreal, February 2005.

66. Email Conversations, Gary Muzzey, Osram Sylvania., Exeter, New Hampshire, February 2005.
67. Defoe, J. "Data Acquisition System for HCCI Research Engine Design and Implementation," Work Term Report, University of Windsor, December 2004.
68. Christensen, M., Hultqvist, A., Johansson, B., "Demonstrating the Multi-Fuel Capability of a Homogeneous Charge Compression Ignition Engine with Variable Compression Ratio," Society of Automotive Engineers, 1999-0103679.
69. Kohl, W.L., "Methanol As An Alternative Fuel Choice: An Assessment," The John Hopkins Foreign Policy Institute, Washington D.C, pp. 236. 1990.
70. Varaprasada, R.R., et al., "Alcohol Fuelling: Effect of Induction Swirl on Aldehyde Emissions," VII International Symposium on Alcohol Fuels, pp. 438. November 1988.
71. US Department of Energy, date accessed Sept. 2005, "http://www.eia.doe.gov/oiaf/aeo/pdf/aeotab_3.pdf."

APPENDICES

Appendix A: Engine Specifications and Function

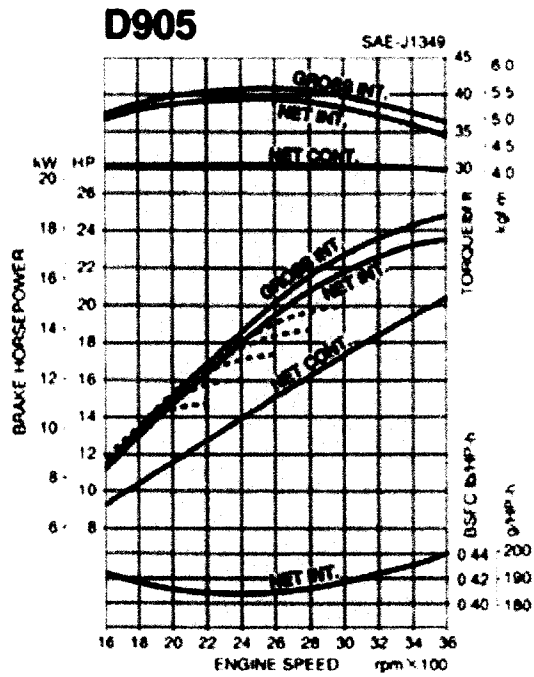
A.1: Kubota D905 Engine Specifications

Engine Type	Vertical 4-cycle liquid cooled diesel
Number of cylinders	3
Bore & Stroke [mm(in)]	72.0 X 73.6 (2.83 X 2.90)
Total Displacement [L(cu.in)]	0.898 (54.8)
Gross Intermittent Power [kW(HP)]	15.5 (20.8) @ 3000 RPM 18.5 (24.8) @ 3600 RPM
Net Intermittent Power [kW(HP)]	14.9 (20) @ 3000 RPM 17.5 (23.5) @ 3600 RPM
Net Continuous Power [kW(HP)]	13.0 (17.4) @ 3000 RPM 15.2 (20.4) @ 3600 RPM
No load high idling speed	3800
No load low idling speed	800
Direction of Rotation	Counter-clockwise (from flywheel side)
Dry Weight [kg(lbs)]	110.0 (242.5)
Compression Pressure	412 to 469 psi, Limit 327 psi

A.2 Factory Valve timing for Kubota D905

Valve Timing	Factory Specification
Intake Valve Open	0.24 rad. (14°) before TDC
Intake Valve Close	0.52 rad. (30°) after TDC
Exhaust Valve Open	0.96 rad. (55°) before BDC
Exhaust Valve Close	0.24 rad. (17°) after TDC

A.3: Performance Curve for Kubota D905 Engine



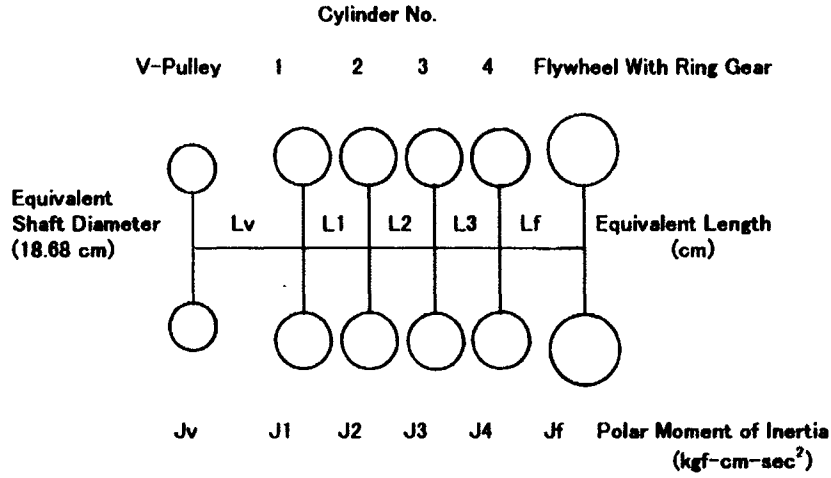
A.4 Cooling System Specifications for Kubota D905

Thermostat's Valve Opening Temperature	69.5 to 72.5°C
Temperature Thermostat Completely Open	85°C
Radiator Water Tightness	Water tightness at 137 kPa (20 psi)
Radiator Cap Air Leakage	> 10 seconds 88 to 59 kPa, (13 to 9 psi)
Cooling System Capacity	4.73 L (1.24 gal)
Engine Block Heater Power	400 W, 120 Volt

A.5 Cylinder Head Removal/Assembly specifications

Tightening torques	Metric Units	SI Units
Cylinder head cover cap nut	6.9 to 8.8 Nm	5.1 to 6.5 ft-lb
Cylinder head bolts	63.7 to 68.6 Nm	47.0 to 50.6 ft-lb
Rocker arm bracket nuts	21.6 to 26.5 Nm	15.9 to 19.5 ft-lb
Valve Clearance	0.145 to 0.185 mm	0.0057 to 0.0072 in

A.6 Kubota D905 Engine Balancing Specifications for Polar Moment of Inertia



Model	Equivalent Length (cm)					Polar Moment of Inertia (kgf-cm-sec ²)					
	Lv	L1	L2	L3	Lf	Jv	J1	J2	J3	J4	Jf
D905	20200	2520	2520	—	1863	0.013	0.049	0.029	0.049	—	1.810
D1005	20200	2520	2520	—	1863	0.013	0.049	0.029	0.049	—	1.810
D1105	20200	2520	2520	—	1863	0.013	0.051	0.031	0.051	—	1.810
D1105-T	20200	2520	2520	—	1863	0.013	0.051	0.031	0.051	—	1.810
V1305	20200	2520	2520	2520	1863	0.012	0.039	0.039	0.039	0.039	1.810
V1505	20200	2520	2520	2520	1863	0.012	0.041	0.041	0.041	0.041	1.810
V1505-T	20200	2520	2520	2520	1863	0.012	0.041	0.041	0.041	0.041	1.810

Notes :	3 Cylinder Models	Flywheel 16239-2511Δ
		V-Pulley 16229-7428Δ
	4 Cylinder Models	Flywheel 16259-2511Δ
		V-Pulley 16249-7428Δ

Appendix B: Engine Design Calculations

B.1 Engine Output Power

Design Constraint: Engine Output Power less than 25 hp.

$$P_{\text{design}} \leq 25 \text{ hp}, \quad (\text{B.1})$$

Kubota D905 Gross Intermittent Output Power:

$$P_{\text{engine}} = 24.8 \text{ hp @ 3600 RPM}, \quad (\text{B.2})$$

Since, $P_{\text{engine}} \leq P_{\text{design}}$ The design constraint has been met.

B.2 Chamber Pressure

Chamber Design Pressure constraint:

$$p_d \leq 180 \text{ bar} \quad (\text{B.3})$$

Kubota D906 compression pressure:

$$p_c = 469 \text{ psi} = 3233.6 \text{ kPa} \quad (\text{B.4})$$

Assuming a combustion pressure (p_{cp}) rise of 50%:

$$p_{cp} = 3233.6 \times 0.5 = 1616.8 \text{ kPa} \quad (\text{B.5})$$

The total pressure (p_t) or the impressed load becomes:

$$p_t = p_{cp} + p_c \quad (\text{B.6})$$

$$p_t = 3233.6 + 1616.8 = 4850.5 \text{ kPa} \quad (\text{B.7})$$

Based on Shigley and Mischke the assumed that the factor of safety:

$$n_d = 4.0 \quad (\text{B.8})$$

Using the Philon Factor of Safety Method given by the equation:

$$p_{lf} = n_d \times p_t \quad (\text{B.9})$$

Substitute and solve, $p_{lf} = 4.0 \times 4850.5 \text{ kPa} = 19402 \text{ kPa}$ (B.10)

Unit conversion, $1 \text{ bar} = 0.00001 \text{ kPa}$ (B.11)

Estimated loss of function pressure, $p_{lf} = 194.02 \text{ bar}$ (B.12)

Since this is greater than our chamber design pressure (180 bar) it can be concluded that the Kubota D905 satisfy the constraint for chamber design pressure.

B.3 Operating Temperature

Operating temperautre constraint:

$$T_d = 75^\circ\text{C} \quad (\text{B.13})$$

Kubota D905 Thermostat Operating Temperature Range:

$$71^\circ\text{C} < T_{op} < 90^\circ\text{C} \quad (\text{B.14})$$

Since the desired HCCI operating temperature is within the temperature range of the Kubota thermostat, the thermostat does not need to be changed, and has met the operating range constraint.

B.4 Ramp Time to Reach Operating Temperature

The desired quantity is the ramp time (T_r) which is defined as an estimate for the elapsed time required for the cooling system to reach operating temperature (T_{op}) of 75°C .

Assumptions: Cooling system is a constant volume liquid,

$$V = 5.73 \text{ L} = 0.00573 \text{ m}^3, \quad (\text{B.15})$$

Comprised of a 50/50 solution of ethylene glycol and water with a specific heat given by,

$$C_p = C_v = 3.338 \text{ kJ/kg}\cdot^\circ\text{C}, \quad (\text{B.16})$$

With initial and final pressures,

$$p_1 = 14.7 \text{ psi} = 1 \text{ bar}, \quad (\text{B.17})$$

$$p_2 = 20 \text{ psi} = 1.38 \text{ bar}, \quad (\text{B.18})$$

The power delivered from the heater is:

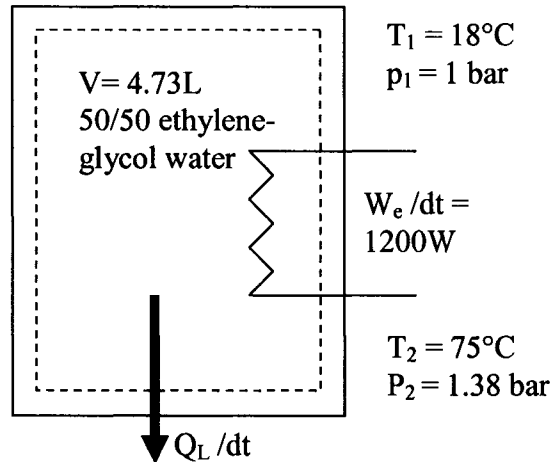
$$W_e / dt = 1200 \text{ W}, \quad (\text{B.19})$$

If we assume a heat loss of 1190 W for our cooling system:

$$Q_L / dt = 1190 \text{ W}, \quad (\text{B.20})$$

Developing the general cooling system schematic as follows:

$$(\text{B.21})$$



And we begin with writing the energy equation on a rate basis for our control mass.

$$dE_{\text{sys}} / dt = E_{\text{in}} / dt - E_{\text{out}} / dt \quad (\text{B.22})$$

Now applying this to our system we get:

$$dU / dt = W_e / dt - Q_L / dt, \quad (\text{B.23})$$

Assuming Constant specific heats:

$$du / dt = m C_v (T_2 - T_1), \quad (\text{B.24})$$

where m = mass and using the following;

$$m = \rho V, \quad (\text{B.25})$$

where ρ is density and V is volume, given density of 50/50 mix:

$$\rho = 1017 \text{ kg/m}^3, \quad (\text{B.26})$$

Equation B.22 becomes:

$$dt = \rho V C_v (T_2 - T_1) / (W_e - Q_L) \quad (\text{B.27})$$

$$dt = 1017 * (0.00573) * (3.338) * (75 - 18) / (1200 - 1190)$$

$dt = 110.5$ seconds approximately 1.6 minutes to warm up the Kubota engine to the operating temperature.

B.5 Variable Compression Ratio Option 1

Kubota D905 Technical Specifications

Stroke (mm)	Vs (cc) (.898L) total	Bore (mm)	CR
73.6	299	72	22
Swept Volume (cc)	Prechamber Vpc (cc)	Slack Volume (cc)	Clearance Vc (cc)
299	9	5.25	14.25

Option 1

Vary clearance volume by ordering several gaskets of varying thicknesses from Gasket Works USA.	Gasket Works USA, http://www.headgasket.com/whoweare.html Available Material thicknesses: 0.022, .032, .040, .043, .054, .063, .070, .086, .093, and .125 inches
---	--

Compression Ratio	Clearance Volume	w/ prechamber	w/ prechamber	w/o prechamber	w/o prechamber
CR	Vc (cc)	t(mm)	t(inch)	t(mm)	t(inch)
8	42.76	8.292	0.326	10.503	0.413
9	37.42	6.979	0.275	9.190	0.362
10	33.26	5.958	0.235	8.169	0.322
11	29.93	5.141	0.202	7.352	0.289
12	27.21	4.473	0.176	6.684	0.263
13	24.94	3.916	0.154	6.127	0.241
14	23.03	3.445	0.136	5.655	0.223
15	21.38	3.041	0.120	5.251	0.207
16	19.96	2.691	0.106	4.901	0.193
17	18.71	2.384	0.094	4.595	0.181
18	17.61	2.114	0.083	4.325	0.170
19	16.63	1.874	0.074	4.084	0.161
20	15.75	1.659	0.065	3.869	0.152
21	14.97	1.465	0.058	3.676	0.145
22	14.25	1.290	0.051	3.501	0.138
23	13.61	1.131	0.045	3.342	0.132
24	13.01	0.986	0.039	3.196	0.126
25	12.47	0.853	0.034	3.063	0.121

B.6 Detailed Calculations for B.5

Given Bore (D_p), Stroke (L_s), Engine displacement (V_d) we can calculate the clearance volume (V_c) for any compression ratio.

Determine swept volume V_s for a 3 cylinder engine:

$$V_s = V_d / 3, \quad (\text{B.28})$$

$$V_s = 0.898 \text{ L} / 3 = 0.299 \text{ L or } 299 \text{ cm}^3 (\text{cc}), \quad (\text{B.29})$$

Then V_c is calculated using the following equation and varying compression ratio CR:

$$V_c = (V_s - 1) / \text{CR}, \quad (\text{B.30})$$

For CR 8:1, $V_c = (299 - 1) / 8 = 42.76 \text{ cc}, \quad (\text{B.31})$

For CR 25:1, $V_c = (299 - 1) / 25 = 12.47 \text{ cc}, \quad (\text{B.32})$

The gasket thickness can be determined using volume, and geometry as follows; the clearance volume minus pre-chamber volume (V_{pc}) equals the net volume. When the net volume V_{net} is divided by the piston area (A_p) we get the required gasket thickness. This can be seen in the expression:

$$V_{net} = V_c - V_{pc}, \quad (B.33)$$

$$t \times A_p = V_c - V_{pc}, \quad (B.34)$$

Gasket thickness, $t = (V_c - V_{pc}) / A_p \quad (B.35)$

Where piston area is defined as:

$$A_p = \Pi \times (D_p/2)^2, \quad (B.36)$$

Therefore B.33 becomes, $t = 10 \times [4(V_c - V_{pc}) / (\Pi \times ((D_p/10))^2)] \text{ (mm)} \quad (B.37)$

For CR 8:1, $t = 10 \times [4(12.47-9) / (\Pi \times ((72/10))^2)] \quad (B.38)$
 $t = 8.292 \text{ mm,}$

For CR 25:1 $t = 10 \times [4(42.76-9) / (\Pi \times ((72/10))^2)] \quad (B.39)$
 $t = 0.853 \text{ mm,}$

A similar calculation is performed for the case without a pre-chamber, this changes equation B.31 to:

$$V_{net} = V_c, \quad (B.40)$$

All other substitutions remain the same.

B.7 Variable Compression Ratio Option 2

Option 2

Modify Stock Kubota head with Secondary Piston using kubota head gasket

Vpc (low CR) (cc)	Vpc (high CR) (cc)	Slack Volume Vsl	Dsp (cm)
16.13	9	5.25	1.732

Low Compression Ratio Pre-chamber

Compression Ratio	Clearance Volume	New Pre-chamber Volume	Delta Volume	Piston position
CR	Vc (cc)	Vpcn (cc)	dV (cc)	Lp(cm)
15	21.38	16.13	0.00	0.000
16	19.96	14.70	1.43	0.605
17	18.71	13.45	2.67	1.134
18	17.61	12.35	3.77	1.601
19	16.63	11.38	4.75	2.017

High Compression Ratio Pre-chamber

23	13.61	8.35	0.65	0.275
24	13.01	7.76	1.24	0.526
25	12.47	7.22	1.78	0.756

The clearance volume V_c is calculated using equation B.28. The slack Volume (V_{sl}) is defined as the original clearance volume minus the original pre-chamber volume:

$$V_{sl} = 14.25\text{cc} - 9\text{cc} = 5.25\text{cc}, \quad (B.41)$$

where 9cc is the original pre-chamber volume. The new pre-chamber volume (V_{pcn}) is defined as:

$$V_{pcn} = V_c - V_{sl}, \quad (B.42)$$

The delta volume (dV) is defined as the amount of volume that must be removed from the pre-chamber to attain the desired clearance volume and hence CR:

$$dV = V_{pc} - V_{pcn}, \quad (B.43)$$

Where $V_{pc}=16.13\text{cc}$ for low compression ratio range and $V_{pc}=9\text{ cc}$ for high compression ratio range. Given the secondary piston diameter (D_{sp}):

$$D_{sp} = 1.732\text{ cm} \quad (B.44)$$

The piston plunge depth (L_p) is defined as:

$$L_p = 4 / ((\Pi dV)/(D_{sp})^2), \quad (B.45)$$

For 17:1:

$$L_p = 4 / ((\Pi \times 2.67\text{cc})/(1.732\text{cm})^2), \quad (B.46)$$

$$L_p = 1.134\text{ cm}, \quad (B.47)$$

For 25:1:

$$L_p = 4 / ((\Pi \times 1.78)/(1.732\text{cm})^2), \quad (B.48)$$

$$L_p = 0.756\text{ cm}, \quad (B.49)$$

Therefore a method of adjusting and securing and sealing the secondary piston will have to be developed in the prototype fabrication phase.

Appendix C: Drive System Specifications

C.1 Emerson Motor Model # H15E1D Specifications

Horsepower	15
Poles	2
RPM (full load)	3535 / 2920
Weight	280 lbs
Phase	3
Frequency	60 / 50
Voltage	480
Rotor Inertia (lb-ft ²)	3.2
Torque (lb-ft)	22.2

C.4 Allen Bradley 1336 Variable Speed Drive

Voltage	460V 60Hz
Torque	Constant Torque
Motor Horsepower	15 HP
Max Output (Amps.)	27.2 A (380-460V) CT
Horsepower	15 HP
Enclosure Type	NEMA Type 1 - CE
Control Interface	L4, Contact Closure
Human Interface Module	HA1, Programmer/Controller w/Analog
Communications Options	GM2, RS232/422/485DF1/DH485

C.5 Allen Bradley 1336-WB035 Brake Chopper

Duty Cycle	For 20, 50, and 100% duty cycle
Current (A)	35 A rms
Voltage (V)	380-480 Vac

C.6 McMaster-Carr Multi-Flex shaft coupler

Hub OD	O'all Lg.	Available Bore Sizes	Bore Depth	Torque, in. lbs.	Max. rpm	Maximum Misalignment			Hubs Each	Rubber Elements Each		
						Parallel	Angular	Axial				
2 1/16"	2"	3/8" to 7/8"	13/16"	60	9200	0.010"	1°	0.125"	6507K1 □ •	\$5.70	6507K69	\$3.44
2 1/2"	2 3/8"	1/2" to 1"	7/8"	120	7600	0.010"	1°	0.125"	6507K2 •	6.71	6507K71	4.22
3 1/4"	2 7/8"	1/2" to 1 1/8"	1 1/16"	240	7600	0.015"	1°	0.125"	6507K3 •	10.60	6507K72	8.48
4"	3 5/16"	5/8" to 1 3/8"	1 7/32"	450	6000	0.015"	1°	0.125"	6507K4 •	14.83	6507K73	14.12
4 5/8"	3 15/16"	3/4" to 1 7/8"	1 27/32"	725	5250	0.020"	1°	0.125"	6507K5	21.19	6507K74	18.34
5 1/2"	4 7/16"	7/8" to 2 3/8"	2 3/32"	1135	4500	0.020"	1°	0.125"	6507K6	28.24	6507K75	24.02
6 11/32"	5 1/16"	1" to 2 7/8"	2 13/32"	1800	3750	0.025"	1°	0.125"	6507K7	42.36	6507K76	28.24

C.7 IPC Resistor Specifications

IPC Resistors Inc.	DB445-11A-GALV
Resistance	23 ohms
Absorption Power	11125 watts

Appendix D: Drive System Design Calculations

D.1 Sizing of AC Motor for Motoring of Kubota D905

Kubota D905 Maximum Gross Intermittent Output Power and Torque:

$$P_{\text{gross}} = 24.8 \text{ hp @ 3600 RPM,} \quad (\text{D.1})$$

$$\tau_{\text{gross}} = 42 \text{ ft-lbs @ 2200 RPM,} \quad (\text{D.2})$$

Plint and Martyr suggest that the amount of motoring torque required (τ_{req}) to motor an engine seldom exceeds 30 percent at steady state operation. This motoring torque is also directly related to the friction losses of the engine:

$$\tau_{\text{req}} = 0.3 \times 42 \text{ ft-lbs,} \quad (\text{D.3})$$

$$\tau_{\text{req}} = 12.6 \text{ ft-lbs,} \quad (\text{D.4})$$

Therefore the maximum required torque the AC motor must provide is 12.6 ft-lbs. From Appendix C.3 the **Emerson Motors Model # H15E1D** can supplied torque (τ_{sup}) at full load of:

$$\tau_{\text{sup}} = 22.2 \text{ ft-lbs,} \quad (\text{D.5})$$

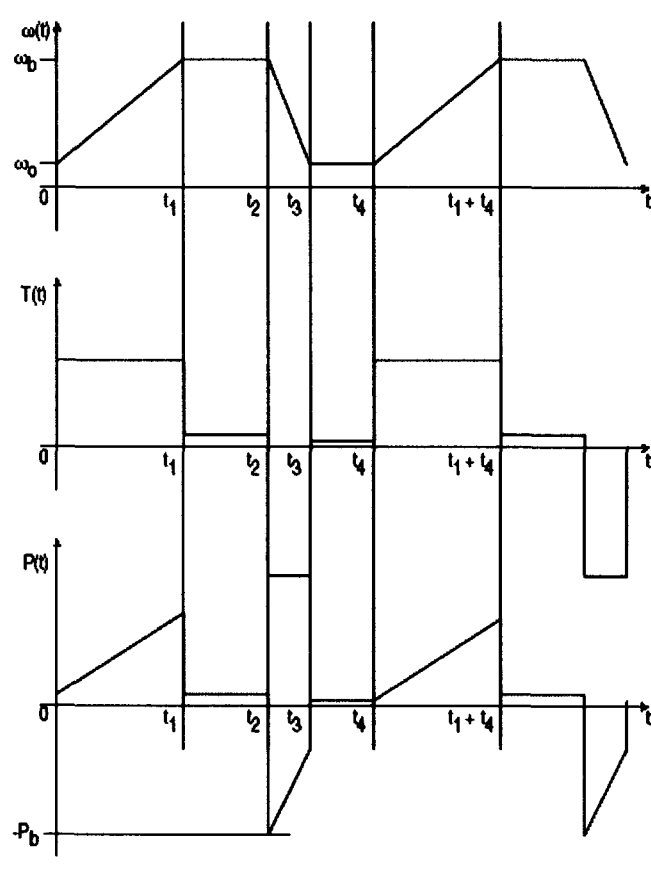
Since, $\tau_{\text{sup}} > \tau_{\text{req}}$, (D.6)

Therefore, the Emerson Motors Model # H15E1D would be able to provide enough torque for the steady state motoring of the Kubota D905 for all engine speeds (0 to 3600 RPM).

D.2 Sizing of AC Motor for Braking of Kubota D905

A 15 HP, 2 pole, 480 volt motor and Kubota D905 engine is accelerated and decelerated as depicted in the figure below.

- The cycle period t_4 is 50 seconds and the motoring time is $t_2 - t_1$ is 30 seconds.
- The acceleration time t_1 is 4 seconds, and the deceleration time $t_3 - t_2$ is 16 seconds.
- The maximum rated speed is 3600 RPM and is to be decelerated to 0 RPM in 16 seconds.
- The Kubota engine inertia is 9.7 lb-ft² and is directly coupled to the AC motor.
- The AC Motor Inertia is 3.2 lb-ft².
- The stub shaft and coupler Inertia is approximated by 0.5 lb-ft²



Step 1. Calculate the necessary values to choose an acceptable dynamic brake.

$$\text{Rated Power} = 15 \text{ HP} \times 746 \text{ watts/HP} = 11.185 \text{ kW} \quad (\text{D.7})$$

$$\text{Rated Speed} = \omega_b = 3600 \text{ RPM} = 2\pi \times 3600/60 = 376.99 \text{ rad/s}, \quad (\text{D.8})$$

$$\text{Lower Speed} = \omega_o = 0 \text{ RPM} = 2\pi \times 0/60 = 0 \text{ rad/s}, \quad (\text{D.9})$$

Total Inertia (J_T) by adding the AC motor (J_{AC}), Kubota Engine(J_{D905}), and Coupling Inertias (J_C) as follows:

$$J_T = J_{AC} + J_C + J_{D905}, \quad (\text{D.10})$$

The rotational moment of inertia for the Kubota D905 engine is given in Appendix A.12. However, the units that were given (kg-cm-s^2) are not familiar units (kg-m^2) or (lb-ft^2) also a conversion could not be found. It is apparent that the largest source of rotational inertia is the flywheel, since in is 1 order of magnitude larger than the values for all other components of the engine (see A.12).

$$J_v = 0.013, J_1 = 0.049, J_2 = 0.029, J_3 = 0.049, J_f = 1.810, \quad (\text{D.11})$$

$$J_{\text{tot}} = J_v + J_1 + J_2 + J_3 + J_f = 1.95, \quad (\text{D.12})$$

The percent ratio of inertia ($\%J_{F\text{-tot}}$) comparing flywheel to the rest of the engine is:

$$\%J_{F-tot} = \frac{J_F}{J_{tot}}, \quad (D.13)$$

$$\%J_{F-tot} = \frac{1.95}{1.81}, \quad (D.14)$$

$$\%J_{F-tot} = 1.077, \quad (D.15)$$

Multiplying this by the flywheel inertia 9.01 lb-ft² given in the schematic in Appendix A.12 yields:

$$J_{D905} = 1.077 \times 9.01 = 9.706 \text{ lb-ft}^2, \quad (D.16)$$

Now using equation D.10 we can find the total inertia of the system:

$$J_T = J_{AC} + J_C + J_{D905},$$

$$J_T = 3.2 + 9.706 + 0.5 = 13.4 \text{ lb-ft}^2, \quad (D.17)$$

$$1 \text{ lb-ft}^2 = 0.138255 \text{ kg-m}^2 \quad (D.18)$$

Therefore the total system inertia is:

$$J_T = 13.4 \text{ lb-ft}^2 = 1.852 \text{ kg-m}^2 \quad (D.19)$$

Step 2. Determine peak braking power (P_b) by using the following equation:

$$P_b = \frac{J_T[\omega_b(\omega_b - \omega_o)]}{(t_3 - t_2)}, \quad (D.20)$$

$$P_b = \frac{1.852 \times [376.99 \times (376.99 - 0)]}{(16)}, \quad (D.21)$$

$$P_b = 16.455 \text{ kW}, \quad (D.22)$$

Note that this is less than 1.5 times the rated Power for the motor.

Step 3. Calculate Minimum Power Requirements for the Dynamic Braking Resistors.

Determine the average braking power that must be dissipated by the resistor.

$$P_{avg} = \left[\frac{(t_3 - t_2)}{t_4} \right] \times \frac{P_b}{2} \times \left[\frac{(\omega_b - \omega_o)}{\omega_b} \right], \quad (D.23)$$

$$P_{avg} = \left[\frac{16}{50} \right] \times \frac{16.455}{2} \times \left[\frac{(376.99 - 0)}{376.99} \right], \quad (D.24)$$

$$P_{avg} = 2.633 \text{ kW}, \quad (D.25)$$

Note that the average braking power $P_{avg} = 2.633 \text{ kW}$ is less than the peak braking power $P_b = 16.455 \text{ kW}$.

Step 4. Calculate the Maximum Dynamic Braking Resistance Value

$$R_{db1} = \frac{0.9 \times (V_d)^2}{P_b}, \quad (D.26)$$

where,

R_{db1} = Maximum allowable value for the dynamic braking resistor. (ohms)

V_d = DC bus voltage the chopper module regulates to 750 VDC for 460 Vrms.

P_b = Peak braking power calculated in earlier. (watts)

$$R_{db1} = \frac{0.9 \times (750)^2}{16455} = 30.765 \text{ ohms} \quad (D.27)$$

The selection of the dynamic braking resistance value should be less than $R_{db1} = 30.76$ ohms. If the value is greater the drive can trip the DC bus over-voltage.

Step 5. Selecting a Resistor

Select a resistor bank from the supplier that has:

- A resistance value that is less than the value calculated (R_{db1}) = 30.76 in ohms.
- A power value greater than the average power value calculated $P_{avg} = 2633$ W.

The IPC resistor bank model # DB445-11A-GALV has a resistance of 23 ohms which is less than (R_{db1}) and dissipation power of 11,125 W which is greater than P_{avg} . Therefore, this resistor will be adequate to perform the required braking.

D.3 Verifying Starting Torque Requirements

To determine the amount of starting torque required on the flywheel of the Kubota D905 will require calculation based on the starter performance. The performance data available is for a 1.4 kW starter. This information can be scaled down to reflect more accurately the 1 kW starter that is supplied with the Kubota D905.

From Kubota Canada, $\tau_{1.4kW} = 13.24$ Nm, (D.28)
Scaled down for 1kW starter,

$$\tau_{1kW} = \frac{\tau_{1.4kW}}{1.4}, \quad (D.29)$$

$$\tau_{1kW} = \frac{13.24 \text{ Nm}}{1.4} = 9.457 \text{ Nm}, \quad (D.30)$$

Thus, the amount of starting torque or load on the starter for the D905 engine is 9.45 Nm.

From Inspection of Starter, $N_{starter} = 9$, (D.31)

From Inspection of flywheel, $N_{flywheel} = 98$, (D.32)

The gear reduction (R_g) from the starter to flywheel is:

$$R_g = \frac{N_{starter}}{N_{flywheel}}, \quad (D.33)$$

$$R_g = \frac{9}{98} = 0.0918 \quad (D.34)$$

Thus, the gear reduction is 0.0918. The flywheel torque required to turn the engine over at 1000 RPM is determined as follows:

$$\tau_{flywheel} = \frac{\tau_{1kW}}{R_g}, \quad (D.35)$$

$$\tau_{flywheel} = \frac{9.457}{0.0918} = 102.97 \text{ Nm} \quad (D.36)$$

$$1 \text{ Nm} = 0.737562 \text{ ft-lbs} \quad (D.37)$$

$$\tau_{flywheel} = 75.953 \text{ ft-lbs} \quad (D.38)$$

Thus, the amount of torque at the flywheel during starting is 75.95 ft-lbs. This is the amount of torque that our AC motor must provide in order to be able to match the starter performance. However, for this design only 1 cylinder will be enabled and the other 2 cylinders will not have compression, therefore the starting torque will be approximately 1/3 of the actual flywheel torque.

$$\tau_{flywheel} = \frac{75.953}{3} = 25.317 \text{ ft-lbs} \quad (D.39)$$

From D.5 the maximum amount of torque that the **H15E1D** can provide is:

$$\begin{aligned} \tau_{sup} &= 22.2 \text{ ft-lbs,} \\ \text{Since, } \tau_{sup} &< \tau_{flywheel}, \end{aligned} \quad (D.40)$$

Therefore, the **H15E1D** cannot provide enough torque to overcome the actual flywheel torque. The solution to this is to utilize the 1kW starter during starting to assist the AC motor during start-up, and then disengage the starter once the engine is being motored by the AC motor.

D.4 Selection of Coupler Torque Capacity

Initial selection is based on the maximum rated torque of the engine with consideration given to the type of engine and number of cylinder, dynamometer characteristics and inertia.

Kubota D905 has a maximum net rated continuous torque of:

$$\tau_{net} = 30 \text{ ft-lbs @ 2200 RPM,}$$

And from Plint and Martyr Table 8.4, the service factor ($F_{service}$) are listed for range of engine and dynamometer types. For this application the service factor is:

$$F_{service} = 4.5, \quad (D.41)$$

The maximum rated torque multiplied by the service factor must not exceed the maximum permitted torque (T_{per}) of the coupler.

$$\tau_{per} = F_{service} \times \tau_{net}, \quad (D.42)$$

$$\tau_{per} = 4.5 \times 30 \text{ ft.lbs} = 135 \text{ ft.lbs} \quad (D.43)$$

The maximum torque of the McMaster-Carr coupler # 6507K7 from Appendix C.6 is:

$$\tau_{max} = 1800 \text{ in-lbs} = 150 \text{ ft-lbs,} \quad (D.44)$$

Since, $\tau_{\max} \geq \tau_{per}$, (D.45)

Therefore the coupler should be more than adequate to handle the torque from the motor.

D.5 Variable Frequency/Speed Calculations

This AC motor is designed to run at a fixed speed of 3600RPM. A variable speed drive changes the input line frequency (60 hz) to a desired frequency (f) hz. This varies the shaft speed of the AC motor according to the following equation:

$$Speed = \frac{120 \times f}{N_{poles}}, \quad (D.46)$$

Varying the desired frequency from (0 to 60 Hz) in increments of 10 Hz we can see how the speed of the AC motor changes in the following table

Frequency (Hz)	Shaft Speed (RPM)
0	0
10	600
20	1200
30	1800
40	2400
50	3000
60	3600

D.6 Determining Maximum Torque on Coupler During Emergency Stop

A calculation was needed to determine the maximum Torque on the coupler during an emergency stop. The engine was assumed to be running at 3600 RPM and the deceleration time for the emergency stop was set at 2 seconds.

The inertia of the Kubota Engine is given by equation D.16.

$$J_{D905} = 9.706 \text{ _lbft}^2 = 0.409 \text{ kg.m}^2 \quad (D.47)$$

The Torque applied to the coupler during deceleration can be determined as follows:

$$\sum \tau_{Coupler} = J_{D905} \alpha \quad (D.48)$$

Where α is the angular acceleration of the system and is given by:

$$\alpha = \frac{\omega}{t} = \frac{2\pi N[rpm]}{60 \times t[s]} = \frac{2\pi 3600rpm}{60 \times 2s} = 188.5 \text{ rad / s}^2 \quad (D.49)$$

$$\tau_{coupler} = J_{D905} \alpha = 0.409 \text{ kgm}^2 \times 188.5 \text{ rad / s}^2$$

$$\tau_{coupler} = 77.09 \text{ Nm} = 56.9 \text{ ft.lbs}$$

The maximum torque of the McMaster-Carr coupler # 6507K7 from Equation D.44.

$$\tau_{\max} = 150 \text{ ft-lbs}, \quad (D.50)$$

Since, $\tau_{\max} \geq \tau_{coupler}$, (D.51)

Therefore the coupler will survive emergency braking of the engine from 3600 RPM.

Appendix E: Engine Testing

E.1 VCR Design Calculations (Borrowed from Appendix B.7)

Option 2

Modify Stock Kubota head with Secondary Piston using kubota head gasket

Vpc (low CR) (cc)	Vpc (high CR) (cc)	Slack Volume Vsl	Dsp (cm)
16.13	9	5.25	1.732

Low Compression Ratio Pre-chamber

Compression Ratio	Clearance Volume	New Pre-chamber Volume	Delta Volume	Piston position
CR	Vc (cc)	Vpcn (cc)	dV (cc)	Lp(cm)
15	21.38	16.13	0.00	0.000
16	19.96	14.70	1.43	0.605
17	18.71	13.45	2.67	1.134
18	17.61	12.35	3.77	1.601
19	16.63	11.38	4.75	2.017

High Compression Ratio Pre-chamber

22	14.25	9.00	0.00	0.000
23	13.61	8.35	0.65	0.275
24	13.01	7.76	1.24	0.526
25	12.47	7.22	1.78	0.756

E.2 VCR Secondary Piston Prototype Experiment Summary

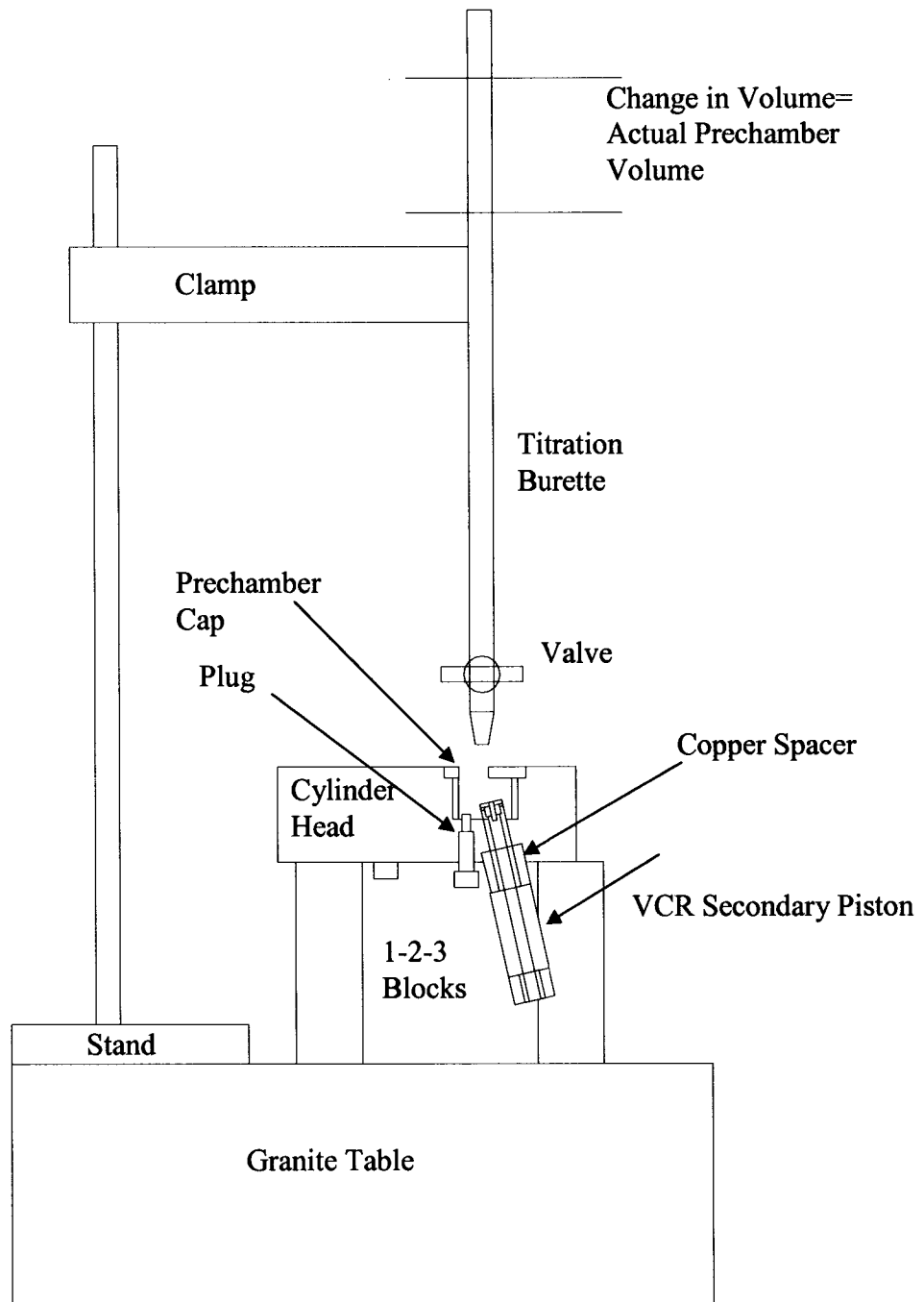
The following prototyping experiment was performed on November 18, 2003.

Objective: To verify the VCR design calculations and to determine the actual spacer length required to obtain the necessary pre-chamber volume.

The calculated prechamber volume for each compression ratio needs to be achieved in the actual prechamber by adjusting the spacer length. The prechamber volumes for each compression ratio are listed above in E.1.

E.3 Experimental Setup VCR

Items needed: Titration buret, stand, clamp, granite table, 1-2-3 levelling blocks, 1 liter of acetone, cylinder head with prechamber installed, various copper spacers.



E.4 Procedure VCR

1. Remove cylinder head from the engine and strip down.
2. Remove original prechamber cap by using a blunt punch and hammer.
3. Install modified prechamber cap (either high CR or low CR).
4. Select CR for test and note the corresponding calculated prechamber volume. This volume should be achieved with adjustment of spacer length and will be compared to actual prechamber volume. See Table below

5. Make an initial guess as to the length of copper spacer and machine to length.
6. Install copper spacer on VCR secondary piston and then install in cylinder head.
7. Setup the experiment according to experimental setup figure above.
8. Fill titration burette with acetone until it reaches the zero mark at the top.
9. Open valve of burette and fill prechamber to the top flush with machined surface of cylinder head.
10. Record the value of the change in volume of the titration burette. This is the actual prechamber volume using the selected copper spacer.
11. If actual value matches calculated value then that is the correct spacer length.
12. If actual value is greater than calculated value then shorten spacer length slightly and repeat from step 5.
13. If actual value is less than calculated value then a longer spacer is required. Its best to use a slightly longer spacer value than expected and machine to the correct length.

Experiment Table

CR	Trial Number	Calculated Prechamber Volume (cc)	Spacer Length (inches)	Actual Prechamber Volume (cc)
22	1	9.00		
	2	9.00		
	3	9.00		

E.5 Results VCR

For High CR prechamber Cap

CR	Trial Number	Calculated Prechamber Volume (cc)	Spacer Length (inches)	Actual Prechamber Volume (cc)
22	1	9.00	0.3	7.5
	2	9.00	0.356	8.1
	3	9.00	0.447	9.05
25	1	7.22	0.26	7.6
	2	7.22	0.23	7.2

For Low CR prechamber Cap

CR	Trial Number	Calculated Prechamber Volume (cc)	Spacer Length (inches)	Actual Prechamber Volume (cc)
15	1	16.13	1.0	16.6
	2	16.13	0.95	16.2
17	1	13.45	0.62	13.45
19	1	11.38	0.26	11
	2	11.38	0.3	11.5

E.6 Summary of Results VCR

CR	Trial Number	Calculated Prechamber Volume (cc)	Spacer Length (inches)	Actual Prechamber Volume (cc)
25	2	7.22	0.23	7.2
22	3	9.0	0.447	9.05
19	2	11.38	0.3	11.5
17	1	13.45	0.62	13.45
15	2	16.13	0.95	16.2

E.7 VCR Leak Test

The following verification experiment was performed on June 23, 2004.

Objective: To verify the VCR secondary piston and prechamber design and ensure no leakage occurs.

E.8 Experimental Setup VCR Leak Test

Items needed: vacuum tester, suction cup, cylinder head with prechamber and VCR installed, various copper spacers.

E.9 Procedure VCR Leak Test

Note: Cylinder head must already be removed from engine.

1. Install VCR secondary piston with spacers into the cylinder head and tighten.
2. Install plug into glow plug hole and tighten.
3. Install modified prechamber into the cylinder head.
4. Install suction cup on vacuum tester.
5. Place suction cup over prechamber opening.
6. Draw vacuum on prechamber.
7. Record vacuum pressure observed on indicator of vacuum tester along with observations using the experimental matrix below.

Experiment Table

Test #	Vacuum Drawn (in.Hg.)	Observations

E.10 Results VCR Leak Test

Test #	Cylinder #	Vacuum Drawn (in.Hg.)	Observations
1	2	15 but leaking	VCR, Plug installed. Result: severe leakage occurred cylinder #2.
2	2	25 but leaking	Tightened VCR further. Result: Improved but leakage cylinder #2.
3	3	27 no leakage	Installed fuel injector, glow plug. Result: no leakage occurred on cylinder # 3.
4	2	10 severe leaking	Install fuel injector, glow plug. Result: severe leakage, vacuum tester broken.
5	3	27 no leakage	Install fuel injector, plug, To test plug seal. Result: no leakage, plug seal is good.
6	2	25 no leakage	Remove pressure transducer cap from VCR and fill hole with puddy. Install VCR and plug. Result: no leakage, therefore transducer cap seal is faulty.
7	2	27 no leakage	Install pipe plug on VCR and remove transducer cap. Result: no leakage
8	2	27 slight leakage	Tighten transducer cap further and reinstall. Result: tip gasket deformed further creating tighter seal, however still leaking slightly.
9	2	27 no leakage	Put Teflon tape on tip screw thread and washer. Result: Teflon allows further tightening, creates perfect seal, no leakage.

E.11 Engine Compression Test

The following verification experiment was performed on July 20, 2004.

Objective: To verify the functionality of the Modified Kubota Engine and VCR mechanism by measuring compression pressure.

E.12 Experimental Setup Engine Compression Test

Items needed: diesel compression tester, glow plug hole adapter.

Kubota D905 Compression Specification: 412 to 469 psi, Minimum limit 327 psi

E.13 Procedure Engine Compression Test

1. Remove custom plug from glow plug hole and install adapter.
2. Ensure the VSD is turned off by using the secondary disconnect.
3. Connect compression tester to adapter.
4. Run starter for 15 seconds and observe compression pressure.
5. Record compression pressure and then release pressure using release valve.
6. Repeat if necessary. Best results obtained when engine is warm.

E.14 Results Engine Compression Test

The engine was run with the 22:1 spacer, high CR prechamber, and the VCR mechanism.

Test #	Compression Pressure (psi.)	Observations
1	0	No compression, valves leaking, send to M/C shop
2	415	Compression OK, engine was cold
3	450	Compression OK, engine was warm

E.15 Engine Systems Check Procedure (Prior to Motoring or Running Engine)

1. Ensure coolant level is full with only a slight air bubble in the top coolant line with a 50/50 mixture of coolant and water.
2. Ensure oil level is full to top mark of dipstick by using 15W40 diesel engine oil.
3. Ensure the coupler is fastened properly.
4. Ensure all safety guarding is secure and not interfering with any rotational components.
5. Ensure all components are fastened and secure to prevent vibration.
6. Install desired compression ratio spacer, keep in mind the installed prechamber cap limits which compression ratios you can run.
7. Perform compression test to verify compression ratio. (see E.13.)
8. If any problems with compression test remove head a perform leak test on prechamber (see E.9.)
9. If compression is fine then engine is ready for experiments, and follow procedure for motoring the engine coupled (see K.4.)

E.16 Engine Peak Pressure Calculation for Motoring

We calculate the peak pressure for an isentropic compression:

$$pV^\gamma = \text{const.} \quad (\text{E.1})$$

And:
$$\frac{p_2}{p_1} = CR^\gamma \quad (\text{E.2})$$

Where CR=25 is the compression ratio of the engine, and $\gamma=1.4$ for air. Rearranging equation E2 we get:

$$p_2 = p_1 \times CR^\gamma \quad (\text{E.3})$$

And reading the MAP sensor we get ($p_1=98.8 \text{ kPa} = 0.988 \text{ bar}$).

$$p_2 = .988 \times 25^{1.4} = 89.51 \text{ bar or } 8951 \text{ kPa.}$$

This is consistent with the pressure transducer measurement of 9000 kPa (90 bar).

Appendix F: Intake System Design Calculations

F.1 Heater Sizing

The desired quantity is the electrical power of the heater in units of watts (P_{heater}) which is defined as the amount of power required to heat the intake air from 0 °C to maximum operating temperature (T_{op}) of 300°C, assuming the engine is operating at 3600 RPM.

Known Quantities:

$$\text{Inlet Temperature } T_1 = 0^\circ\text{C} = 273 \text{ K}, \quad (\text{F.1})$$

$$\text{Exit Temperature } T_2 = 300^\circ\text{C} = 573 \text{ K}, \quad (\text{F.2})$$

From Appendix B.6

$$\text{Engine Displacement (} V_d \text{)} = 898 \text{ cc} \quad (\text{F.3})$$

$$\text{Cylinder Displacement (} V_d/3 \text{)} = 299 \text{ cc} \quad (\text{F.4})$$

The specific heat used for air was borrowed from Cengel and Boles,

$$C_p = 1.08 \text{ kJ/kg}\cdot^\circ\text{C}, \quad (\text{F.8})$$

With initial and final pressures,

$$p_1 = p_2 = 14.7 \text{ psi} = 1 \text{ atm}, \quad (\text{F.9})$$

The density of air (from Cengel and Boles):

$$\rho_{\text{air}} = 1.201, \quad [\text{kg/m}^3] \quad (\text{F.10})$$

If we assume a heat loss for the intake piping and ethanol vaporization of 40 %:

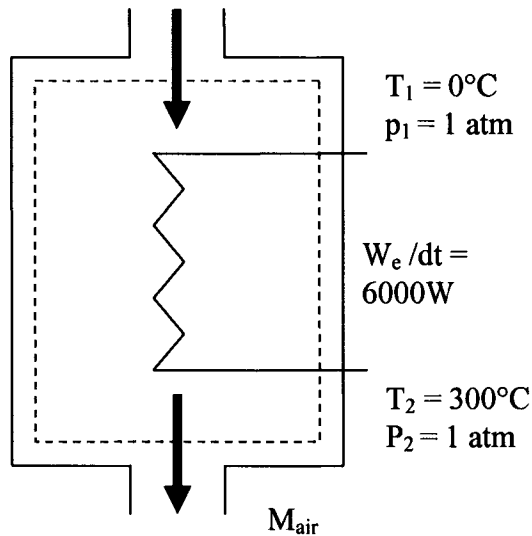
$$\text{Loss Factor (} F_{\text{loss}} \text{)} = 1.4, \quad (\text{F.11})$$

And if we assume an oversize factor of 10%:

$$\text{Oversize Factor (} F_{\text{os}} \text{)} = 1.1, \quad (\text{F.12})$$

Also we must assume steady state operation and that the heater and intake system have reached thermal equilibrium with the environment.

Heater Control Volume Schematic:



And we begin with writing the energy equation on a rate basis for our control volume.

$$dE_{\text{sys}}/dt = E_{\text{in}}/dt - E_{\text{out}}/dt \quad (\text{F.13})$$

Now applying this to our system we get:

$$dh/dt = W_e/dt, \quad (\text{F.14})$$

$$\dot{W}_e = \dot{m} \times C_p \times \Delta T \quad (\text{F.15})$$

where:

$$\dot{m} = \rho_{\text{air}} \times \dot{V} \quad (\text{F.16})$$

and \dot{V} is volumetric flowrate and $\Delta T = T_2 - T_1 = 300^\circ\text{C}$ or K.

Therefore the electric power becomes

$$\dot{W}_e = \rho_{\text{air}} \times \dot{V} \times C_p \times \Delta T \quad (\text{F.17})$$

With Loss factors the electric power becomes:

$$\dot{W}_e = F_{\text{loss}} \times F_{\text{os}} \times \rho_{\text{air}} \times \dot{V} \times C_p \times \Delta T \quad (\text{F.18})$$

F.2 Electrical Power Requirements for Intake Air Flow

RPM	Cycle Time (s)	Volume flowrate (cc/s)	Volume flowrate (m3/s)	Volume flowrate (cfm)	Mass flowrate of Air (kg/s)	Electric Power (kW) Adiab	Electric Power (kW) with loss fact.	Electric Power (kW) with loss O/S
500	0.240	1247.2	0.0012	2.642	0.0015	0.4857	0.6800	0.74797
1000	0.120	2494.4	0.0025	5.285	0.0030	0.9714	1.3600	1.4959
1500	0.080	3741.6	0.0037	7.928	0.0045	1.4571	2.0399	2.2439
2000	0.060	4988.8	0.0050	10.570	0.0060	1.9428	2.7199	2.9915
2500	0.048	6236.1	0.0062	13.213	0.0075	2.4285	3.3999	3.7398
3000	0.040	7483.3	0.0075	15.856	0.0090	2.9142	4.0799	4.4878
3600	0.033	8980.0	0.0090	19.027	0.0108	3.4970	4.8958	5.3854

F.3 Detailed Calculations for F.2 For 3600 RPM

$$\text{Cycle Time (t}_c\text{): } t_c = \frac{120}{RPM}, \quad (\text{F.19})$$

$$t_c = \frac{120}{3600} = 0.0333 \text{ seconds.} \quad (\text{F.20})$$

Volumetric flowrate (\dot{V}) in units of [cc/s] assuming volumetric efficiency (η_v) is 1.0 :

$$\dot{V} = \eta_v \frac{V_s}{t_c}, \quad (\text{F.21})$$

$$\dot{V} = \frac{299cc}{0.0333sec} = 8980 \text{ cc/sec.} \quad (\text{F.22})$$

Convert volumetric flowrate (\dot{V}) to units of [m³/s]:

$$\dot{V} = \frac{\dot{V}}{1000000}, \quad (\text{F.23})$$

$$\dot{V} = \frac{8980cc/sec}{1000000} = 0.008980 \text{ m}^3/\text{s} = 8.98 \text{ L/s} \quad (\text{F.24})$$

Convert volumetric flowrate (\dot{V}) to units of [cfm]:

$$\dot{V} = \dot{V} \times 60 \times 35.315, \quad (\text{F.25})$$

$$\dot{V} = 0.00898 \times 60 \times 35.315 = 19.0275 \text{ cfm,} \quad (\text{F.26})$$

Mass flowrate (\dot{m}) in units of [kg/s]:

$$\dot{m} = \dot{V} \times \rho_{air}, \quad (\text{F.27})$$

$$\dot{m} = 0.00898 \times 1.201 = 0.01078 \text{ kg/s.} \quad (\text{F.28})$$

Heater Power from without losses (F.15)

$$\dot{W}_e = 0.01078 \times 1.08 \times 300 = 3.49 \text{ kW,} \quad (\text{F.29})$$

Heater Power with Intake Losses

$$\dot{W}_e = 1.4 \times 3.49kW = 4.89 \text{ kW,} \quad (\text{F.30})$$

Electric Heater Power with Intake Losses and Oversize Factor

$$\dot{W}_e = 1.1 \times 4.89kW = 5.38 \text{ kW,} \quad (\text{F.31})$$

Thus, the Electric Heater Power requirement for a single cylinder Kubota D905 is 5.4 kW, and therefore the heater selected must have a power rating greater than this.

From Appendix G.1 we have a list of high quality process air heaters from Omega. The Omega SH-73343 is a 6 kW heater with a voltage of 240 V. Therefore, this air heater will be sufficient for single cylinder operation.

F.4 Calculation of Intake Air Flow Rate

The same quantities used in Appendix F.1, F.2, F.3 are also used in the following equation except the flow rate is representative of all three cylinders as opposed to just a single cylinder. The reason for over-sizing of the flowmeter is to allow for future research to be performed on the entire engine, whereas the heater would only be required for single cylinder operation.

Multiply volumetric flowrate (\dot{V}) to all three cylinders to units of [L/s]:

$$\dot{V} = \dot{V} \times 3, \text{ [L/s]} \quad (\text{F.32})$$

From (F.24) for one cylinder the flow rate is 8.98 L/s

$$\dot{V}_{\text{calculated}} = 8.98 \times 3 = 26.94 \text{ L/s} \quad (\text{F.32})$$

Therefore, the engine will have a maximum calculated flowrate of 26.94 L/s.

RPM	Cycle Time (s)	All Three Cylinders			
		Volumetric flowrate (cc/m)	Volumetric flowrate (m3/m)	Volumetric flowrate (L/s)	Mass flowrate of Air (kg/s)
500	0.240	224500	0.22	3.74	0.27
1000	0.120	449000	0.45	7.49	0.54
1500	0.080	673500	0.67	11.22	0.81
2000	0.060	898000	0.90	14.96	1.08
2500	0.048	1122500	1.12	18.7	1.35
3000	0.040	1347000	1.35	22.45	1.62
3500	0.034	1571500	1.57	26.18	1.89
3600	0.033	1616400	1.62	26.94	1.94

F.5 Selection of Laminar Flow Element

scfm = standard cubic feet per minute

acfm = actual cubic feet per minute

cfm = Cubic feet per minute

Note that scfm = acfm = cfm at 29.92" Hg. Abs and 70°F

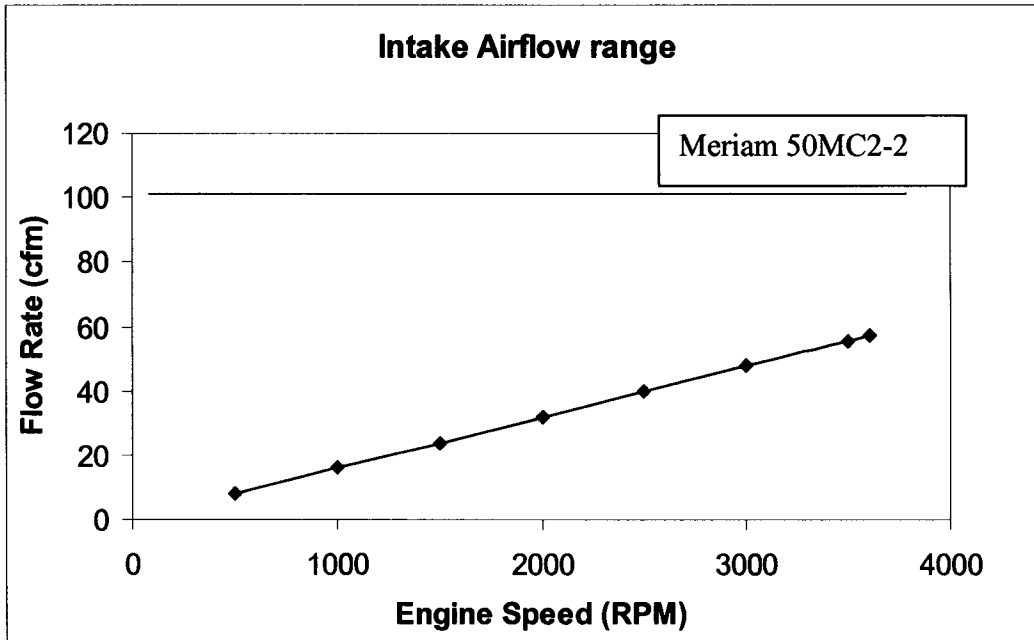
The gas flowing is AIR at a flow rate $\dot{V}_{\text{calculated}}$ of 26.94 L/s or 57 scfm.

The pressure of the flowing AIR is 29.92" Hg. Abs.

The temperature of the AIR is 70°F

Since this flow is at standard condition, the LFE can be selected directly from the capacity chart given in Appendix G.3.

There are two LFE that have a flow rate range covering the expected flow rate of our Kubota D905 engine, (see figure below). The 50MC2-2 was selected because it had a slightly larger range from 0-100 scfm and has hose end attachments that will be easier to utilize with the intake for the research engine.



F.6 Calculation of Differential Pressure

The differential pressure $\Delta p_{calculated}$ of the flow through the LFE is calculated using the following equation:

$$\Delta p_{calculated} = \dot{V}_{calculated} \times \frac{\Delta p_{LFE}}{\dot{V}_{LFE}}, \quad (F.25)$$

where, Δp_{LFE} is the catalog differential pressure rating = 10" H₂O, Appendix G.3

\dot{V}_{LFE} is the catalog flow rate range = 100 scfm, Appendix G.3

Therefore, the calculated differential pressure reading when the engine is at 3600 RPM or flows AIR at a rate of 57 scfm.

$$\Delta p_{calculated} = 57 \text{ scfm} \times \frac{8" \text{ H}_2\text{O}}{100 \text{ scfm}} = 4.56 \text{ inches H}_2\text{O}. \quad (F.26)$$

F.7 Observance of Reynold's Number for the LFE selected.

To maintain laminar flow with linearity through the LFE consideration must be given to the Reynolds number for the maximum flow condition. Meriam LFE elements will produce linear flow characteristics when the Reynolds number is 150 at 4" H₂O differential and 300 at 8" H₂O differential. It should be noted that true linearity will not be retained at elevated Reynolds number. However, a calibration made at the operating condition will be fully usable and repeatable.

The maximum allowable Reynolds number to maintain laminar flow at the differential pressure calculated in {F.26} is determined by interpolating between the following:

$$Re_1 = 150 @ 4''H_2O, \quad (F.27)$$

$$Re_{max} = ? @ 4.56''H_2O \quad (F.28)$$

$$Re_2 = 300 @ 8''H_2O \quad (F.29)$$

Interpolating:

$$Re_{max} = \frac{(300 - 150) \times (4.56 - 4)}{4} + 150 = 171.1 \quad (F.30)$$

Thus the maximum Reynolds number allowable to maintain laminar flow is 171.1.

To calculate the Reynolds number ($Re_{calculated}$) for the 50MC2-2 LFE we use the following equation:

$$Re_{calculated} = \frac{228 \times \gamma_{air} \times p_{air} \times \Delta p}{\nu_{air}}, \quad (F.31)$$

Where:

$Re_{calculated}$ = Reynold's Number calculated

γ_{air} = Specific gravity of air = 1.0

p_{air} = absolute pressure of air flowing through the LFE = 29.92"Hg. Abs.

Δp = differential pressure calculated for the LFE selected (F.26). = 4.56"H₂O

ν_{air} = viscosity of air at the flowing temperature (70°F) [in micropoise] = 181.87 μP

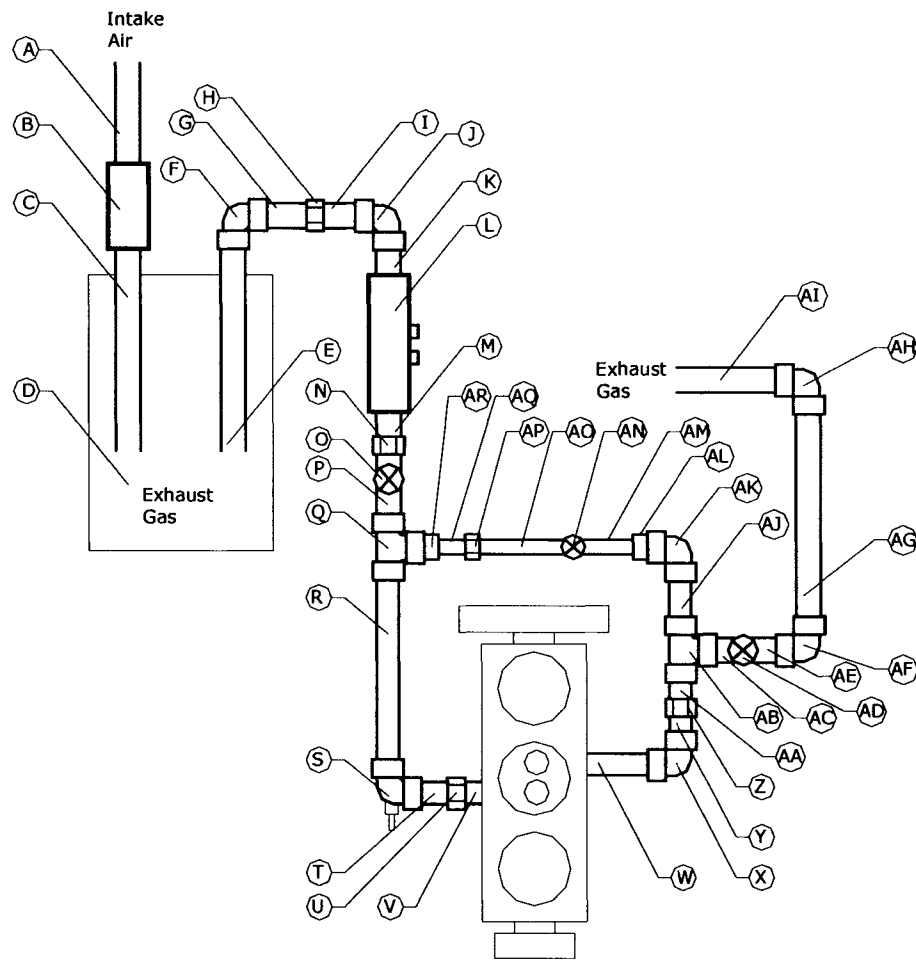
Quantities were borrowed from Meriam Data sheet available on website.

$$Re_{calculated} = \frac{228 \times 1.0 \times 29.92 \times 4.56}{181.87} = 171.04 = 171. \quad (F.28)$$

Since, $Re_{calculated} \leq Re_{max}$ therefore the flow through the LFE should remain laminar.

Also the flow remains laminar and the range of the 50MC2-2 LFE is satisfactory (as indicated in F.5), therefore the LFE selected is an satisfactory choice for our flow meter.

F.8 Intake Piping System Schematic



Item	Description	Item	Description
A	1.5" ABS 1 before LFE	W	1.5" GS 6 after engine
B	Meriam LFE	X	1.5" GS elbow 2
C	1.5" ABS 2 after LFE	Y	1.5" GS 7 after elbow
D	Surge Tank	Z	1.5" GS Coupler 3
E	1.5" ABS 3 out of surge tank	AA	1.5" GS 8 after coupler
F	1.5" ABS Elbow 1	AB	1.5" GS Tee 2
G	1.5" ABS 4 after elbow 1	AC	1.5" GS 9 after Tee
H	1.5" ABS Coupler 1	AD	1.5" Brass Gate Valve (Exh)
I	1.5" ABS 5 after coupler	AE	1.5" GS 10 after gate valve
J	1.5" ABS Elbow 2	AF	1.5" GS Elbow 3
K	1.5" ABS 6 before heater	AG	1.5" GS 11 after elbow
L	Omega Heater	AH	1.5" GS Elbow 4
M	1.5" GS 1 after heater	AI	1.5" GS 12 after elbow
N	1.5" GS Coupler 1	AJ	1.5" GS 13 after Tee
O	1.5" Throttle Valve	AK	1.5" GS Elbow 5
P	1.5" GS 2 after throttle	AL	1.5" to 1" GS reducer 1
Q	1.5" GS Tee 1	AM	1" GS 1 after reducer
R	1.5" GS 3 after Tee	AN	1" Brass Gate Valve (EGR)
S	1.5" GS Elbow 1	AO	1" GS 2 after gate valve
T	1.5" GS 4 after elbow	AP	1" GS coupler
U	1.5" GS Coupler 2	AQ	1.5" to 1" GS Reducer 2
V	1.5" GS 6 before engine		

Material	Melting Temperature (°C)
ABS-plastic plumbing piping	80-125
Galvanized Steel – 1040 (40% carbon)	738

F.9 Intake Piping Flow Resistance Excel Program Inputs

The purpose of this program is to determine the pressure loss associated with the intake piping system for various engine speeds, EGR and Exhaust Valve positions, and heater temperatures. The program inputs are listed in tables below. A desired engine speed is entered and the program calculates the pressure loss for each component of the system and summarizes the resistance for each of the legs of the system.

<u>Engine Properties</u>				<u>Relevant Properties of Air:</u>	
Engine Displacement	898	cc		T (deg C)	25
Cylinder Displacement	299.33	cc		ρ (kg/m ³)	1.184
Cycle time (s)	Q -cc/s	Q - m3/s		γ (N/m ³)	11.61
0.033	8980	8.980E-03		μ (N-s/m ²)	1.85E-05
				ν (m ² /s)	1.56E-05

<u>No. turns from fully closed:</u>					<u>Valve Positions:</u>		
EGR				0.0	EGR Valve:	100	% Closed
Exhaust				6.5	Exhaust Valve:	0.00	% Closed
					Throttle:	0.00	% Closed
	Rv	Rg	L- L	Open Area	Desired Heater Exit Temp (deg. K):		
	(mm)	(mm)	turns	(mm²):	300		
EGR Valve:	12.7	13.97	5.0	0.00			
Exhaust Valve:	19.05	20.955	6.5	1140.09			

Select Desired Engine RPM:

F.10 Intake Piping Flow Resistance Excel Program Outputs

Resistances:	kg/m⁷	Height Change (m)
		0.28876
Intake to first tee	7381902.26	
EGR Pipe	23057227122648800.00	Engine Pressure Rise (Pa)
Exhaust system	2827076.72	1030.63
First tee to engine	1377771.33	
Engine to second tee	1235426.75	
EGR Pipe	23057227122648800.00	
Flowrates:	m³/s	cfm
Intake/Exhaust:	8.98E-03	19.0275
Engine:	8.98E-03	19.0275
EGR:	1.98E-12	0.0000
		Iterations:
		2

F.11 Intake Piping Flow Resistance Excel Program Results

The following table of results are for a flow rate calculated based on an engine speed of 3600 RPM, with the EGR valve fully closed. The lettering corresponds to the legend and drawing shown in Appendix F.8. The coloring corresponds to the legend listed below.

NoElements		StartRow		Legend	
19	6	35	54	Intake to first tee	First tee to engine
9		67		EGR Pipe	
8	9	76	67	Exhaust system	EGR Pipe

	Dia. (mm)	Length (mm)	Height (mm)	Roughness (mm)	Vel (m/s)	Re #	Loss Coef.	Friction Factor	Pressure Loss (Pa)
A	38.1	508	-508	0.0015	7.877	19237	0.00	0.0262	6.94
B	38.1	368.3	-368.3	0.0015	7.877	19237	0.50	0.0262	23.40
C	38.1	254	-254	0.0015	7.877	19237	0.00	0.0262	3.47
D	38.1	0	0	0	7.877	19237	1.00	0.0261	36.73
D	38.1	0	0	0	7.877	19237	0.80	0.0261	29.38
E	38.1	115	115	0.0015	7.877	19237	0.00	0.0262	4.24
F	38.1	60	60	0.0015	7.877	19237	0.30	0.0262	13.23
G	38.1	298	0	0.0015	7.877	19237	0.00	0.0262	7.53
H	43	20	0	0.015	6.184	17045	0.10	0.0276	2.55
I	38.1	585	0	0.0015	7.877	19237	0.00	0.0262	14.78
J	38.1	60	0	0.0015	7.877	19237	3.00	0.0262	111.70
K	38.1	115	0	0.0015	7.877	19237	0.00	0.0262	2.91
L	35	305	0	0.3	9.334	20941	5.00	0.0389	-6.986E+03

M	38.1	155	0	0.15	7.877	19237	0.00	0.0331	4.94
N	38.1	30	0	0.15	7.877	19237	0.08	0.0331	3.89
N	38.1	70	0	0.15	7.877	19237	0.00	0.0331	2.23
O	38.1	45	0	0.015	7.877	19237	1.297 E-01	0.0270	5.932E+00
P	38.1	15	0	0.15	7.877	19237	0.00	0.0331	0.48
Q	38.1	45	0	0.15	7.877	19237	0.90	0.0331	34.49
Q	38.1	45	0	0.15	7.877	19237	0.90	0.0331	34.49
R	38.1	282	0	0.15	7.877	19237	0.00	0.0331	8.99
S	38.1	60	0	0.15	7.877	19237	1.50	0.0331	57.00
T	38.1	132	0	0.15	7.877	19237	0.00	0.0331	4.21
U	38.1	25	0	0.15	7.877	19237	0.08	0.0331	3.74
V	38.1	84	0	0.15	7.877	19237	0.00	0.0331	2.68

ENGINE

-1030.63

AB	38.1	45	0	0.15	0.000	0	0.90	0.0052	0.00
AK	38.1	22	0	0.15	0.000	0	0.00	0.0052	0.00
AL	38.1	60	0	0.15	0.000	0	1.50	0.0052	0.00
AM	31.75	16	0	0.15	0.000	0	0.14	0.0054	0.00
AN	25.4	138	0	0.15	0.000	0	0.00	0.0055	0.00
AO	25.4	51	0	0.15	0.000	0	1.000 E+10	0.0055	9.446E-08
AP	25.4	235	0	0.15	0.000	0	0.00	0.0055	0.00
AQ	31.75	22	0	0.15	0.000	0	0.14	0.0054	0.00
Q-90°	38.1	76	0	0.15	0.000	0	2.00	0.0052	0.00
AB-90°	38.1	76	76	0.15	7.877	19237	2.00	0.0331	76.76
AC	38.1	140	140	0.15	7.877	19237	0.00	0.0331	6.09
AD	38.1	51	51	0.15	7.877	19237	9.449 E-02	0.0331	5.689E+00
AE	38.1	55	140	0.15	7.877	19237	0.00	0.0331	3.38
AF	38.1	60	60	0.15	7.877	19237	1.50	0.0331	57.69
AG	38.1	700	0	0.15	7.877	19237	0.00	0.0331	22.32
AI	38.1	60	60	0.15	7.877	19237	1.50	0.0331	57.69
AJ	38.1	140	140	0.15	7.877	19237	0.00	0.0331	6.09

Piping Leg	Description	Summary of Pressure Loss (Pa)
A to Q	Intake to first tee	308.82
Q to V	First tee to engine	111.10
W to AB	Engine to second tee	99.63
AB to AI	Exhaust system	235.72
AB to Q	EGR	No flow

F.12 Visual Basic Macro for Intake Piping Analysis

Function Colebrook(roughness As Double, diameter As Double, Reynolds As Double) As Double

```

On Error GoTo default
Dim LHS As Double, RHS As Double, f As Double, lastf As Double
f = 0.0001 ' guess value
Do
    lastf = f
    RHS = -2# * Log((roughness / diameter) / 3.7 + 2.51 / (Reynolds * f ^ 0.5)) / Log(10)
    f = 1 / (RHS ^ 2)
Loop While Abs(f - lastf) > 1 * 10 ^ -7
Colebrook = f
If f > 0 Then Exit Function
default:
Colebrook = 0
End Function

```

Function AreaCalc(rv As Single, rg As Single, totTurns As Single, curTurns As Single) As Single

```

Dim PI As Single, tv As Single, tg As Single, h As Single, a As Single, b As Single
PI = 4 * Atn(1)
h = (curTurns / totTurns) * 2 * rv
a = (8 * rg ^ 2 * h * rv + 12 * h ^ 2 * rv * rg - 8 * h * rv ^ 2 * rg - 4 * rg ^ 2 * h ^ 2 + 4 * h ^ 3 * rv - 4 * h ^ 3 * rg - 4 * h ^ 2 * rv ^ 2 - h ^ 4)
If a < 0 Then: a = 0
a = a ^ (1 / 2) / (h - rv + rg) / rg
b = (2 * rg ^ 2 + h ^ 2 - 2 * h * rv + 2 * h * rg - 2 * rv * rg) / rg / (h - rv + rg)
tg = 2 * Atan2_JD(a, b)
a = (8 * rg ^ 2 * h * rv + 12 * h ^ 2 * rv * rg - 8 * h * rv ^ 2 * rg - 4 * rg ^ 2 * h ^ 2 + 4 * h ^ 3 * rv - 4 * h ^ 3 * rg - 4 * h ^ 2 * rv ^ 2 - h ^ 4)
If a < 0 Then: a = 0
a = a ^ (1 / 2) / rv / (h - rv + rg)
b = (h ^ 2 - 2 * h * rv + 2 * h * rg - 2 * rv * rg + 2 * rv ^ 2) / rv / (h - rv + rg)
tv = 2 * Atan2_JD(a, b)
AreaCalc = PI * rv ^ 2 - ((0.5 * tg * rg ^ 2 - rg ^ 2 * Sin(0.5 * tg) * Cos(0.5 * tg)) + (0.5 * tv * rv ^ 2 - rv ^ 2 * Sin(0.5 * tv) * Cos(0.5 * tv)))
End Function

```

Function Atan2_JD(y As Single, x As Single) As Single

```

Dim PI As Single
PI = 4 * Atn(1)
' Normal range of atn is -pi/2 to pi/2, need to expand to -pi to pi
If x > 0 Then
    Atan2_JD = Atn(y / x)
Elseif x < 0 Then
    Atan2_JD = Atn(y / x) + PI
Elseif x = 0 And y > 0 Then
    Atan2_JD = PI / 2
Elseif x = 0 And y < 0 Then
    Atan2_JD = -PI / 2
Elseif x = 0 And y = 0 Then
    Atan2_JD = 0
End If
End Function

```

Function heatPres(Pin As Double, V As Double, D As Double, Tout As Double) As Variant

```

Dim Q As Double, Tout_max As Double
Q = V * Atn(1) * (D / 1000) ^ 2 ' Calculates flowrate through heater
Tout_max = -5868490.265 * Q ^ 2 + 51242.764 * Q + 749.718 ' maximum exit temperature at flowrate
If Tout > Tout_max Then
    heatPres = "Exit temp. too high!" ' limit exit T to max"
Else
    heatPres = Pin * (Tout / 294.111111) ^ (1.4 / 0.4) ' compute exit pressure from heater ' (assumes isentropic).
End If
End Function

```



```

Function Valve_KL(Vtype As String, Pcent_Closed As Double) As Double
' This function computes the loss coefficient for butterfly and gate valves.
Dim a As Double, t As Double, m As Double, b As Double
' Set the values of the coefficients:
If Vtype = "gate" Then
    a = 0.0944898949
    t = 0.0651200439
    m = 399999999.32
    b = -29999999932#
ElseIf Vtype = "butterfly" Then
    a = 0.1296730544
    t = 0.1053022044
    m = 399999986#
    b = -29999998600#
End If

If Pcent_Closed <= 75# Then
    Valve_KL = a * Exp(t * Pcent_Closed)
Else
    Valve_KL = m * Pcent_Closed + b
End If
End Function

Sub PipingSystem()
Dim i As Integer, j As Integer, k As Integer, x As Integer ' Counters: i -> rows, j -> columns, k, x -> others
Dim f As Double, L As Double, D As Double, KL As Double, rho As Double, a As Double, _
    gamma As Double, RPM As Double, dH As Double, dPeng As Double, R(1, 2) As Double, _
    iO As Double, il As Double, Q(2) As Double, Rcoef(1, 1) As Double, e As Double, _
    V As Double, Re As Double, nu As Double, y As Integer, lastQ0 As Double
Dim noElements(1, 2) As Double, startRow(1, 2) As Double ' Recall that indexes start at 0.

Sheets(3).Activate
' This subroutine is actually a function which solves a system of equations.
' The system is the set of coupled equations governing flow in the piping around an HCCI test engine.
' Store data to variables (non-reused):
rho = Cells(4, 10).Value ' air density
gamma = Cells(5, 10).Value ' air specific weight
RPM = Cells(12, 4).Value ' engine RPM
nu = Cells(7, 10).Value ' kinematic viscosity
For i = 0 To 1
    For j = 0 To 2
        noElements(i, j) = Cells(17 + j, 2 + i).Value
        ' Stores number of piping elements in each resistive term
        startRow(i, j) = Cells(22 + j, 2 + i).Value
        ' Stores starting row for each relevant resistive term's piping element details
    Next j
Next i

' First, the "outer loop" will be considered. This is the intake up to the first tee, going along the
' EGR pipe, to the EGR/exhaust split tee, and out along the exhaust back to atmospheric conditions.
' There are three sets of resistances in this loop:
' 1. intake up to first tee
' 2. EGR pipe
' 3. Exhaust system
' There are two "currents" that appear in this loop:
' 1. Flowrate measured by LFE (negative in this equation)
' 2. Flowrate through engine (calculated, f(RPM)) (positive in this equation)
' The only "driving force" terms in this loop are hydrostatic pressure changes due to elevation differences.
' These will be computed first. They will form the "augment" side of the final matrix equation.
dH = 0 ' initialise term value (will be in mm)
For k = 0 To 49
    ' Add up all the hydrostatic terms for this term
    dH = dH + Cells(35 + k, 5).Value
Next k
dH = -dH / 1000 ' converts to m and changes sign for placement on RHS of equation
' The first row of the R array will contain the resistances listed above.
' Next, consider the "inner loop". This is the loop containing the engine and the EGR pipe.
' There are three sets of resistances in this loop:
' 1. from first tee to engine

```

```

' 2. from engine to second tee
' 3. EGR pipe (between the two tees)
' There are two "currents" that appear in this loop:
' 1. Flowrate measured by LFE (negative in this equation)
' 2. Flowrate through engine (calculated, f(RPM)) (positive in this equation)
' The only "driving force" term in this loop is the pressure rise across the engine. It
' will be determined by the equation solutions.
' Note at this point that one of the "currents", i.e. flowrates, is known!
' The flowrate through the engine depends on RPM only and is thus input as:
Q(1) = Cells(10, 4).Value ' m^3/s
' The rest of the solution procedure is iterative:
' Initial guesses for the other flowrates:
Q(0) = 0.5 * Q(1)
Q(2) = 0.5 * Q(1)
' Next, the six resistance terms must be computed for the two loops:
y = 1 ' initialise iteration counter
Do ' commence iteration loop
For i = 0 To 1
  For j = 0 To 2
    R(i, j) = 0
    For k = 1 To noElements(i, j)
      L = Cells(startRow(i, j) - 1 + k, 4).Value ' Length (mm)
      D = Cells(startRow(i, j) - 1 + k, 3).Value ' Diameter (mm)
      e = Cells(startRow(i, j) - 1 + k, 6).Value ' Roughness (mm)
      a = Atn(1) * (D / 1000) ^ 2 ' Area in m^2
      If i = 0 And (j = 0 Or j = 2) Then
        x = 0 ' flow through main intake/exhaust
      ElseIf (i = 0 And j = 1) Or (i = 1 And j = 2) Then
        x = 2 ' flow through EGR pipes
      ElseIf i = 1 And (j = 0 Or j = 1) Then
        x = 1 ' flow through engine
      End If
      V = Q(x) / a ' Velocity of flow (m/s)
      Cells(startRow(i, j) - 1 + k, 7).Formula = V
      Re = Abs(V) * D / nu / 1000 ' Reynolds number
      Cells(startRow(i, j) - 1 + k, 8).Formula = Re
      f = Colebrook(e, D, Re) ' friction factor
      Cells(startRow(i, j) - 1 + k, 10).Formula = f
      KL = Cells(startRow(i, j) - 1 + k, 9).Value ' Loss coefficient
      R(i, j) = R(i, j) + ((f * L / D) + KL) / (a ^ 2)
    Next k
    R(i, j) = R(i, j) * rho / 2 ' Resistance term (final form -- base units, kg/m^7)
  Next j
Next i

' Now that the resistances have been computed, the coefficients of the "currents"
' can be determined as follows:

Rcoef(0, 0) = R(0, 0) + R(0, 1) + R(0, 2) ' outer current eq., outer current coef.
Rcoef(0, 1) = -R(0, 1) ' outer current eq., inner current coef.
Rcoef(1, 0) = -R(1, 2) ' inner current eq., outer current coef.
Rcoef(1, 1) = R(1, 0) + R(1, 1) + R(1, 2) ' inner current eq., inner current coef.

lastQ0 = Q(0) ' store last value for comparison purposes
' Now the two loop equations can be solved for the unknowns (Q(0) and dPeng):
Q(0) = ((gamma * dH - Rcoef(0, 1) * Q(1) ^ 2) / Rcoef(0, 0)) ^ 0.5
dPeng = Rcoef(1, 0) * Q(0) ^ 2 + Rcoef(1, 1) * Q(1) ^ 2
' Currents are equivalent to the square of flowrates. There are three flowrates of interest (in m^3/s):
' 1. Flowrate through LFE / exhaust
' 2. Flowrate through engine (KNOWN)
' 3. Flowrate through EGR pipe

Q(2) = -Q(0) + Q(1) ' positive with flow going from exhaust towards intake
' Now that the flowrates are known, the pressure drop between any two points can be calculated from:
' dP = gamma * dH + R * Q ^ 2

' Program output:
' resistances:
i = 0
  For j = 0 To 2

```

```

    Cells(18 + j, 7).Formula = R(i, j)
  Next j
i = 1
  For j = 0 To 2
    Cells(18 + j + 3, 7).Formula = R(i, j)
  Next j
' flowrates:
For k = 0 To 2
  Cells(27 + k, 7).Formula = Q(k)
Next k
' pressure rise:
Cells(22, 10).Formula = dPeng
' iteration counter:
Cells(30, 10).Formula = y
' height change:
Cells(16, 10).Formula = dH
y = y + 1
Loop While Abs(Q(0) - lastQ0) > 1 * 10 ^ -9 ' End iteration loop
End Sub

```

F.13 MATLAB EGR program description

This M-file was written to enable the calculation of percent EGR based on a measurement of the volume fraction of CO₂ in the intake manifold of an engine. It is intended to be used with the a method of measuring CO₂ such as available with the OTC emissions analyzer. This program was modified by Jeff Defoe (University of Windsor) and originally written by D.M. Arthur of University of Alberta (Edmonton).

The following inputs must be entered into the program for a calculation to be performed:

Relative humidity (ϕ) of air at ambient conditions:

$$\phi = 0.75, \quad (\text{F.29})$$

Ambient pressure (P) of air:

$$P = 101.325 \text{ kPa}, \quad (\text{F.30})$$

Saturation Pressure (P_g) of water at ambient temperature 25 °C:

$$P_g = 3.169 \text{ kPa} \quad (\text{F.31})$$

Mass flow rate of air ($m_{\text{dot_air}}$). This is the mass flowrate of air entering the intake manifold (before mixing with EGR gases) at 4000 RPM.

$$m_{\text{dot_air}} = 0.01279 \text{ kg/s}, \quad (\text{F.32})$$

Mole/Volume fraction of CO₂. This is the measured volume fraction of CO₂ in the intake given from the emission analyzer:

$$N_{\text{CO2}} = \text{various}, \quad (\text{F.33})$$

Composition of fuel (fuel), the number of atoms of C, H, O and N in the fuel:

$$\begin{array}{ccc} \text{C} & \text{H} & \text{O} & \text{N} \\ \text{fuel}=[& 2 & 6 & 1 & 0]; \end{array} \quad (\text{F.34})$$

Composition of additives (adds), the number of atoms of C, H, O and N in each of the additives present in the fuel:

$$\begin{array}{ccc} \text{C} & \text{H} & \text{O} & \text{N} \\ \text{adds}=[& 0 & 0 & 0 & 0]; \end{array} \quad (\text{F.35})$$

Mole fraction of fuel (a), fraction of combustible mixture (fuel + additives) that is made up of fuel:

$$a = 1.0, \quad \text{F.36}$$

Mole fraction of additives (b), fraction of combustible mixture (fuel + additives) that is made up of each additive:

$$b = 0.0, \quad \text{(F.37)}$$

Equivalence ratio (equiv), value counts both fuel and additives as combustibles in calculation of air/combustibles ratio (Set for HCCI range):

$$\text{equiv} = 0.4, \quad \text{(F.38)}$$

PROGRAM OUTPUT:

1. Mass percentage of EGR (m_EGR_percent), percentage of mass entering the cylinder that is re-circulated exhaust gas.

$$m_EGR_percent = ?, \quad \text{(F.39)}$$

F.14 EGR Calculation Summary

For various mass flow rates of CO2 we have corresponding % EGR calculations:

Mass flowrate of CO2	% EGR
.005	9.7122
.01	18.38
.015	27.7767
.02	37.3513
.025	46.997
.03	56.8315
.035	66.8158
.04	76.9556
.045	87.2547
.05	97.7167

F.15 MATLAB EGR program

See the m-file code below for a detailed explanation of how the calculation is performed. All steps are commented for clear explanations.

```
clear
clc

% Program Inputs:
% -----

% Relative humidity:
phi=0.75;
% Atmospheric Pressure (kPa):
P=101.325;
% Saturation Pressure of water at T:
Pg=3.169; % This is for 25 degrees C (in kPa)

% Absolute humidity:
w=0.622*phi*Pg/(P-phi*Pg);
```

```

m_dot_air=.01279; % mass flow rate of air (kg/s)
% The current version of this program does not use the following data:
% P_sample % pressure measured in intake
% P_sat % saturation pressure of H2O
N_CO2=0.02; % Mole Fraction of CO2 in intake (w/o water)

% Gas Constants
Ru=8.314; % universal gas constant

% C H O N
fuel=[2 6 1 0]; % composition of fuel
adds=[0 0 0 0
      0 0 0 0]; % composition of additives

a=1.0; % mole fractions of combustible mixture
b=[0.0
  0.0]; % a -> fuel, b-> additives

equiv=0.4; % equivalence ratio

% Molar Masses:
M_ADDS=12.01*adds(:,1)+2.015/2*adds(:,2)+16*adds(:,3)+14.005*adds(:,4); % vector of additive molar masses
M_FUEL=12.01*fuel(1,1)+2.015/2*fuel(1,2)+16*fuel(1,3)+14.005*fuel(1,4);
M_CO2=44.01;
M_O2=32;
M_N2=28.01;
M_H2O=18.02;
% Molar mass of dry air:
M_dry_air=(1*M_O2+3.773*M_N2)/(1+3.773);
M_COMB=a*M_FUEL;
for k=1:size(b,1)
    M_COMB=M_COMB+(b(k,1).*M_ADDS(k,1));
end
M_COMB=M_COMB/(sum(b)+a);

delta=w*4.773*(M_dry_air/M_H2O); % humidity factor

% Molar mass of air with humidity:
M_air=(1*M_O2+3.773*M_N2+delta*M_H2O)/(1+3.773+delta);

% C H O N
air=[0 2*delta delta+2 3.773*2]; % composition of air

% END INPUT
% C H O N
addsum=[0 0 0 0]; %adds the atoms from all additives

for i=1:4
    for j=1:size(adds,1)
        addsum(1,i)=addsum(1,i)+b(j,1)*adds(j,i);
    end
end
atoms=a*fuel+addsum; % total numbers of atoms for fuel + additives.
% Here atoms [=] [C H O N].
% now compute the air coefficient requirement for
% the stoichiometric case.
x=atoms(1,1)+atoms(1,2)/4-atoms(1,3)/2;
% The actual air coefficient is x/equiv:
y=x/equiv;

% Determine coefficients of products: CO2, H2O, fuel, O2, N2.
% Three cases: stoichiometric, rich, or lean.

if equiv==1.0 % stoichiometric
    f=0;
    o=0;
    n=(atoms(1,4)+y*air(1,4))/2;
    h=(atoms(1,2)+2*delta*y)/2;

```

```

c=atoms(1,1);
elseif equiv>1.0 % rich
o=0;
% system of 3 equations in 3 unknowns to solve
% for c,f,h
M=[2/atoms(1,3) 1 1/atoms(1,3)
0 atoms(1,2)/2 1
1 atoms(1,1) 0 ];
A=[1+(2+delta)*y/atoms(1,3)
(atoms(1,2)+2*delta*y)/2
atoms(1,1)];
B=M/A;

c=B(1,1);
f=B(2,1);
h=B(3,1);
n=(atoms(1,4)+y*air(1,4)-f*atoms(1,4))/2;
elseif equiv<1.0 % lean
f=0;
c=atoms(1,1);
h=(atoms(1,2)+y*2*delta)/2;
o=(atoms(1,1)+y*(2+delta)-2*c-h)/2;
n=(atoms(1,4)+y*air(1,4))/2;
end

% Determine fuel mass flow rate from equivalence ratio:
m_dot_COMB=m_dot_air*(M_COMB/M_air)/y;
% Molar flow rates of combustibles and air:
n_dot_COMB=m_dot_COMB/M_COMB; % molar flow rate of combustibles
n_dot_air=m_dot_air/M_air; % molar flow rate of air (oxidiser)
% since mass is conserved, n_dot*M=const for the mixture (both before and
% after combustion).
% Compute average molar mass of intake (before EGR) and exhaust:
M_IN=(M_COMB+y*M_air)/(1+y);
M_EX=(c*M_CO2+h*M_H2O+f*M_COMB+o*M_O2+n*M_N2)/(c+h+f+o+n);
% Compute molar flow rates of total intake and total exhaust:
n_dot_IN=(m_dot_air+m_dot_COMB)/M_IN;
n_dot_EX=(m_dot_air+m_dot_COMB)/M_EX;
% Molar flow rates - total exhaust:
n_dot_CO2=(c/(c+h+n+f+o))*n_dot_EX; % CO2 content (depends on combustibles)
n_dot_H2O=(h/(c+h+n+f+o))*n_dot_EX; % H2O content from combustibles and air
n_dot_N2=(n/(c+h+n+f+o))*n_dot_EX; % N2 content from combustibles and air
n_dot_COMB_rich=(f/(c+h+n+f+o))*n_dot_EX;; % remaining fuel if mixture is rich
n_dot_O2_lean=(o/(c+h+n+f+o))*n_dot_EX;; % remaining oxygen if mixture is lean

% Solve combustion equation with a given combustible composition for unknown "mu"

mu=-N_CO2*(n_dot_IN)/(N_CO2*n_dot_EX-n_dot_CO2);
% mu is the fraction of the flow diverted from exhaust to EGR

% calculate molar flow rate of CO2, N2 and H2O, and combustibles in EGR:
n_dot_CO2_EGR=mu*n_dot_CO2;
n_dot_N2_EGR=mu*n_dot_N2;
n_dot_H2O_EGR=mu*n_dot_H2O;
n_dot_COMB_EGR=mu*n_dot_COMB_rich;
n_dot_O2_EGR=mu*n_dot_O2_lean;

% mole fraction of intake that is from EGR (after EGR mixing):
N_EGR=(n_dot_CO2_EGR+n_dot_N2_EGR+n_dot_H2O_EGR+n_dot_COMB_EGR+n_dot_O2_EGR)/(n_dot_CO2_EGR+n_dot_
N2_EGR+n_dot_H2O_EGR+n_dot_COMB_EGR+n_dot_O2_EGR+n_dot_air+n_dot_COMB);
% Molar mass of EGR:
M_EGR=M_EX;
% Molar mass of intake (after EGR mixing):
M_i=(M_IN*n_dot_IN+M_EGR*mu*n_dot_EX)/(n_dot_IN+mu*n_dot_EX);

% mass fraction of EGR
m_EGR=N_EGR*M_EGR/M_i;
m_EGR_percent=m_EGR*100

% End of program

```

Appendix G: Intake System Specifications

G.1 Specifications for Omega SH Series Air Heater

Max. Static Pressure: 10 psi	10 psi
Max. Exit Air Temp:	760°C
Max. Inlet Air Temp:	55°C
Exit Connection:	1-1/2" NPT
Inlet Connection:	1-1/4" NPT
Control:	Closed Loop: 4-20mADC Or pulsed DC (3-32V, etc.)
Over-temp Circuit:	Dual Input Limit Card

System (Heater + Over-Temp)	Power Rating (kW)	Max. Volts	Max. Current Draw (Amps)	Replacement Element P/N
SH-73343	6	240-1 phase	25.0	SH-73351
SH-73344	6	480-3 phase	7.2	SH-73352

G.2 Features for Omega CNI Series Controllers

Measured Process Voltage	0-100 mV, 0-1 V, 0-10 V ranges.
Process current	0-20 mA
Communications	RS-232
Control Type	Manual ON-off, Full Autotune PID
User Defined rate of rise to Setpoint	Soak: 00.00 to 99.59
Input Types	J, K, T, E, R, S, B, C, N, J-DIN, RTD 100 ohm, 500 ohm & 1k ohm

G.3 Specifications for Meriam Laminar Flow Meter

Model #	Nominal Airflow Range SCFM @ 8"H20	Description
50MC2-2	0-100	Designed for use with low pressure applications. Line connections are for hose.
50MY15-2 1/2	0-60	Stainless steel welded unit with fused matrix. Line connections are flanges
50MH10-2	0-40	Stainless steel welded unit with fused matrix. Line connections are threaded.



Cert. No.: 091404130358
 Filename: 79962001.1NU
 Program: LAMINAR 1.47

CERTIFICATE OF CALIBRATION
 LAMINAR FLOW ELEMENT

CUSTOMER: PEACOCK INSTRUMENTATION
8600 ST PATRICK
LASALLE QC H8N 1V1 CANADA

CUSTOMER ORDER NUMBER: 9196683

MERIAM ORDER NUMBER: 799620

MODEL NO.: 50MC2-2 SERIAL NO.: 799620-U1

FLOW CURVE/TABLE NO.: 36558

DATE OF CALIBRATION: 09-14-2004

AS RECEIVED CONDITION: In Tolerance Out of Tolerance NA

AS LEFT CONDITION : In Tolerance Out of Tolerance NA

CALIBRATION INTERVAL: To be determined by customer based on usage of LFE.

FLOW STANDARD SERIAL NO.	LAST CALIBRATION	NEXT CALIBRATION
WMMH10-3	FEBRUARY 2004	FEBRUARY 2005

Meriam Process Technologies certifies that the Laminar Flow Element listed above has been calibrated and correlated at several points of flow rate in accordance with procedure A35822 using the standard listed above. Meriam's calibration program is controlled per the requirements of ISO/IEC 17025 and is traceable to the National Institute of Standards and Technology. The expanded uncertainty (U) (k=2 at a confidence level of approximately 95%) of the actual volumetric flowrate of this unit determined by measurements taken by Meriam's calibration system was +/- 0.72% of reading over the calibrated range. (U) includes contribution from the uncertainty of the measurements used to determine the calibration coefficients. In/Out of tolerance statements are the opinions of Meriam and are based on data from measurements taken, procedures utilized, and professional experience. This certificate is provided as a support for our customer and shall not be reproduced, except in full, without the written consent of Meriam Process Technologies.

Issued by: Christine McCutcheon Date: 9/14/04

G.5 Certificate of Calibration for Meriam LFE 50MC2-2 Page 2 of 2

Cert. No.: 091404130358
 Filename: 79962001.INU
 Program: LAMINAR 1.47

Standard

Customer name: PEACOCK INSTRUMENTATION
 Customer address: 8600 ST PATRICK
 LASALLE QC H8N 1V1 CANADA
 Customer order no.: 9196683
 Meriam order no.: 799620

LFE model no.: 50MC2-2 Plot no.: 113
 LFE serial no.: 799620-U1 Working master serial no.: WMMH10-3
 Curve no.: 36558 Master master serial no.: MMMH10-3
 Calibration date: 09-14-2004
 Today's date: 09-14-2004

Calibration data from flow lab utt = Unit Under Test
 mas = Master

RH %	Tutt DEG F	TMAS# DEG F	PSutt PSIA	PSMAS PSIA	DPutt In H2O	DPmas In H2O
52.2	72.5	74.9	14.416	14.379	1.006	1.020
52.4	72.6	74.8	14.411	14.336	2.003	2.044
51.2	72.6	74.8	14.406	14.287	3.003	3.089
50.1	72.6	74.7	14.397	14.235	3.997	4.142
49.6	72.6	74.6	14.387	14.179	5.005	5.233
48.8	72.4	74.4	14.377	14.122	5.992	6.305
48.3	72.4	74.3	14.364	14.061	6.937	7.374
47.8	72.3	74.2	14.347	13.989	8.025	8.608

Master LFE A0 = 2.28008E+03 A3 = 0.00000E+00 A6 = 0.00000E+00
 Coefficients: A1 = -1.20219E+06 A4 = 0.00000E+00 A7 = 0.00000E+00
 A2 = -2.51408E+11 A5 = 0.00000E+00 A8 = 0.00000E+00

Room conditions at start (inlet read): 72.4 DEG F 14.421 PSIA 51.6 RH
 Room conditions at end: (inlet read): 72.3 DEG F 14.415 PSIA 50.0 RH

Reduced data, based on master life coefficients:

DATA POINT	DP utt InH2O@4C	FLOW IN ACFM BASED ON MASTER	CFM* (DATA) BASED ON MASTER	CFM* (CURVE) B*DP+C*DP^2	PERCENT ERROR**
1	1.006	12.607618	12.640987	12.690468	0.39
2	2.003	25.132554	25.201546	25.217304	-0.06
3	3.003	37.726412	37.831212	37.756705	-0.20
4	3.997	50.177063	50.313159	50.186770	-0.25
5	5.005	62.775346	62.967501	62.761001	-0.33
6	5.992	74.858142	75.074670	75.040979	-0.04
7	6.937	86.536146	86.783536	86.755531	-0.03
8	8.025	99.534282	99.808765	100.212618	0.40

*CFM = ACFM x (Flowing viscosity in Micropoise / 181.87)
 ** PERCENT ERROR = ((CURVE-DATA) / DATA) * 100

A Least Squares Fit of the CFM(DATA) yields the following formula and LFE utt coefficients used to generate the CFM(CURVE) values:

$$CFM(CURVE) = (B \times DP) + (C \times DP^2) \quad \text{Where } B = 1.26268E+01 \\ C = -1.73314E-02$$

A Flow of 99.905235 CFM produces a UUT DP of 8.00 In H2O

TERMINAL NON-LINEARITY = 0.956 % FOR DETAILS SEE
 INDEPENDENT NON-LINEARITY = 0.144 % FILE NO. 501:440

G.6 Honewell ST 3000 Transmitter Model # STD904 Specifications

For detailed wiring diagrams and installation instructions consult manual entitled "ST 3000 Smart Transmitter, Release 300 and SFC Smart Field Communicator Model STS103, Installation Guide" Honewyell Inc., July 2000, Phoenix, USA.

34-ST-03-74
Page 4

Specifications - Performance Under Rated Conditions* - Model STD904

Parameter	Description
Upper Range Limit inH ₂ O mbar	400 (39.2°F/4°C is standard reference temperature for inH ₂ O range) 1000
Minimum Span inH ₂ O mbar	16 Note: Recommended minimum span in square root mode is 20 inH ₂ O (50 mbar). 40
Turndown Ratio	25 to 1
Zero Elevation and Suppression	-5 to +100% URL.
Accuracy (Reference - includes combined effects of linearity, hysteresis, and repeatability) • Accuracy includes residual error after averaging successive readings. • For HART use Analog Mode specifications.	In Analog Mode: ±0.15% of calibrated span or upper range value (URV), whichever is greater, terminal based. For URV below reference point (25 inH ₂ O), accuracy equals: $\pm 0.075 + 0.075 \left(\frac{25 \text{ inH}_2\text{O}}{\text{span inH}_2\text{O}} \right) \text{ or } \pm 0.075 + 0.075 \left(\frac{52 \text{ mbar}}{\text{span mbar}} \right) \text{ in } \% \text{ span}$ In Digital Mode: ±0.125% of calibrated span or upper range value (URV), whichever is greater, terminal based. For URV below reference point (25 inH ₂ O), accuracy equals: $\pm 0.05 + 0.075 \left(\frac{25 \text{ inH}_2\text{O}}{\text{span inH}_2\text{O}} \right) \text{ or } \pm 0.05 + 0.075 \left(\frac{52 \text{ mbar}}{\text{span mbar}} \right) \text{ in } \% \text{ span}$
Zero Temperature Effect per 28°C (60°F)	In Analog Mode: ±0.325% of span. For URV below reference point (50 inH ₂ O), effect equals: $\pm 0.0125 + 0.3125 \left(\frac{50 \text{ inH}_2\text{O}}{\text{span inH}_2\text{O}} \right) \text{ or } \pm 0.0125 + 0.3125 \left(\frac{125 \text{ mbar}}{\text{span mbar}} \right) \text{ in } \% \text{ span}$ In Digital Mode: ±0.3125% of span. For URV below reference point (50 inH ₂ O), effect equals: $\pm 0.3125 \left(\frac{50 \text{ inH}_2\text{O}}{\text{span inH}_2\text{O}} \right) \text{ or } \pm 0.3125 \left(\frac{125 \text{ mbar}}{\text{span mbar}} \right) \text{ in } \% \text{ span}$
Combined Zero and Span Temperature Effect per 28°C (60°F)	In Analog Mode: ±0.6% of span. For URV below reference point (50 inH ₂ O), effect equals: $\pm 0.20 + 0.40 \left(\frac{50 \text{ inH}_2\text{O}}{\text{span inH}_2\text{O}} \right) \text{ or } \pm 0.20 + 0.40 \left(\frac{125 \text{ mbar}}{\text{span mbar}} \right) \text{ in } \% \text{ span}$ In Digital Mode: ±0.575% of span. For URV below reference point (50 inH ₂ O), effect equals: $\pm 0.175 + 0.40 \left(\frac{50 \text{ inH}_2\text{O}}{\text{span inH}_2\text{O}} \right) \text{ or } \pm 0.175 + 0.40 \left(\frac{125 \text{ mbar}}{\text{span mbar}} \right) \text{ in } \% \text{ span}$
Zero Static Pressure Effect per 1000 psi (70 bar)	±0.3% of span. For URV below reference point (50 inH ₂ O), effect equals: $\pm 0.0125 + 0.2875 \left(\frac{50 \text{ inH}_2\text{O}}{\text{span inH}_2\text{O}} \right) \text{ or } \pm 0.0125 + 0.2875 \left(\frac{125 \text{ mbar}}{\text{span mbar}} \right) \text{ in } \% \text{ span}$
Combined Zero and Span Static Pressure Effect per 1000 psi (70 bar)	±0.6% of span. For URV below reference point (50 inH ₂ O), effect equals: $\pm 0.20 + 0.40 \left(\frac{50 \text{ inH}_2\text{O}}{\text{span inH}_2\text{O}} \right) \text{ or } \pm 0.20 + 0.40 \left(\frac{125 \text{ mbar}}{\text{span mbar}} \right) \text{ in } \% \text{ span}$
Stability	±0.03% of URL per year

*Performance specifications are based on reference conditions of 25°C (77°F), zero (0) static pressure, 10 to 55% RH.

G.7 Functional Capability of OTC Emission Analyzer

- Communicates to a PC with OTC software to view live and recorded data in highly detailed graphics.
- Printouts available through PC or OTC printer.
- Works on 12 VDC, 110V/60 Hz, 220V/50 Hz power sources.
- Software is menu driven and user friendly, icons are available throughout the software.
- Can record 20 plus events with record times of 7 minutes per event.
- Can be serviced in the field by end user. The NO_x cell, O₂ cell, and pump are replaceable.
- The MicroGAs analyzer is not designed for use on diesel or two-cycle engines. The particulate will clog hoses, filters and internal components.
- Measurement Ranges
 - Hydrocarbons (HC): 0-30000 ppm
 - Carbon Monoxide (CO): 0-15%
 - Carbon Dioxide (CO₂): 0-20%
 - Oxides of Nitrogen (NO_x): 0-5000 ppm
 - Oxygen (O₂): 0-25%

Appendix H: Fuel System Design Calculations

H.1 Fuel System Requirements

The desired quantity is the required fuel flow rate of the fuel system in units of kilograms per seconds (kg/s) or pounds per hour (lb/h) which is determined from calculating the amount of air fuel mixture required by the engine at stoichiometric operation, and maximum engine speed (3600 RPM).

Known Quantities:

Engine Displacement	898	cc	From B.6
Cylinder Displacement	299.333333	cc	From B.6
Clearance Volume	20	cc	From B.6
Cylinder Volume	319.333333	cc	From B.6
Density of air	1.201923077	kg/m ³	From Cengal and Boles
Density of ethanol	789	kg/m ³	From Cengal and Boles
AFR _s	8.957		

RPM	Cycle Time (s)	Volume flowrate (cc/s)	Volume flowrate (m ³ /s)	Mass flowrate of mixture (kg/s)	Mass flowrate of fuel (stoich) (kg/s)	Mass flowrate of fuel (phi=.5) (kg/s)	Mass flowrate of fuel (stoich) (lb/h)	Mass flowrate of fuel (phi=.5) (lb/h)
500	0.240	1247.22	0.0012	0.0015	1.506E-04	7.926E-05	1.198	0.631
1000	0.120	2661.11	0.0027	0.0032	3.212E-04	1.691E-04	2.556	1.345
1500	0.080	3991.67	0.0040	0.0048	4.818E-04	2.537E-04	3.834	2.018
2000	0.060	5322.22	0.0053	0.0064	6.425E-04	3.382E-04	5.111	2.691
2500	0.048	6652.78	0.0067	0.0080	8.031E-04	4.228E-04	6.389	3.363
3000	0.040	7983.33	0.0080	0.0096	9.637E-04	5.073E-04	7.667	4.036
3600	0.033	9580.00	0.0096	0.0115	1.156E-03	6.088E-04	9.200	4.843

Cycle time calculations were performed identically to Appendix F.3 equation F.19. Volumetric flow rate calculations were performed identically to Appendix F.3 equations F.21, F.23.

Convert to volumetric flowrate to mass flow rate of mixture (\dot{m}_{mix}) to units of [kg/s]:

$$\dot{m}_{mix} = \rho_{air} \times \dot{V}_{mix}, \quad (H.1)$$

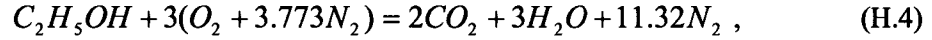
Where the density of air (ρ_{air}) is 1.201923 kg/m³ and where \dot{V} is 0.008980 m³/s from F.24 for a maximum engine speed of 3600 RPM. Solving equation H.1:

$$\dot{m}_{mix} = 1.201923 \text{ kg} / \text{m}^3 \times 0.00898 \text{ m}^3 / \text{s} = 0.0115 \text{ kg} / \text{s} \quad (H.2)$$

Now we can solve for mass flow rate of fuel (\dot{m}_{fuel}) at stoichiometric ratio by using the following equation modified from Heywood:

$$\dot{m}_{fuel} = \frac{\dot{m}_{mix}}{AFR_s + 1}, \quad (H.3)$$

Where the stoichiometric ($\Phi = 1.0$) air fuel ratio of ethanol AFR_s was determined from the overall combustion equation:



to be $AFR_s = 8.957$. Therefore, Equation H.3 for ethanol becomes

$$\dot{m}_{fuel} = \frac{\dot{m}_{mix}}{8.987 + 1}, \quad (H.5)$$

$$\dot{m}_{fuel} = \frac{0.0115kg/s}{8.957 + 1} = 0.00156 \text{ kg/s} \quad (H.6)$$

Convert mass flow rate of fuel to units of pounds per hour (lb/h):

$$\dot{m}_{fuel} = \dot{m}_{fuel} \times 2.21lb/kg \times 3600sec/hour, \quad (H.7)$$

$$\dot{m}_{fuel} = 0.00156kg/s \times 2.21lb/kg \times 3600s/h = 9.2 \text{ lb/h} \quad (H.8)$$

For an HCCI equivalence ratio $\Phi = 0.5$, the air fuel ratio $AFR_{\Phi=0.5}$ is defined as:

$$AFR_{\Phi=0.5} = \frac{AFR_s}{\Phi}, \quad (H.9)$$

$$\text{Equation H.9 becomes: } AFR_{\Phi=0.5} = \frac{8.957}{0.5} = 17.914 \quad (H.10)$$

Then for an equivalence ratio of $\Phi = 0.5$ using Equation H.5 & H.7 the mass flow rate of fuel becomes:

$$\dot{m}_{fuel} = \frac{0.0115kg/s}{17.914 + 1} = 0.000608 \text{ kg/s} \quad (H.11)$$

$$\text{and } \dot{m}_{fuel} = 0.000608kg/s \times 2.21lb/kg \times 3600s/h = 4.84 \text{ lb/h} \quad (H.12)$$

Furthermore, to ensure that our fuel system will supply fuel at the adequate rate for three cylinders we multiply the fuel flow rate in H.6 and H.8 by three to get

$$\dot{m}_{fuel} = 3 \times \dot{m}_{fuel} = 3 \times 0.00156 \text{ kg/s} = 0.00468 \text{ kg/s or } 27.6 \text{ lb/h}, \quad (H.13)$$

Therefore, the amount of fuel that our engine will require if all three cylinders were to be enabled is 0.00468 kg/s or 27.6 lb/h. The volumetric flow rate of fuel \dot{V}_{fuel} is given by:

$$\dot{V}_{fuel} = \frac{\dot{m}_{fuel}}{\rho_{ethanol}}, \quad (m^3/s) \quad (H.14)$$

where the density of ethanol ($\rho_{ethanol}$) is 789 kg/m³. Solving H.14 yeilds:

$$\dot{V}_{fuel} = \frac{0.00468 \text{ kg} / \text{s}}{789 \text{ kg} / \text{m}^3} = 0.000005932 \text{ m}^3/\text{s} = 0.00593 \text{ L/s} \quad (\text{H.15})$$

Converting volumetric flow rate of fuel to gallons per hour (gal/h) we get:

$$\dot{V}_{fuel} = \dot{V}_{fuel} (\text{m}^3 / \text{s}) \times 264.17 (\text{gal} / \text{m}^3) \times 3600 (\text{s} / \text{h}) \quad (\text{H.16})$$

$$\dot{V}_{fuel} = 0.000005932 (\text{m}^3 / \text{s}) \times 264.17 (\text{gal} / \text{m}^3) \times 3600 (\text{s} / \text{h}) \quad (\text{H.17})$$

$$\dot{V}_{fuel} = 5.64 \text{ gal/h} \quad (\text{H.18})$$

Therefore the fuel flow rate requirement for three cylinder operation of the fuel system is 5.64 gal/h or 0.00593 L/s.

H.2 Fuel Pump Selection:

Accel Model 310-74701 electronic fuel injection (EFI) fuel pump. The Fuel flow rate of the pump (\dot{V}_{pump}) is:

$$\dot{V}_{pump} = 26 \text{ gal/hr @ 45 psi.} \quad (\text{H.19})$$

The factor of oversize ($F_{O/S}$) is determined by:

$$F_{O/S} = \frac{\dot{V}_{pump}}{\dot{V}_{fuel}}, \quad (\text{H.20})$$

where \dot{V}_{fuel} is 5.64 gal/h from equation H.18 and substituting along with H.19 into H.20 we get:

$$F_{O/S} = \frac{26}{5.64} = 4.6, \quad (\text{H.21})$$

Therefore the selection of the Accel Model 310-74701 fuel pump will be more than adequate for the proposed engine, since the factor of oversize is 4.6.

H.3 Fuel Tank Selection:

Fuel volume storage limit (V_{limit}) is:

$$V_{limit} = 5 \text{ L} \quad (\text{H.22})$$

The JAZ 547-250-001-01 Vertical Fuel Tank was selected. It has dimensions of 6" by 6" by 12" and is compatible with the fuel pump selected earlier and alcohol fuels (see Appendix I.2.)

The volume capacity (V_{tank}) of the fuel tank is:

$$V_{tank} = 1 \text{ gal} = 3.7842 \text{ L} \quad (\text{H.23})$$

Since:

$$V_{tank} \leq V_{limit} \quad (\text{H.24})$$

And the JAZ fuel tank is alcohol compatible. Therefore, the JAZ fuel tank will meet the design constraints.

H.4 Fuel Injector Selection

The fuel flow rate for one cylinder was determined earlier (H.8) to be:

$$\dot{m}_{fuel} = 0.00156kg / s = \text{or } 9.2 \text{ lb/h,}$$

The dynamic flow rate (\dot{m}_{inj}) of the Delphi Multec 2 # 2532087 injector from Appendix I.3 is:

$$\dot{m}_{inj} = 17.305 \text{ lb/h or } 2.1804 \text{ g/s,} \quad (\text{H.25})$$

Since: $\dot{m}_{fuel} \leq \dot{m}_{inj}$ (H.26)

Therefore, the Delphi Multec 2 injector will meet the design constraints.

H.5 Fuel Regulator and Gauge Selection

The system pressure (P_{sys}) of the fuel system will be within the following range as determined from the constraints:

$$P_{sys} = 2 \text{ to } 5 \text{ bar} \quad (\text{H.27})$$

or, $P_{sys} = 29 \text{ to } 72.5 \text{ psig,}$ (H.28)

Additionally, the nominal system pressure (P_{nom}) for is:

$$P_{nom} = 3.1 \text{ bar or } 45 \text{ psig,} \quad (\text{H.29})$$

From Appendix I.4, the Mallory Regulator Model # 4309 has a regulator pressure range (P_{reg}) of:

$$P_{reg} = 30\text{-}100 \text{ psi,} \quad (\text{H.30})$$

Since, $P_{reg} \approx P_{sys}$ (H.31)

And the nominal system pressure is within the limits of the pressure regulator:

$$30 \text{ psi} \leq P_{nom} \leq 100 \text{ psi,} \quad (\text{H.32})$$

And since, the regulator is both gasoline and alcohol compatible.

Therefore, the Mallory Pressure Regulator meets the design constraints of the fuel system.

From Appendix I.5, the Omega Model # PGS 25L 160 has a pressure range (P_{reg}) of:

$$P_{gauge} = 0\text{-}160 \text{ psi,} \quad (\text{H.30})$$

Since, the pressure regulator range is within the range of the pressure gauge.

$$\frac{0 \leq 30 \text{ psi} \leq P_{reg} \leq 100 \text{ psi} \leq 160 \text{ psi}}{P_{reg}} \quad (\text{H.31})$$

And since, the pressure gauge is both gasoline and alcohol compatible. Therefore, the Omega Pressure gauge meets the design constraints of the fuel system.

Appendix I: Fuel and ECU System Specification

I.1 Fuel Pump Specifications

ACCEL	Model # 310-74710
Electronic Fuel Injection (EFI) fuel pump	Alcohol compatibility
Volumetric Flow rate Capacity	26 gal/h
Operating Pressure	45 psi

I.2 Fuel Tank Specifications

JAZ	Model # 547-250-001-01
Dimensions	6" x 6" x 12"
Volume Capacity	1 US gallon
Vertical design	Alcohol compatibility

I.3 Fuel Injector Specifications

Delphi Multec 2 Short	Product # FJ10063 or 2532087
Operating Pressure	58 psi or (400 kPa)
Static Flow Rate	22 lbs/h or (2.76 g/s)
Dynamic Flow Rate	17.305 lb/h or (2.1804 g/s)
Pulse width / Repetition Rate	2.0 ms / 10.0 ms
Fuel Compatibility	Gasoline/alcohol

I.4 Fuel Pressure Regulator

Mallory Racing Regulator	Model # 4309
Fuel compatibility	Gasoline/alcohol
Pressure Range	30 – 100 psi
Type	Adjustable, Return style

I.5 Fuel Pressure Gauge

Omega	Model # PGS 25L 160
Type	Stem Mount
Fuel compatibility	Gasoline/alcohol
Pressure Range	0 – 160 psig
Material	316 stainless steel

I.6 Fuel Filter

JAZ	547-836-006-11
Type	Inline with -06 AN male ends
Fuel Compatibility	Gasoline/alcohol
Finish/Material	Blue Anodized aluminium
Dimensions	5-1/8" long x 1-1/8" diameter

I.7 Fuel Connectors

Aeroquip	Various Model Numbers
Types	Swivel Hose ends, AN to NPT, AN union, AN coupler.
Fuel Compatibility	Gasoline/alcohol
Finish/Material	Blue anodized aluminium

I.8 Fuel Hose

Aeroquip	Model # 023-FCA0620
Type	High stress steel braided hose
Material	Elastomer inner tube, partial stainless inner wire, and full stainless outer wire braid
Temperature Range	-49°C to 150°C

I.9 Electronic Control Unit (ECU)

034EFI	Stage 3b
Operating Temperature	-40 to +85°C
Current Consumption	0.05-16 Amperes
Injector Impedance	High or low impedance, 12+ ohms recom.
Maximum RPM	16000
Trigger Modes	5 window hall effect sensor
Injection Timing Resolution	1 microsecond to 65.535 millisecond
Communications	High Speed RS-232
Programming Platform	MS Windows98, 2000,
Throttle Position Sensor	3 wire universal
Coolant Temperature Sensor	GM type, 2700 ohm @ 25°C
Intake Air Temperature Sensor	GM type, 2700 ohm @ 25°C
Auxiliary Input	0 – 5 Volt dc
Manifold Pressure	1 to 2.65 bar provided in enclosure
Oxygen Sensor	1, 3 or 4 wire universal, for closed loop

Appendix J: Data Acquisition System Specifications

J.1 Thermocouple Specifications

Omega	K-Type, Model # KMQSS-010
Quick Disconnect Temperature Probes	Alcohol compatibility
Temperature Calibration Range	-270 to 1372°C (-454 to 2501°F)
EMF over Temperature Range	-6.458 to 54.886 mV
Yellow Lead (+) Material	Nickel-Chromium
Red Lead (-) Material	Nickel-Aluminum
Length	6 inches

J.2 In-cylinder Pressure Transducer Specifications

Kistler	Model # 6052A
Measuring Range	0 -250 bar
Sensitivity	19.2 pC/bar
Linearity	0.3 <= +/- %FSO
Serial Number	1073915

J.3 Charge Amplifier Specifications

Kistler	Model # 5004
Measurement Range	10 – 999000 pC
Scale Settings (1,2,3,4,5 sequence)	0.0002 – 10000000 MU / Volt
Sensor Sensitivity	0.01 – 9990 pC/MU 0.01 – 9990 mV/MU

Where MU: is mechanical unit (bar, psi, lb, g, etc.)

J.4 Rotary Encoder Specifications

Gurley Precision Instruments Inc.	Model # 9125S-03600H-5L01-C18SQ-06
Dimensions	2.5" dia. x 2.7" long body; 3/8" shaft dia.
Output communications	RS-422 differential line driver output
Resolution	3600 cycles per revolution

J.5 In-cylinder Pressure Calibration Sheet

201502 # 2
-ACC1

KISTLER

Kistler Instrumente AG Winterthur,
Switzerland

Eulachstrasse 22, PO Box 304, CH-8408 Winterthur
Telephone + 41 - 52 224 11 11
Telefax + 41 - 52 224 14 14
E-mail sales@kistler.ch
Internet www.kistler.com

KALIBRIERSCHEIN DRUCK

CALIBRATION CERTIFICATE PRESSURE

Typ	Type	6052A
Serien-Nr	Serial No	1073915
Betriebstemperaturbereich	Operating Temperature Range	°C -50 ... 350
Messbereich	Measuring Range	bar 0 ... 250
Hochtemperatur-Kalibrierung bei	High Temperature Calibration at	°C 200,250,300,350

Messungen		Measurements	
Kalibrierter Bereich / Calibrated Range	Empfindlichkeit / Sensitivity	Linearität / Linearity	
bar	µC/bar	≤ ± %FSO	
0 ... 250 (23°C)	-18,4	0,1	
0 ... 50 (23°C)	-18,4	0,1	
0 ... 250 (200°C)	-18,7	0,2	
0 ... 50 (200°C)	-18,7	0,1	
0 ... 250 (250°C)	-18,9	0,2	
0 ... 50 (250°C)	-18,8	0,1	
0 ... 250 (300°C)	-19,0	0,3	
0 ... 50 (300°C)	-18,9	0,4	
0 ... 250 (350°C)	-19,2	0,3	←
0 ... 50 (350°C)	-19,1	0,3	

Umgebungstemperatur	Ambient Temperature	°C 24 ±1
Relative Feuchte	Relative Humidity	% 46 ±5
Kalibriert durch	Calibrated by	E. Weniger
Datum	Date	28.11.00

Wir bestätigen, dass das oben identifizierte Gerät nach den vorgeschriebenen Verfahren geprüft wurde. Alle Messmittel sind auf nationale Normale rückverfolgbar, die Bezugsnormale über die von Kistler betriebene SCS (Swiss Calibration Service) Kalibrierstelle Nr. 049, akkreditiert nach EN 45001.

We confirm that the device identified above was tested by the prescribed procedures. All measuring devices are traceable to national standards, the reference standards through the SCS (Swiss Calibration Service) Calibration Laboratory No. 049, operated by Kistler and accredited per EN 45001.

Referenz Geräte	Reference Equipment	Typ / Type	Serien-Nr. / Serial No
Sensor (Gebrauchsnormale)	Sensor (Working Standard)	Kistler 7005	492692
Ladungsverstärker	Charge Amplifier	Kistler 5011A	333916
Leitwertschleifer	Charge Calibrator	Kistler 5306A1	530622

J.6 Data Acquisition Card Specifications

National Instruments	NI PCI-6071E
Type	High Speed Multi-function
Maximum Sampling Rate	1.25 Mega Samples/sec
Analog Channels	64
Digital Channels	32
Input Resolution	12 bits
Input Range	+/- 0.05 to +/- 10 V

J.7 Data Acquisition Speed Calculation

The sampling rate (\dot{N}_{card}) of the National Instruments PCI-6071-E DAQ is:

$$\dot{N}_{card} = 1.25 \times 10^6 \text{ samples / sec}, \quad (J.1)$$

The number of sensors ($N_{sensors}$) that require sampling is determined from 6 thermocouples, 1 in-cylinder pressure, 1 encoder and 1 air flow meter.

$$N_{sensors} = 9, \quad (J.2)$$

The available sampling rate (\dot{N}_{sensor}) per channel is determined using the following equation:

$$\dot{N}_{sensor} = \frac{\dot{N}_{card}}{N_{sensors}}, \quad (J.3)$$

$$\dot{N}_{sensor} = \frac{1.25 \times 10^6 \text{ samples / sec}}{9}, \quad (J.4)$$

$$\dot{N}_{sensor} = 138,888.8 \text{ samples / sec}, \quad (J.5)$$

Since there is a switching delay between channels, a maximum rate of approximately 90% of this value so \dot{N}_{sensor} becomes:

$$\dot{N}_{sensor} = 0.90 \times 138,888.8 \text{ samples / sec} = 125,000 \text{ samples/sec}, \quad (J.6)$$

Recall that the functional requirement of the DAQ system is an accuracy of 1/10 CAD at 2000 RPM. The required sampling rate ($\dot{N}_{required}$) required for this is determined from:

$$\omega = 2000 \text{ rpm} \cdot \frac{1 \text{ min}}{60 \text{ s}} = 33.3 \frac{\text{rot}}{\text{s}}, \quad (J.7)$$

where ω is the engine speed,

$$N_{datapoints} = 10 \frac{\text{pts}}{\text{CAD}} \cdot 360 \frac{\text{CAD}}{\text{rot}} = 3600, \quad (J.8)$$

where $N_{datapoints}$ is the number of data points per crank angle degree (CAD).

$$\dot{N}_{required} = \omega \cdot pts \text{ per rot} = 33.\bar{3} \cdot 3600 = 120,000 \frac{samples}{sec} \quad (J.9)$$

and $\dot{N}_{required}$ is the required sampling rate.

Since
$$\dot{N}_{required} \leq \dot{N}_{sensor} \quad (J.10)$$

Therefore, the National Instruments PCI-6071-E DAQ is adequately sized to perform the required function.

J.8 Terminal Box

Pin	Channel	Device	Pin	Channel	Device
0	AI Ground	Flowmeter Ground	28	P 0,5	DB 9 Pin 5
2	AI Ground	Encoder Ground	29	P 0,2	DB 9 Pin 6
3	AI 0	Cold-junction compensation signal	30	P 0,6	DB 9 Pin 7
4	AI 8		31	P 0,3	DB 9 Pin 8
5	AI 1	Thermocouple 1 (+ / -)	32	P 0,7	DB 9 Pin 9
6	AI 9	Thermocouple 2 (+ / -)	34	+ 5 V	Encoder Power
7	AI 2		51	AI 16	BNC Input 1 (+ / -)
8	AI 10	Thermocouple 3 (+ / -)	52	AI 24	
9	AI 3		Thermocouple 4 (+ / -)	53	AI 17
10	AI 11	Thermocouple 5 (+ / -)		54	AI 25
11	AI 4		Thermocouple 6 (+ / -)	55	AI 18
12	AI 12	Reserved for extra thermocouple		56	AI 26
13	AI 5		BNC Output 1	57	AI 19
14	AI 13	BNC Output 2		58	AI 27
15	AI 6		Ground for AO 0 & 1	59	AI 20
16	AI 14	DB 9 Pin 1		60	AI 28
17	AI 7		DB 9 Pin 2	61	AI 21
18	AI 15	DB 9 Pin 3		62	AI 29
20	AO 0		DB 9 Pin 4	63	AI 22
21	AO 1	Encoder channel A		64	AI 30
23	AO Ground		Encoder channel B	65	AI 23
24	D Ground	Encoder Index signal		66	AI 31
25	P 0,0			67	AI 32
26	P 0,4		69	AI 33	
27	P 0,1		71	AI 34	

Appendix K: Drive System Testing

K.1 Drive System Motoring and Emergency Braking

Objective: To verify the functionality of drive system in both motoring and emergency braking modes (performed on August 5, 2004).

K.2 Experimental Setup Motoring/Braking

Items needed: Stop watch

K.3 Procedure for Motoring without Engine Coupled

1. Remove coupler between AC motor and Kubota Engine.
2. Ensure safety guarding is installed correctly.
3. Ensure that both disconnects are in the OFF position.
4. Ensure that both disconnects have the appropriate fuses installed.
5. Connect cable for drive to 600V outlet on north wall of combustion lab.
6. Turn main 600 V disconnect to ON position using left hand and looking away.
7. Wait approximately 1 min to give auto-transformer chance to stabilize.
8. Turn secondary 480 V disconnect to ON position using left hand and looking away.
9. Ensure that no fault codes appear in the VSD display. At this point the VSD should be ON and is ready to start using.
10. Set the speed dial to approximately $\frac{1}{4}$ rotation.
11. For motoring without engine coupled simple turn on the VSD by pushing the green button, wait for shaft to begin rotating.
12. Make sure to give approximately 30 minutes of idling time at 17.0 (1000 RPM) to give the engine and fluids a chance to warm up.
13. Using the table below determine the input frequency for the VSD to attain the desired shaft speed. Starting with 9.0 and working your way up in 1.0 frequency increments to the maximum speed of the drive 3535 RPM.
14. For all tests record observations using the table below.
15. To turn off drive first slow engine gradually to lower than 14.0 then turn off using RED button.

K.4 Procedure for Motoring with Engine Coupled

1. Follow Procedure E.15 to ensure engine system checks have been performed.
2. Ensure coupler between AC motor and Kubota Engine is securely installed.
3. Ensure safety guarding is installed correctly.
4. Ensure that both disconnects are in the OFF position.
5. Ensure that both disconnects have the appropriate fuses installed.
6. Connect cable for drive to 600V outlet on north wall of combustion lab.
7. Turn main 600 V disconnect to ON position using left hand and looking away.
8. Wait approximately 1 min to give auto-transformer chance to stabilize.
9. Turn secondary 480 V disconnect to ON position using left hand and looking away.
10. Ensure that no fault codes appear in the VSD display. At this point the VSD should be ON and is ready to start using.
11. Set the speed dial to approximately $\frac{1}{4}$ rotation, 13.0.

12. For motoring with engine coupled turn on the VSD by pushing the green button, and then click starter on for 3 seconds, the starter will provide the starting torque required and the AC motor will take over once the starter has succeeded in turning the engine over. Wait for shaft to begin rotating then turn off starter. **DANGER: DO NOT RUN STARTER TOO LONG OR WHILE ENGINE IS RUNNING.**
13. Make sure to give approximately 30 minutes of idling time at 17.0 (1000RPM) to give the engine and fluids a chance to warm up.
14. Using the table below determine the input frequency for the VSD to attain the desired shaft speed.
15. Starting with 12.0 and working your way up in 1.0 frequency increments to the maximum speed of the drive 60.0 (3535) RPM.
16. For all tests record observations using the table below.
17. To turn off drive first slow engine gradually to lower than 14.0 then turn off using red STOP button.

K.5 Procedure for Emergency Braking with Engine Coupled

1. Follow Steps 1 to 14 from K.4.
2. Select desired speed and then when ready to begin emergency braking press red STOP button on VSD. The engine and AC motor will be brought to a complete stop very quickly.
3. For all tests record observations using the table below.

Frequency/Speed Table

Input Frequency (Hz)	Desired Speed (RPM)	Observations
9	530.25	
10	589.17	
11	648.08	
12	707.00	
13	765.92	
14	824.83	

K.6 Results Motoring without Engine Coupled

Input Frequency (Hz)	Desired Speed (RPM)	Observations
9	530.25	Functioning perfectly, no signs of distress.
10	589.17	Functioning perfectly, no signs of distress.
11	648.08	Functioning perfectly, no signs of distress.
12	707.00	Functioning perfectly, no signs of distress.
13	765.92	Functioning perfectly, no signs of distress.
14	824.83	Functioning perfectly, no signs of distress.
15	883.75	Functioning perfectly, no signs of distress.
16	942.67	Functioning perfectly, no signs of distress.
17	1001.58	Functioning perfectly, no signs of distress.
18	1060.50	Functioning perfectly, no signs of distress.
19	1119.42	Functioning perfectly, no signs of distress.
20	1178.33	Functioning perfectly, no signs of distress.
21	1237.25	Functioning perfectly, no signs of distress.
22	1296.17	Functioning perfectly, no signs of distress.
23	1355.08	Functioning perfectly, no signs of distress.
24	1414.00	Functioning perfectly, no signs of distress.
25	1472.92	Functioning perfectly, no signs of distress.
26	1531.83	Functioning perfectly, no signs of distress.
27	1590.75	Functioning perfectly, no signs of distress.
28	1649.67	Functioning perfectly, no signs of distress.
29	1708.58	Functioning perfectly, no signs of distress.
30	1767.50	Functioning perfectly, no signs of distress.

31	1826.42	Functioning perfectly, no signs of distress.
32	1885.33	Functioning perfectly, slight distress noticed.
33	1944.25	Functioning perfectly, slight distress noticed.
34	2003.17	Functioning perfectly, slight distress noticed.
35	2062.08	Functioning perfectly, slight distress noticed.
36	2121.00	Functioning perfectly, slight distress noticed.
37	2179.92	Functioning perfectly, slight distress noticed.
38	2238.83	Functioning well, vibration is noticed.
39	2297.75	Functioning well, vibration is noticed.
40	2356.67	Functioning well, vibration is noticed.
41	2415.58	Functioning well, vibration is noticed.
42	2474.50	Functioning well, vibration is noticed.
43	2533.42	Functioning well, vibration is noticed.
44	2592.33	Functioning well, vibration is noticed.
45	2651.25	Functioning well, vibration is noticed.
46	2710.17	Functioning well, vibration is noticed.
47	2769.08	Functioning well, vibration is noticed.
48	2828.00	Functioning well, vibration is noticed.
49	2886.92	Functioning well, vibration is noticed.
50	2945.83	Functioning well, vibration is noticed.
51	3004.75	Functioning well, vibration is noticed.
52	3063.67	Functioning well, vibration is noticed.
53	3122.58	Functioning well, vibration is noticed.
54	3181.50	Functioning well, vibration is noticed.
55	3240.42	Functioning well, vibration is noticed.
56	3299.33	Functioning well, vibration is noticed.
57	3358.25	Functioning well, vibration is noticed.
58	3417.17	Functioning well, vibration is noticed.
59	3476.08	Functioning well, vibration is noticed.
60	3535.00	Functioning well, vibration is noticed.

K.7 Results Motoring with Engine Coupled and with compression

Input Frequency (Hz)	Desired Speed (RPM)	Observations
9	530.25	Will not run. Severe vibration.
10	589.17	Will not run. Severe vibration.
11	648.08	Will not run. Severe vibration.
12	707.00	Functioning poorly, some vibration.
13	765.92	Functioning fair, some vibration.
14	824.83	Functioning fair, some vibration.
15	883.75	Functioning well, some vibration.
16	942.67	Functioning well, slight vibration.
17	1001.58	Functioning well, slight vibration.
18	1060.50	Functioning well, slight vibration.
19	1119.42	Functioning well, slight vibration.
20	1178.33	Functioning well, slight vibration.
21	1237.25	Functioning well, slight vibration.
22	1296.17	Functioning well, slight vibration.
23	1355.08	Functioning well, slight vibration.
24	1414.00	Functioning well, slight vibration.
25	1472.92	Functioning well, some vibration.
26	1531.83	Functioning well, some vibration.
27	1590.75	Functioning well, some vibration.
28	1649.67	Functioning well, some vibration.
29	1708.58	Functioning well, stronger vibration.
30	1767.50	Functioning well, stronger vibration. Noise level increased.
31	1826.42	Functioning well, stronger vibration. Noise level increased.
32	1885.33	Functioning well, stronger vibration. Noise level increased.
33	1944.25	Functioning well, stronger vibration. Noise level increased.
34	2003.17	Functioning well, stronger vibration. Noise level increased.
35	2062.08	Functioning well, stronger vibration. Noise level increased.
36	2121.00	Functioning well, stronger vibration. Noise level louder.
37	2179.92	Functioning well, stronger vibration. Noise level louder.
38	2238.83	Functioning well, stronger vibration. Noise level louder.
39	2297.75	Functioning well, stronger vibration. Noise level louder.
40	2356.67	Functioning well, heavy vibration. Noise level louder.
41	2415.58	Functioning well, heavy vibration. Noise level louder.
42	2474.50	Functioning well, heavy vibration. Noise level louder.

43	2533.42	Functioning well, heavy vibration. Noise level louder.
44	2592.33	Functioning well, heavy vibration. Noise level louder.
45	2651.25	Functioning well, heavy vibration. Noise level louder.
46	2710.17	Functioning well, heavy vibration. Noise level louder.
47	2769.08	Functioning well, heavy vibration. Noise level louder.
48	2828.00	Functioning well, heavy vibration. Noise level very loud.
49	2886.92	Functioning well, heavy vibration. Noise level very loud.
50	2945.83	Functioning well, heavy vibration. Noise level very loud.
51	3004.75	Functioning well, severe vibration. Noise level extremely loud.
52	3063.67	Noise too severe to continue.
53	3122.58	-
54	3181.50	-
55	3240.42	-
56	3299.33	-
57	3358.25	-
58	3417.17	-
59	3476.08	-
60	3535.00	-

K.8 Results for Braking with Engine Coupled.

Input Frequency (Hz)	Desired Speed (RPM)	Observations
12	707.00	Stopped perfectly, resistor banks not used. ½ sec
15	883.75	Stopped perfectly, resistor banks not used. ½ sec
20	1178.33	Stopped perfectly, resistor banks not used. ½ sec
25	1472.92	Stopped well, resistor banks used. 1 sec
30	1767.50	Stopped well, resistor banks used. 1 sec
35	2062.08	Stopped well, resistor banks used. 1.5 sec
40	2356.67	Stopped well, resistor banks used. 1.5 sec
45	2651.25	Stopped satisfactorily, resistor banks used. 2 sec
50	2945.83	Stopped satisfactorily, resistor banks used. 2 sec

Appendix L: Fuel and ECU System Testing

L.1 Fuel System Testing

Objective: To verify the functionality of fuel system components: Fuel pump operation, Regulator and fuel gauge operation, No leaks in system (performed on October 27, 2004).

L.2 Experimental Setup

Items needed:

Stop watch, 10 mm allen wrench, small adjustable wrench, 5 litres of ethanol

L.3 Procedure

1. Ensure all components, fittings and tighten properly.
2. Ensure 12 Volt electrical power is available to fuel pump via switch.
3. Pour 2 L of ethanol fuel into fuel tank.
4. Turn on fuel pump for 60 seconds to check function.
5. Check system for leaks and repair if necessary.
6. Check fuel pressure gauge and adjust pressure regulator until 45 psi is reached.
7. Check return line to ensure no blockage and fuel is returning to fuel tank.
8. At this point turn on fuel pump, you could turn on the ECU and fire the injector.
9. When completed simply turn off power switch to fuel pump.

CAUTION: TAKE APPROPRIATE PRECAUTIONS WHEN USING FLAMMABLE LIQUIDS.

L.4 Results

Component	Function Level	Observations
Fuel Pump	OK, Working Correctly	Initially no fuel pressure but once regulator screw was tightened pressure varied.
Fuel Fittings and Hoses	OK, No leaks	All fittings tightened properly, no leaks.
Fuel Regulator and Gauge	OK, Variable fuel pressure from 0 to 100 psi	Set at 45 psi, fuel pressure decreases as battery voltage decreases.
Fuel Tank	OK, No leaks	Holding fuel, no leaks
Fuel Injector	OK, Working Correctly, need calibration.	Injecting correctly, but need better clamping method to hold injector in place.

L.4 ECU System Testing

Objective: To verify the functionality of ECU system and calibrate the fuel injector, (performed on November, 18, 2004).

L.5 Experimental Setup

Items needed: Stop watch, weigh scale, small plastic bucket, 5 litres ethanol, 5 litres gasoline.

L.6 Procedure for running ECU

1. Perform engine systems check according to procedure in E.14.
2. Perform steps 2 through 10 of motoring procedure in K.4.
3. Check to make sure all loose items are put away, or fastened down to the apparatus fixture.
4. Turn on both exhaust fans to help ventilate the fumes.
5. Put on a pair of safety glasses and use hearing protection if necessary.
6. Turn on power to PC and load 883ECU program and click on monitor screen.
7. Turn on ECU power and ensure connection is established between ECU and computer.
8. Look over the monitor screen and ensure that all required sensor are responding and working correctly. Check:
 - a. Throttle position sensor (0 to 75%) depending on position.
 - b. Intake air temp (10 to 30°C).
 - c. Coolant temp (10 to 30°C initially and climbing as engine temp increases)
 - d. MAP pressure sensor (95 to 105 kPa).
 - e. Battery Voltage (12 to 14 volts).
 - f. Hall sensor (responds to changes in engine speed)
9. At this point you should be ready to motor the engine with fuel, but before you continue you need to select the correct fuel injector scalar for the equivalence ratio you want to run. This is dependant on the fuel type and equivalence ratio and engine RPM. Experiments to determine the injector scalar were performed and the procedure and results are available below. Once the correct injector scalar value has been inputted into the basic mapping window, you are ready to begin motoring the engine and injecting fuel. Follow procedure K.4 steps 10 through 14 to begin motoring the engine.
10. Follow the fuel system procedure steps 1 through 9 as appropriate.
11. Set the throttle position at 65% and set to desired engine speed in RPM. You should be able to here the injector ticking which means it is injecting fuel at the prescribed equivalence ratio and hence pulse width. Note that it is best to initially run the injector outside the intake manifold into a bucket to verify spray pattern.
12. Before combustion can be achieved the data acquisition system needs to be operating, to determine the airflow rate and ensure intake and coolant temperatures are adequate and recorded. Further detail is available in Appendix N.
13. To stop injecting fuel, simply turn off the fuel pump switch.

L.7 Results for ECU Functional Test

Component	Function Level	Observations
Throttle Position Sensor	OK, Working	Varies from 1 – 75 %
Intake Air Temp. Sensor	OK, Working	Responds to changes in air temp. -10 –100 °C
Coolant Temp. Sensor	OK, Working	Responds to changes in coolant temp. (0 – 90°C)
MAP sensor	OK, Working	Responds to changes in manifold pressure. (95 – 105 kPa)

Battery Voltage Indicator	OK, Working	Voltage is read accurately.
Hall Sensor	OK, Working	Responds to cam trigger, but has a glitch in signal. Injector responds to hall sensor by ticking.

L.8 Procedure for Determining Injector Scalar

1. Follow steps 1 through 8 of procedure L.6 as appropriate.
2. Remove injector with lines and regulator from injection port of intake.
3. Turn on weigh scale, zero, clean bucket and place plastic bucket on weigh scale and zero.
4. Place bucket on top of table top and place injector assembly over bucket and secure.
5. At this point you should be ready to motor the engine with fuel but without compression (it is best to remove the VCR secondary piston since no combustion is desired.)
6. Before you continue you need to input the mass of mixture, dynamic flowrate of the injector and the engine speed desired into Fuel System Design Calcs2.xls in order to calculate the theoretical injector pulse width required.
 - a. The program calculates the mass of fuel injected after 4 min of running at the desired engine speed and throttle position of 65% and fuel pressure of 45 psi.
 - b. Four equivalence ratios are selected to perform sample test (0.35, 0.50, 0.70 and 0.85.)
7. Using the Basic Mapping window of the 883ECU, by trial and error input the injector scalar value and adjust this value until the pulse width displayed in the window matches the value calculated in the spreadsheet. This scalar value is entered into the spreadsheet as the initial guess scalar.
8. Now the engine is motored at the desired engine speed, and the fuel pump and injector can be turned on.
9. Using the stopwatch ensure the injector operates and sprays into the plastic container for 4 minutes, and then turn off the injector and pump.
10. Place plastic bucket on weigh scale and measure the mass of fuel in grams.
11. Enter the mass of fuel into the spreadsheet under initial fuel mass. The program calculates the ratio between the theoretical mass of fuel and initial mass of fuel, and this ratio is multiplied by the initial guess scalar to determine the actual scalar.
12. Enter the required scalar into the basic mapping window and repeat the test again.
13. Record the final mass of fuel in the spreadsheet and compare to theoretical amount of fuel. These two values should be very close (within 1 gram) repeat if necessary.
14. Repeat these steps for the other equivalence ratios and engine speeds of 625, 1000, 1500, and 2000 RPM. These results are interpolated and extrapolated to provide fuelling information from 625 to 3000 RPM.

L.9 Results for scalar calibration 625 RPM

Mmix 0.35977564 g Dyn. Flowrate 2.1804 g/s
 Engine Speed 625 RPM
 * Note: all calculations are performed at Cycle Time 192 ms
 wide-open throttle (though TPS shows assuming VSD is correct measurement for RPM
 65%). Fuel Pressure 45 psi

Phi	Ethanol		Theoretical	Initial Guess Scalar	Initial Fuel mass (g)	Ratio	Required Scalar	Final Fuel (g)
	Mfuel (mg)	Pulse Width (ms)	Fuel after 4 min (g)					
0.10	3.61	1.66	4.52				5.19	
0.15	5.42	2.49	6.77				6.61	
0.20	7.23	3.31	9.03				8.03	
0.25	9.03	4.14	11.29				9.45	
0.30	10.84	4.97	13.55				10.87	
0.35	12.65	5.80	15.81	10.80	14	1.1291	12.19	16.00
0.40	14.45	6.63	18.07				13.71	
0.45	16.26	7.46	20.32				15.13	
0.50	18.07	8.29	22.58	15.80	21	1.0753	16.78	23.00
0.55	19.87	9.11	24.84				17.97	
0.60	21.68	9.94	27.10				19.39	
0.65	23.49	10.77	29.36				20.81	
0.70	25.29	11.60	31.62	21.80	31	1.0198	22.03	30.00
0.75	27.10	12.43	33.87				23.65	
0.80	28.91	13.26	36.13				25.07	
0.85	30.71	14.09	38.39	26.30	38	1.0102	26.87	36.00
0.90	32.52	14.91	40.65				27.92	
0.95	34.33	15.74	42.91				29.34	
1.00	36.13	16.57	45.17				30.76	

L.10 Results for scalar calibration 1000 RPM

Mmix 0.35977564 g Dyn. Flowrate 2.1804 g/s
 Engine Speed 1000 RPM
 * Note: all calculations are performed at Cycle Time 120 ms
 wide-open throttle (though TPS shows
 65%).

Phi	Ethanol		Theoretical	Initial Guess Scalar	Initial Fuel mass (g)	Ratio	Required Scalar	Final Fuel (g)
	Mfuel (mg)	Pulse Width (ms)	Fuel after 4 min (g)					
0.10	3.61	1.66	7.23				3.44	
0.15	5.42	2.49	10.84				4.72	
0.20	7.23	3.31	14.45	5.41	13	1.111783	6.01	15
0.25	9.03	4.14	18.07				7.28	
0.30	10.84	4.97	21.68				8.56	

0.35	12.65	5.80	25.29	12.19	31	0.815905	9.95	25
0.40	14.45	6.63	28.91				11.12	
0.45	16.26	7.46	32.52				12.40	
0.50	18.07	8.29	36.13	16.78	44	0.821203	13.78	35
0.55	19.87	9.11	39.75				14.97	
0.60	21.68	9.94	43.36				16.25	
0.65	23.49	10.77	46.97				17.53	
0.70	25.29	11.60	50.59	22.03	59	0.857392	18.89	50
0.75	27.10	12.43	54.20				20.09	
0.80	28.91	13.26	57.81				21.37	
0.85	30.71	14.09	61.43	26.57	72	0.853139	22.67	62
0.90	32.52	14.91	65.04				23.94	
0.95	34.33	15.74	68.65				25.22	
1.00	36.13	16.57	72.27				26.50	

L.11 Results for scalar calibration 1500 RPM

Mmix 0.359775641 g Dyn. Flowrate Engine Speed 2.1804 g/s 1500 RPM

* Note: all calculations are performed at wide-open throttle (though TPS shows 65%).

Cycle Time 80 ms

Phi	Ethanol		Theoretical	Initial Guess Scalar	Initial Fuel mass (g)	Ratio	Required Scalar	Final Fuel (g)
	Mfuel (mg)	Pulse Width (ms)	Fuel after 4 min (g)					
0.10	3.61	1.66	10.84				2.88	
0.15	5.42	2.49	16.26				4.16	
0.20	7.23	3.31	21.68	6.00	27	0.802954	4.82	22
0.25	9.03	4.14	27.10				6.72	
0.30	10.84	4.97	32.52				8.00	
0.35	12.65	5.80	37.94	12.20	48	0.790408	9.64	39
0.40	14.45	6.63	43.36				10.56	
0.45	16.26	7.46	48.78				11.84	
0.50	18.07	8.29	54.20	15.00	61	0.888615	13.33	53
0.55	19.87	9.11	59.62				14.41	
0.60	21.68	9.94	65.04				15.69	
0.65	23.49	10.77	70.46				16.97	
0.70	25.29	11.60	75.88	18.00	75	1.011722	18.21	76
0.75	27.10	12.43	81.30				19.53	
0.80	28.91	13.26	86.72				20.81	
0.85	30.71	14.09	92.14	21.00	89	1.03527	21.74	92
0.90	32.52	14.91	97.56				23.38	
0.95	34.33	15.74	102.98				24.66	
1.00	36.13	16.57	108.40				25.94	

L.12 Results for scalar calibration 2000 RPM

Mmix 0.359775641 g Dyn. Flowrate 2.1804 g/s
 Engine Speed 2000 RPM

* Note: all calculations are performed at Cycle Time 60 ms wide-open throttle (though TPS shows 65%).

Phi	Ethanol		Theoretical	Initial Guess Scalar	Initial Fuel mass (g)	Ratio	Required Scalar	Final Fuel (g)
	Mfuel (mg)	Pulse Width (ms)	Fuel after 4 min (g)					
0.10	3.61	1.66	14.45				2.35	
0.15	5.42	2.49	21.68				3.61	
0.20	7.23	3.31	28.91	4.45	27	1.070606	4.76	29
0.25	9.03	4.14	36.13				6.14	
0.30	10.84	4.97	43.36				7.41	
0.35	12.65	5.80	50.59	9.64	57	0.887476	8.56	51
0.40	14.45	6.63	57.81				9.94	
0.45	16.26	7.46	65.04				11.20	
0.50	18.07	8.29	72.27	13.78	79	0.914758	12.61	72
0.55	19.87	9.11	79.49				13.73	
0.60	21.68	9.94	86.72				15.00	
0.65	23.49	10.77	93.95				16.26	
0.70	25.29	11.60	101.17	18.00	105	0.963545	17.34	100
0.75	27.10	12.43	108.40				18.79	
0.80	28.91	13.26	115.63				20.06	
0.85	30.71	14.09	122.85	21.75	125	0.982816	21.38	123
0.90	32.52	14.91	130.08				22.59	
0.95	34.33	15.74	137.31				23.86	
1.00	36.13	16.57	144.53				25.12	

L.13 Summary of Results for scalar calibration 625 - 3000 RPM

Phi	Measured Scalar Values				Extrapolated Scalar	
	RPM					
	625	1000	1500	2000	2500	3000
0.10	5.19	3.44	2.88	2.35	1.80	1.25
0.15	6.61	4.72	4.16	3.61	3.06	2.51
0.20	8.03	6.01	4.82	4.76	3.95	3.32
0.25	9.45	7.28	6.72	6.14	5.58	5.01
0.30	10.87	8.56	8.00	7.41	6.84	6.26
0.35	12.19	9.95	9.64	8.56	7.99	7.30
0.40	13.71	11.12	10.56	9.94	9.36	8.77
0.45	15.13	12.40	11.84	11.20	10.62	10.02
0.50	16.78	13.78	13.33	12.61	12.06	11.48
0.55	17.97	14.97	14.41	13.73	13.14	12.52
0.60	19.39	16.25	15.69	15.00	14.40	13.77
0.65	20.81	17.53	16.97	16.26	15.66	15.02
0.70	22.03	18.89	18.21	17.34	16.60	15.83
0.75	23.65	20.09	19.53	18.79	18.18	17.53
0.80	25.07	21.37	20.81	20.06	19.44	18.78
0.85	26.57	22.67	21.74	21.38	20.64	19.99
0.90	27.92	23.94	23.38	22.59	21.96	21.28
0.95	29.34	25.22	24.66	23.86	23.22	22.54
1.00	30.76	26.50	25.94	25.12	24.48	23.79

Appendix M: Intake System Testing

M.1 Intake Air Flow Testing

The following verification experiment was performed on November 26, 2004.

Objective: To verify the functionality of intake system by performing experiments using the airflow meter and ensuring no leaks in system.

M.2 Procedure

1. Ensure all components and fittings of the intake system are tightened properly.
2. Follow engine testing procedure in Appendix E.15.
3. Follow drive system start-up procedure steps 1 to 14 in Appendix K.4.
4. Connect power to 24 Volt flow meter power supply.
5. Start PC and load Labview 7.1 software and open Research Engine Data Acquisition.
6. Load the 883ECU program and open the monitor screen. Ensure the throttle position sensor is set at 70 %.
7. Scroll down to Flow Meter output screen and observe output on screen.
8. Record output when changing engine speed using table below.
9. When completed simply turn off VSD to stop the engine.

Throttle Position:		Single Cylinder		
		70.00%	CORRECTED	
RPM	Cycle Time (s)	Volumetric flowrate (cfm)	Volumetric flowrate (cfm)	Vol. Eff., %
0		-0.8		
800	0.150			
1000	0.120			
1500	0.080			
2000	0.060			
2500	0.048			
3000	0.040			

M.3 Calculations

Corrected Volumetric Flowrate = Actual Volumetric Flow rate – (Actual Volumetric Flowrate at 0 RPM). (L.1)

$$\text{Volumetric Efficiency: } \eta_v = \frac{2\dot{m}_a}{\rho_{air} V_d N} \quad (L.2)$$

$$\text{Heat Transfer Rate to the Air from Heater: } Q_{HT} = \dot{m}_a C_p \Delta T \quad (L.3)$$

M.4 Results

Engine Displacement	898	cc
Cylinder Displacement	299.333	cc
Clearance Volume	20	cc
Cylinder Volume	319.333	cc
Density of Air	1.20192	kg/m ³

THEORETICAL:

		Single Cylinder			
RPM	Cycle Time (s)	Volumetric flowrate (cc/m)	Volumetric flowrate (L/s)	Volumetric flowrate (cfm)	Mass flowrate of Air (kg/s)
800	0.150	119733	1.9956	4.2294	0.0400
1000	0.120	149667	2.4944	5.2867	0.0500
1500	0.080	224500	3.7417	7.9301	0.0750
2000	0.060	299333	4.9889	10.5734	0.0999
2500	0.048	374167	6.2361	13.2168	0.1249
3000	0.040	449000	7.4833	15.8601	0.1499

ACTUAL:

		Single Cylinder			
		70.00%	CORRECTED		
RPM	Cycle Time (s)	Volumetric flowrate (cfm)	Volumetric flowrate (cfm)	Volumetric flowrate (L/s)	Vol. Eff., %
0		-0.8			
800	0.150	3.3000	4.1000	1.9345	96.9413%
1000	0.120	4.2000	5.0000	2.3592	94.5768%
1500	0.080	6.3000	7.1000	3.3500	89.5327%
2000	0.060	8.8500	9.6500	4.5532	91.2666%
2500	0.048	10.8500	11.6500	5.4969	88.1456%
3000	0.040	11.5000	12.3000	5.8036	77.5530%

M.5 Intake Air Preheater Testing

The following verification experiment was performed on November 29, 2004.

Objective: To verify the functionality of intake air preheater system by performing experiments using the preheater and preheater controller.

Items Needed: Stopwatch

M.6 Procedure

1. Ensure all components, and fittings in the intake system are tightened properly.
2. Follow engine testing procedure in Appendix E.15.
3. Follow drive system start-up procedure steps 1 to 14 in Appendix K.4.
4. Ensure Preheater Disconnect on North East corner of Combustion lab is in the OFF position and that the laser disconnect is also in the OFF position.
5. Connect power to 240 Volt preheater wall plug. (Located on north wall of combustion lab.)
6. Start PC and load Labview 7.1 software and open Research Engine Data Acquisition and begin running program.
7. Load the 883ECU program and open the monitor screen. Ensure the throttle position sensor is set at 70 %.
8. Scroll down to temperature output screen and observe output on screen.
9. Review Operation Manual for Omega Preheater Controller and follow procedures for setting temperature set points and operation.
10. Begin running engine and turn on exhaust fan. Engine must be running while preheater is running to prevent burn up of heater element.
11. Install heater tape on intake manifold and turn ON and allow intake piping to heat up.
12. Turn ON preheater disconnect, and then turn ON preheater controller. At this point the preheater controller is ready to be set and the preheater will turn on once the controller has been set.
13. Ensure that temperature set points are not more than 50 °C higher than the air temperature before the intake valve. Only small gains should be made and temperature ramp-up needs to give enough time for temperature soaking of intake manifold.
14. The temperature set-points are (50 °C, 100 °C, 150 °C, 200 °C). Starting at 50°C vary the engine speed from 625, 1000, 1500 to 2000 RPM. Ensure that temperature reaches equilibrium before making final reading.
15. Record output from screen when changing engine speed using table below.
16. When completed simply turn off heater controller, turn OFF heater disconnect and turn off VSD to stop the engine.

Set Point	Experiment #1			
	50 °C		100 °C	
	Heater Exit Temp (°C)	Heater Tape Setting (%)	Heater Exit Temp	Heater Tape Setting
RPM				
625				
1000				
1500				
2000				

M.7 Results

Experiment One: Heater tape installed without insulation

Set Point		Experiment #1				
		50°C			100°C	
RPM	Heater Exit Temp (°C)	Heater Tape Setting (%)	Calculated Heater Transferred (W)	Heater Exit Temp	Heater Tape Setting	Calculated Heater Transferred (W)
625	50	15	71.25	148	25	282.82
1000	50.5	18	115.72	156	28	480.15
1500	51.3	25	177.73	152	30	699.50
2000	54	25	255.62	142	25	863.58

Experiment Two: Heater tape installed with insulation

Set Point		100°C			150°C		
RPM	Heater Exit Temp	Heater Tape Setting	Calculated Heater Power (W)	Heater Exit Temp	Heater Tape Setting	Calculated Heater Power (W)	
625	109	20	198.62	191	25	375.66	
1000	116	20	341.98	192	25	604.51	
1500	119	20	528.51	206	25	979.30	
2000	114	20	670.14	185	25	1160.65	

Set Point		200°C			250°C		
RPM	Heater Exit Temp	Heater Tape Setting	Calculated Heater Power (W)	Heater Exit Temp	Heater Tape Setting	Calculated Heater Power (W)	
625	314	35	641.21	420	35	870.06	
1000	278	35	901.58	370	35	1219.38	
1500	318	35	1559.63	400	35	1984.51	
2000	270	35	1747.89	280	35	1816.98	

Appendix N: HCCI Gasoline Combustion Experiments

N.1 HCCI gasoline combustion experiment

The following verification experiment was performed on February 16-18, 2005.

Objective: To verify the functionality of the research engine system by performing HCCI combustion verification experiments.

N.2 Procedure

1. Ensure all components, and fittings in the intake system are tightened properly.
2. Follow engine testing procedure in Appendix E.15.
3. Follow drive system start-up procedure steps 1 to 14 in Appendix K.4.
4. Perform gasoline injector scalar calibration experiments using the procedure in Appendix L.8, except ensure values are for gasoline rather than ethanol.
5. Connect power to 24 Volt flow meter power supply.
6. Start PC and load Labview 7.1 software and open Research Engine Data Acquisition.vi and begin running program.
7. Load the 883ECU program and open the monitor screen. Ensure the throttle position sensor is set at 70 %.
8. Scroll down to Flow Meter output screen and observe output on screen.
9. Before combustion can begin, heater tape must be set to 40 % and be heating the intake manifold for 30 minutes. Engine temperature must be at least 30°C preferably 40°C. Battery must be fully charged and charger should be plugged in.
10. The initial engine speed will be 750 RPM. Using this engine speed and injector scalar summary chart, select an appropriate equivalence ratio, and then read scalar value and enter into 883ECU program. Note: Richer mixtures tend to ignite more readily than leaner mixtures, therefore start with a richer mixture like $\Phi=0.8$ and get the engine to ignite, then be prepared to lean out the mixture quickly, as HCCI mode has a tendency to run off, and severe knocking can occur, which will damage the engine. If engine noise becomes severe or system failure is observed, turn off fuel pump to shut of fuel injector and pump simultaneously.
11. Once HCCI has been achieved lean-out fuel mixture to 0.3 slowly and you should be able to get steady HCCI at that engine speed.
12. Acquire data once HCCI is steady, for 10 seconds at a time. Use in-cylinder pressure screen to ensure you have HCCI combustion before you begin acquiring data. Keep in mind the data acquisition rate is quite fast, and the file sizes can get enormous if the system is left on for longer than 10 seconds.
13. When completed simply turn off the fuel, VSD to stop the engine.
14. Post-processing of the raw data file will be required. The binary file will need to be converted to a text file using Convert Binary to Text program.

15. MS Excel is used to import the text data files created using “Convert Binary to Text.VI” into a standard .XLS file.
16. Up to 15 files may be imported at once. Fill in the bordered cells as appropriate and click the IMPORT button.
17. Once the data is imported into Excel, any desired post-processing can be performed easily.
18. Obtain a representative sample of the HCCI combustion event and perform analysis and construct graphs. P-V diagram, P-CAD, and perform calculations to determine indicated power.

$$W_{c,i} = \frac{(v_1 - v_2) [p_1 + 4(p_1 + p_2) + p_2]}{6 \cdot 10}$$

Engine Speed	3000	RPM
Compression		
Work	341.43	Nm
Expansion Work	393.7736	Nm
Indicated Work	52.35	Nm
Indicated Power	3925.99	W
Indicated Power	5.264838	HP

N.4 Results

UPR Prss (bar)	PRC Press (bar)	CA	CAD	Indicated Work	volume
-3.72	7.80	297.93	-82.07	#REF!	129.99
-8.79	2.70	298.02	-81.98	0.043387	129.77
-3.72	7.80	298.10	-81.90	0.043387	129.58
-3.72	7.80	298.18	-81.82	0.064461	129.34
-3.72	7.80	298.26	-81.74	0.06446	129.13
-3.60	7.90	298.35	-81.65	0.064874	128.91
-3.42	8.10	298.43	-81.57	0.068114	128.70
-3.54	8.00	298.51	-81.49	0.068528	128.49
-3.42	8.10	298.60	-81.40	0.068527	128.27
-3.60	7.90	298.68	-81.32	0.068113	128.06
-3.54	8.00	298.76	-81.24	0.065724	127.84
-3.54	8.00	298.84	-81.16	0.068114	127.63
-3.05	8.40	298.93	-81.07	0.067768	127.41
-3.36	8.10	299.01	-80.99	0.068179	127.20
-3.42	8.10	299.09	-80.91	0.06694	126.98
-3.42	8.10	299.17	-80.83	0.066939	126.77
-3.17	8.30	299.26	-80.74	0.067766	126.56
-3.30	8.20	299.34	-80.66	0.06818	126.34
-3.23	8.30	299.42	-80.58	0.068179	126.13
-3.36	8.10	299.50	-80.50	0.067766	125.91
-3.42	8.10	299.59	-80.41	0.068964	125.70
-3.78	7.70	299.67	-80.33	0.065287	125.49
-3.42	8.10	299.75	-80.25	0.065286	125.27
-2.99	8.50	299.83	-80.17	0.068593	125.06
-2.81	8.70	299.92	-80.08	0.071071	124.85
-2.99	8.50	300.00	-80.00	0.071072	124.63
-3.42	8.10	300.08	-59.92	0.068593	124.42
-2.93	8.60	300.17	-59.83	0.069005	124.21
-2.93	8.60	300.25	-59.75	0.071072	123.99
-2.99	8.50	300.33	-59.67	0.070658	123.78
-3.17	8.30	300.41	-59.59	0.069419	123.57
-3.05	8.40	300.50	-59.50	0.069031	123.35
-2.93	8.60	300.58	-59.42	0.070246	123.14
-2.75	8.80	300.66	-59.34	0.071898	122.93
-2.99	8.50	300.74	-59.26	0.071485	122.71
-2.93	8.60	300.83	-59.17	0.070659	122.50
-2.75	8.80	300.91	-59.09	0.071898	122.29
-2.93	8.60	300.99	-59.01	0.071899	122.08
-2.69	8.80	301.07	-58.93	0.071898	121.86
-2.69	8.80	301.16	-58.84	0.072725	121.65
-2.58	8.90	301.24	-58.76	0.073138	121.44

-2.62	8.90	301.32	-58.68	0.073578	121.23
-2.56	8.90	301.40	-58.60	0.07355	121.01
-2.50	9.00	301.49	-58.51	0.073965	120.80
-2.44	9.10	301.57	-58.43	0.07479	120.59
-2.82	8.90	301.65	-58.35	0.074378	120.38
-2.75	8.80	301.74	-58.26	0.073138	120.17
-2.62	8.90	301.82	-58.18	0.073137	119.95
-2.32	9.20	301.90	-58.10	0.074791	119.74
-2.81	8.70	301.98	-58.02	0.073964	119.53
-1.77	9.70	302.07	-57.93	0.076031	119.32
-2.14	9.40	302.15	-57.85	0.076952	119.11
-2.32	9.20	302.23	-57.77	0.076857	118.90
-2.38	9.10	302.31	-57.69	0.075617	118.68
-2.20	9.30	302.40	-57.60	0.076031	118.47
-2.44	9.10	302.48	-57.52	0.076031	118.26
-2.08	9.40	302.56	-57.44	0.076443	118.05
-2.20	9.30	302.64	-57.36	0.07727	117.84
-2.20	9.30	302.73	-57.27	0.076856	117.63
-2.14	9.40	302.81	-57.19	0.07727	117.42
-1.89	9.60	302.89	-57.11	0.07851	117.21
-2.01	9.50	302.98	-57.02	0.078952	117.00
-1.89	9.60	303.06	-56.94	0.078922	116.79
-1.95	9.50	303.14	-56.86	0.078923	116.58
-1.77	9.70	303.22	-56.78	0.079336	116.37
-1.89	9.60	303.31	-56.69	0.079749	116.16
-1.95	9.50	303.39	-56.61	0.078923	115.95
-1.89	9.60	303.47	-56.53	0.078922	115.74
-1.71	9.80	303.55	-56.45	0.080163	115.53
-2.38	9.10	303.64	-56.36	0.078097	115.32
-1.59	9.90	303.72	-56.28	0.078509	115.11
-1.71	9.80	303.80	-56.20	0.081432	114.90
-1.59	9.90	303.88	-56.12	0.081402	114.69
-1.59	9.90	303.97	-56.03	0.081815	114.48
-1.40	10.10	304.05	-55.95	0.082642	114.27
-1.34	10.20	304.13	-55.87	0.083882	114.06
-1.28	10.20	304.21	-55.79	0.084294	113.85
-1.22	10.30	304.30	-55.70	0.084708	113.64
-1.28	10.20	304.38	-55.62	0.084707	113.43
-1.40	10.10	304.46	-55.54	0.083882	113.22
-1.40	10.10	304.55	-55.45	0.083498	113.01
-1.40	10.10	304.63	-55.37	0.083499	112.81
-1.53	10.00	304.71	-55.29	0.083054	112.60
-1.10	10.40	304.79	-55.21	0.084295	112.39
-1.28	10.20	304.88	-55.12	0.085121	112.18
-1.10	10.40	304.96	-55.04	0.08512	111.97
-1.10	10.40	305.04	-54.96	0.085948	111.76
-1.04	10.50	305.12	-54.88	0.08638	111.55
-0.18	11.30	305.21	-54.79	0.09008	111.35
-0.98	10.50	305.29	-54.71	0.09008	111.14
-0.98	10.50	305.37	-54.63	0.086773	110.93
-1.04	10.50	305.45	-54.55	0.086806	110.72
-0.92	10.60	305.54	-54.46	0.087187	110.52
-0.85	10.80	305.62	-54.38	0.087601	110.31
-0.73	10.80	305.70	-54.30	0.088428	110.10
-0.73	10.80	305.79	-54.21	0.089253	109.90
-0.87	10.80	305.87	-54.13	0.089252	109.69
-0.73	10.80	305.95	-54.05	0.089253	109.48
-0.67	10.80	306.03	-53.97	0.089253	109.27
-0.55	11.00	306.12	-53.88	0.090079	109.07
-0.87	10.80	306.20	-53.80	0.09008	108.86
-0.81	10.90	306.28	-53.72	0.089699	108.65
-0.55	11.00	306.36	-53.64	0.090492	108.45
-0.55	11.00	306.45	-53.55	0.090906	108.24
-0.43	11.10	306.53	-53.47	0.091319	108.04
-0.37	11.10	306.61	-53.39	0.091732	107.83
-0.43	11.10	306.69	-53.31	0.091733	107.62
-0.43	11.10	306.78	-53.22	0.091732	107.42
-0.18	11.30	306.86	-53.14	0.092559	107.21
-2.99	8.50	306.94	-53.06	0.081816	107.01
-0.81	10.90	307.02	-52.98	0.080162	106.80
-0.12	11.40	307.11	-52.89	0.092179	106.60
-0.18	11.30	307.19	-52.81	0.093799	106.39
0.24	11.70	307.27	-52.73	0.095038	106.18
0.00	11.50	307.36	-52.64	0.095984	105.98
0.00	11.50	307.44	-52.56	0.095038	105.78
0.12	11.60	307.52	-52.48	0.09545	105.57
0.24	11.70	307.60	-52.40	0.096278	105.37
0.12	11.60	307.69	-52.31	0.096278	105.16
0.06	11.60	307.77	-52.23	0.095984	104.96
0.31	11.80	307.85	-52.15	0.096891	104.75
0.31	11.80	307.93	-52.07	0.097553	104.55
0.37	11.90	308.02	-51.98	0.097931	104.34
0.49	12.00	308.10	-51.90	0.098756	104.14
0.31	11.80	308.18	-51.82	0.098344	103.94
0.49	12.00	308.26	-51.74	0.098343	103.73
0.79	12.30	308.35	-51.65	0.10041	103.53
0.55	12.00	308.43	-51.57	0.10041	103.33
0.73	12.20	308.51	-51.49	0.099996	103.12
0.55	12.00	308.60	-51.40	0.099997	102.92
0.73	12.20	308.68	-51.32	0.099996	102.72

0.73	12.20	308.76	-51.24	0.10088	102.51
0.24	11.70	308.84	-51.16	0.098757	102.31
0.79	12.30	308.93	-51.07	0.09917	102.11
0.85	12.40	309.01	-50.99	0.102062	101.91
1.22	12.70	309.09	-50.91	0.103716	101.70
0.73	12.20	309.17	-50.83	0.102888	101.50
1.22	12.70	309.26	-50.74	0.102889	101.30
1.10	12.60	309.34	-50.66	0.104542	101.10
1.77	13.30	309.42	-50.58	0.10702	100.90
1.16	12.70	309.50	-50.50	0.107435	100.69
1.28	12.80	309.59	-50.41	0.105407	100.49
1.22	12.70	309.67	-50.33	0.105389	100.29
1.34	12.80	309.75	-50.25	0.105367	100.09
1.28	12.80	309.83	-50.17	0.105782	99.89
1.40	12.90	309.92	-50.08	0.106194	99.69
1.46	13.00	310.00	-50.00	0.107021	99.49
1.59	13.10	310.08	-49.92	0.107848	99.29
1.65	13.10	310.17	-49.83	0.10826	99.08
1.59	13.10	310.25	-49.75	0.108261	98.88
1.65	13.10	310.33	-49.67	0.10826	98.68
1.77	13.30	310.41	-49.59	0.109087	98.48
1.89	13.40	310.50	-49.50	0.110367	98.28
1.89	13.40	310.58	-49.42	0.11074	98.08
1.71	13.20	310.66	-49.34	0.109913	97.88
1.83	13.30	310.74	-49.26	0.109501	97.68
1.83	13.30	310.83	-49.17	0.109914	97.49
2.01	13.50	310.91	-49.09	0.110739	97.29
2.01	13.50	310.99	-49.01	0.111567	97.09
2.01	13.50	311.07	-48.93	0.111565	96.89
2.20	13.70	311.16	-48.84	0.112393	96.69
2.08	13.60	311.24	-48.76	0.112806	96.49
2.32	13.80	311.32	-48.68	0.113261	96.29
2.20	13.70	311.40	-48.60	0.113831	96.09
2.38	13.90	311.49	-48.51	0.114046	95.89
2.38	13.90	311.57	-48.43	0.114871	95.70
1.95	13.50	311.65	-48.35	0.11322	95.50
3.23	14.70	311.74	-48.26	0.116525	95.30
2.58	14.10	311.82	-48.18	0.119003	95.10
2.75	14.20	311.90	-48.10	0.118938	94.91
2.01	13.50	311.98	-48.02	0.114458	94.71
2.62	14.10	312.07	-47.93	0.114046	94.51
2.93	14.40	312.15	-47.85	0.117808	94.31
2.62	14.10	312.23	-47.77	0.117765	94.12
2.93	14.40	312.31	-47.69	0.117783	93.92
2.87	14.40	312.40	-47.60	0.119004	93.72
2.99	14.50	312.48	-47.52	0.119418	93.53
3.17	14.70	312.56	-47.44	0.120656	93.33
3.23	14.70	312.64	-47.36	0.121484	93.13
3.30	14.80	312.73	-47.27	0.121895	92.94
3.17	14.70	312.81	-47.19	0.121897	92.74
3.23	14.70	312.89	-47.11	0.121484	92.55
3.72	15.20	312.98	-47.02	0.123595	92.35
3.54	15.00	313.06	-46.94	0.124788	92.16
3.48	15.00	313.14	-46.86	0.123963	91.96
3.38	14.90	313.22	-46.78	0.12355	91.77
3.54	15.00	313.31	-46.69	0.123548	91.57
3.60	15.10	313.39	-46.61	0.124376	91.38
3.66	15.20	313.47	-46.53	0.125201	91.18
4.03	15.50	313.55	-46.45	0.126855	90.99
3.72	15.20	313.64	-46.36	0.126855	90.79
3.85	15.30	313.72	-46.28	0.126028	90.60
3.78	15.30	313.80	-46.20	0.126488	90.40
3.91	15.40	313.88	-46.12	0.126855	90.21
3.97	15.50	313.97	-46.03	0.12768	90.02
4.21	15.70	314.05	-45.95	0.128922	89.82
3.66	15.20	314.13	-45.87	0.127682	89.63
4.09	15.60	314.21	-45.79	0.127267	89.44
4.21	15.70	314.30	-45.70	0.129335	89.24
4.21	15.70	314.38	-45.62	0.129746	89.05
4.39	15.90	314.46	-45.54	0.130574	88.86
4.82	16.30	314.55	-45.45	0.133054	88.67
4.39	15.90	314.63	-45.37	0.133102	88.47
4.52	16.00	314.71	-45.29	0.131812	88.28
4.52	16.00	314.79	-45.21	0.132227	88.09
4.58	16.10	314.88	-45.12	0.13264	87.90
4.70	16.20	314.96	-45.04	0.133485	87.71
4.76	16.30	315.04	-44.96	0.134293	87.51
4.21	15.70	315.12	-44.88	0.132226	87.32
4.94	16.40	315.21	-44.79	0.13264	87.13
4.94	16.40	315.29	-44.71	0.135533	86.94
4.64	16.10	315.37	-44.63	0.134292	86.75
5.00	16.50	315.45	-44.55	0.134755	86.56
5.19	16.70	315.54	-44.46	0.137186	86.37
5.07	16.60	315.62	-44.38	0.137599	86.18
5.25	16.70	315.70	-44.30	0.137597	85.99
5.19	16.70	315.79	-44.21	0.138012	85.80
5.25	16.70	315.87	-44.13	0.13801	85.61
5.62	17.10	315.95	-44.05	0.139685	85.42
5.49	17.00	316.03	-43.97	0.140905	85.23
5.74	17.20	316.12	-43.88	0.141316	85.04

5.88	17.20	316.20	-43.80	0.142144	84.85
5.55	17.10	316.28	-43.72	0.141782	84.86
5.74	17.20	316.38	-43.64	0.141729	84.48
5.88	17.40	316.45	-43.55	0.142971	84.29
5.88	17.40	316.53	-43.47	0.143797	84.10
6.16	17.70	316.61	-43.39	0.145035	83.91
7.08	18.60	316.69	-43.31	0.149995	83.72
5.98	17.50	316.78	-43.22	0.149167	83.54
5.88	17.40	316.86	-43.14	0.14421	83.35
6.04	17.50	316.94	-43.06	0.14421	83.16
6.29	17.80	317.02	-42.98	0.145881	82.97
6.35	17.80	317.11	-42.89	0.147156	82.79
6.29	17.80	317.19	-42.81	0.147103	82.80
6.47	18.00	317.27	-42.73	0.147929	82.41
6.59	18.10	317.36	-42.64	0.149167	82.23
6.65	18.20	317.44	-42.58	0.149995	82.04
6.71	18.20	317.52	-42.48	0.150407	81.85
6.77	18.30	317.60	-42.40	0.150822	81.67
7.08	18.60	317.69	-42.31	0.152474	81.48
7.02	18.50	317.77	-42.23	0.153299	81.30
7.02	18.50	317.85	-42.15	0.152888	81.11
6.96	18.50	317.93	-42.07	0.152943	80.93
7.08	18.60	318.02	-41.98	0.153301	80.74
7.08	18.60	318.10	-41.90	0.153712	80.58
7.26	18.80	318.18	-41.82	0.154541	80.37
7.69	19.20	318.26	-41.74	0.157018	80.19
7.39	18.90	318.35	-41.65	0.157433	80.00
7.45	18.90	318.43	-41.57	0.156193	79.82
7.69	19.20	318.51	-41.49	0.157431	79.84
7.75	19.30	318.60	-41.40	0.159086	79.45
7.57	19.10	318.68	-41.32	0.156871	79.27
7.26	18.80	318.76	-41.24	0.156663	79.09
8.18	19.70	318.84	-41.16	0.159066	78.90
7.63	19.10	318.93	-41.07	0.160325	78.72
8.24	19.70	319.01	-40.99	0.160324	78.54
8.12	19.60	319.09	-40.91	0.162392	78.36
8.12	19.60	319.17	-40.83	0.161976	78.17
8.24	19.70	319.26	-40.74	0.162392	77.99
8.30	19.80	319.34	-40.66	0.163218	77.81
8.42	19.90	319.42	-40.58	0.164042	77.63
8.48	20.00	319.50	-40.50	0.164871	77.45
8.54	20.00	319.59	-40.41	0.165344	77.27
8.67	20.20	319.67	-40.33	0.16611	77.08
8.73	20.20	319.75	-40.25	0.166935	76.90
8.79	20.30	319.83	-40.17	0.16735	76.72
9.03	20.50	319.92	-40.08	0.168588	76.54
9.03	20.50	320.00	-40.00	0.169416	76.36
9.22	20.70	320.08	-39.92	0.170243	76.18
9.09	20.60	320.17	-39.83	0.170654	76.00
9.03	20.50	320.25	-39.75	0.169829	75.82
9.03	20.50	320.33	-39.67	0.169414	75.64
9.28	20.80	320.41	-39.59	0.170656	75.46
9.52	21.00	320.50	-39.50	0.172784	75.29
9.70	21.20	320.58	-39.42	0.174375	75.11
9.84	21.10	320.66	-39.34	0.174788	74.93
9.84	21.10	320.74	-39.26	0.174375	74.75
9.70	21.20	320.83	-39.17	0.174788	74.57
9.89	21.40	320.91	-39.09	0.176025	74.39
9.89	21.40	320.99	-39.01	0.176854	74.22
9.89	21.40	321.07	-38.93	0.176852	74.04
10.38	21.90	321.16	-38.84	0.17892	73.86
10.31	21.80	321.24	-38.76	0.180573	73.68
10.58	22.10	321.32	-38.68	0.181465	73.51
10.25	21.80	321.40	-38.60	0.181397	73.33
10.44	21.90	321.49	-38.51	0.180573	73.15
10.74	22.20	321.57	-38.43	0.182223	72.98
10.62	22.10	321.65	-38.35	0.183052	72.80
10.74	22.20	321.74	-38.26	0.183052	72.63
10.88	22.40	321.82	-38.18	0.184289	72.45
11.29	22.80	321.90	-38.10	0.186771	72.28
10.99	22.50	321.98	-38.02	0.187182	72.10
10.93	22.40	322.07	-37.93	0.185531	71.93
11.66	23.20	322.15	-37.85	0.188492	71.75
10.88	22.40	322.23	-37.77	0.188424	71.58
11.35	22.90	322.31	-37.69	0.187182	71.40
11.47	23.00	322.40	-37.60	0.189683	71.23
11.54	23.00	322.48	-37.52	0.190077	71.05
11.66	23.20	322.56	-37.44	0.190901	70.88
11.78	23.30	322.64	-37.36	0.192143	70.71
11.84	23.30	322.73	-37.27	0.192554	70.53
11.98	23.50	322.81	-37.19	0.193382	70.36
12.02	23.50	322.89	-37.11	0.194209	70.19
12.33	23.80	322.98	-37.02	0.195519	70.02
12.15	23.60	323.06	-36.94	0.195859	69.84
11.78	23.30	323.14	-36.86	0.193795	69.67
12.33	23.80	323.22	-36.78	0.194622	69.50
12.45	24.00	323.31	-36.69	0.197512	69.33
12.57	24.10	323.39	-36.61	0.198754	69.16
12.70	24.20	323.47	-36.53	0.199578	68.99
12.63	24.10	323.55	-36.45	0.199568	68.81

12.82	24.30	323.64	-36.36	0.199994	68.64
13.31	24.80	323.72	-36.28	0.202884	68.47
13.06	24.60	323.80	-36.20	0.2042	68.30
13.18	24.70	323.88	-36.12	0.203713	68.13
13.00	24.50	323.97	-36.03	0.203297	67.96
13.12	24.60	324.05	-35.95	0.202886	67.79
13.00	24.50	324.13	-35.87	0.202886	67.62
13.55	25.00	324.21	-35.79	0.204536	67.45
13.73	25.20	324.30	-35.70	0.207431	67.29
13.73	25.20	324.38	-35.62	0.208255	67.12
13.98	25.50	324.46	-35.54	0.209497	66.95
14.04	25.50	324.55	-35.45	0.210737	66.78
14.16	25.70	324.63	-35.37	0.21164	66.61
14.10	25.60	324.71	-35.29	0.211974	66.44
14.40	25.90	324.79	-35.21	0.212803	66.28
14.34	25.80	324.88	-35.12	0.21363	66.11
14.47	26.00	324.96	-35.04	0.21404	65.94
15.08	26.60	325.04	-34.96	0.217348	65.78
14.40	25.90	325.12	-34.88	0.216933	65.61
14.83	26.30	325.21	-34.79	0.215696	65.44
15.08	26.60	325.29	-34.71	0.218588	65.28
14.95	26.50	325.37	-34.63	0.219412	65.11
15.44	26.90	325.45	-34.55	0.220734	64.95
15.20	26.70	325.54	-34.46	0.221481	64.78
15.44	26.90	325.62	-34.38	0.221481	64.61
15.44	26.90	325.70	-34.30	0.222304	64.45
15.69	27.20	325.79	-34.21	0.223547	64.29
15.75	27.20	325.87	-34.13	0.224784	64.12
15.75	27.20	325.95	-34.05	0.224786	63.96
16.24	27.70	326.03	-33.97	0.226852	63.79
16.11	27.60	326.12	-33.88	0.228502	63.63
15.93	27.40	326.20	-33.80	0.227265	63.47
16.17	27.70	326.28	-33.72	0.227761	63.30
16.38	27.90	326.36	-33.64	0.229742	63.14
16.42	27.90	326.45	-33.55	0.230571	62.98
15.56	27.10	326.53	-33.47	0.227266	62.81
16.05	27.60	326.61	-33.39	0.226023	62.65
16.91	28.40	326.69	-33.31	0.231398	62.49
16.91	28.40	326.78	-33.22	0.2347	62.33
17.21	28.70	326.86	-33.14	0.235943	62.17
17.15	28.70	326.94	-33.06	0.237183	62.00
17.40	28.90	327.02	-32.98	0.238006	61.84
17.52	29.00	327.11	-32.89	0.239335	61.68
17.46	29.00	327.19	-32.81	0.239662	61.52
17.64	29.10	327.27	-32.73	0.240075	61.36
17.52	29.00	327.36	-32.64	0.240072	61.20
17.82	29.30	327.44	-32.56	0.240901	61.04
18.01	29.50	327.52	-32.48	0.242965	60.88
18.13	29.60	327.60	-32.40	0.244207	60.72
18.37	29.90	327.69	-32.31	0.24586	60.56
18.25	29.70	327.77	-32.23	0.24827	60.41
18.74	30.20	327.85	-32.15	0.247513	60.25
17.33	28.80	327.93	-32.07	0.243882	60.09
18.74	30.20	328.02	-31.98	0.243794	59.93
18.88	30.40	328.10	-31.90	0.250402	59.77
19.29	30.80	328.18	-31.82	0.252685	59.62
19.10	30.60	328.26	-31.74	0.253708	59.46
19.17	30.70	328.35	-31.65	0.253298	59.30
19.41	30.90	328.43	-31.57	0.254537	59.14
19.53	31.00	328.51	-31.49	0.255774	58.99
19.53	31.00	328.60	-31.40	0.25619	58.83
19.41	30.90	328.68	-31.32	0.255774	58.67
19.78	31.30	328.76	-31.24	0.25711	58.52
19.96	31.50	328.84	-31.16	0.259496	58.36
20.14	31.80	328.93	-31.07	0.260736	58.21
20.69	32.20	329.01	-30.99	0.263625	58.05
20.39	31.90	329.09	-30.91	0.264868	57.90
20.32	31.80	329.17	-30.83	0.263212	57.74
20.57	32.10	329.26	-30.74	0.264041	57.59
20.81	32.30	329.34	-30.66	0.266107	57.44
21.61	33.10	329.42	-30.58	0.270236	57.28
20.94	32.40	329.50	-30.50	0.270653	57.13
21.06	32.60	329.59	-30.41	0.268684	56.98
21.30	32.80	329.67	-30.33	0.270239	56.82
21.18	32.70	329.75	-30.25	0.270649	56.67
21.55	33.00	329.83	-30.17	0.271479	56.52
21.42	32.90	329.92	-30.08	0.272302	56.37
21.97	33.50	330.00	-30.00	0.274371	56.21
21.48	33.00	330.08	-29.92	0.274785	56.06
22.09	33.60	330.17	-29.83	0.275195	55.91
22.46	34.00	330.25	-29.75	0.27933	55.76
22.28	33.80	330.33	-29.67	0.280153	55.61
22.40	33.90	330.41	-29.59	0.279743	55.46
22.71	34.20	330.50	-29.50	0.281498	55.31
22.64	34.10	330.58	-29.42	0.282222	55.16
22.77	34.30	330.66	-29.34	0.282632	55.01
22.95	34.40	330.74	-29.26	0.283875	54.86
23.13	34.60	330.83	-29.17	0.285115	54.71
23.25	34.80	330.91	-29.09	0.286764	54.56
23.50	35.00	330.99	-29.01	0.288421	54.41

23.56	35.10	331.07	-28.93	0.289657	54.26
23.80	35.30	331.16	-28.84	0.2909	54.11
23.99	35.50	331.24	-28.78	0.292553	53.97
24.05	35.50	331.32	-28.68	0.293486	53.82
24.17	35.70	331.40	-28.60	0.294202	53.67
24.48	36.00	331.49	-28.51	0.296272	53.52
24.35	35.90	331.57	-28.43	0.297094	53.38
24.66	36.20	331.65	-28.35	0.297924	53.23
24.84	36.30	331.74	-28.28	0.299577	53.09
24.96	36.50	331.82	-28.18	0.300813	52.94
24.29	35.80	331.90	-28.10	0.298751	52.79
25.15	36.60	331.98	-28.02	0.29918	52.65
24.90	36.40	332.07	-27.93	0.301643	52.50
25.51	37.00	332.15	-27.85	0.303406	52.36
25.63	37.10	332.23	-27.77	0.306189	52.21
25.88	37.40	332.31	-27.69	0.307838	52.07
26.12	37.60	332.40	-27.60	0.309908	51.92
26.67	38.20	332.48	-27.52	0.313213	51.78
26.31	37.80	332.56	-27.44	0.314038	51.64
26.43	37.90	332.64	-27.36	0.3128	51.49
26.61	38.10	332.73	-27.27	0.314038	51.35
26.73	38.20	332.81	-27.19	0.315279	51.21
28.14	39.60	332.89	-27.11	0.321477	51.07
26.98	38.50	332.98	-27.02	0.322834	50.92
26.73	38.20	333.06	-26.94	0.316928	50.78
27.34	38.80	333.14	-26.86	0.318172	50.64
27.53	39.00	333.22	-26.78	0.321477	50.50
27.71	39.20	333.31	-26.69	0.323126	50.36
27.71	39.20	333.39	-26.61	0.323957	50.22
27.95	39.50	333.47	-26.53	0.325192	50.08
27.95	39.50	333.55	-26.45	0.326436	49.94
28.14	39.60	333.64	-26.38	0.326849	49.80
28.44	39.90	333.72	-26.28	0.328498	49.66
28.56	40.10	333.80	-26.20	0.330688	49.52
28.87	40.40	333.88	-26.12	0.332834	49.38
25.45	37.00	333.97	-26.03	0.319821	49.24
28.87	40.40	334.05	-25.95	0.319825	49.10
28.56	40.10	334.13	-25.87	0.332834	48.96
29.54	41.00	334.21	-25.79	0.335109	48.83
29.60	41.10	334.30	-25.70	0.339245	48.69
29.66	41.20	334.38	-25.62	0.340068	48.55
29.91	41.40	334.46	-25.54	0.341311	48.41
30.15	41.70	334.55	-25.45	0.343378	48.28
30.33	41.80	334.63	-25.37	0.345156	48.14
30.21	41.70	334.71	-25.29	0.345028	48.00
30.88	42.40	334.79	-25.21	0.34751	47.87
30.82	42.30	334.88	-25.12	0.349989	47.73
30.21	41.70	334.96	-25.04	0.347092	47.60
31.13	42.80	335.04	-24.96	0.348336	47.46
31.31	42.80	335.12	-24.88	0.352877	47.33
31.92	43.40	335.21	-24.79	0.356187	47.19
31.49	43.00	335.29	-24.71	0.357013	47.06
28.50	40.00	335.37	-24.63	0.34296	46.92
32.10	43.60	335.45	-24.55	0.345569	46.79
32.17	43.70	335.54	-24.46	0.360732	46.66
32.23	43.70	335.62	-24.38	0.361146	46.52
32.23	43.70	335.70	-24.30	0.361141	46.39
32.71	44.20	335.79	-24.21	0.363212	46.26
33.08	44.60	335.87	-24.13	0.366928	46.13
32.96	44.50	335.95	-24.05	0.36817	46.00
33.20	44.70	336.03	-23.97	0.368583	45.86
33.26	44.80	336.12	-23.88	0.369818	45.73
33.51	45.00	336.20	-23.80	0.371063	45.60
33.87	45.40	336.28	-23.72	0.373677	45.47
33.69	45.20	336.36	-23.64	0.374364	45.34
34.30	45.80	336.45	-23.55	0.376021	45.21
35.16	46.70	336.53	-23.47	0.382219	45.08
33.94	45.40	336.61	-23.39	0.380562	44.95
34.61	46.10	336.69	-23.31	0.378087	44.82
34.42	45.90	336.78	-23.22	0.380149	44.69
34.91	46.40	336.86	-23.14	0.381393	44.56
35.77	47.30	336.94	-23.06	0.387178	44.44
35.40	46.90	337.02	-22.98	0.389239	44.31
35.46	47.00	337.11	-22.89	0.388145	44.18
35.64	47.10	337.19	-22.81	0.388831	44.05
35.95	47.40	337.27	-22.73	0.390483	43.93
36.07	47.60	337.36	-22.64	0.392545	43.80
36.19	47.70	337.44	-22.56	0.393789	43.67
36.25	47.80	337.52	-22.48	0.394611	43.55
36.58	48.10	337.60	-22.40	0.396268	43.42
36.56	48.10	337.69	-22.31	0.397508	43.30
36.62	48.10	337.77	-22.23	0.397503	43.17
37.66	49.20	337.85	-22.15	0.402053	43.05
37.29	48.80	337.93	-22.07	0.405093	42.92
37.41	48.90	338.02	-21.98	0.403706	42.80
37.11	48.60	338.10	-21.90	0.402875	42.67
37.78	49.30	338.18	-21.82	0.404533	42.55
37.72	49.20	338.26	-21.74	0.407007	42.42
38.76	50.30	338.35	-21.65	0.411144	42.30
38.33	49.80	338.43	-21.57	0.413823	42.18

38.70	50.20	338.51	-21.49	0.413205	42.06
38.70	50.20	338.60	-21.40	0.414863	41.93
38.88	50.40	338.68	-21.32	0.415684	41.81
39.06	50.60	338.76	-21.24	0.417494	41.69
39.06	50.60	338.84	-21.16	0.418189	41.57
39.37	50.90	338.93	-21.07	0.419408	41.45
39.61	51.10	339.01	-20.99	0.421469	41.33
39.49	51.00	339.09	-20.91	0.421887	41.21
40.10	51.80	339.17	-20.83	0.423948	41.09
40.28	51.80	339.26	-20.74	0.427259	40.97
40.59	52.10	339.34	-20.66	0.429325	40.85
40.71	52.20	339.42	-20.58	0.430673	40.73
40.85	52.10	339.50	-20.50	0.430978	40.61
40.95	52.50	339.59	-20.41	0.432375	40.49
41.75	53.20	339.67	-20.33	0.436763	40.37
41.38	52.90	339.75	-20.25	0.438411	40.25
41.58	53.10	339.83	-20.17	0.438003	40.14
41.93	53.40	339.92	-20.08	0.440063	40.02
41.93	53.40	340.00	-20.00	0.441308	39.90
42.42	53.90	340.08	-19.92	0.443374	39.79
38.25	47.80	340.17	-19.83	0.420229	39.67
42.54	54.00	340.25	-19.75	0.420648	39.55
42.42	53.90	340.33	-19.67	0.445848	39.44
42.85	54.30	340.41	-19.59	0.447093	39.32
43.27	54.80	340.50	-19.50	0.450976	39.21
43.46	55.00	340.58	-19.42	0.453705	39.09
43.70	55.20	340.66	-19.34	0.455352	38.98
43.88	55.40	340.74	-19.26	0.45701	38.86
44.07	55.60	340.83	-19.17	0.458663	38.75
44.19	55.70	340.91	-19.09	0.459897	38.64
44.49	56.00	340.99	-19.01	0.461556	38.52
44.80	56.30	341.07	-18.93	0.464029	38.41
44.80	56.30	341.16	-18.84	0.465274	38.30
45.10	56.60	341.24	-18.76	0.466514	38.19
45.35	56.80	341.32	-18.68	0.46875	38.07
45.84	57.30	341.40	-18.60	0.471467	37.96
44.68	56.20	341.49	-18.51	0.468993	37.85
46.02	57.50	341.57	-18.43	0.469814	37.74
46.14	57.60	341.65	-18.35	0.475805	37.63
46.02	57.50	341.74	-18.26	0.475805	37.52
46.69	58.20	341.82	-18.18	0.476078	37.41
46.75	58.30	341.90	-18.10	0.48139	37.30
47.18	58.70	341.98	-18.02	0.48345	37.19
47.24	58.70	342.07	-17.93	0.485109	37.08
47.36	58.90	342.15	-17.85	0.486111	36.97
47.79	59.30	342.23	-17.77	0.488414	36.86
47.85	59.40	342.31	-17.69	0.490474	36.75
48.03	59.50	342.40	-17.60	0.491307	36.65
48.34	59.80	342.48	-17.52	0.49296	36.54
48.71	60.20	342.56	-17.44	0.495846	36.43
48.28	59.80	342.64	-17.36	0.495852	36.33
49.01	60.50	342.73	-17.27	0.497086	36.22
46.02	57.50	342.81	-17.19	0.487588	36.11
49.44	60.90	342.89	-17.11	0.489241	36.01
49.56	61.10	342.98	-17.02	0.504299	35.90
49.56	61.10	343.06	-16.94	0.504937	35.80
50.11	61.60	343.14	-16.86	0.507009	35.69
50.23	61.70	343.22	-16.78	0.509488	35.59
50.48	62.00	343.31	-16.69	0.511135	35.48
50.80	62.10	343.39	-16.61	0.512794	35.38
50.96	62.50	343.47	-16.53	0.514853	35.28
51.33	62.80	343.55	-16.45	0.517752	35.17
51.45	63.00	343.64	-16.38	0.519818	35.07
51.45	63.00	343.72	-16.28	0.520638	34.97
52.49	64.00	343.80	-16.20	0.524967	34.86
52.25	63.70	343.88	-16.12	0.527869	34.76
52.31	63.80	343.97	-16.03	0.526836	34.66
52.80	64.30	344.05	-15.95	0.529322	34.56
52.98	64.50	344.13	-15.87	0.532214	34.46
53.16	64.70	344.21	-15.79	0.533861	34.36
53.34	64.80	344.30	-15.70	0.535107	34.26
53.47	65.00	344.38	-15.62	0.53634	34.16
53.83	65.30	344.46	-15.54	0.538413	34.06
54.14	65.60	344.55	-15.45	0.540892	33.96
54.08	65.60	344.63	-15.37	0.542328	33.86
54.50	66.00	344.71	-15.29	0.543778	33.76
54.69	66.20	344.79	-15.21	0.546264	33.66
54.99	66.50	344.88	-15.12	0.54833	33.56
55.36	66.90	344.96	-15.04	0.551215	33.47
55.48	67.00	345.04	-14.96	0.553288	33.37
56.03	67.50	345.12	-14.88	0.555781	33.27
55.85	67.30	345.21	-14.79	0.557007	33.18
55.79	67.30	345.29	-14.71	0.556181	33.08
56.52	68.00	345.37	-14.63	0.559066	32.98
56.58	68.10	345.45	-14.55	0.562583	32.89
56.82	68.30	345.54	-14.46	0.563618	32.79
57.01	68.50	345.62	-14.38	0.565271	32.70
57.37	68.90	345.70	-14.30	0.567744	32.60
57.82	69.10	345.79	-14.21	0.57023	32.51
58.11	69.60	345.87	-14.13	0.573115	32.41

58.04	69.50	345.95	-14.05	0.574775	32.32
58.29	69.80	346.03	-13.97	0.575602	32.23
58.41	69.90	346.12	-13.88	0.577247	32.13
58.59	70.10	346.20	-13.80	0.578494	32.04
59.08	70.80	346.28	-13.72	0.581598	31.95
59.20	70.70	346.36	-13.64	0.583859	31.86
59.88	71.40	346.45	-13.55	0.587171	31.77
60.00	71.50	346.53	-13.47	0.590477	31.67
60.06	71.60	346.61	-13.39	0.591296	31.58
60.42	71.90	346.69	-13.31	0.592958	31.49
60.36	71.90	346.78	-13.22	0.594189	31.40
60.61	72.10	346.86	-13.14	0.595022	31.31
60.85	72.40	346.94	-13.06	0.597088	31.22
61.16	72.70	347.02	-12.98	0.59956	31.13
61.48	73.00	347.11	-12.89	0.602286	31.05
61.48	73.00	347.19	-12.81	0.603287	30.96
61.95	73.50	347.27	-12.73	0.605353	30.87
61.95	73.50	347.38	-12.64	0.607411	30.78
62.58	74.10	347.44	-12.56	0.609898	30.69
62.68	74.20	347.52	-12.48	0.612783	30.61
62.74	74.20	347.60	-12.40	0.613204	30.52
63.17	74.70	347.69	-12.31	0.61527	30.43
64.09	75.60	347.77	-12.23	0.621047	30.35
63.23	74.70	347.85	-12.15	0.621065	30.26
63.78	75.30	347.93	-12.07	0.62004	30.17
64.51	76.00	348.02	-11.98	0.625187	30.09
64.33	75.80	348.10	-11.90	0.627245	30.00
64.39	75.90	348.18	-11.82	0.62884	29.92
64.94	76.40	348.26	-11.74	0.629311	29.84
64.82	76.30	348.35	-11.65	0.630972	29.75
65.19	76.70	348.43	-11.57	0.632211	29.67
65.25	76.70	348.51	-11.49	0.633858	29.59
65.55	77.10	348.60	-11.40	0.635517	29.50
65.80	77.30	348.68	-11.32	0.637989	29.42
66.22	77.70	348.76	-11.24	0.640708	29.34
66.10	77.60	348.84	-11.16	0.641715	29.26
66.59	78.10	348.93	-11.07	0.643388	29.18
66.71	78.20	349.01	-10.99	0.645839	29.09
66.89	78.40	349.09	-10.91	0.647087	29.01
67.02	78.50	349.17	-10.83	0.648319	28.93
67.20	78.70	349.26	-10.74	0.649586	28.85
67.63	79.10	349.34	-10.66	0.652045	28.77
67.75	79.20	349.42	-10.58	0.654104	28.69
67.87	79.40	349.50	-10.50	0.655351	28.62
67.38	78.90	349.59	-10.41	0.654349	28.54
67.87	79.40	349.67	-10.33	0.654111	28.46
68.54	80.00	349.75	-10.25	0.658649	28.38
68.66	80.20	349.83	-10.17	0.661982	28.30
68.79	80.30	349.92	-10.08	0.663194	28.23
69.21	80.70	350.00	-10.00	0.665288	28.15
69.27	80.80	350.08	-9.92	0.667334	28.07
69.58	81.10	350.17	-9.83	0.668979	28.00
70.01	81.50	350.25	-9.75	0.671879	27.92
69.82	81.30	350.33	-9.67	0.672898	27.84
70.13	81.80	350.41	-9.59	0.673119	27.77
70.58	82.10	350.50	-9.50	0.67687	27.69
70.37	81.90	350.58	-9.42	0.677864	27.62
70.92	82.40	350.66	-9.34	0.678898	27.55
71.11	82.60	350.74	-9.26	0.681797	27.47
71.04	82.50	350.83	-9.17	0.68221	27.40
71.47	83.00	350.91	-9.09	0.683854	27.33
71.72	83.20	350.99	-9.01	0.686755	27.25
71.84	83.30	351.07	-8.93	0.687988	27.18
72.51	84.00	351.16	-8.84	0.6913	27.11
72.33	83.80	351.24	-8.76	0.693368	27.04
72.33	83.80	351.32	-8.68	0.692791	26.97
72.14	83.60	351.40	-8.60	0.691705	26.89
72.45	83.90	351.49	-8.51	0.692127	26.82
73.06	84.60	351.57	-8.43	0.69625	26.75
73.73	85.20	351.65	-8.35	0.701831	26.68
73.18	84.70	351.74	-8.26	0.702044	26.61
73.55	85.00	351.82	-8.18	0.701209	26.55
73.79	85.30	351.90	-8.10	0.703897	26.48
73.91	85.40	351.98	-8.02	0.705341	26.41
74.04	85.50	352.07	-7.93	0.708176	26.34
74.16	85.70	352.15	-7.85	0.707872	26.27
74.65	86.10	352.23	-7.77	0.709895	26.20
74.65	86.10	352.31	-7.69	0.711539	26.14
75.38	86.90	352.40	-7.60	0.714853	26.07
75.07	86.60	352.48	-7.52	0.716919	26.00
75.28	86.80	352.56	-7.44	0.718497	25.94
75.68	87.20	352.64	-7.36	0.718985	25.87
74.34	85.80	352.73	-7.27	0.714845	25.81
75.91	87.30	352.81	-7.19	0.715287	25.74
76.05	87.50	352.89	-7.11	0.722291	25.68
76.72	88.20	352.98	-7.02	0.726274	25.61
76.29	87.80	353.06	-6.94	0.727241	25.55
76.54	88.00	353.14	-6.86	0.726423	25.49
76.23	87.70	353.22	-6.78	0.72801	25.42
76.90	88.40	353.31	-6.69	0.727854	25.36

76.97	88.50	353.39	-6.61	0.730668	25.30
77.21	88.70	353.47	-6.53	0.732199	25.24
77.58	89.10	353.55	-6.45	0.734687	25.17
77.45	89.00	353.64	-6.36	0.735927	25.11
77.70	89.20	353.72	-6.28	0.736331	25.05
78.00	89.50	353.80	-6.20	0.736674	24.99
77.64	89.40	353.88	-6.12	0.739233	24.93
77.39	88.90	353.97	-6.03	0.736745	24.87
78.37	89.90	354.05	-5.95	0.738819	24.81
78.31	89.80	354.13	-5.87	0.742538	24.75
78.55	90.10	354.21	-5.79	0.743356	24.69
78.80	90.30	354.30	-5.70	0.745431	24.64
78.92	90.40	354.38	-5.62	0.746661	24.58
79.04	90.50	354.46	-5.54	0.747497	24.52
78.98	90.50	354.55	-5.45	0.74791	24.46
79.28	90.80	354.63	-5.37	0.749422	24.41
79.53	91.00	354.71	-5.29	0.751207	24.35
79.71	91.20	354.79	-5.21	0.752869	24.29
79.71	91.20	354.88	-5.12	0.753695	24.24
79.71	91.20	354.96	-5.04	0.753686	24.18
80.14	91.60	355.04	-4.96	0.755348	24.13
80.32	91.80	355.12	-4.88	0.757818	24.07
80.44	91.90	355.21	-4.79	0.759067	24.02
80.51	92.00	355.29	-4.71	0.759893	23.96
80.57	92.10	355.37	-4.63	0.76071	23.91
80.87	92.40	355.45	-4.55	0.762649	23.85
81.30	92.80	355.54	-4.46	0.765285	23.80
80.99	92.50	355.62	-4.38	0.765678	23.75
81.05	92.60	355.70	-4.30	0.764642	23.70
81.42	92.90	355.79	-4.21	0.768505	23.64
81.48	93.00	355.87	-4.13	0.768148	23.59
81.48	93.00	355.95	-4.05	0.768571	23.54
81.67	93.20	356.03	-3.97	0.769397	23.49
81.54	93.00	356.12	-3.88	0.769388	23.44
81.85	93.30	356.20	-3.80	0.76981	23.39
81.97	93.50	356.28	-3.72	0.772156	23.34
81.60	93.10	356.36	-3.64	0.771041	23.29
82.21	93.70	356.45	-3.55	0.771876	23.24
82.40	93.90	356.53	-3.47	0.775162	23.19
82.76	94.30	356.61	-3.39	0.777652	23.14
82.52	94.00	356.69	-3.31	0.778074	23.10
82.70	94.20	356.78	-3.22	0.777652	23.05
82.82	94.30	356.86	-3.14	0.778901	23.00
82.58	94.10	356.94	-3.06	0.778488	22.96
83.01	94.50	357.02	-2.98	0.779305	22.91
83.13	94.60	357.11	-2.89	0.781664	22.86
83.19	94.70	357.19	-2.81	0.782207	22.82
83.37	94.90	357.27	-2.73	0.783446	22.77
83.37	94.90	357.36	-2.64	0.784283	22.73
83.50	95.00	357.44	-2.56	0.784688	22.68
83.68	95.20	357.52	-2.48	0.785916	22.64
83.80	95.30	357.60	-2.40	0.787185	22.59
83.62	95.10	357.69	-2.31	0.788752	22.55
83.62	95.10	357.77	-2.23	0.785916	22.51
84.05	95.50	357.85	-2.15	0.787578	22.46
83.56	95.10	357.93	-2.07	0.787864	22.42
84.05	95.50	358.02	-1.98	0.787578	22.38
84.23	95.70	358.10	-1.90	0.790048	22.34
84.05	95.50	358.18	-1.82	0.790058	22.30
84.53	96.00	358.26	-1.74	0.791288	22.25
84.35	95.90	358.35	-1.65	0.79296	22.21
84.72	96.20	358.43	-1.57	0.793776	22.17
84.72	96.20	358.51	-1.49	0.795006	22.13
84.72	96.20	358.60	-1.40	0.795016	22.09
84.84	96.30	358.68	-1.32	0.79542	22.05
84.72	96.20	358.76	-1.24	0.795718	22.02
84.84	96.30	358.84	-1.16	0.795429	21.98
84.96	96.50	358.93	-1.07	0.796669	21.94
85.08	96.60	359.01	-0.99	0.797899	21.90
85.14	96.60	359.09	-0.91	0.798322	21.86
85.14	96.60	359.17	-0.83	0.798312	21.83
85.39	96.90	359.26	-0.74	0.799581	21.79
85.27	96.80	359.34	-0.66	0.800388	21.75
85.27	96.80	359.42	-0.58	0.799965	21.72
86.30	97.80	359.50	-0.50	0.804107	21.68
85.63	97.10	359.59	-0.41	0.805639	21.65
85.69	97.20	359.67	-0.33	0.802867	21.61
85.57	97.10	359.75	-0.25	0.802857	21.58
85.75	97.30	359.83	-0.17	0.80328	21.54
85.82	97.30	359.92	-0.08	0.804097	21.51
85.82	97.30	0.00	-380.00	-3502	21.48
85.88	97.40	0.08	-359.92	0.801599	21.44
85.88	97.40	0.16	-359.84	0.802011	21.41
85.94	97.40	0.25	-359.75	0.802021	21.38
86.30	97.80	0.33	-359.67	0.803658	21.35
86.12	97.60	0.41	-359.59	0.804481	21.32
86.12	97.60	0.49	-359.51	0.803658	21.29
86.43	97.90	0.58	-359.42	0.804893	21.25
86.30	97.80	0.66	-359.34	0.805716	21.22
86.30	97.80	0.74	-359.26	0.805315	21.19

86.18	97.70	0.82	-359.18	0.804893	21.16
86.43	97.90	0.91	-359.09	0.805305	21.14
86.55	98.00	0.99	-359.01	0.80654	21.11
86.88	97.40	1.07	-359.93	0.804481	21.08
86.61	98.10	1.15	-358.85	0.804893	21.05
86.55	98.00	1.24	-358.76	0.807373	21.02
86.91	98.40	1.32	-358.68	0.808598	20.99
86.67	98.20	1.40	-358.60	0.809422	20.97
86.73	98.20	1.48	-358.52	0.808598	20.94
87.04	98.50	1.58	-358.44	0.809834	20.91
87.04	98.50	1.65	-358.35	0.811079	20.89
86.67	98.20	1.73	-358.27	0.809834	20.86
87.10	98.60	1.81	-358.19	0.810245	20.84
87.22	98.70	1.89	-358.11	0.812304	20.81
87.59	99.10	1.98	-358.02	0.814362	20.79
87.59	99.10	2.06	-357.94	0.816009	20.76
87.46	99.00	2.14	-357.86	0.815607	20.74
87.65	99.10	2.22	-357.78	0.815598	20.72
87.83	99.30	2.31	-357.69	0.816833	20.69
87.95	99.50	2.39	-357.61	0.818479	20.67
88.07	99.60	2.47	-357.53	0.819715	20.65
88.28	99.80	2.55	-357.45	0.82096	20.63
88.20	99.70	2.63	-357.37	0.821361	20.61
88.75	100.20	2.72	-357.28	0.823008	20.59
88.93	100.40	2.80	-357.20	0.82589	20.56
89.84	101.30	2.88	-357.12	0.830419	20.54
89.54	101.00	2.96	-357.04	0.832889	20.52
89.78	101.30	3.05	-356.95	0.832899	20.51
89.84	101.30	3.13	-356.87	0.834124	20.49
90.33	101.80	3.21	-356.79	0.836183	20.47
90.58	102.10	3.29	-356.71	0.839477	20.45
90.64	102.10	3.38	-356.62	0.840712	20.43
91.19	102.70	3.46	-356.54	0.843182	20.41
91.49	103.00	3.54	-356.46	0.846898	20.40
91.86	103.40	3.62	-356.38	0.849769	20.38
92.35	103.80	3.71	-356.29	0.853063	20.36
92.96	104.50	3.79	-356.21	0.857592	20.35
92.96	104.50	3.87	-356.13	0.860474	20.33
93.38	104.90	3.95	-356.05	0.862131	20.31
93.87	105.40	4.03	-355.97	0.865826	20.30
94.38	105.90	4.12	-355.88	0.869943	20.28
95.78	107.30	4.20	-355.80	0.877766	20.27
95.34	106.80	4.28	-355.72	0.881471	20.26
96.01	107.50	4.36	-355.64	0.882295	20.24
96.62	108.10	4.45	-355.55	0.887647	20.23
97.23	108.70	4.53	-355.47	0.892598	20.22
97.96	109.50	4.61	-355.39	0.898351	20.20
98.14	109.80	4.69	-355.31	0.902057	20.19
99.37	110.90	4.78	-355.22	0.907821	20.18
99.98	111.50	4.86	-355.14	0.915854	20.17
101.56	113.10	4.94	-355.06	0.924701	20.16
101.62	113.10	5.02	-354.98	0.931288	20.15
102.54	114.00	5.11	-354.89	0.934993	20.14
103.03	114.50	5.19	-354.81	0.940757	20.13
103.94	115.40	5.27	-354.73	0.946521	20.12
104.82	116.40	5.35	-354.65	0.954355	20.11
105.65	117.20	5.43	-354.57	0.961755	20.10
106.57	118.10	5.52	-354.48	0.968754	20.09
107.54	119.00	5.60	-354.40	0.976164	20.08
108.58	120.10	5.68	-354.32	0.984399	20.07
109.44	120.90	5.76	-354.24	0.992221	20.07
110.53	122.00	5.85	-354.15	1.000044	20.06
111.63	123.10	5.93	-354.07	1.009113	20.05
112.49	124.00	6.01	-353.99	1.017335	20.05
113.71	125.20	6.09	-353.91	1.025981	20.04
114.50	126.00	6.18	-353.82	1.034216	20.04
116.27	127.80	6.26	-353.74	1.044933	20.03
116.82	128.30	6.34	-353.66	1.054369	20.03
116.04	129.50	6.42	-353.58	1.061388	20.02
116.53	130.00	6.51	-353.49	1.068387	20.02
120.06	131.60	6.59	-353.41	1.077033	20.02
121.09	132.60	6.67	-353.33	1.087738	20.01
122.13	133.60	6.75	-353.25	1.095985	20.01
122.62	134.10	6.83	-353.17	1.102148	20.01
124.08	135.60	6.92	-353.08	1.110382	20.00
124.76	136.50	7.00	-353.00	1.120283	20.00
124.94	137.00	7.08	-352.92	1.126027	20.00
124.94	137.50	7.16	-352.84	1.130144	20.00
124.94	138.00	7.25	-352.75	1.134261	20.00
124.94	138.50	7.33	0.00	4876.823	20.00
124.94	139.00	7.41	0.09	1.195262	20.00
124.94	139.50	7.49	0.17	1.199569	20.00
124.94	140.00	7.58	0.26	1.203976	20.00
124.94	140.50	7.66	0.34	1.208184	20.00
124.94	141.00	7.74	0.43	1.212491	20.01
124.94	141.50	7.82	0.52	1.216798	20.01
124.94	142.00	7.90	0.60	1.221105	20.01
124.94	142.50	7.99	0.69	1.225413	20.01
124.94	143.00	8.07	0.78	1.22972	20.02
124.94	143.50	8.15	0.86	1.234027	20.02

124.94	144.00	8.23	0.95	1.238334	20.03
124.94	144.50	8.32	1.03	1.242642	20.03
124.94	145.00	8.40	1.12	1.246949	20.04
124.94	145.50	8.48	1.21	1.251256	20.04
124.94	146.00	8.56	1.29	1.255563	20.05
124.94	146.50	8.65	1.38	1.259871	20.05
124.94	147.00	8.73	1.46	1.264178	20.06
124.94	147.50	8.81	1.55	1.268485	20.07
124.94	148.00	8.89	1.64	1.272792	20.08
124.94	148.50	8.98	1.72	1.2771	20.08
124.94	149.00	9.06	1.81	1.281407	20.09
124.94	149.50	9.14	1.90	1.285714	20.10
124.94	150.00	9.22	1.98	1.290021	20.11
124.94	150.50	9.30	2.07	1.294329	20.12
124.94	151.00	9.39	2.15	1.298636	20.13
124.94	151.50	9.47	2.24	1.302943	20.14
124.94	152.00	9.55	2.33	1.30725	20.15
124.94	152.50	9.63	2.41	1.311558	20.17
124.94	153.00	9.72	2.50	1.315865	20.18
124.94	153.50	9.80	2.58	1.320172	20.19
124.94	154.00	9.88	2.67	1.324479	20.20
124.94	154.50	9.96	2.76	1.328787	20.22
124.94	155.00	10.05	2.84	1.333094	20.23
124.94	155.00	10.13	2.93	1.335248	20.24
124.94	154.50	10.21	3.02	1.333094	20.26
124.94	154.00	10.29	3.10	1.328787	20.27
124.94	153.50	10.38	3.19	1.324479	20.29
124.94	153.00	10.46	3.27	1.320172	20.31
124.94	153.20	10.54	3.36	1.31888	20.32
124.94	152.50	10.62	3.45	1.316742	20.34
124.94	152.00	10.70	3.53	1.314542	20.36
124.94	151.80	10.79	3.62	1.308543	20.37
124.94	153.50	10.87	3.70	1.315019	20.39
124.94	153.00	10.95	3.79	1.320157	20.41
124.94	152.80	11.03	3.88	1.317157	20.43
124.94	152.00	11.12	3.96	1.312865	20.45
124.94	151.50	11.20	4.05	1.30725	20.47
124.94	151.00	11.28	4.13	1.302943	20.49
124.94	150.00	11.36	4.22	1.298482	20.51
124.94	149.70	11.45	4.31	1.290868	20.53
124.94	149.00	11.53	4.39	1.286576	20.55
124.94	148.20	11.61	4.48	1.280115	20.57
124.94	147.50	11.69	4.57	1.273669	20.59
124.94	146.80	11.77	4.65	1.267624	20.62
124.94	146.00	11.86	4.74	1.261163	20.64
124.94	145.00	11.94	4.82	1.25341	20.66
124.94	144.00	12.02	4.91	1.244781	20.69
124.94	143.00	12.10	5.00	1.236195	20.71
124.94	142.00	12.19	5.08	1.227566	20.74
124.94	141.00	12.27	5.17	1.218952	20.76
124.94	138.20	12.35	5.25	1.202584	20.79
124.94	138.40	12.43	5.34	1.191385	20.81
124.94	138.10	12.52	5.43	1.190941	20.84
124.94	137.90	12.60	5.51	1.188815	20.87
124.94	137.50	12.68	5.60	1.186217	20.89
124.94	137.20	12.76	5.69	1.183202	20.92
124.94	137.00	12.85	5.77	1.181048	20.95
124.94	136.80	12.93	5.86	1.179325	20.98
124.94	136.40	13.01	5.94	1.176741	21.01
124.78	136.30	13.09	6.03	1.174587	21.03
124.51	136.00	13.17	6.12	1.172984	21.06
123.78	135.30	13.26	6.20	1.168557	21.09
123.72	135.20	13.34	6.29	1.165111	21.13
123.23	134.70	13.42	6.37	1.162527	21.16
122.86	134.40	13.50	6.46	1.159081	21.19
122.50	134.00	13.59	6.55	1.156066	21.22
122.38	133.90	13.67	6.63	1.153912	21.25
121.58	133.10	13.75	6.72	1.150038	21.28
121.28	132.80	13.83	6.81	1.145298	21.32
120.85	132.30	13.92	6.89	1.141852	21.35
120.48	132.00	14.00	6.98	1.138406	21.38
118.96	130.50	14.08	7.06	1.130653	21.42
119.08	130.80	14.16	7.15	1.124623	21.45
119.26	130.80	14.25	7.24	1.125915	21.49
118.84	130.30	14.33	7.32	1.124623	21.52
118.47	130.00	14.41	7.41	1.121177	21.56
117.92	129.40	14.49	7.49	1.117301	21.60
117.98	129.50	14.57	7.58	1.115147	21.63
117.74	129.20	14.66	7.67	1.114288	21.67
116.58	128.10	14.74	7.75	1.108255	21.71
115.84	127.30	14.82	7.84	1.100072	21.75
115.72	127.20	14.90	7.93	1.096195	21.79
115.30	126.80	14.99	8.01	1.094041	21.82
114.75	126.20	15.07	8.10	1.089734	21.86
114.58	126.10	15.15	8.18	1.086719	21.90
113.95	125.50	15.23	8.27	1.083704	21.94
113.59	125.10	15.32	8.36	1.079397	21.98
113.10	124.60	15.40	8.44	1.07552	22.03
112.55	124.00	15.48	8.53	1.070782	22.07
112.08	123.60	15.56	8.61	1.066475	22.11

112.06	123.60	15.65	8.70	1.064752	22.15
111.33	122.80	15.73	8.79	1.061308	22.19
110.84	122.30	15.81	8.87	1.065707	22.24
110.47	122.00	15.89	8.96	1.052261	22.28
110.05	121.50	15.97	9.05	1.048815	22.32
109.58	121.10	16.06	9.13	1.044939	22.37
108.89	120.40	16.14	9.22	1.040201	22.41
108.09	119.60	16.22	9.30	1.03374	22.46
107.73	119.20	16.30	9.39	1.028571	22.50
107.67	119.20	16.39	9.48	1.026848	22.55
107.30	118.80	16.47	9.56	1.025137	22.60
106.87	118.40	16.55	9.65	1.021668	22.64
106.28	117.80	16.63	9.73	1.017372	22.69
105.96	117.50	16.72	9.82	1.013496	22.74
105.47	117.00	16.80	9.91	1.01005	22.79
105.10	116.60	16.88	9.99	1.006185	22.83
104.68	116.20	16.96	10.08	1.002716	22.88
104.08	115.60	17.04	10.17	0.998432	22.93
103.64	115.10	17.13	10.25	0.993671	22.98
103.52	115.00	17.21	10.34	0.991098	23.03
102.97	114.50	17.29	10.42	0.988514	23.08
101.81	113.30	17.37	10.51	0.981192	23.13
101.28	112.80	17.46	10.60	0.973881	23.18
101.44	112.90	17.54	10.68	0.972135	23.24
100.95	112.50	17.62	10.77	0.970854	23.29
100.71	112.20	17.70	10.85	0.967839	23.34
100.10	111.60	17.79	10.94	0.963963	23.39
99.87	111.20	17.87	11.03	0.959668	23.45
99.00	110.50	17.95	11.11	0.954906	23.50
98.75	110.30	18.03	11.20	0.951052	23.56
98.27	109.80	18.12	11.28	0.948015	23.61
98.02	109.50	18.20	11.37	0.94458	23.67
97.47	109.00	18.28	11.46	0.941145	23.72
96.98	108.50	18.38	11.54	0.939816	23.78
96.68	108.20	18.44	11.63	0.933392	23.83
96.13	107.60	18.53	11.72	0.929494	23.89
95.76	107.30	18.61	11.80	0.925639	23.95
94.67	106.20	18.69	11.89	0.919598	24.00
95.03	106.50	18.77	11.97	0.916141	24.06
94.67	106.20	18.86	12.06	0.916163	24.12
93.93	105.40	18.94	12.15	0.911404	24.18
93.57	105.10	19.02	12.23	0.906687	24.24
93.08	104.60	19.10	12.32	0.90322	24.30
92.90	104.40	19.19	12.40	0.900215	24.36
92.22	103.70	19.27	12.49	0.896349	24.42
91.61	103.10	19.35	12.58	0.890729	24.48
91.25	102.70	19.43	12.66	0.888442	24.54
90.64	102.10	19.52	12.75	0.882115	24.60
90.58	102.10	19.60	12.84	0.879551	24.66
90.15	101.60	19.68	12.92	0.877387	24.73
89.80	101.10	19.76	13.01	0.873069	24.79
89.29	100.80	19.84	13.09	0.869644	24.85
88.81	100.30	19.93	13.18	0.866178	24.92
88.38	99.90	20.01	13.27	0.862321	24.98
87.95	99.50	20.09	13.35	0.858866	25.04
87.59	99.10	20.17	13.44	0.85542	25.11
87.04	98.50	20.26	13.52	0.851113	25.17
86.73	98.20	20.34	13.61	0.847226	25.24
86.24	97.70	20.42	13.70	0.8438	25.31
85.88	97.40	20.50	13.78	0.840344	25.37
85.39	96.90	20.59	13.87	0.836899	25.44
84.96	96.50	20.67	13.96	0.833022	25.51
84.17	95.70	20.75	14.04	0.827844	25.57
84.05	95.50	20.83	14.13	0.823556	25.64
83.44	94.90	20.91	14.21	0.820091	25.71
83.50	95.00	21.00	14.30	0.817956	25.78
83.01	94.50	21.08	14.39	0.816224	25.85
79.35	90.80	21.16	14.47	0.798133	25.92
81.85	93.30	21.24	14.56	0.792965	25.99
81.91	93.40	21.33	14.64	0.804154	26.06
81.30	92.80	21.41	14.73	0.802019	26.13
80.93	92.40	21.49	14.82	0.797703	26.20
80.51	92.00	21.57	14.90	0.794257	26.27
79.90	91.40	21.66	14.99	0.78996	26.35
79.59	91.10	21.74	15.08	0.786073	26.42
79.22	90.70	21.82	15.16	0.783058	26.49
78.80	90.30	21.90	15.25	0.779612	26.56
78.43	89.90	21.99	15.33	0.776166	26.64
78.13	89.60	22.07	15.42	0.773151	26.71
77.76	89.30	22.15	15.51	0.770567	26.79
77.33	88.80	22.23	15.59	0.767121	26.86
76.66	88.20	22.31	15.68	0.762383	26.94
77.33	88.80	22.40	15.76	0.762383	27.01
76.23	87.70	22.48	15.85	0.76023	27.09
75.62	87.10	22.56	15.94	0.752907	27.16
75.81	87.30	22.64	16.02	0.751184	27.24
74.89	86.40	22.73	16.11	0.748178	27.32
74.52	86.00	22.81	16.20	0.74257	27.40
74.04	85.50	22.89	16.28	0.738876	27.47
73.79	85.30	22.97	16.37	0.735987	27.55

73.43	84.90	23.06	16.45	0.733094	27.63
73.00	84.50	23.14	16.54	0.720657	27.71
72.57	84.10	23.22	16.63	0.726202	27.79
72.33	83.80	23.30	16.71	0.723179	27.87
71.59	83.10	23.39	16.80	0.71888	27.95
71.41	82.90	23.47	16.88	0.715004	28.03
71.04	82.50	23.55	16.97	0.712427	28.11
70.98	82.20	23.63	17.06	0.709388	28.19
70.25	81.80	23.71	17.14	0.706397	28.28
69.95	81.40	23.80	17.23	0.702943	28.36
69.70	81.20	23.88	17.32	0.700359	28.44
69.09	80.60	23.96	17.40	0.696921	28.53
69.03	80.50	24.04	17.49	0.693882	28.61
68.48	80.00	24.13	17.57	0.691322	28.69
68.24	79.70	24.21	17.66	0.687868	28.78
67.99	79.20	24.29	17.75	0.684422	28.86
67.50	79.00	24.37	17.83	0.681415	28.95
67.20	78.70	24.46	17.92	0.679238	29.03
66.59	78.10	24.54	18.00	0.675385	29.12
66.22	77.70	24.62	18.09	0.67107	29.21
65.73	77.20	24.70	18.18	0.667201	29.29
65.80	77.30	24.78	18.26	0.66547	29.38
65.25	76.70	24.87	18.35	0.663301	29.47
64.88	76.40	24.95	18.44	0.659448	29.55
64.51	76.00	25.03	18.52	0.656425	29.64
64.33	75.80	25.11	18.61	0.653848	29.73
63.96	75.50	25.20	18.69	0.651697	29.82
63.48	75.00	25.28	18.78	0.648234	29.91
63.29	74.80	25.36	18.87	0.645228	30.00
62.81	74.30	25.44	18.95	0.642211	30.09
63.35	74.90	25.53	19.04	0.642649	30.18
62.07	73.60	25.61	19.12	0.639627	30.27
61.71	73.20	25.69	19.21	0.632297	30.36
61.77	73.30	25.77	19.30	0.631012	30.45
61.16	72.70	25.86	19.38	0.628858	30.55
60.73	72.20	25.94	19.47	0.624128	30.64
60.36	71.90	26.02	19.55	0.620875	30.73
59.94	71.40	26.10	19.64	0.617222	30.83
59.57	71.10	26.18	19.73	0.613783	30.92
59.27	70.80	26.27	19.81	0.611206	31.01
59.27	70.80	26.35	19.90	0.609907	31.11
58.84	70.30	26.43	19.99	0.607753	31.20
58.72	70.20	26.51	20.07	0.605182	31.30
58.04	69.50	26.60	20.16	0.601723	31.39
57.80	69.30	26.68	20.24	0.597853	31.49
57.74	69.20	26.76	20.33	0.596554	31.59
57.13	68.60	26.84	20.42	0.593539	31.68
56.88	68.40	26.93	20.50	0.590086	31.78
56.40	67.90	27.01	20.59	0.587078	31.88
55.79	67.30	27.09	20.67	0.582347	31.98
55.85	67.30	27.17	20.76	0.579758	32.07
55.42	66.90	27.26	20.85	0.578026	32.17
55.54	67.00	27.34	20.93	0.576741	32.27
54.93	66.40	27.42	21.02	0.574587	32.37
54.69	66.20	27.50	21.11	0.571148	32.47
53.89	65.40	27.58	21.19	0.566834	32.57
53.96	65.50	27.67	21.28	0.563812	32.67
53.65	65.10	27.75	21.36	0.562527	32.77
52.98	64.50	27.83	21.45	0.558226	32.87
53.22	64.70	27.91	21.54	0.556497	32.98
52.80	64.30	28.00	21.62	0.555635	33.08
52.43	63.90	28.08	21.71	0.552183	33.18
51.70	63.20	28.16	21.79	0.547451	33.28
51.82	63.30	28.24	21.88	0.544873	33.39
51.70	63.20	28.33	21.97	0.544867	33.49
51.27	62.80	28.41	22.05	0.542713	33.59
51.33	62.90	28.49	22.14	0.540984	33.70
50.54	62.00	28.57	22.23	0.537545	33.80
50.29	61.80	28.66	22.31	0.533244	33.91
50.05	61.50	28.74	22.40	0.531084	34.01
49.80	61.30	28.82	22.48	0.528938	34.12
50.17	61.70	28.90	22.57	0.529779	34.23
49.26	60.80	28.98	22.66	0.527638	34.33
48.89	60.40	29.07	22.74	0.522045	34.44
48.95	60.50	29.15	22.83	0.520747	34.55
48.34	59.80	29.23	22.91	0.518188	34.65
48.16	59.70	29.31	23.00	0.514704	34.76
48.03	59.50	29.40	23.09	0.51343	34.87
47.61	59.10	29.48	23.17	0.51084	34.98
47.18	58.70	29.56	23.26	0.507394	35.09
47.00	58.50	29.64	23.35	0.504816	35.20
46.94	58.40	29.73	23.43	0.503508	35.31
46.51	58.00	29.81	23.52	0.50137	35.42
46.20	57.70	29.89	23.60	0.498349	35.53
45.84	57.30	29.97	23.69	0.495334	35.64
45.47	57.00	30.05	23.78	0.492324	35.75
45.35	56.80	30.14	23.86	0.490154	35.86
44.98	56.50	30.22	23.95	0.488017	35.97
44.86	56.40	30.30	24.03	0.486289	36.09
44.31	55.80	30.38	24.12	0.483279	36.20

44.01	55.50	30.47	24.21	0.479397	36.31
44.01	55.50	30.55	24.29	0.478094	36.43
43.76	55.30	30.63	24.38	0.477249	36.54
43.88	55.40	30.71	24.47	0.476813	36.66
43.27	54.80	30.80	24.55	0.474664	36.77
43.03	54.50	30.88	24.64	0.470771	36.89
42.72	54.20	30.96	24.72	0.468204	37.00
42.54	54.00	31.04	24.81	0.466044	37.12
42.72	54.20	31.13	24.90	0.466044	37.23
42.05	53.80	31.21	24.98	0.464327	37.35
41.75	53.20	31.29	25.07	0.460004	37.47
41.44	52.90	31.37	25.15	0.457005	37.58
41.14	52.60	31.45	25.24	0.454415	37.70
41.08	52.60	31.54	25.33	0.453123	37.82
40.83	52.30	31.62	25.41	0.451838	37.94
40.59	52.10	31.70	25.50	0.449666	38.06
40.28	51.80	31.78	25.59	0.447528	38.17
39.49	51.00	31.87	25.67	0.442785	38.29
39.79	51.30	31.95	25.76	0.440637	38.41
39.49	51.00	32.03	25.84	0.440632	38.53
39.31	50.80	32.11	25.93	0.438468	38.65
38.94	50.40	32.20	26.02	0.435899	38.78
38.94	50.40	32.28	26.10	0.434171	38.90
38.51	50.00	32.36	26.19	0.432453	39.02
38.39	49.90	32.44	26.27	0.430294	39.14
38.21	49.70	32.53	26.36	0.428997	39.26
38.02	49.50	32.61	26.45	0.427279	39.38
37.88	49.20	32.69	26.53	0.425126	39.51
37.29	48.80	32.77	26.62	0.422115	39.63
37.23	48.70	32.85	26.70	0.419657	39.75
36.80	48.30	32.94	26.79	0.417798	39.88
36.74	48.20	33.02	26.88	0.41565	40.00
36.56	48.10	33.10	26.96	0.414788	40.13
36.32	47.80	33.18	27.05	0.41307	40.25
36.07	47.60	33.27	27.14	0.410912	40.38
35.95	47.40	33.35	27.22	0.409184	40.50
35.83	47.30	33.43	27.31	0.407897	40.63
35.48	47.00	33.51	27.39	0.406178	40.76
35.16	46.70	33.60	27.48	0.403589	40.88
34.91	46.40	33.68	27.57	0.401005	41.01
34.73	46.20	33.76	27.65	0.398847	41.14
35.22	46.70	33.84	27.74	0.400144	41.27
34.36	45.90	33.92	27.82	0.398856	41.39
34.12	45.60	34.01	27.91	0.394113	41.52
33.94	45.40	34.09	28.00	0.39196	41.65
33.75	45.30	34.17	28.08	0.390663	41.78
33.51	45.00	34.25	28.17	0.388945	41.91
33.26	44.80	34.34	28.26	0.386796	42.04
32.96	44.50	34.42	28.34	0.384637	42.17
32.96	44.50	34.50	28.43	0.383341	42.30
32.90	44.40	34.58	28.51	0.382915	42.43
32.41	43.90	34.67	28.60	0.38033	42.56
32.41	43.90	34.75	28.69	0.378181	42.70
32.47	44.00	34.83	28.77	0.376607	42.83
31.92	43.40	34.91	28.86	0.376449	42.96
31.82	43.10	35.00	28.94	0.372577	43.09
31.25	42.80	35.08	29.03	0.369997	43.23
31.25	42.80	35.16	29.12	0.368701	43.36
30.88	42.40	35.24	29.20	0.366878	43.49
31.01	42.50	35.32	29.29	0.365681	43.63
30.03	41.50	35.41	29.38	0.361809	43.76
30.52	42.00	35.49	29.46	0.35966	43.90
30.21	41.70	35.57	29.55	0.360517	44.03
29.72	41.20	35.65	29.63	0.357071	44.17
29.91	41.40	35.74	29.72	0.355775	44.30
29.66	41.20	35.82	29.81	0.355779	44.44
28.99	40.50	35.90	29.89	0.351908	44.58
29.42	40.90	35.98	29.98	0.35061	44.71
32.41	43.90	36.07	30.06	0.385259	44.85
28.81	40.30	36.15	30.15	0.362662	44.99
28.81	40.30	36.23	30.24	0.347164	45.13
28.75	40.20	36.31	30.32	0.346738	45.26
28.38	39.90	36.40	30.41	0.345011	45.40
28.20	39.70	36.48	30.50	0.342861	45.54
27.95	39.50	36.56	30.58	0.341126	45.68
27.89	39.40	36.64	30.67	0.339846	45.82
28.02	39.50	36.72	30.75	0.339842	45.96
27.47	39.00	36.81	30.84	0.338119	46.10
27.28	38.80	36.89	30.93	0.335108	46.24
27.28	38.80	36.97	31.01	0.334235	46.38
27.04	38.50	37.05	31.10	0.332954	46.52
26.73	38.20	37.14	31.18	0.330366	46.66
26.49	38.00	37.22	31.27	0.328212	46.81
26.61	38.10	37.30	31.36	0.327766	46.95
26.31	37.80	37.38	31.44	0.326913	47.09
26.55	38.10	37.47	31.53	0.326824	47.23
25.94	37.40	37.55	31.62	0.325197	47.38
26.00	37.50	37.63	31.70	0.322617	47.52
25.70	37.20	37.71	31.79	0.321752	47.66
24.96	36.50	37.80	31.87	0.317437	47.81

25.39	36.90	37.88	31.96	0.316156	47.95
25.21	36.70	37.96	32.05	0.317014	48.10
25.15	36.60	38.04	32.13	0.315718	48.24
24.78	36.30	38.12	32.22	0.314006	48.39
24.66	36.20	38.21	32.30	0.312272	48.53
24.48	36.00	38.29	32.39	0.310991	48.68
24.17	35.70	38.37	32.48	0.308823	48.82
23.90	35.30	38.45	32.56	0.305811	48.97
33.02	44.50	38.54	32.65	0.343727	49.12
23.86	35.40	38.62	32.74	0.344145	49.27
23.74	35.20	38.70	32.82	0.304099	49.41
23.38	34.90	38.78	32.91	0.301931	49.56
23.38	34.90	38.87	32.99	0.300843	49.71
23.13	34.80	38.95	33.08	0.299361	49.86
23.32	34.80	39.03	33.17	0.29892	50.01
23.38	34.90	39.11	33.25	0.300222	50.16
22.77	34.30	39.19	33.34	0.298058	50.31
22.64	34.10	39.28	33.42	0.294809	50.46
22.58	34.10	39.36	33.51	0.293761	50.61
22.28	33.80	39.44	33.60	0.292459	50.76
22.09	33.60	39.52	33.68	0.290315	50.91
21.91	33.40	39.61	33.77	0.288582	51.06
21.91	33.40	39.69	33.85	0.287718	51.21
21.79	33.30	39.77	33.94	0.2873	51.36
21.87	33.20	39.85	34.03	0.286429	51.51
21.30	32.80	39.94	34.11	0.284272	51.67
21.24	32.70	40.02	34.20	0.282135	51.82
21.24	32.70	40.10	34.29	0.281688	51.97
20.94	32.40	40.18	34.37	0.280412	52.13
20.75	32.30	40.27	34.46	0.278673	52.28
20.32	31.80	40.35	34.54	0.276088	52.43
20.81	32.30	40.43	34.63	0.276104	52.59
20.39	31.90	40.51	34.72	0.276519	52.74
20.20	31.70	40.59	34.80	0.273951	52.90
20.08	31.60	40.68	34.89	0.272643	53.05
20.02	31.50	40.76	34.97	0.271784	53.21
20.75	32.30	40.84	35.06	0.274809	53.38
19.78	31.30	40.92	35.15	0.273935	53.52
19.96	31.50	41.01	35.23	0.270505	53.68
19.59	31.10	41.09	35.32	0.269628	53.83
19.29	30.80	41.17	35.41	0.268616	53.99
18.74	30.20	41.25	35.49	0.262748	54.15
18.92	30.40	41.34	35.58	0.261013	54.31
18.80	30.30	41.42	35.66	0.261459	54.46
18.74	30.20	41.50	35.75	0.260583	54.62
18.55	30.10	41.58	35.84	0.259724	54.78
18.68	30.20	41.67	35.92	0.259733	54.94
18.55	30.10	41.75	36.01	0.259724	55.10
17.88	29.40	41.83	36.09	0.256287	55.26
18.37	29.90	41.91	36.18	0.255414	55.42
17.94	29.40	41.99	36.27	0.255417	55.58
17.88	29.40	42.08	36.35	0.253272	55.74
17.52	29.00	42.16	36.44	0.25154	55.90
17.58	29.10	42.24	36.53	0.250257	56.06
17.46	29.00	42.32	36.61	0.250245	56.22
17.33	28.80	42.41	36.70	0.248956	56.38
17.15	28.70	42.49	36.78	0.247673	56.54
17.40	28.90	42.57	36.87	0.248095	56.71
16.97	28.50	42.65	36.96	0.247242	56.87
16.97	28.50	42.74	37.04	0.24551	57.03
16.72	28.20	42.82	37.13	0.244215	57.20
16.11	27.60	42.90	37.21	0.24035	57.36
16.66	28.20	42.98	37.30	0.240342	57.52
16.05	27.60	43.06	37.39	0.24035	57.69
16.36	27.90	43.15	37.47	0.23905	57.85
16.11	27.60	43.23	37.56	0.239047	58.02
16.60	28.10	43.31	37.65	0.239919	58.18
16.24	27.70	43.39	37.73	0.240342	58.34
15.50	27.00	43.48	37.82	0.235612	58.51
15.93	27.40	43.56	37.90	0.234312	58.68
15.50	27.00	43.64	37.99	0.234309	58.84
15.26	26.80	43.72	38.08	0.231738	59.01
15.38	26.90	43.81	38.16	0.231294	59.17
14.65	26.10	43.89	38.25	0.22829	59.34
14.77	26.30	43.97	38.33	0.225697	59.51
14.71	26.20	44.05	38.42	0.226125	59.68
14.83	26.30	44.14	38.51	0.226139	59.84
14.89	26.40	44.22	38.59	0.226987	60.01
14.77	26.30	44.30	38.68	0.226987	60.18
14.65	26.10	44.38	38.77	0.225697	60.35
14.40	25.90	44.46	38.85	0.223972	60.52
13.61	25.10	44.55	38.94	0.219677	60.69
14.16	25.70	44.63	39.02	0.218803	60.86
14.16	25.70	44.71	39.11	0.2214	61.03
13.98	25.50	44.79	39.20	0.220526	61.20
13.98	25.50	44.88	39.28	0.219667	61.37
13.73	25.20	44.96	39.37	0.218383	61.54
13.55	25.00	45.04	39.45	0.216219	61.71
13.61	25.10	45.12	39.54	0.215801	61.88
13.55	25.00	45.21	39.63	0.215788	62.05

13.92	25.40	45.29	39.71	0.217083	82.22
13.37	24.90	45.37	39.80	0.21886	82.39
13.12	24.60	45.45	39.89	0.213204	82.57
12.82	24.30	45.54	39.97	0.210632	82.74
13.00	24.50	45.62	40.06	0.210189	82.91
12.76	24.30	45.70	40.14	0.210191	83.08
13.73	25.20	45.78	40.23	0.213214	83.26
12.70	24.20	45.86	40.32	0.212778	83.43
12.33	23.80	45.95	40.40	0.208753	83.60
12.27	23.80	46.03	40.49	0.20502	83.78
12.33	23.80	46.11	40.57	0.205023	83.95
12.33	23.80	46.19	40.66	0.20503	84.13
12.15	23.60	46.28	40.75	0.204161	84.30
12.08	23.60	46.36	40.83	0.203307	84.48
12.15	23.60	46.44	40.92	0.203297	84.65
12.02	23.50	46.52	41.01	0.202869	84.83
11.72	23.20	46.61	41.09	0.201153	85.01
11.72	23.20	46.69	41.18	0.199854	85.18
11.54	23.00	46.77	41.26	0.19899	85.36
10.50	22.00	46.85	41.35	0.193833	85.53
11.35	22.90	46.94	41.44	0.193391	85.71
11.23	22.70	47.02	41.52	0.196415	85.89
11.11	22.60	47.10	41.61	0.195118	86.07
11.11	22.60	47.18	41.69	0.194683	86.24
11.17	22.70	47.26	41.78	0.195125	86.42
10.86	22.40	47.35	41.87	0.194252	86.60
10.99	22.50	47.43	41.95	0.1934	86.78
10.80	22.30	47.51	42.04	0.192963	86.96
10.86	22.40	47.59	42.12	0.19253	87.14
10.56	22.10	47.68	42.21	0.191879	87.32
10.62	22.10	47.76	42.30	0.190376	87.50
10.50	22.00	47.84	42.38	0.189956	87.68
10.25	21.80	47.92	42.47	0.188653	87.86
10.25	21.80	48.01	42.56	0.187794	88.04
10.19	21.70	48.09	42.64	0.18737	88.22
9.95	21.40	48.17	42.73	0.185838	88.40
9.83	21.30	48.25	42.81	0.183928	88.58
10.38	21.90	48.33	42.90	0.186069	88.76
11.11	22.60	48.42	42.99	0.19167	88.94
9.64	21.10	48.50	43.07	0.188231	89.13
9.70	21.20	48.58	43.16	0.182192	89.31
9.77	21.30	48.66	43.24	0.183065	89.49
9.52	21.00	48.75	43.33	0.182192	89.67
9.64	21.10	48.83	43.42	0.181333	89.86
9.16	20.70	48.91	43.50	0.180047	90.04
9.28	20.80	48.99	43.59	0.178749	90.22
9.16	20.70	49.08	43.68	0.178755	90.41
9.03	20.50	49.16	43.76	0.177455	90.59
8.91	20.40	49.24	43.85	0.176164	90.78
8.97	20.50	49.32	43.93	0.176171	90.96
8.91	20.40	49.41	44.02	0.176164	91.15
5.62	17.10	49.49	44.11	0.161526	91.33
8.73	20.20	49.57	44.19	0.160657	91.52
8.48	20.00	49.65	44.28	0.173149	91.70
8.36	19.90	49.73	44.36	0.171863	91.89
8.48	20.00	49.82	44.45	0.171857	92.07
8.42	19.90	49.90	44.54	0.171863	92.26
7.87	19.40	49.98	44.62	0.169273	92.45
8.06	19.80	50.06	44.71	0.167979	92.63
8.18	19.70	50.15	44.80	0.169279	92.82
8.18	19.70	50.23	44.88	0.169704	93.01
7.93	19.40	50.31	44.97	0.168417	93.19
8.06	19.60	50.39	45.05	0.167981	93.38
7.26	18.80	50.48	45.14	0.165395	93.57
7.81	19.30	50.56	45.23	0.16411	93.76
7.87	19.40	50.64	45.31	0.166689	93.95
7.75	19.30	50.72	45.40	0.166894	94.14
7.63	19.10	50.81	45.48	0.165396	94.32
7.45	18.90	50.89	45.57	0.163672	94.51
7.32	18.80	50.97	45.66	0.162389	94.70
7.08	18.60	51.05	45.74	0.161087	94.89
7.32	18.80	51.13	45.83	0.161095	95.08
7.08	18.60	51.22	45.92	0.161089	95.27
7.08	18.60	51.30	46.00	0.160228	95.46
7.14	18.60	51.38	46.09	0.160235	95.65
7.39	18.90	51.46	46.17	0.161518	95.84
6.65	18.20	51.55	46.26	0.159803	96.04
6.84	18.30	51.63	46.35	0.157213	96.23
6.84	18.30	51.71	46.43	0.157042	96.42
6.71	18.20	51.79	46.52	0.15722	96.61
6.71	18.20	51.88	46.60	0.15678	96.80
6.53	18.00	51.96	46.69	0.155928	96.99
6.65	18.20	52.04	46.78	0.155019	97.19
6.29	17.80	52.12	46.86	0.155059	97.38
6.35	17.80	52.20	46.95	0.153342	97.57
6.10	17.60	52.29	47.04	0.152473	97.76
6.29	17.80	52.37	47.12	0.152462	97.96
6.04	17.50	52.45	47.21	0.152042	98.15
6.04	17.50	52.53	47.29	0.150752	98.35
6.04	17.50	52.62	47.38	0.150757	98.54

5.55	17.10	52.70	47.47	0.149027	78.73
6.04	17.50	52.78	47.55	0.149036	78.93
5.86	17.40	52.86	47.64	0.15032	79.12
5.68	17.20	52.95	47.72	0.149029	79.32
5.86	17.40	53.03	47.81	0.149034	79.51
6.04	17.50	53.11	47.90	0.150321	79.71
4.46	16.00	53.19	47.98	0.144296	79.90
5.37	16.90	53.28	48.07	0.141705	80.10
5.68	17.20	53.36	48.16	0.146876	80.30
5.19	16.70	53.44	48.24	0.148019	80.49
5.37	16.90	53.52	48.33	0.144722	80.69
5.25	16.70	53.60	48.41	0.144727	80.88
5.25	16.70	53.69	48.50	0.143859	81.08
5.25	16.70	53.77	48.59	0.14386	81.28
4.82	16.30	53.85	48.67	0.142143	81.48
5.55	17.10	53.93	48.76	0.14386	81.67
5.00	16.50	54.02	48.84	0.14472	81.87
4.64	16.10	54.10	48.93	0.140421	82.07
4.94	16.40	54.18	49.02	0.139982	82.27
4.82	16.30	54.26	49.10	0.14085	82.47
5.07	16.60	54.35	49.19	0.141707	82.66
4.70	16.20	54.43	49.27	0.141275	82.86
4.58	16.10	54.51	49.36	0.139129	83.06
4.76	16.30	54.59	49.45	0.139552	83.26
4.58	16.10	54.68	49.53	0.139558	83.46
5.07	16.60	54.76	49.62	0.140845	83.66
4.33	15.80	54.84	49.71	0.139552	83.86
4.15	15.70	54.92	49.79	0.135683	84.06
4.27	15.80	55.00	49.88	0.135675	84.26
4.39	15.90	55.09	49.96	0.136545	84.46
4.39	15.90	55.17	50.05	0.136967	84.66
4.09	15.60	55.25	50.14	0.135677	84.86
4.15	15.70	55.33	50.22	0.13482	85.06
4.33	15.80	55.42	50.31	0.135675	85.26
4.03	15.50	55.50	50.39	0.134822	85.47
4.03	15.50	55.58	50.48	0.133522	85.67
3.91	15.40	55.66	50.57	0.133092	85.87
3.85	15.30	55.75	50.65	0.132236	86.07
3.30	14.80	55.83	50.74	0.129645	86.27
3.66	15.20	55.91	50.83	0.129222	86.48
3.54	15.00	55.99	50.91	0.130076	86.68
3.54	15.00	56.08	51.00	0.129216	86.88
3.54	15.00	56.16	51.08	0.129221	87.08
3.42	14.90	56.24	51.17	0.128764	87.29
3.30	14.80	56.32	51.26	0.12793	87.49
3.36	14.90	56.40	51.34	0.127922	87.69
3.36	14.90	56.49	51.43	0.128355	87.90
3.36	14.90	56.57	51.51	0.128359	88.10
3.11	14.60	56.65	51.60	0.127062	88.31
3.05	14.80	56.73	51.69	0.125775	88.51
2.87	14.40	56.82	51.77	0.124907	88.72
3.05	14.80	56.90	51.86	0.124909	88.92
2.87	14.40	56.98	51.95	0.124913	89.12
2.87	14.40	57.06	52.03	0.124047	89.33
2.87	14.40	57.15	52.12	0.124052	89.54
2.99	14.50	57.23	52.20	0.124477	89.74
2.87	14.40	57.31	52.29	0.124478	89.95
2.75	14.20	57.39	52.38	0.12319	90.15
2.56	14.10	57.47	52.46	0.121894	90.36
2.75	14.20	57.56	52.55	0.121898	90.56
2.38	13.90	57.64	52.63	0.121032	90.77
2.56	14.10	57.72	52.72	0.1206	90.98
2.50	14.00	57.80	52.81	0.121037	91.18
2.50	14.00	57.89	52.89	0.120602	91.39
2.32	13.80	57.97	52.98	0.119744	91.60
2.14	13.60	58.05	53.07	0.118017	91.81
2.32	13.80	58.13	53.15	0.118016	92.01
2.32	13.80	58.22	53.24	0.118883	92.22
2.14	13.60	58.30	53.32	0.118017	92.43
4.33	15.80	58.38	53.41	0.126636	92.64
2.20	13.70	58.46	53.50	0.127062	92.85
2.20	13.70	58.55	53.58	0.118016	93.05
2.08	13.60	58.63	53.67	0.117592	93.26
1.95	13.50	58.71	53.75	0.116724	93.47
1.77	13.30	58.79	53.84	0.115437	93.68
2.01	13.50	58.87	53.93	0.115433	93.89
2.38	13.90	58.96	54.01	0.118016	94.10
2.14	13.80	59.04	54.10	0.118454	94.31
1.77	13.30	59.12	54.19	0.115862	94.52
1.71	13.20	59.20	54.27	0.114145	94.73
1.65	13.10	59.29	54.36	0.113279	94.94
1.71	13.20	59.37	54.44	0.113278	95.15
1.85	13.10	59.45	54.53	0.113285	95.36
1.46	13.00	59.53	54.62	0.112417	95.57
1.53	13.00	59.62	54.70	0.111992	95.78
1.28	12.80	59.70	54.79	0.111124	95.99
1.53	13.00	59.78	54.87	0.111126	96.20
1.40	12.90	59.86	54.96	0.111156	96.41
1.28	12.80	59.95	55.05	0.110694	96.62
1.28	12.80	60.03	55.13	0.110269	96.84

1.10	12.60	60.11	55.22	0.109402	97.05
1.16	12.70	60.19	55.31	0.108972	97.28
0.98	12.50	60.27	55.39	0.108545	97.47
1.04	12.50	60.38	55.48	0.107679	97.68
0.92	12.40	60.44	55.56	0.107254	97.90
0.92	12.40	60.52	55.65	0.106817	98.11
1.04	12.50	60.60	55.74	0.107249	98.32
0.79	12.30	60.69	55.82	0.106822	98.53
0.73	12.20	60.77	55.91	0.106528	98.75
0.61	12.10	60.85	55.99	0.104869	98.96
0.67	12.20	60.93	56.08	0.104864	99.17
0.61	12.10	61.02	56.17	0.104865	99.39
0.67	12.20	61.10	56.25	0.104869	99.60
0.49	12.00	61.18	56.34	0.104234	99.81
0.73	12.20	61.26	56.42	0.104233	100.03
0.49	12.00	61.34	56.51	0.104238	100.24
0.06	11.60	61.43	56.60	0.10165	100.46
0.49	12.00	61.51	56.68	0.101653	100.67
0.31	11.80	61.59	56.77	0.102511	100.88
0.55	12.00	61.67	56.86	0.10251	101.10
0.49	12.00	61.76	56.94	0.103378	101.31
0.31	11.80	61.84	57.03	0.10251	101.53
0.12	11.60	61.92	57.11	0.100792	101.74
0.18	11.70	62.00	57.20	0.100358	101.96
0.24	11.70	62.09	57.29	0.100787	102.17
0.12	11.60	62.17	57.37	0.100362	102.39
-0.18	11.30	62.25	57.46	0.098634	102.61
0.00	11.50	62.33	57.54	0.098208	102.82
0.00	11.50	62.42	57.63	0.099066	103.04
0.37	11.90	62.50	57.72	0.100787	103.25
0.00	11.50	62.58	57.80	0.100793	103.47

VITA AUCTORIS

Philip S. Zoldak was born in 1976 in Kitchener, Ontario. He grew up working along side his father at the family automotive repair business. He graduated from St. David High School in 1996. From there he went on to study at the University of Waterloo where he attained a B.A.Sc. in Mechanical Engineering in 2002. While a student at University of Waterloo he had several co-op placements in automotive manufacturing and product development with firms such as Magna, Ford, and Toyota. He is currently working as a Development Engineer with International Truck and Engine Company. He is also a candidate for the Master's degree in Mechanical Engineering at the University of Windsor and hopes to graduate in Fall 2005.

VITA AUCTORIS

Philip S. Zoldak was born in 1976 in Kitchener, Ontario. He grew up working along side his father at the family automotive repair business. He graduated from St. David High School in 1996. From there he went on to study at the University of Waterloo where he attained a B.A.Sc. in Mechanical Engineering in 2002. While a student at University of Waterloo he had several co-op placements in automotive manufacturing and product development with firms such as Magna, Ford, and Toyota. He is currently working as a Development Engineer with International Truck and Engine Company. He is also a candidate for the Master's degree in Mechanical Engineering at the University of Windsor and hopes to graduate in Fall 2005.